WADC TECHNICAL REPORT 54-602

REVIEW OF SOUND PROPAGATION IN THE LOWER ATMOSPHERE

WESLEY L. NYBORG
DAVID MINTZER

BROWN UNIVERSITY

MAY 1955

WRIGHT AIR DEVELOPMENT CENTER

AF WP (B, O-12 AUG 55 200

NOTICE

When Government drawings, specifications, or other data are used for any purpose other than in connection with a definitely related Government procurement operation, the United States Government thereby incurs no responsibility nor any obligation whatsoever; and the fact that the Government may have formulated, furnished, or in any way supplied the said drawings, specifications, or other data, is not to be regarded by implication or otherwise as in any manner licensing the holder or any other person or corporation, or conveying any rights or permission to manufacture, use, or sell any patented invention that may in any way be related thereto.

WADC TECHNICAL REPORT 54-602

REVIEW OF SOUND PROPAGATION IN THE LOWER ATMOSPHERE

Wesley L. Nyborg
David Mintzer

Brown University

May 1955

Aero Medical Laboratory
Contract No. AF 33(616)-340
Project No. 7212

Wright Air Development Center
Air Research and Development Command
United States Air Force
Wright-Patterson Air Force Base, Ohio

FOREWORD

The work herein reported was conducted by the Physics Department of Brown University, Providence, Rhode Island, under Contract AF33 (616)-340. It was initiated under USAF Project RDO No. R-695-63 "Sonic and Mechanical Vibration Action of Air Force Personnel", continued under Project R-695-85 "Propagation of Sound Waves Near the Earth's Surface" and finished under Task No. 71709 "Propagation of Sound Waves near the Earth's Surface" of Project No. 7212. Major Horace O. Parrack, Mr. Wolf W. von Wittern and Dr. Henning E. von Gierke served as project engineers for the Aeromedical Laboratory, Wright Air Development Center, during the course of this investigation.

The authors gratefully acknowledge helpful consultations with Professors R. B. Lindsay, R. W. Morse and P. J. Westervelt on matters contained herein. Messrs. D. Brickl, J. S. D. Y. Lee and A. Washington provided considerable assistance in preparation of the technical material. Messrs. S. Cottrell, E. Iannuccillo, F. Jackson, J. Kline and L. Ray helped with numerical work and drafting. The typing was done by Mrs. C. D. Hawes.

ABSTRACT

A critical review is given of available information on sound propagation through the lower atmosphere. The application is to the prediction of sound fields due to aircraft (in flight or on the ground), especially, at distances up to a few miles from the aircraft sound sources. Treatment of the prediction problem requires consideration of a number of topics including (1) absorption processes in the air, (2) boundary effects caused by the earth and (3) refraction of sound due to spatial variations in air temperature and wind. Although a fair amount of information is now available on these topics a considerable amount of research remains to be done before practical solutions will be available.

PUBLICATION REVIEW

This report has been reviewed and is approved.

FOR THE COMMANDER:

JACK BOLLERUD
Colonel, USAF (MC)
Chief, Aero Medical Laboratory
Directorate of Research

TABLE OF CONTENTS

SECTION I

Theory and Laboratory Measurements

Table of Contents

Table of Contents

LIST OF FIGURES

List of Figures

List of Figures

LIST OF TABLES

List of Tables

INTRODUCTION

Airports and their immediate vicinities are becoming more and more subject to intense noise as the tendency to use ever more powerful aircraft continues. Because of increasing human reaction to this situation, the neighborhood aircraft noise problem presents itself as a most serious one. It is evident that in the design and operation of an airport acoustical planning must henceforth play a highly important role.

For such planning to be effective it is, of course, necessary to be able to predict what sound levels will exist, under given conditions, at various points on and in the neighborhood of an airport. To do this one must, in the first place, have information on the aircraft sound sources that will be used. That is, one must know what noise levels exist in the near field of the source, both when operated in the open (either on the ground or in flight) and when modified by enclosures or other shielding structures.

One would then hope to use these near field results as a basis on which to calculate noise levels at large distances from the source, i.e., in the far field. It is, of course, obvious that to do this one must know how the sound field changes with distance. A study of these changes constitutes the subject of propagation of sound through the atmosphere and over the ground. An investigation of sound propagation problems must include a variety of topics for consideration including (a) absorption processes in the air, (b) viscous dissipation and condensation phenomena if fog is present, (c) effects caused by the earth as both an absorbing and a reflecting boundary, and (d) refraction of sound due to spatial variations in air temperature and wind.

It is these problems of sound propagation with which this report is concerned. The principal aim of the report is to give a review of the present state of knowledge of atmospheric acoustics, especially as related to aircraft noise propagation. The attempt has been made to include all suitable material available on this subject, whether in the form of work published in the scientific journals, or in the form of technical reports, or in some cases, in the form of private memoranda.

All such material comes ultimately from either of three kinds of activity, namely, from theory, from laboratory experiments, or from measurements made out-of-doors. In this report each of these three sources makes its contribution, as discussed briefly below:

(1) There is a rather extensive amount of theory available on special topics related to atmospheric acoustics.

In some cases the results are fairly directly applicable to actual out-of-doors situations. In others the theory in its present form is for conditions too idealized to apply in the field. The latter kind of theory can be very useful, however, in suggesting which parameters are likely to be the important ones, and for use in estimating the order-of-magnitude of effects.

(2) Further information on particular aspects of atmospheric acoustics problems comes from the results of laboratory experiments. Some of these results appear to be rather directly applicable to certain field situations, but for most of the experiments this is not true, the conditions being quite different than those obtaining in typical aircraft noise problems. The latter experiments are nevertheless of great importance. Theories can often be tested with comparative ease in the laboratory, where parameters are more readily varied and controlled than in out-of-doors. When theories have been examined critically by means of laboratory tests they can usually be applied to field problems with more confidence and with better judgement.

(3) Finally, there is now available a fair amount of acoustical data obtained from measurements made out-of-doors. Some of these data were taken by using essentially single frequency sound generated by loudspeakers, etc; others were obtained by using noise from actual aircraft. It will be realized that, in general, it is difficult to separate the effect of different parameters in out-of-door measurements since, e.g., the weather is obviously not at the control of the experimenter. Nevertheless, in some cases the experiment was so designed and the conditions so specified that the effect of various parameters could be ascertained. In others only general or "typical" effects could be determined.

In this report Section I is a review of contributions from theory and laboratory measurements to our present knowledge on problems in atmospheric acoustics. In this section are presented what are felt to be the more important formulae for dealing with sound propagation in the lower atmosphere, together with related charts and tables. Ranges of applicability of the formulae are indicated, where possible; this is especially feasible when data from controlled experiments are available for comparison with the theory.

In Section II a review is given of results from measurements made out-of-doors. Comparison is made between the results of different investigators, obtained under quite a variety of different circumstances. Also, where possible, comparison is made with the predictions of pertinent theory from Section I.

In Section III special tables and graphs are given for applying information reviewed in the previous sections; also, recommended procedures are described for dealing with various practical problems.

Section IV contains detailed discussion of needs for future research in the areas treated in this report. Important deficiencies in present-day knowledge are pointed out, and various methods of approach examined.

Appendices I and II contain tables of constants and a chart for converting units of humidity. Appendix III tabulates theoretical absorption coefficients for various parts of the United States. Appendix IV, reviews briefly certain material pertinent to this report, but received too recently to be incorporated into Section II.

SECTION I

THEORY AND LABORATORY MEASUREMENTS

1.1 INTRODUCTION

1.1.1 Actual sound fields which exist in typical out-of-door situations are almost prohibitively difficult to describe in detail. The atmosphere is never homogeneous - there are always variations in temperature and humidity - and it is never quiescent. Thus the medium for sound transmission is not the ideal one to which most current acoustical theory applies. In addition, the boundary conditions are often much less simple than those used in most of currently available wave theory. Thus the terrain may be uneven, both in vegetative covering and in contour; trees and hills, as well as buildings and other man-made structures may complicate description of the lower boundary.

Hence, as would be expected, there exists at the present time no over-all theory which can be used to describe typical out-of-door sound fields with sufficient completeness. There are, however, a number of special theoretical developments which are of much interest. Each of these idealizes the total problem in order to treat some particular aspect of it, and thereby gives specific attention to certain particular parameters. By considering separately these theories for idealized cases, one can develop insight into the parts different parameters play in affecting a sound field. Also, there are a few instances where certain of the idealized theories do apply with fair accuracy to actual out-of-door situations.

The remainder of Section I will be devoted chiefly to a discussion of the special theories and experimental results mentioned above. In order to clarify the organization of this section before going into details, we list below the separate problems to be taken up, together with brief descriptions of them. The idealized conditions assumed in each case are stated, as are also the results from theory and/or experiment as to which parameters appear to be the most important ones.

In most of the topics to be discussed the problem is to describe the sound field in a region of atmosphere above a flat earth. More specifically, the chosen aim is to state the sound pressure p at any point P due to a source, whose pertinent properties are assumed known, localized near another point Q. Unless otherwise stated, it will be assumed in Section I that the source is like a point source and has spherical symmetry. It is realized, however, that directional effects are very important for aircraft as noise sources and that these must finally be taken into account. Another important specialization made implicitly throughout most of Section I is that nonlinear effects are ignored, it being assumed that pressure amplitudes are small in com-

parison to atmospheric pressure, except at points very near the source. (The situation when the pressure amplitude is not small is treated briefly in subsection 1.8.)

For describing the position of source and receiver points Q and P with respect to the earth and each other we use the symbols defined by the sketch in Fig. 1. Here the plane surface S represents the earth's surface and is assumed to be a horizontal plane. The points O and P' are on the surface S and are directly below Q and P, respectively. The source height $\overline{OQ}$ is z_o and the receiver height $\overline{PP'}$ is z. The actual distance from the source point Q to the receiver point P is R, while the horizontal component $\overline{OP'}$ of this distance is r. The four above-defined quantities are related by the equation

$$R^2 = r^2 + (z_o - z)^2 . \qquad (1)$$

As indicated on the figure, ϕ measures the angle between the wind direction and the directed line $\overline{OP'}$.

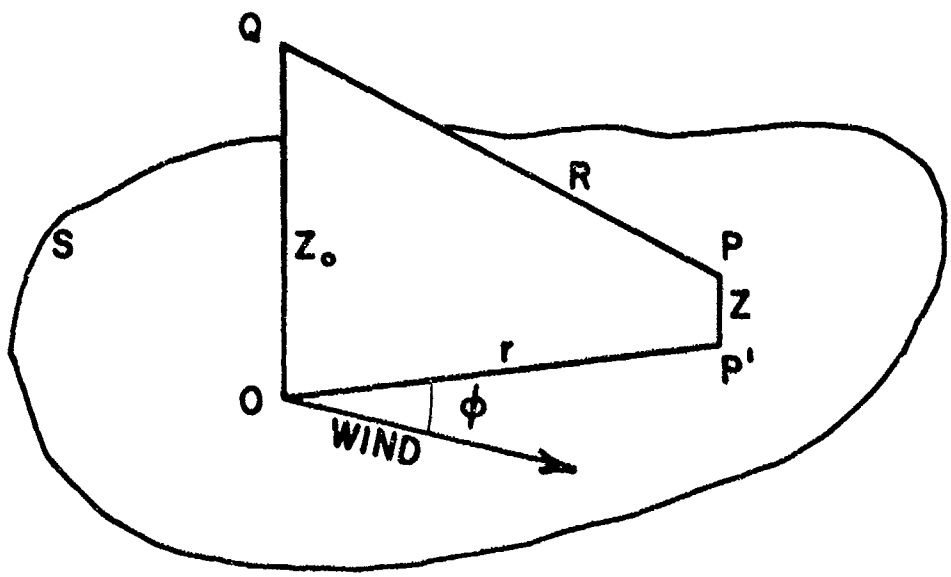

Fig. 1 Geometrical variables for describing sound propagation. S represents horizontal ground surface; Q and P are source and receiver points; O and P' are projections of Q and P on S; ϕ measures the angle between $\overline{OP'}$ and the wind direction.

1.1.2 We now list and briefly describe the topics to be taken up in the remainder of Section I.

1.1.2.1 Sound propagation in homogeneous air

This is the simplest possible case. It is assumed that the humidity and temperature are everywhere the same, that the air is free of particles of fog and smoke and that the bounding surface presented by the earth does not affect the sound field (as if there were no bounding surfaces and the atmosphere were infinite in extent). For typical conditions to be encountered in practical field situations, the main parameters besides the sound frequency are the air temperature, the absolute humidity and the source-receiver distance R. The law giving the sound pressure amplitude p at any point P is assumed to be of the form:

$$p = AR^{-1} e^{-\alpha R} \qquad (2)$$

where the constant A depends on the source strength and the constant α depends on air conditions.

1.1.2.2 Propagation in fog

Here the same conditions hold as in the previous subsection except that the air is assumed to hold in suspension a distribution of small spherical particles, either liquid or solid. The new parameters which prove to be important here are those describing the distribution of particle sizes, those characterizing the material composing the particles, and those, in addition to temperature and humidity, needed to specify the properties of the surrounding air. It is assumed that the sound field is of the form given by Eq. (2), so that R is the important geometrical variable.

1.1.2.3 Propagation over the ground

It is assumed here that the air is homogeneous and that the ground presents a plane uniform surface with known acoustical properties. The air temperature and humidity are assumed relatively unimportant here. Besides the sound frequency and the geometrical quantities z_o, r, and z, the important parameters are those describing the nature of the ground. The general expression for the sound pressure p at any point P is rather complicated. For the special case in which the source and receiver are both very near the ground, it is found that if the ground is absorbing and r is sufficiently great the pressure at P is given simply by

$$p = Br^{-2} , \qquad (3)$$

where B is a constant depending particularly on the source strength, the frequency and the nature of the ground.

1.1.2.4 Propagation in a stratified medium

Here it is assumed (1) that the air is homogeneous except that the temperature and/or wind velocity varies with height and (2) that the ground surface is uniform and of known acoustical properties. The cases of special interest are those where sound shadows exist; such shadows occur when the effective sound velocity decreases with height, so that rays from the source are bent upward. Besides the distances z_o, r, and z, and the sound frequency, the main parameters are those which give the rate of change with height of temperature and wind velocity, and the angle ϕ between the wind direction and the line $\overline{OP'}$ (see Fig. 1). The general expression for the sound field at any point P is fairly involved. If source and receiver are at the same height (i.e., if z_o and z are equal), theory for special cases indicates that a law of the form

$$p = \frac{Ce^{-\alpha r}}{\sqrt{r}} \qquad (4)$$

holds for points inside the shadow region, where C and α are constants.

1.1.2.5 Propagation through a randomly inhomogeneous atmosphere

Here the situation is considered where the wind and temperature vary in space and time, as indeed is always true in the atmosphere. However, it is assumed that in this case (unlike that treated in the previous subsection) the time-averaged air conditions are the same everywhere. Specifically, it is assumed that (a) the time-averaged wind velocity is zero at all points, (b) the time-averaged temperature is the same at all points, and (c) each statistical index of wind and temperature fluctuations, obtained by time-averaging at a point, is the same at all points in the atmosphere.

The pressure amplitude p at any point P will vary with time in an apparently random manner. Theory for the fluctuations due to temperature variations indicate that the main parameters, besides the frequency and the distance R, are two statistical indices, one describing the mean magnitude of the temperature variations and the other the mean "grain size".

For the mean value of p at any distance R from the source there is, as yet, no adequate general theory. It has been suggested that, at least, in some cases the law may be of the form of Eq. (2), where α depends essentially on the frequency and on the same two statistical indices mentioned above.

1.1.2.6 Propagation over a wall

Here the classical methods for treating diffraction by a "straight edge", long known in optics, are applied, with suitable modifications, to the problem of the sound shadow cast by a long wall or building. The usual approximations of Fresnel diffraction are made. Though some consideration is given to reflections from the earth and to refraction by vertical gradients of temperature and wind it is assumed, in the main, that the atmosphere is homogeneous and that ground effects are absent. The most important variables are the sound frequency, the distances z_0, r, z, the height of the wall and its distance from source and receiver.

1.1.2.7 Propagation of high-amplitude sound waves

The problem treated here is that of sound propagation when the small-amplitude approximations of ordinary acoustics are not valid. The more exact form of the basic equations must then be considered, including nonlinear terms; solutions of these cannot be superposed as can those of the linear wave equations. A propagating sound wave, originally sinusoidal with given single frequency, will suffer distortion as it travels; harmonics are generated in such a wave at a rate which depends particularly on the source amplitude, the frequency, and the nature of the wave (e.g., whether it is plane or spherical).

1.1.3 Before proceeding with detailed discussion of the separate topics listed above in subsection 1.1.2, we pause briefly to explain certain conventions which will be followed and terminology which will be used.

In describing the sound field for a given situation one might specify the space distribution of any of a number of quantities, such as pressure amplitude, particle velocity amplitude, etc. As in the preceding discussion we shall, throughout the report, be usually speaking of the pressure amplitude (or of some quantity proportional thereto). The reason for this choice is partly that the pressure, unlike the velocity or displacement, is a scalar quantity and hence is comparatively easy to describe. It is also partly because both laboratory and field data are likely to be in terms of the pressure amplitude, since microphones in use tend to be essentially pressure-indicators.

One may describe any given pressure distribution by (1) stating the amplitude at some reference point P_0 and (2) stating the ratio of the amplitude at any other point P to that at P_0. Under the assumption of linearity the latter ratio will be independent of the amplitude at P_0. In practice, the point P_0 is often chosen near the source, so that the pressure amplitude there may be regarded as characteristic of the source and nearly unaffected by absorption or refraction in the air, and nearly

independent of the earth below. At the same time, since linearity is assumed in most of the situations to be considered here, the reference point P_o, where the amplitude is to be characteristic of the source, should also be supposed sufficiently far from the source; the field at P_o, and at points outward from the source relative to P_o, must be weak enough to permit use of the usual acoustical approximations. (In the field of very powerful noise sources there may be no point P_o which is entirely satisfactory as a reference point. Thus, in such cases it may be that all points which satisfy the weak-field condition are so far from the source that the field at these points is strongly affected by refraction in the air or by "ground effects".)

In acoustics, it is often customary to state the pressure amplitude p at any given point P by specifying a quantity, called the sound pressure level (or, simply, the level) at P, proportional to the logarithm of p. Specifically, in terms of both neper and decibel (db) units we have:

$$\text{Sound level in nepers} = \ln (p/p^*) \tag{5a}$$

$$\text{Sound level in db} = 20 \log_{10} (p/p^*), \tag{5b}$$

where p^* is an arbitrary reference amplitude.

Similarly, in stating the ratio between the amplitudes at any two points, such as P_o and P, it is convenient to specify a quantity proportional to the logarithm of the ratio. This logarithmic ratio is referred to as the loss or attenuation in sound level at P relative to that at P_o, or, when appropriate, as the "loss incurred by a sound wave in traveling from P_o to P", or as the transmission loss between P_o and P, etc. In neper and db units, respectively, we have

$$\text{Loss in nepers} = \ln (p_o/p) \tag{6a}$$

$$\text{Loss in db} = 20 \log_{10} (p_o/p), \tag{6b}$$

where p is the pressure amplitude at P and p_o that at P_o. One may convert between nepers and db by the following relation

$$(\text{Loss in db}) = 8.68\ (\text{Loss in nepers}) \tag{7}$$

In the following discussion, which deals with separate problems, we shall speak of losses due to a number of different mechanisms. As an important example, if Eq. (2) holds and α is essentially zero the loss incurred between any two points is due only to the spreading or divergence of the spherical wave. On the other hand, if α is not zero we consider the loss as due to two causes. Using Eq. (2) in Eqs. (6) we may write for the loss between P_o and P:

$$\text{Loss in nepers} = \ln\left[RR_o^{-1}\, e^{\alpha(R-R_o)}\right] \tag{8a}$$

$$\text{Loss in db} = 20 \log_{10}\left[RR_o^{-1}\, e^{\alpha(R-R_o)}\right], \tag{8b}$$

where R_o and R are the distances from the source to P_o and P, respectively. The right hand sides of each of the latter equations may be written as

$$\text{Loss in nepers} = \ln\left(RR_o^{-1}\right) + \alpha(R-R_o) \tag{9a}$$

$$\text{Loss in db} = 20 \log_{10}\left(RR_o^{-1}\right) + 8.68\,\alpha(R-R_o) \tag{9b}$$

We see that the loss consists of two parts, given by the two terms on the right hand side of either of Eqs. (9). Choosing either of these equations for our attention, the first term on the right hand side gives the loss due to spherical spreading, i.e., the loss which would occur if α were zero. The second term gives the loss associated with α. The latter loss tends to predominate at large distances from the source where the divergence loss is relatively small and the spherical wave propagates essentially like a plane wave. To facilitate discussion throughout the report we shall give distinguishing names to these two particular kinds of losses: the first we shall refer to as the divergence loss or (1/R) loss, and the second the exponential loss. From Eqs. (9) we have that the exponential loss suffered by a spherical wave in traveling radially outward from a reference point P_o to another point P is given as follows:

$$\text{Exponential loss in nepers} = \alpha(R-R_o) \tag{10a}$$

$$\text{Exponential loss in db} = \alpha^*(R-R_o) \tag{10b}$$

where, from Eq. (7), $\alpha^* = 8.68\,\alpha$ and where $(R-R_o)$ is the distance from P_o to P. The exponential loss experienced by an expanding spherical wave is proportional to the distance travelled. The coefficients α and α^* give the loss per unit distance in units of nepers per unit distance and decibels per unit distance, respectively.

1.2 SOUND ABSORPTION IN HOMOGENEOUS AIR

1.2.1 Introduction

We treat here the idealized case of small amplitude sound propagation from a small source in a large body of homogeneous air, re-

flections from boundaries (in particular, the earth) being assumed negligible. Under these conditions Eq. (2) holds, where the constant α depends on the temperature, pressure and molecular composition of the air. The exponential loss is in this case said to be due to absorption and α (whether in nepers or decibels per unit distance) is called the absorption coefficient. Well-known theories exist for calculating the absorption constant α . Also, experimental data taken in the laboratory under controlled conditions are available against which the theories can be checked. These data agree with theoretical expectations for some ranges of parameters. Unfortunately, however, the theory appears to be far from adequate for certain conditions which are very important for aircraft noise problems. Thus, for the lower audible frequencies and fairly high absolute humidities, laboratory determinations of α tend to be much in excess of present theoretical values. Still more unfortunately, adequate laboratory data do not exist at frequencies below 1000 cycles/sec. We are thus at a loss to know what values to expect for α at very low audible and, especially, at sub-audible frequencies.

We give in subsection 1.2 an account of present-day knowledge about the absorption coefficient α in air under different conditions. Formulae resulting from accepted theories are presented in analytical, tabular, and graphical form; the results of laboratory experiments are also displayed, and compared with theoretical predictions.

In Section II the results discussed here will be compared with loss coefficients measured out-of-doors.

In Section III additional tables and charts are presented for convenience in determining α for given field conditions. These computational aids are based on the findings to be discussed in the remainder of subsection 1.2.

In Appendix III average values of α , computed from the charts just mentioned, are tabulated for 80 different stations in the United States, based on average temperature and humidity data from records of the U. S. Weather Bureau.

It is customary to regard the absorption coefficient α as being composed of a number of separate parts, each having a different physical origin. Thus we write

$$\alpha = \alpha_{class} + \alpha_{mol}, \tag{11a}$$

$$\alpha_{class} = \alpha_v + \alpha_c + \alpha_d + \alpha_r , \tag{11b}$$

where α_v, α_c, α_d and α_r are, respectively, the absorption coefficient due to viscosity, conduction (of heat), diffusion (of oxygen and

nitrogen molecules among each other), and radiation (of heat). The sum of these is here designated as α_{class} and is called the classical absorption coefficient. The term α_{mol} is due to intra-molecular causes, and is usually much larger than α_{class} at audible frequencies. It is sometimes referred to as the humidity loss factor because of its strong dependence on the moisture content of the air at any given frequency. We shall discuss α_{class} first, in subsection 1.2.2; α_{mol} will then be taken up, in subsection 1.2.3.

1.2.2 Classical Absorption[1]

The classical absorption is often negligible for typical conditions in aircraft noise propagation problems. We nevertheless shall present the main theoretical results for α_{class}, partly because of their general interest, and partly in order that the reader may apply them to special problems. (For example, if the absorption at either high frequencies or low static pressures is to be considered α_{class} must be taken into account). The four separate terms that combine to make up α_{class}, according to Eq. (11b) are given by the following expressions:

$$\alpha_v = \frac{8}{3} \frac{\pi^2 \eta f^2}{\rho_o c^3} \tag{12}$$

$$\alpha_c = \frac{2\pi^2 f^2 (\gamma-1) K}{\rho_o c^3 c_p} \tag{13}$$

$$\alpha_d = \frac{\gamma-1}{2\gamma} \frac{\omega^2}{c^3} a D_{12} \tag{14}$$

$$\alpha_r = \frac{\gamma-1}{2} \frac{H}{c c_v} \tag{15}$$

The symbols used in Eqs. (12 - 15) have the following meanings:

η : viscosity of air (poise)

f : frequency of the sound (cycles per second)

ω : $2\pi f$

ρ_o : density of air (gm cm^{-3})

c : velocity of sound in air (cm sec^{-1})

γ : (c_p/c_v); ratio of specific heats for air

K : heat conductivity of air (cal cm^{-2} sec^{-1} $[^oC\ cm^{-1}]^{-1}$)

c_p : specific heat of air at constant pressure (cal $gm^{-1}[^oC]^{-1}$)

a : molecular constant for air (0.51)

D_{12} : mutual diffusion coefficient of N_2 and O_2 (cm^2 sec^{-1})

H : coefficient of radiation of air $\doteq 10^{-3}$ (cal sec^{-1} gm^{-1} $^oC^{-1}$)

c_v : specific heat of air at constant volume (cal $gm^{-1}[^oC]^{-1}$)

Tabular values and empirical formulae for those constants which vary with temperature are given in Appendix I. Using these in Eqs. (12 - 15) the separate components of α_{class} can be calculated over a range of temperature. This has been done in preparing Table 1; here ($\alpha_v + \alpha_c$), α_d and α_r are tabulated for temperatures ranging from -150° to 100°C. In converting from the units (nepers/cm) of Eqs. (12 - 15) to the units (db/1000 ft) of Table 1 use was made of the following conversion ratio:

$$(\alpha \text{ in db/1000 ft}) = (264{,}500)(\alpha \text{ in nepers/cm}) \qquad (16)$$

TABLE 1

Calculated Values of Classical Absorption Coefficients

(Frequency f in kc; static pressure p^* in atmospheres; absorption coefficients α_v, etc, in db/1000 ft)

Temperature	($\alpha_v + \alpha_c$)	α_d	α_r
-150°C	.026 f^2/p^*	.0033f^2	.0070
-100	.030 f^2/p^*	.0035f^2	.0058
-50	.033 f^2/p^*	.0037f^2	.0051
0	.036 f^2/p^*	.0038f^2	.0046
50	.038 f^2/p^*	.0040f^2	.0042
100	.039 f^2/p^*	.0041f^2	.0039

Suppose that for definiteness we take the figure of 0.1 db/1000 ft to be the lower limit of absorption losses which are important in ordinary field problems. On this basis we see from Table 1 that α_r is <u>always</u> negligible, that α_d is negligible for frequencies less than about 5 kc,

and that at ordinary static pressures the sum ($\alpha_v + \alpha_c$) is negligible for frequencies less than about 1.5 kc.

Since α_r is negligible, the classical absorption coefficient α class, Eq. (11b), at any given temperature can be obtained by adding ($\alpha_v + \alpha_c$) and α_d at that temperature, using values given by Table 1. Fig. 2 shows α_{class} determined in this way, plotted against frequency for three different temperatures, the static pressure being assumed atmospheric.

For frequencies between the abscissal limits of 1 and 10 kc α_{class} may be read directly from the graph. Also for frequencies outside the latter range the same graph may be readily used, by virtue of the fact that α_{class} is (omitting α_r) proportional to the square of the frequency. Thus suppose a given frequency f is written in the form

$$f = 10^n f^* , \tag{17}$$

where f^* is a number between 1 and 10, and n is an integer. The actual frequency f is thus 10^n times the reference frequency f^*, and the classical absorption coefficient for f is just 10^{2n} times that which would obtain for a frequency f^*. For a frequency of f^* in kc the value of α_{class} may be read directly from the graph in Fig. 2; the latter value is then only to be multiplied by 10^{2n} to yield α_{class} for the given frequency f. For example, the frequency 730 kc may be written as (7.3×10^2) kc. For 7.3 kc α_{class} is 2.1 db/1000 ft at 0°C. Hence for 730 kc at 0°C, α_{class} is 2.1×10^4 db/1000 ft.

If the classical absorption coefficient is to be calculated at pressures other than atmospheric, Table 1 may be used. (This may, of course, be done in any case.) As shown there α_v and α_c vary inversely with the pressure, while α_d is pressure-independent, except insofar as the constants (other than ρ_o) appearing in Eqs. (12 - 14) vary slightly with pressure.

1.2.3 Molecular absorption[2]

Referring back to Eqs. (11) we now consider the second contribution to α, namely, the molecular absorption coefficient α_{mol}. In air the absorption given by α_{mol} is due to the finite rate at which energy is imparted to and from internal vibrations of oxygen molecules when a disturbance, such as a sound wave, passes through air. This time for interchange is strongly influenced by the presence of water molecules - hence the importance of humidity in connection with this last mechanism. Kneser's expression for α_{mol} may be written

$$\alpha_{mol} = \frac{\pi f}{c} \cdot \frac{RC_i}{C_v(C_v + R)} \cdot \frac{f\, f_m}{f_m^2 + f^2} \tag{18}$$

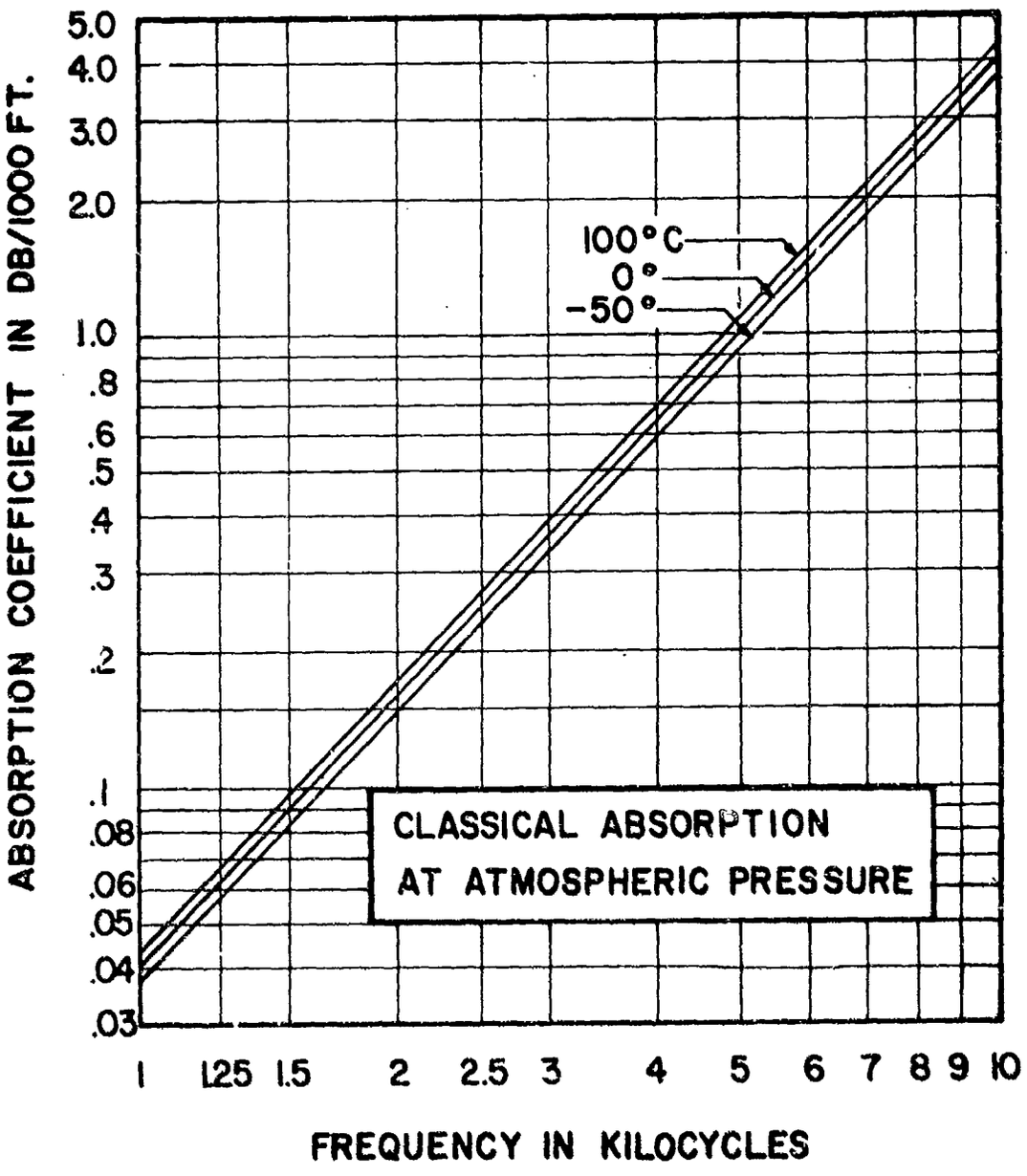

Fig. 2. Classical absorption coefficient α_{class} in air at -50°, 0° and 100°C for frequencies between 1 and 10 kc. This graph may also be used conveniently for determination of α_{class} at any frequency f outside the indicated range by carrying out the following steps (see accompanying Text):

(1) Write $f = 10^n f^*$, where f is in kc, n is an integer and $1 < f^* < 10$;

(2) Determine α_{class} for a frequency f^* (in kc) from the graph;

(3) Multiply the result of Step (2) by 10^{2n}.

where the symbols have the following meanings:

f : sound frequency (cps)

c : phase velocity of sound (cm sec^{-1})

R : molar gas constant $(cal)(mole)^{-1}(^{o}C)^{-1}$

C_v : total heat capacity per mole of air at constant volume $(cal)(mole)^{-1}(^{o}C)^{-1}$

f_m : equal to $(k/2\pi)$, where k is Kneser's rate constant

C_i : vibrational heat capacity per mole $(cal)(mole)^{-1}(^{o}C)^{-1}$

Kneser obtained C_i from spectroscopic data on energy levels in oxygen molecules by using the expression

$$C_i = \frac{E^2}{RT^2} \cdot \frac{e^{-E/RT}}{(1-e^{-E/RT})} \tag{19}$$

in which T is absolute temperature and E the vibrational energy (calories per mole) for the internal oxygen mode involved.

The quantity f_m varies with humidity. According to an empirical formula by Kneser we have

$$f_m = 1.01 \times 10^3 h^2, \tag{20}$$

where f is in cycles per second and h is in grams per cubic meter. (Several different kinds of units for specifying h are in common use; conversion tables and formulae are given in Appendix II.) However, as will be shown later, data by various workers are not in complete agreement and the correct relation between f_m and h is not accurately known. For ease in interpretation and in application to field problems, we recast Eq. (18) in a reduced form and convert units of α_{mol} from nepers per centimeter to decibels per thousand feet, obtaining a quantity w given by

$$w = \frac{\alpha_{mol}}{\alpha_{max}} = \frac{2x}{1 + x^2} \tag{21a}$$

where

$$\alpha_{max} = 264{,}500 \; \frac{\pi f}{2c} \; \frac{RC_i}{C_v(C_v + R)} \tag{21b}$$

$$x = (f_m/f). \tag{21c}$$

From Eq. (21b) we see that α_{max} is proportional to f. The proportionality constant depends mainly on temperature, being nearly independent of ordinary variations in pressure or humidity. Values of α_{max} computed from Eq. (21b) and from tables in Appendix I are plotted versus frequency for various temperatures in Section III, Fig. 41. A plot of selected values, for 20°C only, is given by the straight line in Fig. 3.

The ratio $w = (\alpha_{mol}/\alpha_{max})$ depends only on $x = (f_m/f)$, and f_m, in turn, depends mainly on absolute humidity. When x = o, w = o; as x increases, w rises to a maximum value of unity when x = 1, then falls to zero as x approaches infinity. The value of w for any given x is the same as that for its reciprocal (1/x). We wish to express the ratio w in terms of the humidity h. Let us define a frequency-dependent quantity h_m; the latter gives, for any frequency f, the humidity for which α_{mol} is maximum (i.e., equal to α_{max}) at that frequency. From Eq. (20) we have

$$f = 1.01 \times 10^3 \, h_m^2 \; ; \tag{22}$$

taking the ratio of f_m to f we thus obtain

$$x = (h/h_m)^2. \tag{23}$$

Substituting the above into Eq. (21a) we obtain

$$w = \frac{2(h/h_m)^2}{1 + (h/h_m)^4} \tag{24}$$

A plot of Eq. (22) is given by the curve in Fig. 4; the function given by Eq. (24) is given by the curve in both of Figs. 5 and 6.

One may calculate α_{mol} at 20°C for a given frequency and absolute humidity h by proceeding as follows:

(1) Obtain α_{max} from Fig. 3;

(2) Obtain h_m from Eq. (22); form the ratio h_m/h;

(3) Using the value of (h_m/h) from Step 2, obtain $w = (\alpha_{mol}/\alpha_{max})$ from Eq. (24) or from the curve of Fig. 5 or 6;

(4) Multiply the results of Steps 1 and 3 to obtain $\alpha_{mol} = w \; \alpha_{max}$.

In Section III additional graphs and other aids are given to expedite calculations of α_{mol}.

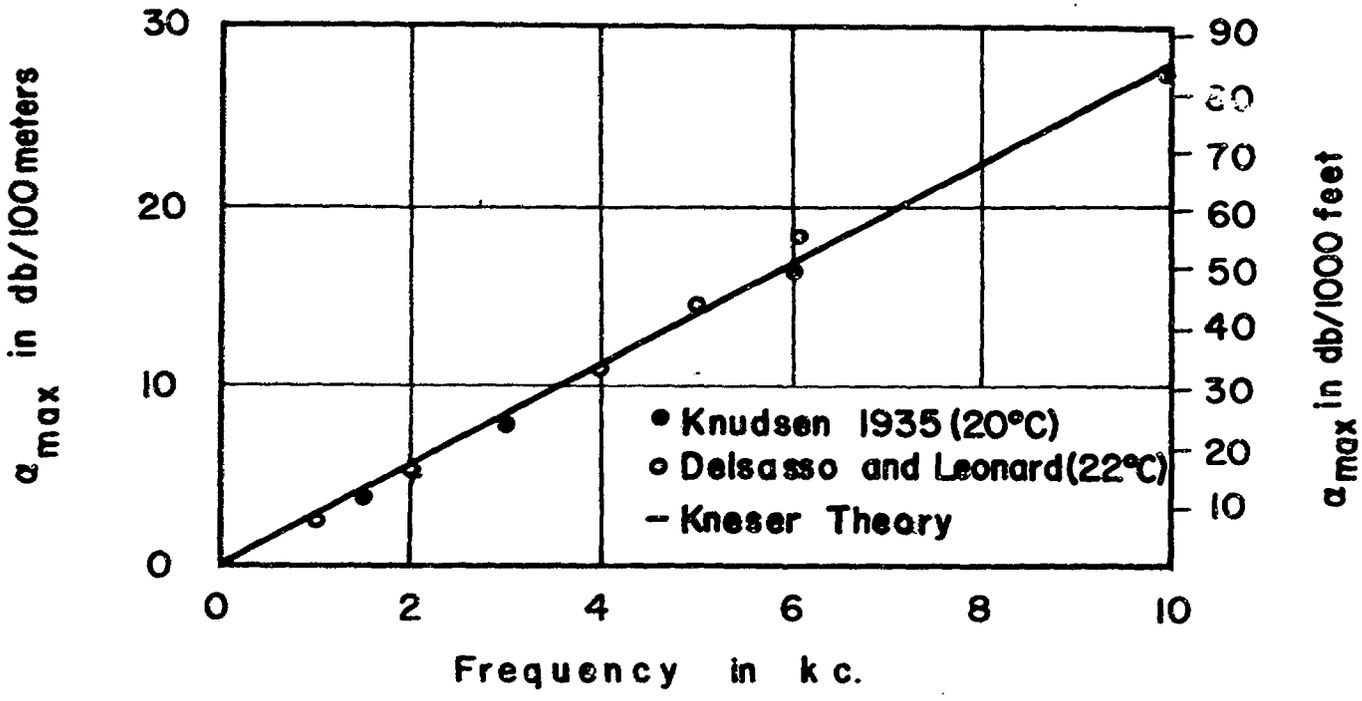

Fig. 3 Solid curve gives α_{max} versus frequency at 20°C from Kneser theory (Eq. 21b). Experimental points give α'_{max}, the peak laboratory value of α at each frequency minus the corresponding value of α_{class}.

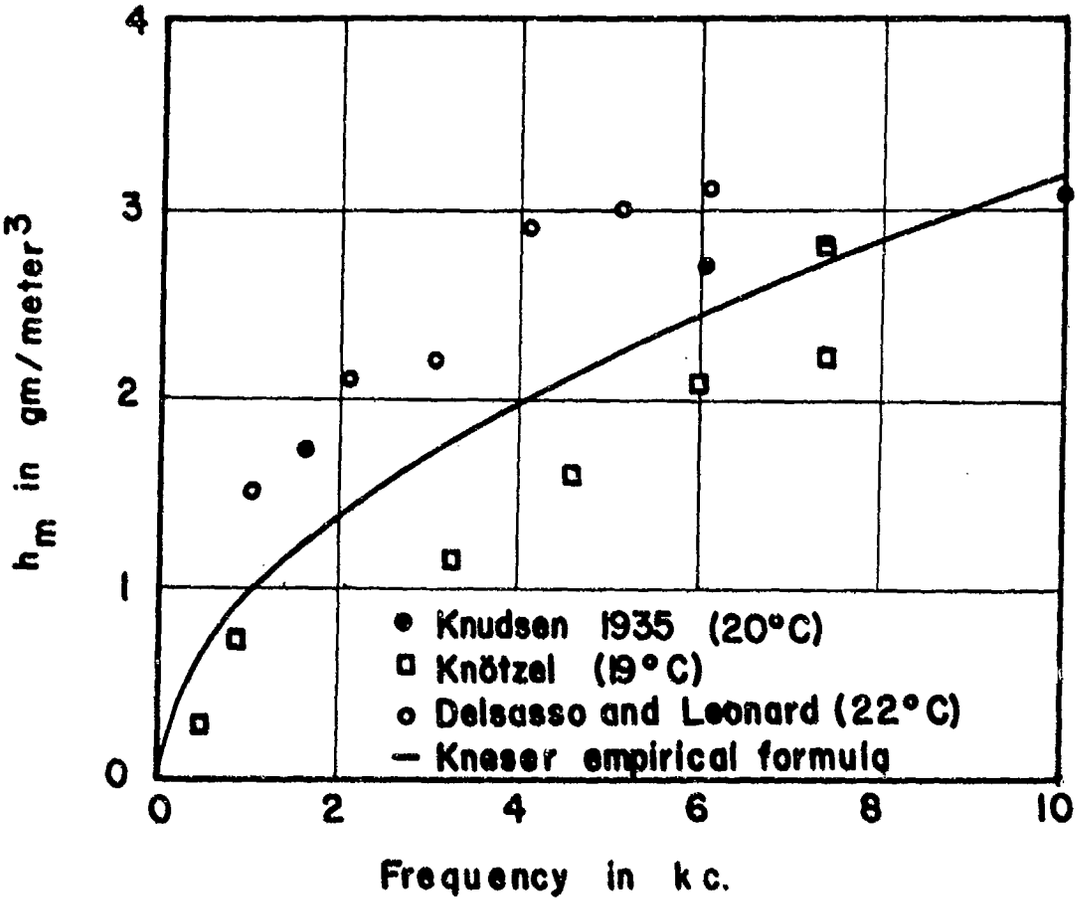

Fig. 4. Solid curve gives h_m versus frequency from Eq. (22). Experimental points give humidities at which peak absorption occurs in laboratory measurements, for various values of the frequency.

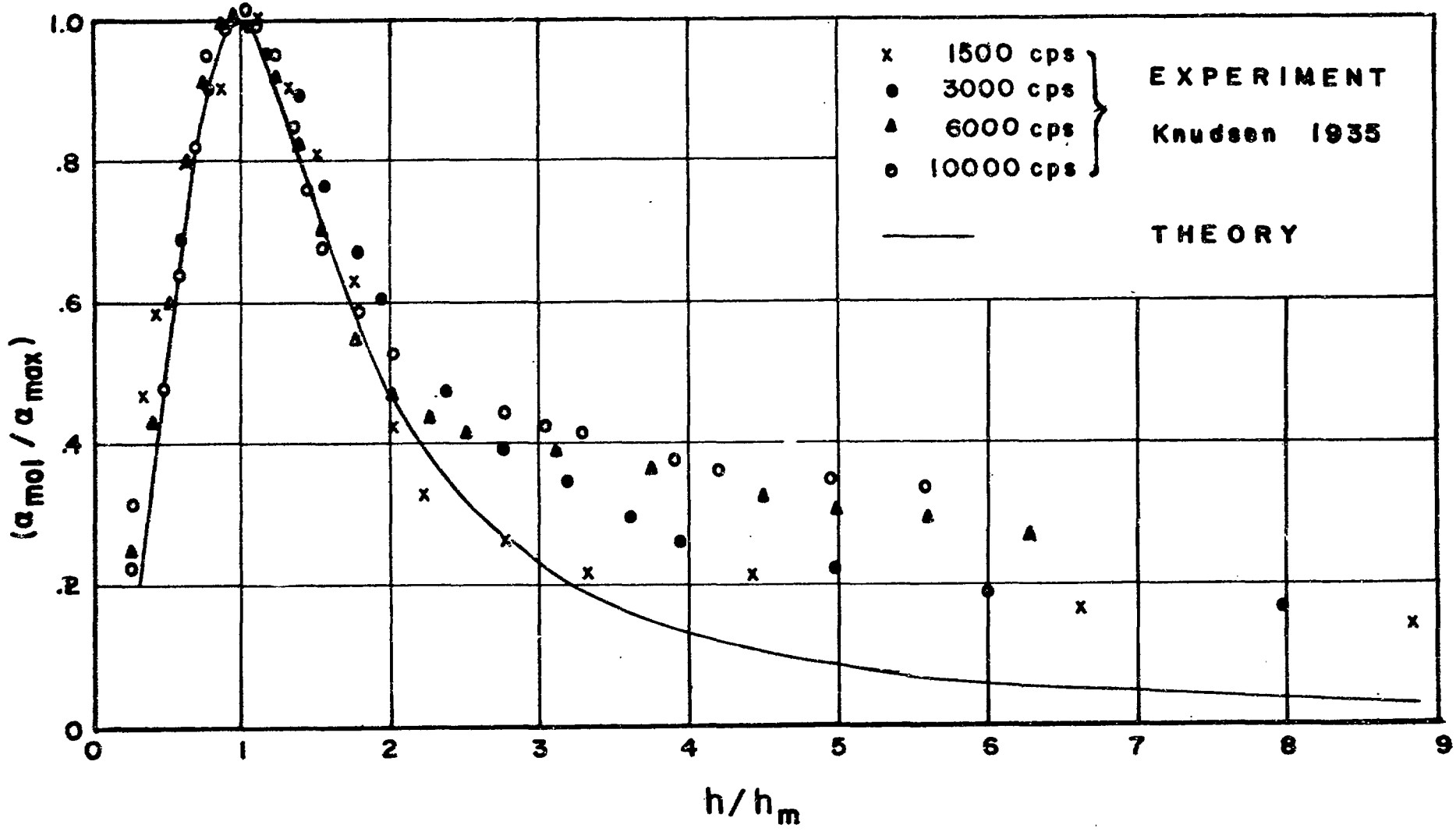

Fig. 5. Solid curve shows $w = (a_{mol}/a_{max})$ plotted against (h/h_m) from Eq. (24). Experimental points give values of (a'/a'_{max}) for various values of (h/h_m), derived from Knudsen's data[3,4] (see Text).

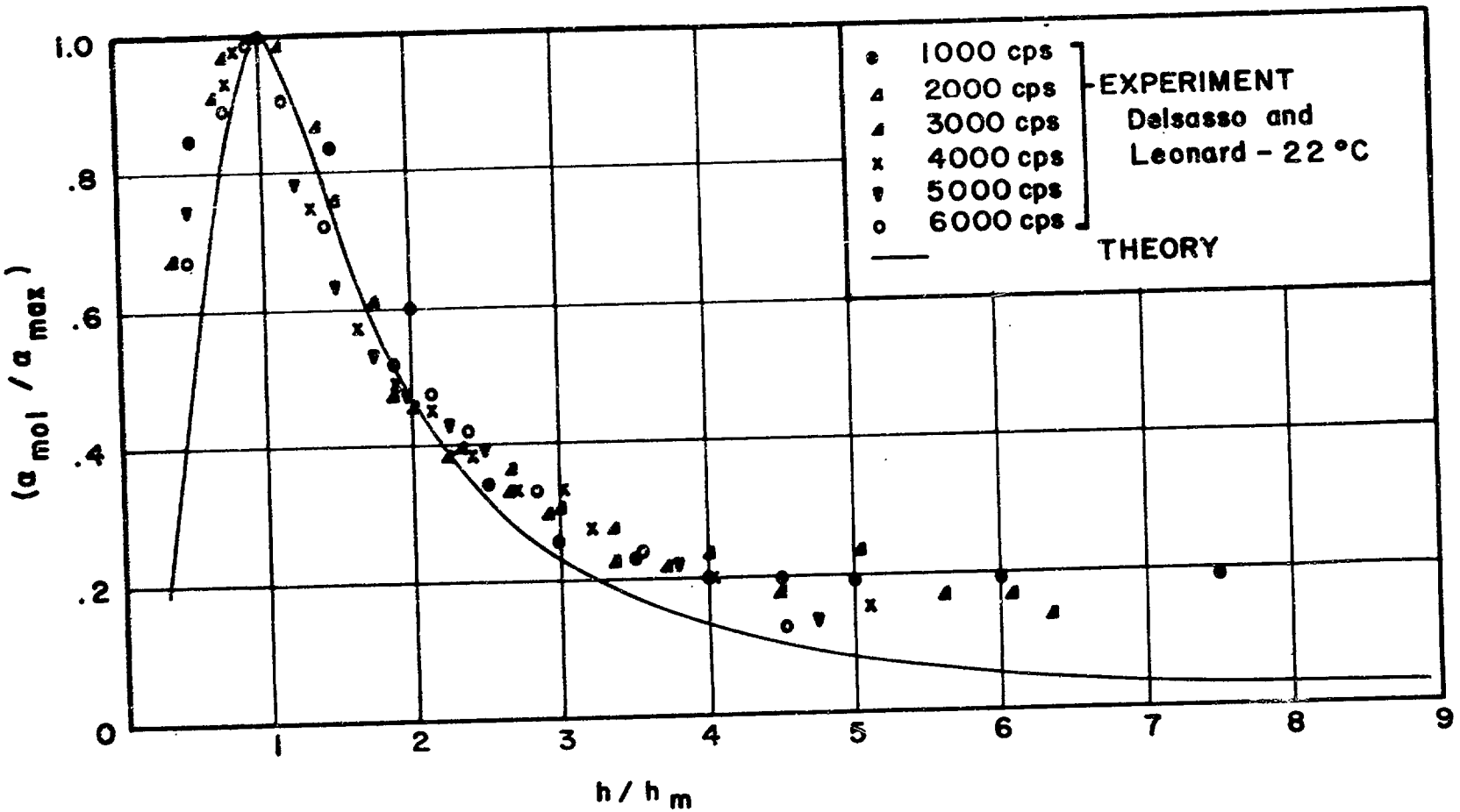

Fig. 6 Solid curve shows $w = (a_{mol}/a_{max})$ plotted against (h/h_m), from Eq. (24). Experimental points give values of (a'/a'_{max}) for various values of (h/h_m), derived from the data of Delsasso and Leonard[6] (see Text).

1.2.4 Laboratory Results[3-10]

The total absorption coefficient α for any specified conditions, as given by Eqs. (11), etc., would be obtained by adding the values of α_{class} and α_{mol}, the latter being calculated by methods described in Sections 1.2.2 and 1.2.3, respectively. These theoretical values may be compared with the results of experimental determinations of α. The laboratory value of α may be defined as the total exponential loss (see Section 1.1.3) per unit distance. In the case of experiments where spherical wave propagation is studied, the experimentally-determined α may equally well be defined as the constant to be used in Eq. (2) in order to fit the latter equation to the observed sound field. When plane wave propagation is used the experimental α may be defined analogously as the constant such that the sound field is fitted by the equation: $p = A \exp(-\alpha x)$.

Measurements of α have been made in laboratory air over a wide range of conditions and with a variety of techniques. Investigators have used frequencies ranging from 1 to 2000 kc and have made determinations in the air for absolute humidities up to about 20 gm/m^3, temperatures ranging from 0° to 55°C and pressures down to 0.002 atmospheres. Under some conditions the observed attenuation agrees rather closely with the α predicted by Eqs. (11). Under most conditions the former is in excess of the theoretical α; this excess varies from a few percent up to a factor of five or more.

The situation is summarized in Fig. 7 for air at atmospheric pressure and at temperatures around 20°C. In the graph, absolute humidity is plotted along the horizontal and frequency along the vertical axis. The entry at any given humidity and frequency gives the ratio of the observed to the theoretical absorption coefficient for these conditions, as found by the experimenters indicated. For example, at a humidity of 12 gm/m^3 and a frequency of 21 kc Rothenberg and Pielemeier[7] measured the absorption coefficient α in air and found it to be about 1.8 times the theoretical value given by $(\alpha_{class} + \alpha_{mol})$.

At the highest frequencies represented in Fig. 7 the absorption is due mainly to α_{class}, and at the lowest frequencies mainly to α_{mol}. By extrapolating from Figs. 2 and 3 one finds that at 20°C the cross-over frequency, where α_{class} just equals α_{max}, is 210 kc. For all frequencies above 210 kc α_{class} is therefore necessarily greater than α_{mol}. For lower frequencies, either term might predominate depending on the humidity; for humidity conditions usually encountered α_{mol} is greater than α_{class} for frequencies less than 10 kc.

In Fig. 7 we see that the observed absorption is rarely, if ever, less than the theoretical value. (Due to experimental errors the fact that a few ratios less than unity do appear may not be significant.) We

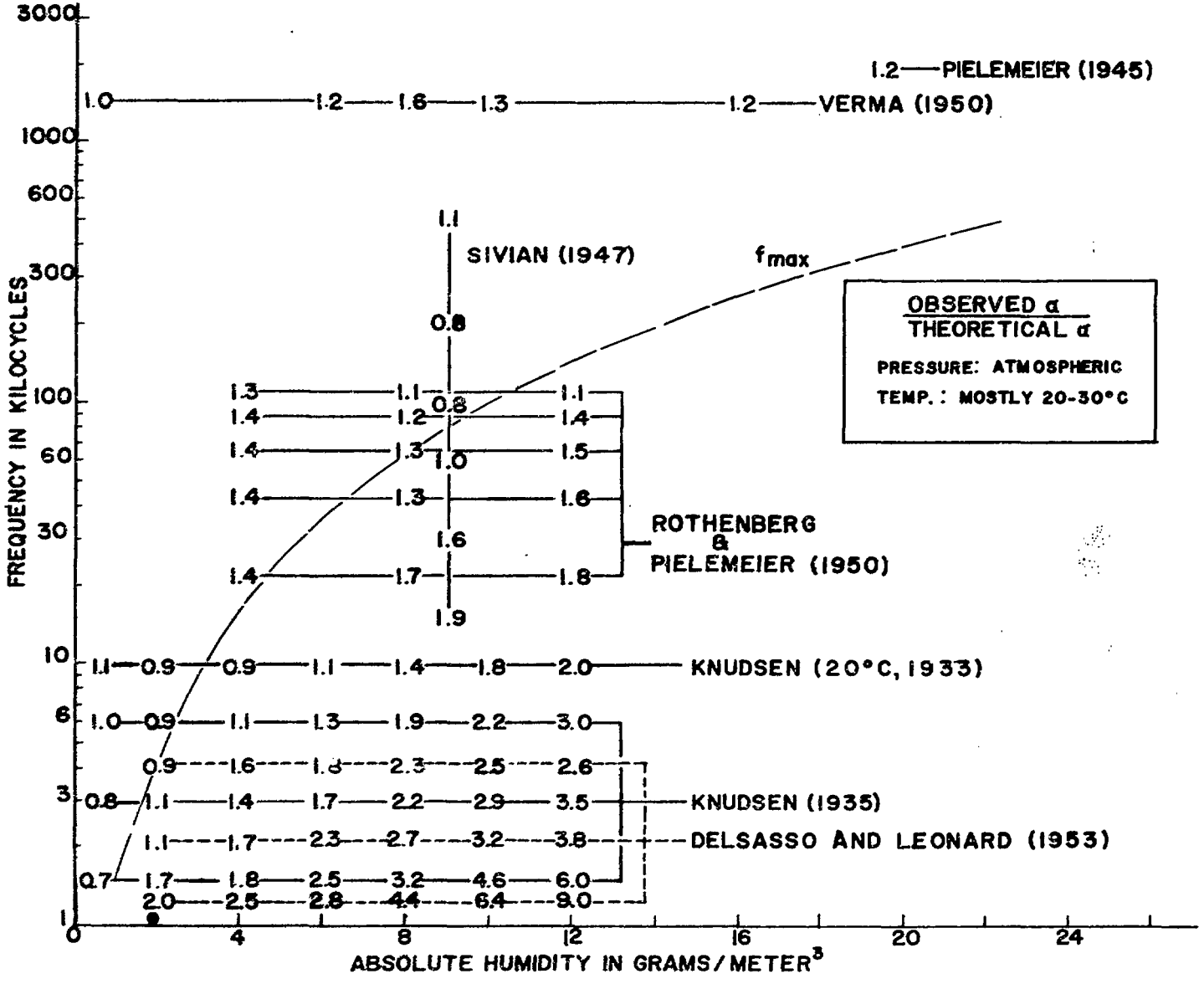

Fig. 7. Comparison between theory and experiment for absorption coefficients in air. Each entry gives the ratio between the observed value of α and the corresponding theoretical value from Eqs. (11), etc. The dashed curve is a plot of f_m versus h from Eq. (20).

also see that the agreement is comparatively good at the higher frequencies; for frequencies above 50 kc most of the indicated ratios are less than 1.5. Agreement is also good in the vicinity of the dashed curve; the latter gives the frequency for maximum molecular absorption as a function of humidity, from Eq. (20). Agreement is generally poor at frequencies of 10 kc or less when the humidity is greater than about 6 gm/m^3.

Because our main interest here is in frequencies below 10 kc, we shall now turn our attention to more detailed consideration of measurements in this range. According to theory the absorption under these conditions should be given mainly by α_{mol}. The most recent laboratory data for the audible range of frequencies are those of Delsasso and Leonard[6]. The latter present experimental plots of α versus h obtained by measuring sound decay in air at atmospheric pressure, at six frequencies and at three different temperatures. (Data are also given for air at pressures less than atmospheric, but these will not be discussed here.) The α vs h plots exhibit peaks or tendencies toward peaks, as the theory for α_{mol} shows they should.

The values h_m of the humidity at which the peaks occur at different frequencies are plotted as open circles in Fig. 4. These h_m-values tend to be appreciably higher than those given by the solid curve, the latter being plotted from Eq. (22). For comparison, the filled circles represent h_m-values obtained from similar data by Knudsen[3,4], and the triangles h_m-values found by Knötzel[5] to be consistent with his data. Pertinent here also, though beyond the scope of Fig. 4, are the results of Rothenberg and Pielemeier[7]. Using frequencies from 22 to 110 kc and pressures down to several cm of Hg, they found their results consistent with the assumption that h_m is given by Kneser's empirical formula, Eq. (22).

It is evident that uncertainty exists as to the humidity value for which maximum absorption occurs at any given frequency. In future work thought should be given to means of reducing this uncertainty. Present theory is of no help on this point. A basic theory for accurately predicting h_{max} from basic molecular considerations would require much more precise knowledge of the mechanism of molecular collisions than is now available.

The situation is otherwise with respect to the actual heights of absorption maxima. Theory for predicting α_{max} is well developed; Eq. (21b) gives α_{max} in terms of rather well-known thermodynamic and spectroscopic constants. Also experimental values of α_{max} (corrected for the small contribution of α_{class}) agree well with each other and with the theory. In Fig. 3 the solid line is plotted from Eq. (21b) for 20°C; the filled circles are from Knudsen[3,4], while the open circles

are from Delsasso and Leonard[6]; the agreement is excellent.

Having examined the present state of knowledge regarding h_m and α_{max} we now consider the overall dependence of α on h. In comparing experiment with theory it will be convenient to speak of a quantity $\alpha' = (\alpha - \alpha_{class})$ where, as before, α is the laboratory value of the absorption coefficient (i.e., α is the total exponential attenuation per unit distance). We shall also refer to a quantity $w' = (\alpha'/\alpha'_{max})$ which gives the ratio of α' at a given humidity and frequency to the maximum value (α'_{max}) of α' at that frequency. If the laboratory value of α is just equal to the theoretical value (Eqs. (11)) the quantity α' will be just equal to α_{mol}; also w' will then equal w and will be given by Eq. (24).

The solid curves in Figs. 5 and 6 are identical plots of $(\alpha_{mol}/\alpha_{max})$ versus (h/h_m), based on Eq. (24). The plotted points in Fig. 5 give w' values and are from Knudsen's experimentally obtained plots of α versus h for various frequencies. Reduction of data for plotting at any given frequency, was accomplished by (1) dividing each α'-value by the peak value α'_{max} for that frequency, and (2) dividing each h-value by that particular humidity value h_m for which the peak occurs. The points in Fig. 6 are the data of Delsasso and Leonard, reduced in the same way. We note that the fit is fairly good near the peak, i.e., for abscissal values ranging from 0.5 to 2. However, at higher (h/h_m) ratios the observed absorption exceeds that predicted by Eq. (24), frequently by factors of two or three. It is not presently known how to account for this discrepancy.

In summary, theory for α_{mol} agrees with laboratory measurements of α' in some respects, not in others. Absorption peaks do occur whose heights are predicted rather accurately by Eq. (21b). However, it is not known with certainty at what humidity the absorption will be maximum at any given frequency. At the higher humidities absorption coefficients obtained experimentally greatly exceed those predicted.

1.3 LOSS COEFFICIENTS IN FOG AND SMOKE

1.3.1 Introduction

Information is available from both theory and experiment relative to acoustic losses due to propagation through fog. In our discussion of present knowledge of this subject, the idealized situation assumed is that of an infinite ocean of air, free of boundaries, in

which exists a uniform distribution of water droplets. The sound field is assumed to have either spherical symmetry, in which case Eq. (2) holds, or plane symmetry, in which case the pressure amplitude along the direction of propagation varies as $\exp(-\alpha x)$. The quantity of interest in either case is the loss coefficient α.

We shall suppose in the following discussion that the actually observed α, i.e., the total exponential loss per unit distance in air containing fog droplets or other suspended matter is the sum of two contributions, namely,

$$\alpha = \alpha_{hom} + \alpha_{susp} . \tag{25}$$

Here α_{hom} represents the loss coefficient in homogeneous air, free of liquid or solid particles; it is this contribution which was discussed in subsection 1.2. The second contribution α_{susp} represents the additional loss per unit distance due to the suspended matter.

According to available theory for acoustic losses due to liquid droplets we may, in turn, represent α_{susp} as due to two rather different mechanisms. One of these has to do with viscous dissipation and heat conduction which takes place near droplets (or suspended particles of any kind) in a sound field. Theory for this process has recently been made available by Epstein and Carhart[11]. The other loss mechanism is a relaxation process which takes place when sound passes through air in which liquid droplets are suspended. The relaxation results from a time lag which exists between the water vapor density in the vicinity of individual droplets and that in the surrounding air, during the cyclic pressure variations of a sound field. Theory for the attenuation due to the latter effects was given by Oswatitsch[12]; Wei[13] has recently examined the Oswatitsch theory critically and suggested modifications.

In the following subsection we give the Epstein-Carhart expressions for α_{vh}, the loss coefficient due to viscosity and heat conduction. In subsection 1.3.3 the Oswatitsch-Wei results are given for the loss coefficient α_e due to relaxation effects. Certain available laboratory results on transmission losses due to fog are then described (subsection 1.3.4) and finally, brief consideration is given to the subject of acoustic losses in aerosols (subsection 1.3.5).

1.3.2 From the Epstein-Carhart theory we have for the loss coefficient, in db/1000 ft.,

$$\alpha_{vh} = (264,500) \cdot \frac{\pi n \xi}{c} \left[3\nu Y_\eta + 2(\gamma-1)\sigma Y_\tau \right] \tag{26}$$

In Eq. (26) Y_η is a function of z and Y_τ a function of y, where z and

y are defined below. In Fig. (8) plots are given of Y_η (z) and Y_τ (y) as functions of their arguments. (In the graphs x represents z for the Y_η plot and y for the Y_τ plot.) All other symbols in Eq. (26) are defined below.

n = number of droplets per unit volume

ξ = radius of droplets

ρ = density of air

c = normal velocity of sound (in homogeneous air)

η = shear viscosity coefficient for air

γ = ratio of specific heats for air

K = thermal conductivity coefficient for air

c_p = specific heat of air at constant pressure

$y/\xi = (\omega/2\sigma)^{1/2}$

$z/\xi = (\omega/2\nu)^{1/2}$

$\sigma = K/\rho c_p$

$\nu = \eta/\rho$

Eq. (26) is subject to the restrictions that the radius ξ of each droplet be small with respect to λ, the wavelength of sound, and that neighboring droplets be sufficiently far apart.

Using constants for air at 20°C (see Tables in Appendix I), Eq. (26) becomes

$$\alpha_{vh} = 24.2n\xi \left[0.453\, Y_\eta (z) + 0.157\, Y_\tau (y) \right] \qquad (27)$$

where

$$y = 4.00\, \xi\, f^{1/2}$$

$$z = 4.56\, \xi\, f^{1/2}$$

In the above equation n is the number of droplets per cm^3 of radius ξ (in cm) and f is the frequency in cycles per second. In actual fogs the droplets are not uniform in size; suppose, however, the distribution can be divided into groups such that n_1 droplets per unit volume are approxi-

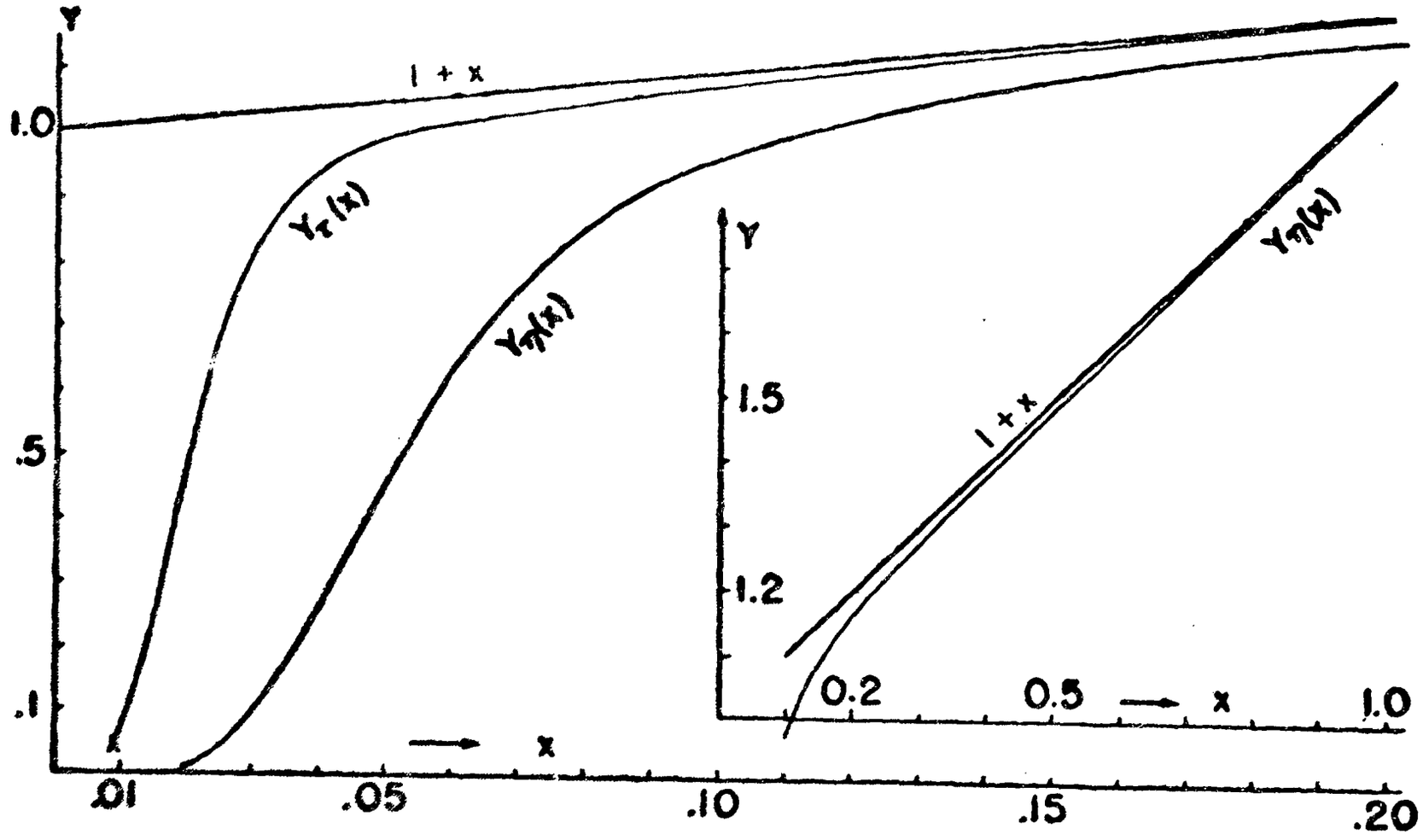

Fig. 8. (From Epstein and Carhart). Plots of the quantities Y_τ and Y_η in the Epstein-Carhart theory, Eq. (26) against dimensionless parameters. In the plot of Y_η (x) against its argument, x represents $z = \xi(\omega/2\nu)^{1/2}$; in the plot of Y_τ (x) the argument x represents $y = \xi(\omega/2\sigma)^{1/2}$. See Text.

mately of radius ξ_1, n_2 of radius ξ_2, etc. One may then determine α_{vh} for each of these groups separately from Eq. (26) or (27) and, finally, add the group-values to obtain the resultant value of α_{vh} for the distribution.

1.3.3 Theory of Oswatitsch, and modifications by Wei

Theoretical expressions for the loss coefficient α_e, due to evaporation processes, are rather involved. Wei's results[13] are particularly so; his general expression takes into account relative motion between droplets and the surrounding air and thus contains terms involving the dimensionless quantity $(\xi^2\omega/\nu)$, where ξ, ω and ν, as before, represent the droplet radius, angular frequency and kinematic viscosity, respectively. For typical fog droplet sizes and for frequencies of the order of 100 cps or less we find that $(\xi^2\omega/\nu) \ll 1$ and terms involving this quantity may be dropped from Wei's expression. The remainder of Wei's expression has nearly the same formal appearance as that of Oswatitsch[12]. We give below the results of Oswatitsch with certain modifications by Wei.

The coefficient α_e is written below in terms of a sequence of intermediate quantities which are ultimately expressed in terms of ordinary physical constants. Thus we have, in nepers per cm,

$$\alpha_e = \frac{\omega}{2w'} \frac{(1 - \frac{w_o^2}{c^2})(\frac{\omega}{\omega'})^2}{\left[1 - (\frac{\omega}{\omega'})^2 g'_{30}\right]^2 - \left[1 - \frac{w_o^2}{c^2}\right]\left[1 - (\frac{\omega}{\omega'})^2 g'_{30}\right] + (\frac{\omega}{\omega'})^2} \tag{28}$$

where w', g'_{30}, w_o and ω' are given in terms of new variables, as follows:

$$\left[\frac{w'}{c}\right]^2 = 1 - \frac{\left[1 - \frac{w_o^2}{c^2}\right]\left[1 - (\frac{\omega}{\omega'})^2 g'_{30}\right]}{\left[1 - (\frac{\omega}{\omega'})^2 g'_{30}\right]^2 + (\frac{\omega}{\omega'})^2} \tag{29}$$

$$\frac{g_{30}'}{g_{30}} = \frac{\left[1 + \gamma(\lambda_s - \lambda_f)\right]}{\left[1 + \lambda_s\lambda_d - \lambda_f\lambda_d\right]^2} \cdot \frac{c_3}{c_p} \cdot \lambda_d \tag{30}$$

$$\frac{w_o^2}{c^2} = \frac{1 + \lambda_s - \lambda_f}{1 + \gamma(\lambda_s - \lambda_f)} \tag{31}$$

$$\frac{\omega'}{\omega^*} = \frac{1 + \gamma(\lambda_s - \lambda_f)}{1 + \lambda_s \lambda_d - \lambda_f \lambda_d} \tag{32}$$

The expressions in Eqs. (29-32) are given by Wei; in Oswatitsch's result the term ($\lambda_f \lambda_d$) in the denominators of Eqs. (30) and (32), and the term λ_f in the numerator of Eq. (31), do not appear.

The quantities ω^*, λ_f, λ_d and λ_s are defined in terms of standard physical constants as follows:

$$\omega^* = 4\pi Dn\xi \tag{33}$$

$$\lambda_f = \frac{\rho_{20} L}{\rho_o c_p T_o} \tag{34}$$

$$\lambda_d = \rho_o c_p \, D/K \tag{35}$$

$$\lambda_s = \frac{\rho_{20} L}{\rho_o c_p p_{20}} \left(\frac{dp_2}{dT}\right)_o . \tag{36}$$

The remaining symbols have the following meanings:

c	:	phase velocity in the limit of infinite frequency; i.e., velocity in dry air.
w'	:	actual phase velocity
L	:	latent heat of condensation for water
ρ_{20}	:	water vapor density
c_3	:	specific heat of liquid water
c_p	:	specific heat of moist air at constant pressure
c_v	:	specific heat of moist air at constant volume
γ	:	c_p/c_v
n	:	number of droplets per cm^3
D	:	coefficient of diffusion of water vapor through air
K	:	coefficient of thermal conductivity of air
T_o	:	absolute temperature
$\left(\frac{dp_2}{dT}\right)_o$	:	rate of increase of water vapor pressure with temperature

ρ_o : density of moist air in sound-free conditions

g_{30} : ratio of water mass in droplet form, in any given volume, to the air mass in that same volume

p_{20} : vapor pressure

In connection with D and K, Wei notes that for small droplets whose radius is not large compared to the mean free path of air molecules, modified values must be used for these coefficients. Thus Oswatitsch suggests that D be replaced by a quantity equal to D divided by the factor $(1 + \xi_k / \xi)$ where ξ_k is a constant, independent of ξ. On the other hand, Langmuir[14] gives quite a different expression for the quantity to replace D in diffusion equations for small droplets. A theoretical result for a compensated heat conduction coefficient to be used in describing heat conduction from small droplets has been given by Howell[15]. In this report we shall ignore these corrections and assume D and K given by their usual values (see Table 2 and Appendix I).

Calculation of α_e from Eqs. (28) - (36) for a given set of conditions is facilitated by Tables 2, 3 and Fig. 9. These were prepared from charts given by Oswatitsch for his equations, which differ little from Eqs. (28) - (36). Fig. 9 shows plots of the dimensionless absorption constant $(2\alpha_e w'/\omega')$ versus the ratio (ω/ω') at two temperatures and for two values of g'_{30}. The absorption constant has its maximum value in the vicinity of $(\omega/\omega') = 10$ and falls off to zero at both large and small values of this ratio. The peak is a very broad one. For $g'_{30} = 0.05$ the quantity $(2\alpha_e w'/\omega')$ falls to one-half its peak value about when $(\omega/\omega') = 0.9$ at the lower limit and when $(\omega/\omega') = 250$ at the upper limit. For $g'_{30} = 0.10$ the upper limit is reduced to about 110. Use of Fig. 9 requires knowledge of ω' and w'. By Eqs. (29) - (32) these are expressed in terms of the temperature-dependent quantities λ_f, λ_s, λ_d and $(1 - w_o^2/c^2)$, values of which are given in Table 2 for temperatures from -10° to 30°C.

TABLE 2

Temperature-Dependent Quantities in Oswatitsch Theory

T(°C)	D	λ_f	λ_s	λ_D	$1-w_o^2/c^2$	A
-10	.195	.0152	.316	1.108	.075	2.61
-5	.202	.0230	.467	1.125	.096	2.75
0	.209	.0340	.680	1.143	.118	2.88
5	.216	.0474	.916	1.160	.136	2.99
10	.223	.0651	1.235	1.175	.154	3.12
15	.230	.0882	1.632	1.192	.168	3.22
20	.238	.118	2.13	1.212	.179	3.32
25	.246	.157	2.78	1.234	.189	3.40
30	.254	.206	3.56	1.251	.198	3.50

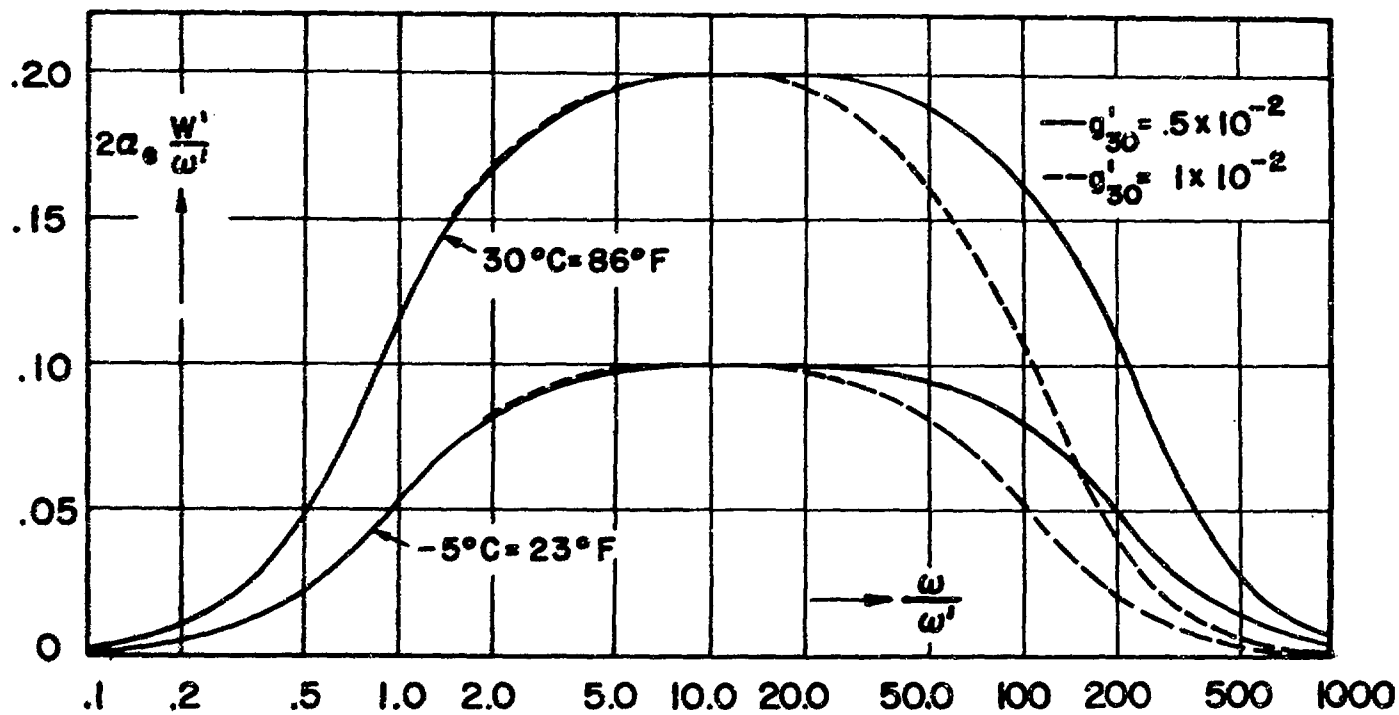

Fig. 9. Dimensionless loss coefficient ($2\alpha_e w'/\omega'$) for fog versus the ratio (ω/ω'). See Text.

The phase velocity w' varies somewhat with both the temperature and the ratio ω/ω', but is practically independent of g'_{30}. In Table 3 values of (w'/c) at 30°C and -5°C, respectively, are given for a series of values of ω/ω'. For temperatures less than 30°C the phase velocity w' in foggy air is always between c and 0.9c. Values of c for different temperatures are given in Appendix I.

TABLE 3

The Sound Velocity in Foggy Air

ω/ω'	0	0.1	0.5	1.0	2.0	10.0	∞
$(w'/c)_{30°}$	0.90	0.90	0.92	0.95	0.98	1.00	1.00
$(w'/c)_{-5°}$	0.95	0.95	0.96	0.98	0.99	1.00	1.00

One may determine ω' for a given fog, consisting of n particles per unit volume of radius ξ at a given temperature by using Eqs. (32) and (33) with values for λ_s, etc. from Tables 2 and 3. More conveniently one may use the equation

$$\omega' = A(T)n\xi^{6}, \tag{37}$$

where the temperature-dependent proportionality constant A is given by

$$A = \frac{1 + \gamma(\lambda_s - \lambda_f)}{1 + \lambda_s \lambda_d - \lambda_f \lambda_d} \cdot 4\pi D, \tag{38}$$

and is tabulated in Table 2.

In summary, one may calculate α_e from Fig. 9 and Tables 2 and 3 by the following procedure:

(1) Determine ω' for given n, ξ and T from Eq. (37) and Table 2.
(2) Form the ratio ω/ω', then find $(2\alpha_e w'/\omega')$ from Fig. 9.
(3) Estimate w' from Table 3 and Appendix I
(4) Determine α_e by multiplying the value of $(2\alpha_e w'/\omega')$ obtained from Fig. 9 in Step 2 by (ω'/w') x 132,200 to obtain units of db/1000 ft.

An example is given in Section III. It should be realized that the Oswatitsch-Wei theory is applicable only to a fog in which the drop-

lets are of uniform radius ξ. Application of the result to actual distributions cannot be done in this case (unlike the Epstein-Carhart case) by dividing the droplet sizes into groups, determining the loss-coefficient separately for each group, then adding these to give the resultant loss coefficient. Further development of the theory is necessary in order to obtain a result which can be applied to a distribution of sizes.

1.3.4 Laboratory Measurements.

Measurements of loss coefficients in artificial fogs have been made by Knudsen, Wilson and Anderson[16], mainly in the 500-8000 cps range, using a reverberation technique. Drop size determinations were made by photographing droplets deposited on an oil-coated glass slide. For one set of measurements the observed droplet distribution, divided into five groups, is given in Table 4 from Epstein and Carhart. The total volume of all drops was 2×10^{-6} cm^3 per cm^3 of air.

TABLE 4

Drop Size Distribution,
for Knudsen, Wilson and Anderson Measurements

Group	Mean Radius	Drops/cm^3
1	3.75×10^{-4}cm	55
2	6.25×10^{-4}	89
3	10.0×10^{-4}	121
4	15.0×10^{-4}	38
5	21.5×10^{-4}	21

Experimental values of α determined by Knudsen, et al for this fog at the various frequencies are given in Table 5 (from Epstein and Carhart). Also shown there are corresponding values of α_{vh}, calculated by Epstein and Carhart from their theory, applied to the distribution given in Table 4.

The Epstein-Carhart coefficient α_{vh}, which represents losses due to viscosity and heat conduction, is sufficient to describe the experimental results given here fairly well at about 500-1000 cps, but is too small at higher frequencies.

At frequencies less than 500 cps the viscosity and heat conduction processes treated by Epstein and Carhart plays a reduced role and

TABLE 5

Loss Coefficients in Artificial Fog

Frequency	α (Experiment)	α_{vh} (Theory)
500 cps	4.3 db/1000 ft.	4.4 db/1000 ft.
1000	6.1	5.0
2000	8.2	5.5
4000	8.8	6.1
6000	10.7	6.5
8000	11.6	6.7

the evaporation mechanics considered by Oswatitsch and Wei apparently becomes the predominant one. Knudsen, et al[16], also made preliminary measurements of the loss coefficient α in fog at lower frequencies, namely, from 27.5 to 350 cps; in this range their measured losses were considerably in excess of those given by α_{vh}.

More recently Wei[13] has made measurements in the 30 - 100 cps range using an impedance tube method. In one of the artificial fogs he investigated there were 5.4×10^3 droplets/cm^3 of average radius 6.6×10^{-4}cm; the ratio of water mass (in droplet form) to air mass was 6.05×10^{-3}. The results are given below in Table 6.

TABLE 6

Measured and Calculated Loss Coefficients in Fog

Frequency	α (Experimental)	α_{visc} (Theoretical)	α_e (Theoretical)
30	7.3 db/1000 ft.	0.2 db/1000 ft.	5.9 db/1000 ft.
35	7.4	0.3	
40	7.8	0.3	5.7
45	7.5	0.4	
50	7.3	0.4	5.5
55	7.3	0.5	
60	6.6	0.5	5.4
65	6.5	0.7	
70	6.5	0.9	5.3
75	6.9	1.1	
80	7.4	1.3	5.1
85	7.3	1.6	
90	7.4	1.8	4.9
95	7.4	2.5	
100	7.5	2.9	4.7

As seen in Table 6, measured values of α are practically independent of frequency, averaging about 7 db/1000 ft over the frequency range given for this (rather heavy) artificial fog.

Shown for comparison is α_{visc}, the calculated coefficient due to viscosity alone, obtained from α_{vh} by letting ν, and therefore Y_τ, equal zero. (The complete Epstein-Carhart theory was not available when Wei made his measurements.) Though negligible at 30 cps, the viscous losses increase rapidly with frequency and account for about one-third of the total exponential loss at 100 cps. Also shown in Table 6 is α_e, the coefficient due to evaporation processes, calculated from Eqs. (28) - (36). (Wei does not explain in detail how theory is applied when, as here, droplets are not uniform in size. See discussion in subsection 1.3.3.) Evidently α_e accounts for most of the observed losses, being far greater than α_{visc} in the 30 cps region, and being about twice as great as α_{visc} in the 100 cps region.

1.3.5 Smoke and dust.

An equivalent analysis to that of Epstein and Carhart for fluid spheres in air has not yet been made available for small solid bodies. in air. However, upon examination one finds that α_{vh}, given by Eq. (26), does not depend significantly on the viscous or elastic properties of the inner medium of the tiny spheres, but only on the corresponding density and heat conductivity. It might therefore be argued that results for rigid spheres would not differ greatly from those, given by Eq. (26), for liquid spheres of equivalent density and heat conductivity. To the extent to which this is true Eq. (26) may be applied to smoke or dust composed of solid spheres. It is not obvious, however, that Eq. (26) (or any theory derived for spherical scatterers) would apply to dusts composed of rough irregularly-shaped particles, as is commonly the case. Viscous losses near rough surfaces are probably much different from those occurring at smooth boundaries.

1.4 SOUND PROPAGATION OVER A PLANE EARTH

1.4.1 Introduction

The propagation of sound through a homogeneous, isotropic atmosphere from a point source above the ground is strongly dependent upon the acoustical characteristics assumed for the ground. Irregularities of the surface (of a size of the order of the sound wavelength or larger), ground type (sand, hard-packed earth, etc.) and ground cover (bare ground,

grass, etc.) all play a role in the determination of the intensity of sound at a distance from the source.

Expressions have been developed for the pressure from a point source above a plane earth for the case[17] in which the earth may be assumed a homogeneous, isotropic "fluid" medium (i.e., no shear effects are taken into account), and for the case[18, 19] in which the earth is acoustically representable by a normal-impedance boundary condition.

The problem of a dipole source above a non-uniform surface[20, 21] has been investigated for the case of electromagnetic waves; however, the corresponding analysis for acoustic waves has not been developed.

When there is no preferred direction at the surface of the ground, or in the ground itself, the "fluid" medium assumption should be valid; this condition has been found to be an adequate representation for sand[22]. However, when the lower medium is porous, and so constituted that air in the pores moves more readily in the vertical than in any other direction, the normal impedance boundary condition should hold. In practice this situation might be approached if the earth were covered by long, vertical-stemmed vegetation, such as meadow grass, and if this vegetation were so dense as to essentially constitute the "lower medium", the ground itself then having no effect on the sound field.

Let us consider a point source of sound, having a harmonic time dependence (sound pressure varying as $\exp(-i\omega t)$, at the point $(0,0,z_o)$, and a receiver at (x,y,z); see Fig. 10. We shall use the following notation for the fluid boundary condition (Case 1) and the normal-impedance boundary condition (Case 2).

ω = angular frequency of source (Case 1 and 2)

$k_1 = \frac{\omega}{c_1}$ propagation constant for air (Case 1 and 2) (39)

$k_2 = \frac{\omega}{c_2}$ propagation constant for earth (Case 1 and 2) (40)

$R_1 = [x^2 + y^2 + (z - z_o)^2]^{\frac{1}{2}}$ distance from source $(0,0,z_o)$ to receiver (x,y,z) (Case 1 and 2) (41)

$R_2 = [x^2 + y^2 + (z + z_o)^2]^{\frac{1}{2}}$ distance from image point $(0,0,-z_o)$ to receiver (x,y,z) (Case 1 and 2) (42)

ψ = specular reflection angle from horizontal (angle between horizontal and line from image point to receiver) (Case 1 and 2)

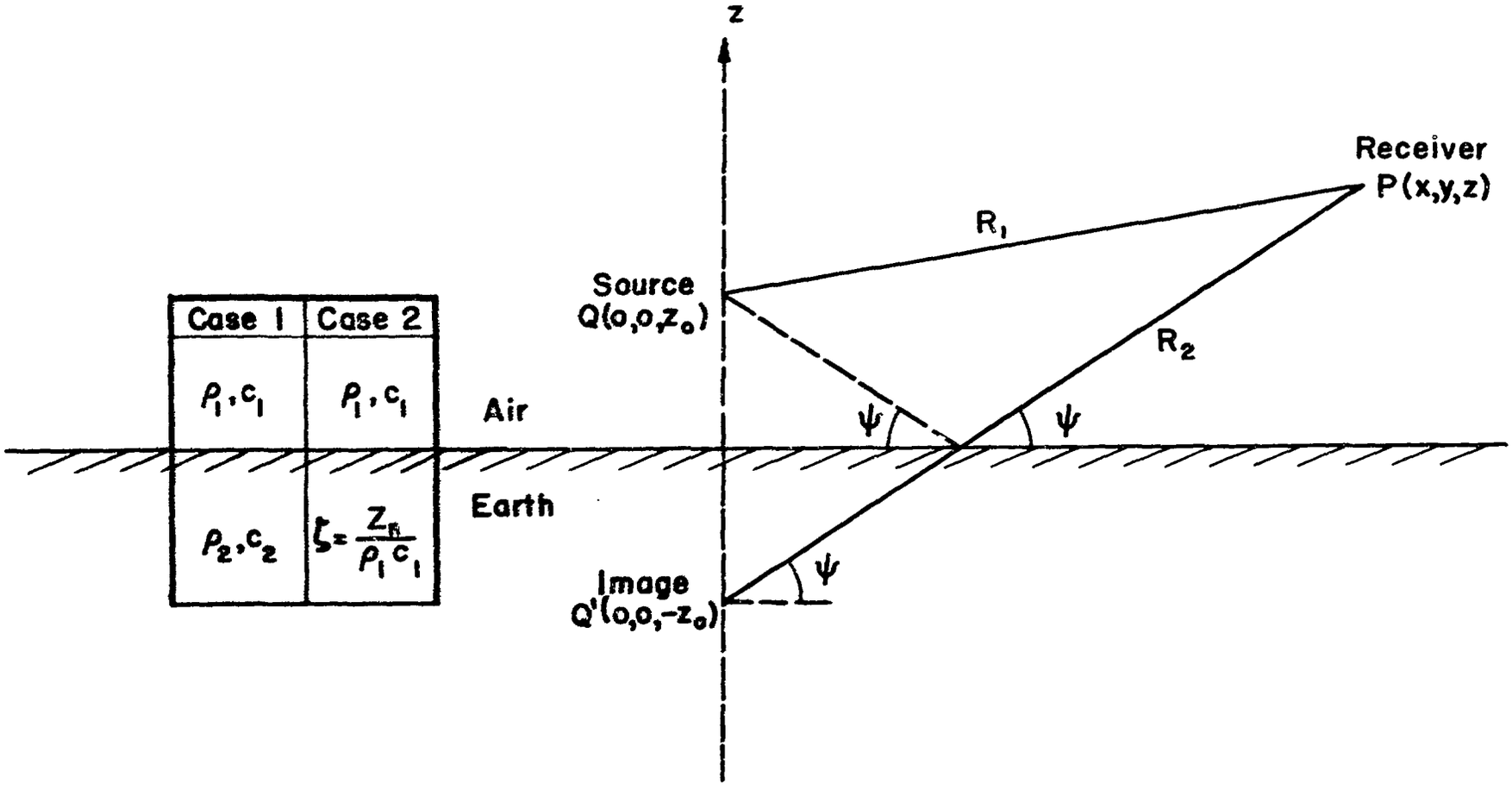

Fig. 10. Geometrical relations for source and receiver above a "fluid" earth (Case 1) or a normal-impedance earth (Case 2).

$$\cos\psi = \frac{(x^2 + y^2)^{\frac{1}{2}}}{R_2} \qquad \sin\psi = \frac{z + z_o}{R_2} \tag{43}$$

$$Z_1 = \rho_1 c_1 = \frac{\omega \rho_1}{k_1} \quad \text{impedance of air (Case 1 and 2)} \tag{44}$$

$$Z_2 = \rho_2 c_2 = \frac{\omega \rho_2}{k_2} \quad \text{impedance of "fluid" earth (Case 1)} \tag{45}$$

$$\zeta = \frac{Z_n}{\rho_1 c_1} \quad \text{specific normal impedance of ground (normal impedance of ground divided by impedance of air) (Case 2)} \tag{46}$$

$$R_p^{(1)} = \frac{Z_2 \sin\psi - Z_1 \left[1-(k_1/k_2)^2 \cos^2\psi\right]^{\frac{1}{2}}}{Z_2 \sin\psi + Z_1 \left[1-(k_1/k_2)^2 \cos^2\psi\right]^{\frac{1}{2}}} \tag{47}$$

plane wave reflection coefficient in the specular direction for reflection from a "fluid" earth (Case 1)

$$R_p^{(2)} = \frac{\zeta \sin\psi - 1}{\zeta \sin\psi + 1} \tag{48}$$

plane wave reflection coefficient in the specular direction for reflection from a normal-impedance boundary (Case 2)

$$\Phi(u) = \frac{2}{\sqrt{\pi}} \int_o^u e^{-v^2}\, dv \tag{49}$$

error function[23] (Case 1 and 2)

1.4.2 Solutions for the General Case*

The problem of a point source of sound in a homogeneous, isotropic atmosphere above a plane boundary below which lies a homogene-

*The methods used in the acoustical case summarized here are analogous to methods developed for the problem of a dipole source of electromagnetic radiation above a plane conducting earth. The method used by Rudnick[17] and by Lawhead and Rudnick[19] is that developed by Sommerfeld, van der Pol and Norton; the method used by Ingard is based upon the solution of the electromagnetic problem by Weyl. For a short summary of these methods, see J. Stratton, Electromagnetic Theory (McGraw-Hill Book Company, Inc., New York, 1951), p. 573; for a complete analysis of all work done on the problem, and an extensive bibliography, see A. Banos, Jr. and J. P. Wesley, "The Horizontal Electric Dipole in a Conducting Half-space", Scripps Institute of Oceanography (Univ. of Calif.) Reference 53-33 (September, 1953).

ous, isotropic "fluid" earth has been treated by Rudnick[17], following the method of Sommerfeld. The incident pressure from the point source, and the reflected (and transmitted) pressure fields are developed in terms of Fourier-Bessel integrals; by applying the boundary conditions at the air-earth interface (continuity of pressure and of normal particle velocity across the interface) an integral expression for the reflected field is found. The integral is then approximated under the assumption that the earth is a highly absorbing medium; specifically, it is assumed that the distance from the image point to the receiver (R_2) is large compared with the distance in which the amplitude of a plane wave traveling in the earth is diminished by a factor of e = 2.72... , i.e., it is assumed that $|R_2 \mathrm{Im}(k_2)| \gg 1$. Laboratory tests made by Lawhead and Rudnick[24] show that the theory is valid at audible frequencies over acoustical absorbing materials such as Fiberglas.

The problem of a point source of sound in a homogeneous, isotropic atmosphere above a plane earth which may be acoustically characterized by a normal-impedance boundary condition has been treated by Ingard[18] in a manner similar to that of Weyl, and by Lawhead and Rudnick[19], following the method used by Rudnick in the "fluid" earth case. Since the method of Lawhead and Rudnick yields results very close to that of Ingard (the results are the same for $\zeta \gg \sin\psi$), their method will not be discussed. Ingard's method is to represent the incident and reflected fields as a (integral) superposition of plane waves; the boundary condition at the surface is that the total pressure divided by the particle velocity normal to the surface is equal to the normal impedance of the surface. In two special cases, to be discussed in subsection 1.4.3, the resulting integral may be evaluated exactly; in the general case the approximation $k_1 R_2 \gg 1$ (distance from image point to receiver is large compared with the wavelength of sound in air) is made.

In both cases (Case 1: "fluid" boundary condition; Case 2: normal-impedance boundary condition) the sound pressure at the receiver is given by

$$p(x,y,z) = \frac{e^{ik_1 R_1}}{R_1} + \frac{e^{ik_1 R_2}}{R_2}\left[R_p + (1-R_p)F(\rho)\right] \qquad (50)$$

(Case 1 and 2)

where the specular-direction plane wave reflection coefficient used is that appropriate to the case under consideration: $R_p^{(1)}$, Eq. (47), for Case 1; $R_p^{(2)}$, Eq. (48), for Case 2. The function $F(\rho)$ is:

$$F(\rho) = 1 - (\pi\rho)^{\frac{1}{2}} e^{\rho}\left[1 - \Phi(\rho^{\frac{1}{2}})\right] \qquad (51)$$

where Φ is the error function, Eq. (49). The "numerical distance", ρ appearing as the argument is given in the two cases as*

$$\rho^{(1)} = \frac{1}{2i} k_1 R_2 \frac{1}{\cos^2\psi} \left[\sin\psi + \left(\frac{Z_1}{Z_2}\right) \sqrt{1 - \left(\frac{k_1}{k_2}\right)^2 \cos^2\psi} \right]^2 \qquad (52)$$

(Case 1)

$$\rho^{(2)} = \frac{1}{2i} k_1 R_2 \frac{(\zeta \sin\psi + 1)^2}{\zeta(\zeta + \sin\psi)} \qquad (53)$$

(Case 2)

Ingard has plotted the magnitude and the phase of $F(\rho)$ as functions of the magnitude of the variable ρ, with the phase of ρ as a parameter; see Figs. 11 and 12.

The Taylor's series and the asymptotic series for $F(\rho)$ are given by Ingard as:

$$F(\rho) = 1 - (\pi\rho)^{\frac{1}{2}} e^{\rho} \left[1 - 2\left(\frac{\rho}{\pi}\right)^{\frac{1}{2}} \left(1 - \frac{\rho}{1\cdot 3} + \frac{\rho^2}{2\cdot 5} - \frac{\rho^3}{3\cdot 7} + \ldots\right) \right] \qquad (54)$$

$$F(\rho) \sim \frac{1}{2\rho} - \frac{1\cdot 3}{(2\rho)^2} + \frac{1\cdot 3\cdot 5}{(2\rho)^3} \ldots \qquad (55)$$

There are three limiting cases of importance for both the fluid boundary condition and the normal-impedance boundary condition:

(1) As R_2 goes to infinity, both $\rho^{(1)}$ and $\rho^{(2)}$ go to infinity, and $F(\rho)$ goes to zero; the expression for the pressure becomes

$$p(x,y,z) \sim \frac{e^{ik_1 R_1}}{R_1} + R_p \frac{e^{ik_1 R_2}}{R_2}, \quad R_2 \to \infty \text{ (Case 1 and 2)} \qquad (56)$$

---

*The following changes from those formulas appearing in the references should be noted: (a) in the numerical distance $\rho^{(1)}$, the factor 1/i replaces Rudnick's factor of i so that Ingard's graphs can be used; (b) the term $1/\cos^2\psi$ in $\rho^{(1)}$ is a correction for a term left out of the expansion leading to Rudnick's final result; (c) in the numerical distance $\rho^{(2)}$, the factor 1/i, instead of i as given by Ingard, is a correction to his reported result. The expression of Lawhead and Rudnick for Case 2 is given by Eqs. (50) and (51), with a numerical distance

$$\rho = \frac{1}{2i} k_1 R_2 (\zeta \sin\psi + 1)^2 / \zeta^2 \cos^2\psi$$

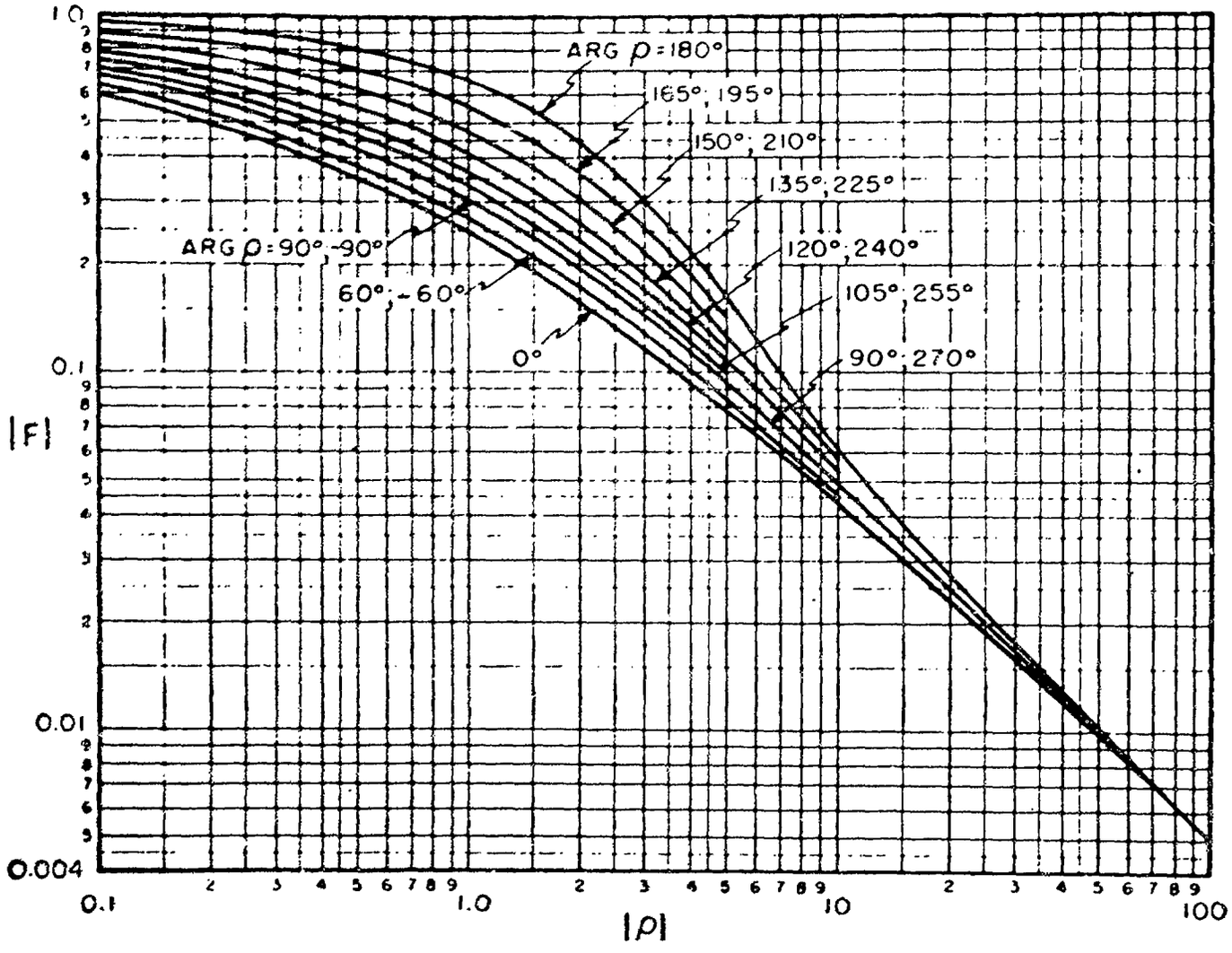

Fig. 11. Graph of the reflection function $F(\rho)$ as a function of the numerical distance ρ. Magnitude of $F(\rho)$ vs magnitude of ρ ; phase of ρ as a parameter.

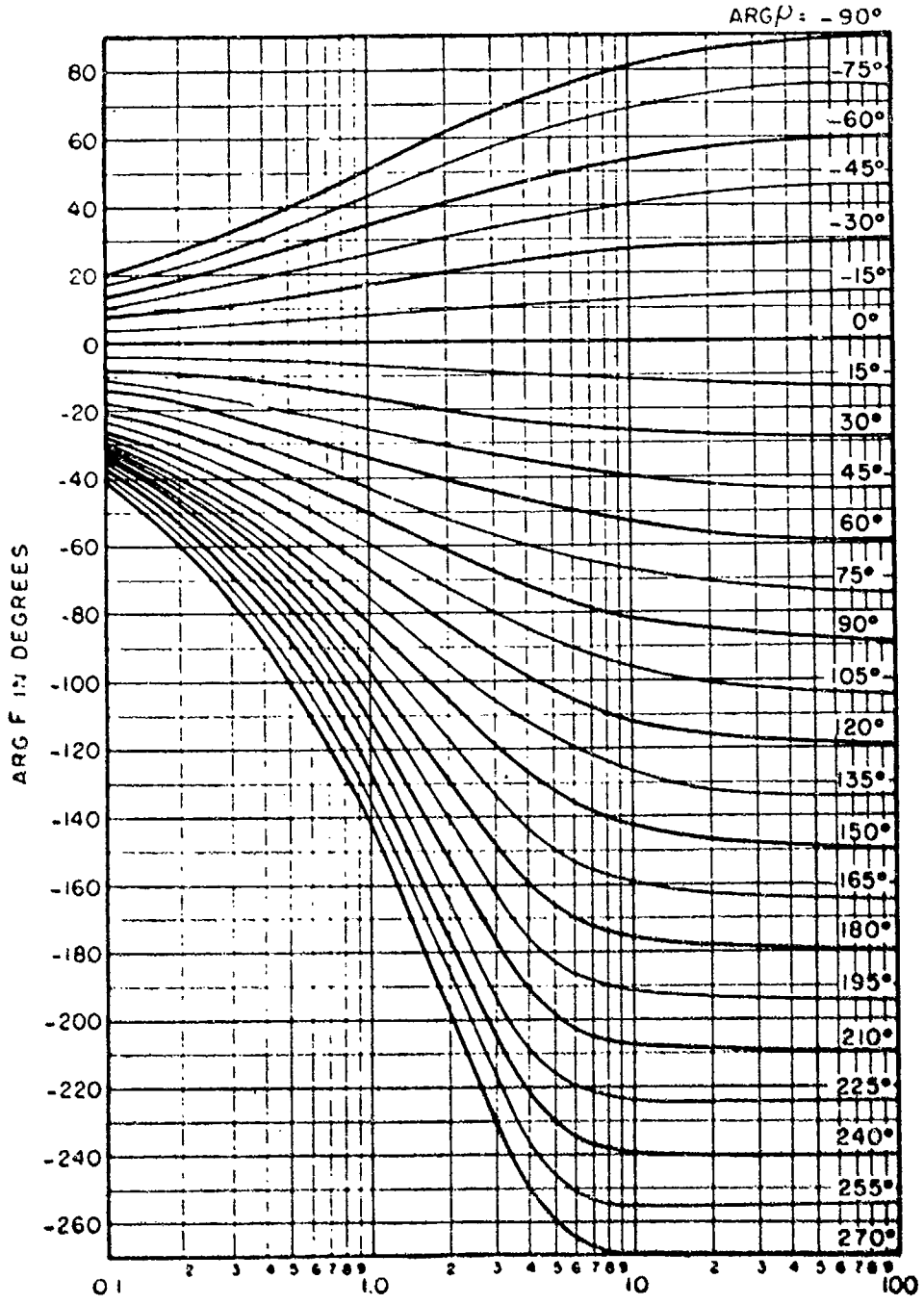

Fig. 12. Graph of the reflection function $F(\rho)$ as a function of the numerical distance ρ. Phase of $F(\rho)$ vs magnitude of ρ; phase of ρ as a parameter.

This corresponds to the usual result that, at large distances from the source, the reflected radiation is that due to an image source having an amplitude equal to the plane-wave reflection coefficient in the specular direction.

(2) As the boundary becomes "acoustically soft" ($\rho_2 \to 0$ for Case 1, or $\zeta \to 0$ for Case 2) both $\rho^{(1)}$ and $\rho^{(2)}$ go to infinity so that $F(\rho)$ goes to zero, while $R_p^{(1)}$ and $R_p^{(2)}$ go to -1; the pressure becomes, as expected,

$$p(x,y,z) = \frac{e^{ik_1R_1}}{R_1} - \frac{e^{ik_1R_2}}{R_2} \tag{57}$$

for pressure-release surface (Case 1 and 2)

(3) As the boundary becomes "acoustically hard" ($\rho_2 \to \infty$ for Case 1, or $\zeta \to \infty$ for Case 2) both $R_p^{(1)}$ and $R_p^{(2)}$ go to + 1; the pressure becomes, as expected,

$$p(x,y,z) = \frac{e^{ik_1R_1}}{R_1} + \frac{e^{ik_1R_2}}{R_2} \tag{58}$$

for hard surface (Case 1 and 2)

1.4.3 Solutions for Special Cases

Two cases of particular importance occur when the source and receiver are on the ground, and when the source and the receiver are in a vertical line.

(1) Source and receiver on ground

For the source at (0,0,0) and the receiver at (x,y,0), we have:

$$R_1 = R_2 = (x^2 + y^2)^{\frac{1}{2}} \equiv r; \qquad \psi = 0; \qquad R_p^{(1)} = R_p^{(2)} = -1 \tag{59}$$

(Case 1 and 2)

The pressure is given by

$$p(x,y,z) = 2F(\rho)\,\frac{e^{ik_1r}}{r} \tag{60}$$

(Case 1 and 2)

where the numerical distances, Eqs. (52) and (53), become

$$\rho^{(1)} = \frac{1}{2i}\, k_1 r\, \left(\frac{Z_1}{Z_2}\right)^2 \left[1 - (k_1/k_2)^2\right] \tag{61}$$

(Case 1)

$$\rho^{(2)} = \frac{1}{2i} k_1 r \frac{1}{\zeta^2} \qquad \text{(Case 2)} \quad (62)$$

For large distances from source to receiver, r goes to infinity, so that $\rho^{(1)}$ and $\rho^{(2)}$ tend to infinity. From Eq. (55), $F(\rho) \sim \frac{1}{2\rho}$, so

$$p^{(1)}(x,y,z) \sim \frac{2i}{k_1 \left[1 - (k_1/k_2)^2\right]} \left(\frac{Z_2}{Z_1}\right)^2 \frac{e^{ik_1 r}}{r^2}, \quad r \to \infty \qquad (63)$$

(Case 1)

$$p^{(2)}(x,y,z) \sim \frac{2i\zeta^2}{k_1} \frac{e^{ik_1 r}}{r^2}, \quad r \to \infty \qquad (64)$$

(Case 2)

For a source and receiver at the boundary (or near it) and for a large distance from source to receiver, the pressure amplitude follows an inverse-square law with distance (as anticipated in Eq. (3), subsection 1.1).

(2) Source and receiver in a vertical line

For the source at $(0,0,z_o)$ and the receiver at $(0,0,z)$, we have:

$$R_1 = |z - z_o|, \; R_2 = (z + z_o); \qquad \psi = 90^\circ \qquad (65)$$

(Case 1 and 2)

$$R_p^{(1)} = \frac{Z_2 - Z_1}{Z_2 + Z_1} \qquad (66)$$

(Case 1)

$$R_p^{(2)} = \frac{\zeta - 1}{\zeta + 1} \qquad (67)$$

(Case 2)

The numerical distances become:*

$$\rho^{(1)} \to \infty \qquad (68)$$

(Case 1)

---

*The numerical distance $\rho^{(2)}$ in Eq. (69) has been taken from Ingard's approximate solution, Eq. (53). However, Ingard has derived[18] an exact solution for the case of $\psi = 90^\circ$; the exact expression for the numerical distance is $\rho = (1/i)k_1 R_2 (1 + 1/\zeta)$, just twice the expression in Eq. (69). For the case of $\zeta = 1$, an exact solution has also been derived for arbitrary angle ψ; this is $\rho = (1/i)k_1 R_2 (1 + \sin\psi)$. Since there is given no approximate solution for angles near $\psi = 90^\circ$, or impedance close to $\zeta = 1$, based on the exact solution for these cases, only the general approximation is used here.

$$\rho^{(2)} = \frac{1}{2i} k_1(z + z_o) \left(\frac{\zeta + 1}{\zeta}\right) \qquad (69)$$

(Case 2)

The pressure is therefore given by

$$p^{(1)}(x,y,z) = \frac{e^{ik_1|z - z_o|}}{|z - z_o|} + \left[\frac{Z_2 - Z_1}{Z_2 + Z_1}\right] \frac{e^{ik_1(z + z_o)}}{(z + z_o)} \qquad (70)$$

(Case 1)

$$p^{(2)}(x,y,z) = \frac{e^{ik_1|z - z_o|}}{|z - z_o|} + \frac{1}{\zeta + 1}\left[(\zeta - 1) + 2F(\rho^{(2)})\right]\frac{e^{ik_1(z+z_o)}}{(z+z_o)} \qquad (71)$$

(Case 2)

1.5 SOUND PROPAGATION IN A STRATIFIED MEDIUM

1.5.1 Introduction

One of the most important effects to be noted in atmospheric acoustics is the change in sound intensity due to acoustic refraction by changes in air temperature and wind velocity with height. The effects of sound refraction are only partially explained by theory, due to the mathematical difficulties inherent in the calculations. These effects, although often noticed, have been carefully measured in the atmosphere in only a few cases; however, the attenuation due to refraction of sound has been well studied for the case of sound propagation in the ocean[25]. The discussion here will be limited to the case of sound velocity changes (due to changes in temperature and wind velocity) in the vertical direction only; changes due to variation of temperature and wind velocity in the horizontal direction have not yet been analyzed.

Micrometeorological measurements will first be discussed in order to give background for obtaining a general expression for the velocity of sound in the presence of the type of wind and temperature variations most usually found to occur. The analysis of the sound field by means of ray theory (geometrical acoustics) will then be discussed. The wave theory of sound attenuation for the cases of a constant sound velocity gradient, and for a linear variation of air temperature with height, over a sound-absorbing earth make up the next sections. Finally, as an illustration of the general theory, an approximate sound attenuation formula is derived for the case of the sound velocity varying in a manner to be expected from the micrometeorological measurements. This

will be later used to analyze a recent set of measurements of sound attenuation in the atmosphere (see subsection 2.3.3).

1.5.2 Temperature Distribution near the Ground

A number of measurements of the dependence upon height of air temperature and wind velocity have been made for the first few tens of meters above the ground[26,27] Only average values will be considered here; the discussion of fluctuations about the mean value will be left to subsection 1.6.

O. G. Sutton[28] and E. L. Deacon[29] have found that the variation of air temperature with height is representable by the following empirical formula for the temperature gradient:

$$\frac{dT}{dz} = -\Gamma - az^{-\delta} \tag{72}$$

where T is the temperature, Γ is the adiabatic lapse rate, and a and δ are experimentally determined constants. The adiabatic lapse rate, 1° Centigrade per 100 meters, is the change in atmospheric temperature with height which must exist if any mass of dry air, moving adiabatically, is to have the same temperature as its surroundings (i.e., a temperature gradient of $-\Gamma$ is the condition for static adiabatic equilibrium of dry air).

When the temperature gradient is $-\Gamma$, that is, when the value of a is zero, the temperature condition is known as an "adiabatic lapse" or "neutral stability" condition. When a is positive, the temperature decreases with height at a rate faster than that given by Γ; this is known as a "super-adiabatic lapse" condition (commonly called a "lapse" condition). When a is negative, and Γ is less than $az^{-\delta}$ the temperature increases with height; this is called an "inversion" condition. The lapse condition is found during the day, when the ground, heated by the sun, heats the lower layers of the atmosphere; this gives rise to the decrease in temperature with height. At night, the ground cools off rapidly, leading to

TABLE 7

Typical values of a (°C), derived from Fig. 13, assuming $\delta = 1$.

	Summer (June)	Winter (January)
Day	0.5	0.1
Night	-0.15	-0.15

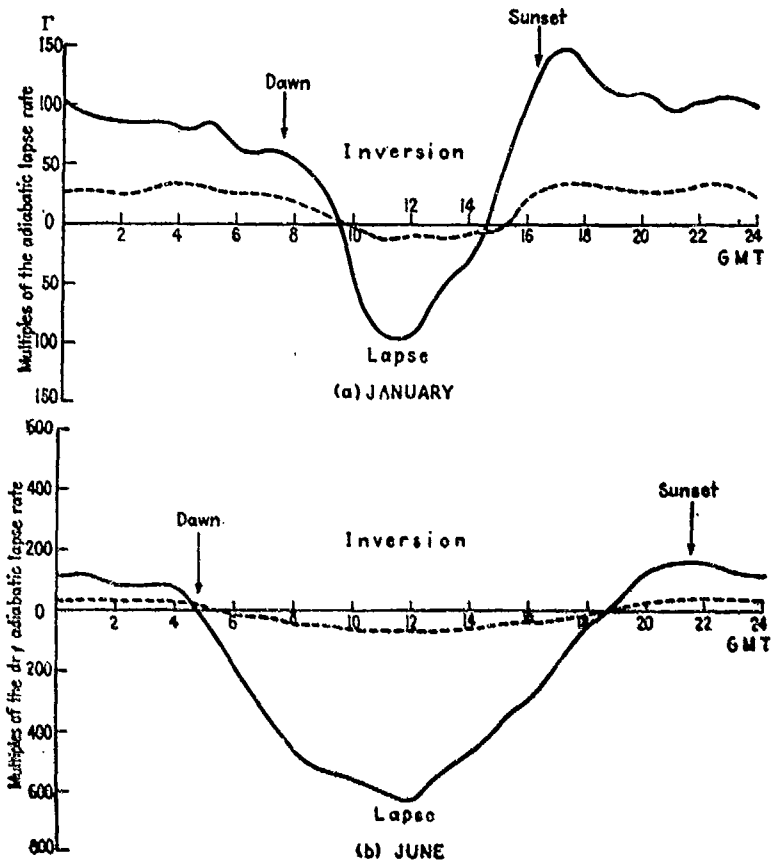

Fig. 13. Diurnal variation of temperature gradients found by Best at Porton, England. Solid line for temperature difference between heights of 2.5 and 30.5 cm; dashed line same for heights of 30.5 and 120 cm. (From O.G. Sutton, Reference 26).

a temperature increase with height, or an inversion. Figure 13 showing the diurnal variation of temperature gradients, illustrates these points. From this figure, one can obtain typical values for the constant a. A few values from Fig. 13 are given in Table 7.

Deacon, using data obtained by A. C. Best, has found that δ, the exponent of z in Eq. (72), is positive and approximately equal to unity. He obtains values of δ greater than unity for lapse conditions, and values less than unity for inversions (typical values being 1.15 and 0.80, respectively); near neutral stability, $\delta \sim 1.10$.

Integration of Eq. (72) leads to:

$$T = T_1 - \Gamma (z - z_1) - \frac{a}{1-\delta}\left[z^{1-\delta} - z_1^{1-\delta}\right] \qquad (73)$$

where T is the temperature at height z, and T_1 the temperature at height z_1.

1.5.3 Wind Velocity Distribution near the Ground

Under conditions of neutral stability, both theory and experiment[30,31] give a variation of mean wind velocity with height of

$$u = \frac{u_*}{k} \ln\left(\frac{z}{\ell}\right) , \quad z \geq \ell \qquad (74)$$

where k is the von Karman constant and is approximately equal to 0.4. The "friction velocity" u_* is found to be proportional to the windspeed, at any given reference height, its value depending upon the roughness of ground. The "roughness length" ℓ is characteristic of a given surface,

TABLE 8

Representative values of ℓ and u_*/u_{200} for natural surfaces, where u_{200} is the wind speed at 200 cm above the ground (neutral stability assumed). From Sutton, Micrometeorology p.233

Type of Surface	ℓ (cm)	u_*/u_{200}
Very smooth (mud flats, ice)	0.001	0.032
Lawn, grass up to 1 cm high	0.1	0.052
Meadow, thin grass up to 10 cm high	0.7	0.072
Thick grass, up to 10 cm high	2.3	0.090
Thin grass, up to 50 cm high	5	0.110
Thick grass, up to 50 cm high	9	0.126

and is roughly proportional to the height above the ground of the protuberances causing the roughness. Table 8 gives representative values of ℓ and of the ratio u_*/u_{200}, where u_{200} is the velocity at a height of 200 cm. It is to be noted from Eq. (74) that $u = 0$ at $z = \ell$.

Deacon has found that under more general thermal conditions, the wind velocity gradient can be given as:

$$\frac{du}{dz} = \frac{u_*}{k\ell^{1-\beta}} z^{-\beta} \tag{75}$$

where u_*, k, ℓ are defined as before, and β is a positive constant of order unity. This expression gives the neutral stability variation of wind velocity with height for $\beta = 1$. Deacon has also determined a relation between β and δ (the corresponding constant for the temperature gradient) of:

$$2\beta - \delta \simeq 0.9 \tag{76}$$

Since $\delta \simeq 1.10$ for neutral stability, this gives $\beta = 1$ in that case, as expected. Integration of Eq. (75) gives:

$$u = \frac{u_*}{k(1-\beta)\ell^{1-\beta}} \left[z^{1-\beta} - \ell^{1-\beta} \right] \quad z \geq \ell \tag{77}$$

where u is the wind velocity at height z and $u = 0$ at a height equal to the roughness length, $z = \ell$. It is to be noted that $z = \ell$ must be taken as the effective height of the ground.

1.5.4 Sound Velocity as a Function of Height

The results of the last two subsections may be used to determine the variation of the velocity of sound with height expected to occur naturally. Since the effect on the sound velocity of temperature and wind changes will be small, Eq. (73) and (77) may be approximated to obtain a simple expression for the sound velocity.

Neglecting the term $-\Gamma(z - z_1)$ in Eq. (73), since its effect will be small, the sound velocity may be written as a function of height using the dependence of air temperature upon height of Eq. (73):

$$c \simeq c_1 \left[1 - \frac{a}{2(1-\delta)\, T_1} \left(z^{1-\delta} - z_1^{1-\delta} \right) \right] \tag{78}$$

where c_1 is the velocity of sound at height z_1, and T_1 is the absolute temperature there.

If sound travels in a medium moving with velocity u, the sound velocity at any point (x,y,z) is given by (for $u \ll c$):

$$c(x,y,z) = c'(x,y,z) + u(x,y,z)\cos\phi \tag{79}$$

where c' is the sound velocity at (x,y,z) in the absence of motion of the medium, and ϕ is the angle between the wind direction and the path of the sound ray through (x,y,z), i.e., if wind and sound ray are in the same direction the sound velocity is increased by the wind. Since it is assumed that there are no variations in sound velocity in the x and y directions, the projection of the ray path on the x-y plane will be a straight line (under the approximation $u \ll c$); the angle ϕ is therefore taken as the angle between the wind direction and the horizontal projection of the line drawn from source to receiver. (See Figure 14a.) Using Eq. (77), Eq. (79) becomes

$$c = c' + \frac{u_*}{k(1-\beta)\,\ell^{1-\beta}}\left[z^{1-\beta} - \ell^{1-\beta}\right]\cos\phi, \quad z \geq \ell$$

Using Eq. (78) for c', the velocity of sound in the absence of wind:

$$c(z) = c_1\left[1 - \frac{a}{2T_1(1-\delta)}\left(z^{1-\delta} - z_1^{1-\delta}\right) + \frac{u_*\cos\phi}{c_1 k(1-\beta)\,\ell^{1-\beta}}\left(z^{1-\beta} - \ell^{1-\beta}\right)\right] \tag{80}$$

Since wind velocities will be small compared with the sound velocity, and temperature changes will be small compared with the absolute temperature, the second and third terms in Eq. (80) may be approximated without much error in the final result. If the velocity of sound at the source (used as a reference point here) is $c_o = c(z_o)$, the velocity of sound at an arbitrary point z is:

$$c(z) \approx c_o\left[1 - \frac{a}{2T_1(1-\delta)}\left(z^{1-\delta} - z_o^{1-\delta}\right) + \frac{u_*\cos\phi}{c_o k(1-\beta)\,\ell^{1-\beta}}\left(z^{1-\beta} - z_o^{1-\beta}\right)\right]$$

$$\approx c_o\left[1 - \frac{a z_o^{1-\delta}}{2T_1}\ln\left(\frac{z}{z_o}\right) + \frac{u_*\cos\phi}{c_o k}\left(\frac{z_o}{\ell}\right)^{1-\beta}\ln\left(\frac{z}{z_o}\right)\right]$$

where the approximation is valid for $(1-\delta)\ln\left(\frac{z}{z_o}\right) \ll 1$, $(1-\beta)\ln(z/z_o) \ll 1$. The sound velocity may therefore be written as:

$$c(z) = c_o\left[1 - B\ln\left(\frac{z}{z_o}\right)\right]; \quad z \geq \ell; \quad B = \frac{a z_o^{1-\delta}}{2T_1} - \frac{u_*}{c_o k}\left(\frac{z_o}{\ell}\right)^{1-\beta}\cos\phi \tag{81}$$

where c_o is the velocity of sound at the reference point z_o; a, δ, β, ℓ and u_*/k are experimentally determined from micrometeorological informa-

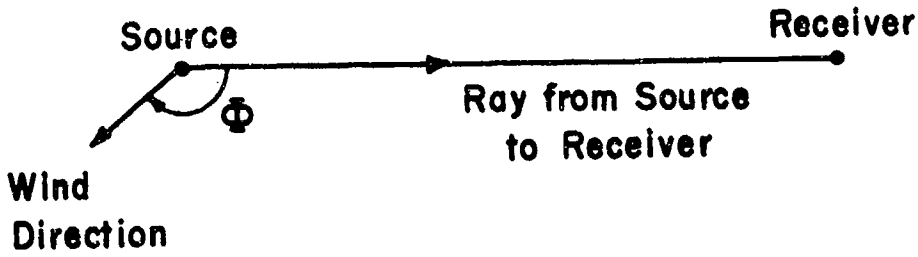

(a)

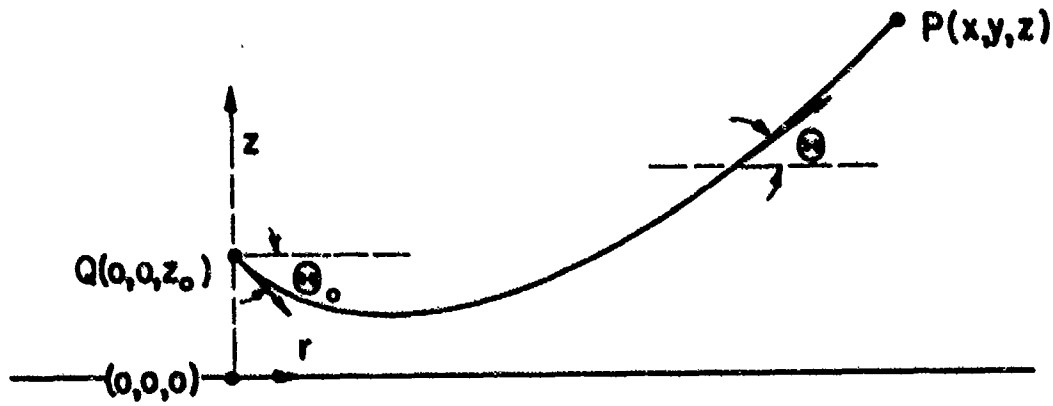

(b)

Fig. 14. Geometrical relations for a sound ray from source to receiver. (a) Projection on x-y plane showing angle between wind direction and ray direction; (b) in vertical plane, showing angles with horizontal made by ray at source and at an arbitrary point along the path.

tion, and ϕ is the angle between the wind direction and the ray path through the point P(x,y,z). The approximations are valid for β and δ near unity, and z near z_o (but, if β and δ are assumed exactly equal to unity, z may have any value). As noted in the discussion of the wind velocity gradient, the "ground" is at height $z = \ell$; it is at this height that the wind velocity becomes zero.

1.5.5 Ray Theory: Shadow Boundary

An important effect due to the variation of sound velocity with height is the formation of shadows in the presence of the ground. In this subsection, a derivation by means of geometrical acoustics will be given of the position of the shadow boundary for the sound velocity varying as in Eq. (81).

A sound ray, in a medium whose sound velocity depends upon height, travels along a path given by Snell's law:

$$c(z) \cos \theta_o = c_o \cos \theta \tag{82}$$

where c(z) is the velocity of sound at a height z, θ is the angle made with the horizontal by the tangent to the ray path through the point (x,y,z), and c_o and θ_o are sound velocity and angle made by the ray at some reference point (in this case, the point at which the source of sound is located); see Fig. 14b. For the case of the sound velocity decreasing with height (e.g., for $B > 0$ in Eq. (81), a given ray from the source will be bent upwards; the presence of the ground causes a region to be formed into which no rays can penetrate, the "shadow zone". Although ray theory leads to an absence of sound in the shadow zone, an application of wave theory shows that sound is diffracted across the shadow boundary, but the sound pressure decreases markedly with distance into the shadow zone; see subsection 1.5.7. Two types of shadow zones may be formed, one in which a single ray from the source forms the shadow boundary (a constant velocity gradient forms this type of shadow zone); and one in which, due to crossing of the rays, the envelope of many rays form the shadow boundary (the inverse-z velocity gradient, treated above, forms this type). These are schematically illustrated in Fig. 15.

The equation of a ray (r as a function of z, z_o, and θ_o) may be found from (see Fig. 14b)

$$r = \int_{z_o}^{z} \frac{dz}{\pm \tan \theta} \tag{83}$$

where $\tan \theta$ is found from Eq. (82), z is the height of the ray at r, and z_o is the height of the source. Since a ray can pass through a

(a)

(b)

Fig. 15. Schematic diagram of the formation of a shadow-zone due to a negative sound velocity gradient: (a) Case for one sound ray forming the shadow boundary; (b) Case for shadow boundary formed by the envelope of many rays.

minimum point (when $\theta = 0$), the integration is carried out in two parts; an integration from z_o to z_m, and from z_m to z, where z_m is the minimum height of the ray, i.e., the height for which $\theta = 0$ (it should be noted that $\tan \theta = dr/dz$ changes sign through the minimum). Carrying out the analysis for the sound velocity dependence of Eq. (81) (and neglecting terms in B^2 as being small compared with unity), the equation of a ray starting from $r = 0$, $z = z_o$, and making an initial angle θ_o with the horizontal, may be written as

$$\sqrt{\frac{B}{2}}\ \frac{r}{z_o} \simeq \frac{z_m}{z_o}\left[1 - B\ln(z_m/z_o)\right]\left[\int_o^w \exp(v^2)\,dv + \int_o^{w_o} \exp(v^2)dv\right]$$

$$- \frac{B}{2}\left[w_o + (z/z_o)w\right] \qquad (84)$$

$$w = \left[\ln(z/z_m)\right]^{\frac{1}{2}}; \qquad w_o = \left[\ln(z_o/z_m)\right]^{\frac{1}{2}}$$

where the minimum height of a ray, i.e., that height for which $\theta = 0$, is:

$$z_m = z_o \exp(-\frac{1}{2B}\tan^2 \theta_o) \qquad (85)$$

As anticipated earlier the rays given by Eq. (84) cross each other, their envelope forming a shadow boundary (see Fig. 15b). The shadow boundary for any given value of z is formed by that ray which has an initial angle giving the maximum radial distance from the source for that value of z; the shadow-forming rays satisfy:

$$\left(\frac{dr}{d\theta_o}\right)_{z=\text{const.}} = 0 \qquad (86)$$

As may be seen from Fig. 15b, the presence of the ground affects the shadow boundary only slightly; the ray which "begins" the shadow boundary at the ground has an initial angle $\theta_o^{(0)}$ such that $\theta = 0$ at the ground:

$$\cos \theta_o^{(0)} = \frac{c_o}{c(\ell)} \qquad (87)$$

where $z = \ell$ is the "ground height" used in the velocity distribution, Eq. (81). (For the case of the shadow zone formed by one ray, as in Fig. 15a, the shadow-forming ray has an initial angle given by Eq. (87).) Using Eq. (86) it is found that the initial ray angle $\theta_o^{(s)}$ which form the shadow boundary at height z is given approximately by:

$$\tan^2 \theta_o^{(s)} \simeq \frac{2B\ln(z/z_o)}{(z/z_o)^2 - 1} \qquad (88)$$

This also approximately satisfies Eq. (87) for the shadow boundary at ground, $z = \ell$, provided that the source is not too close to the ground, i.e., $z_o \gg \ell$.

Using Eq. (88) in Eq. (84), the horizontal distance to the shadow boundary, r_s, is therefore:

$$\frac{r_s}{z_o} = \sqrt{\frac{2}{B}}\left\{e^{-\tau^2}\left[\int_0^{(z\tau/z_o)} \exp(v^2)dv + \int_0^{\tau} \exp(v^2)dv\right] - \frac{B}{2}\left[(z/z_o)^2 + 1\right]\tau\right\}$$

$$\tau = \left[\frac{\ln(z/z_o)}{(z/z_o)^2 - 1}\right]^{\frac{1}{2}} \qquad (89)$$

A graph of these results is given in Fig. 16 for $0.1 \leq (z/z_o) \leq 10$; for this range of variable, it is found that the second term (containing the extra factor of B) is negligible for values of B usually found to occur. Figure 16 is a plot of $\left[(r_s/z_o)\sqrt{B/2}\right]$ vs (z/z_o); for any value of B (less than about 0.1) the distance to the shadow zone may be found from the graph, subject to the condition that the source height be large compared with the roughness length ("ground height") ℓ.

The relation given by the graph, Fig. 16, may be written as:

$$\frac{r_s}{z_o} = \sqrt{\frac{2}{D - M_o\cos\phi}}\ f(z/z) \qquad (90)$$

since B, from the velocity distribution Eq. (81), is:

$$B = \frac{a\ z_o^{1-\delta}}{2T_1} - \frac{u_*}{c_o k}\left(\frac{z_o}{\ell}\right)^{1-\beta}\cos\phi \equiv D - M_o\cos\phi \qquad (91)$$

A polar plot of r_s, the distance to the shadow boundary, vs ϕ, the angle between the wind direction and the line from source to receiver, may be made. It may be seen from Eq. (91) and Fig. 14a, that the distance to the shadow boundary forms a closed curve for $D > M_o$ (i.e., for the temperature effect larger than the effect of wind), so that the source is everywhere enclosed by the shadow region. However, if the effect of wind is greater than that of the temperature variation, so that $D < M_o$, the distance to the shadow boundary, r_s, forms an open curve; this curve gives a shadow zone in directions against the wind, and goes asymptotically to the lines through the source given by:

$$\cos\phi_o = \frac{D}{M_o} \qquad (92)$$

These effects are illustrated in Fig. 17.

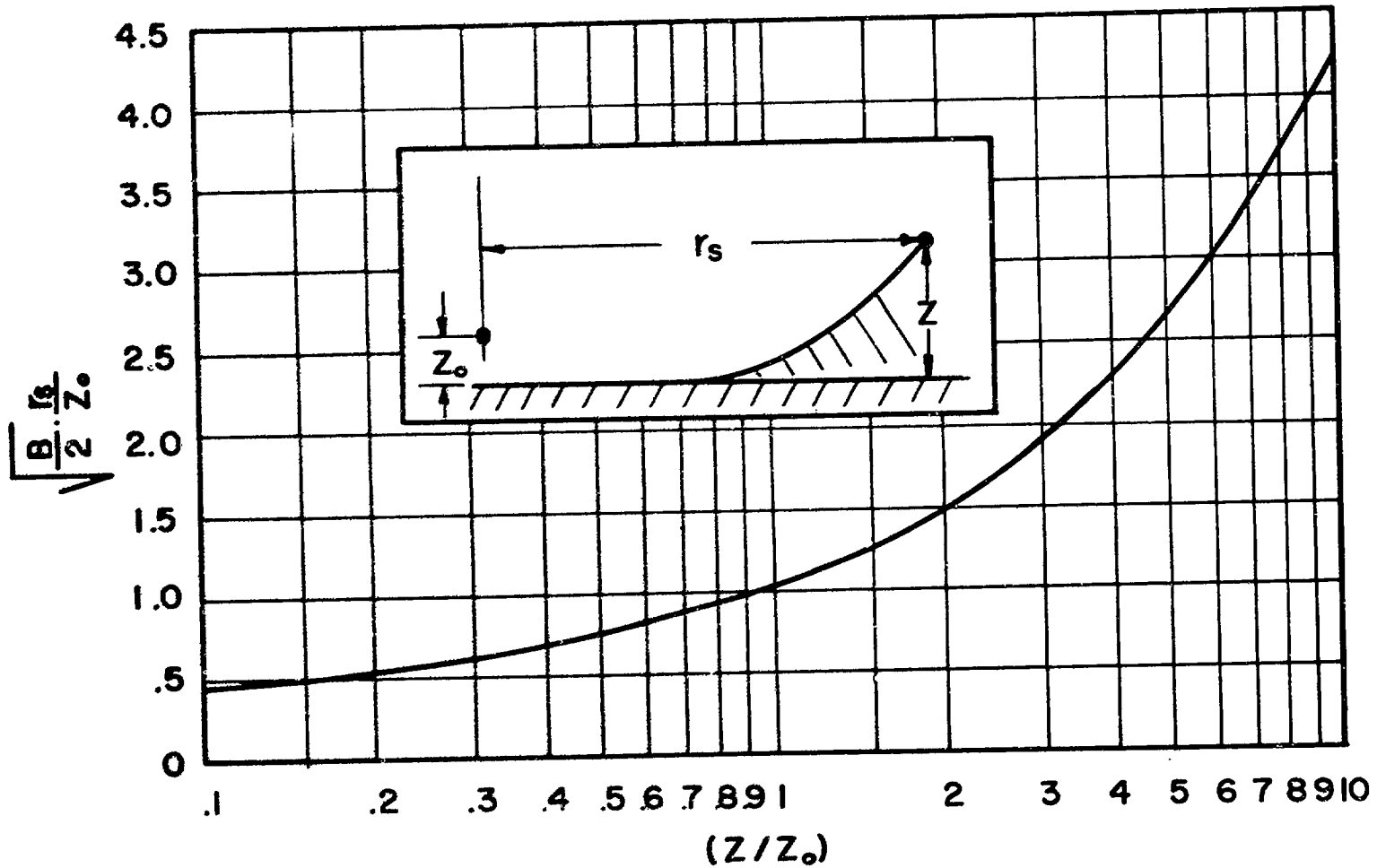

Fig. 16. Graph of distance to shadow boundary (r_s) as a function of height of receiver (z) for arbitrary sound velocity constant (B); height of source is z_o; see Eq. (89).

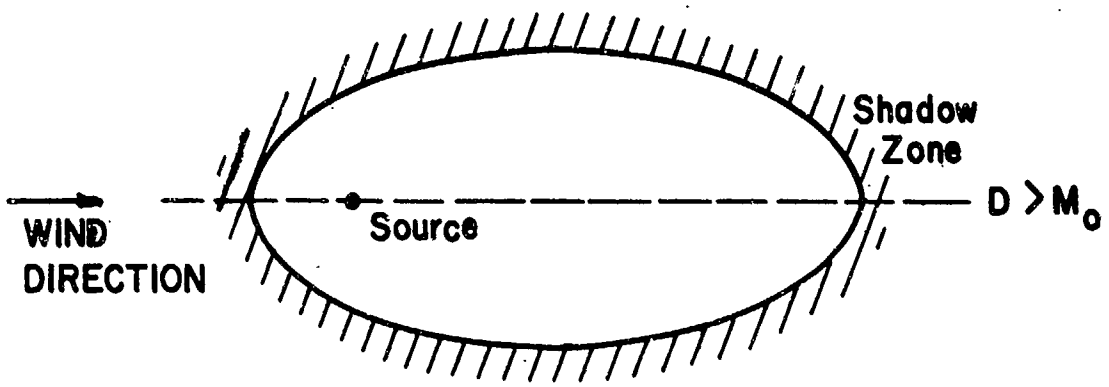

a) Temperature effect greater than effect of wind.

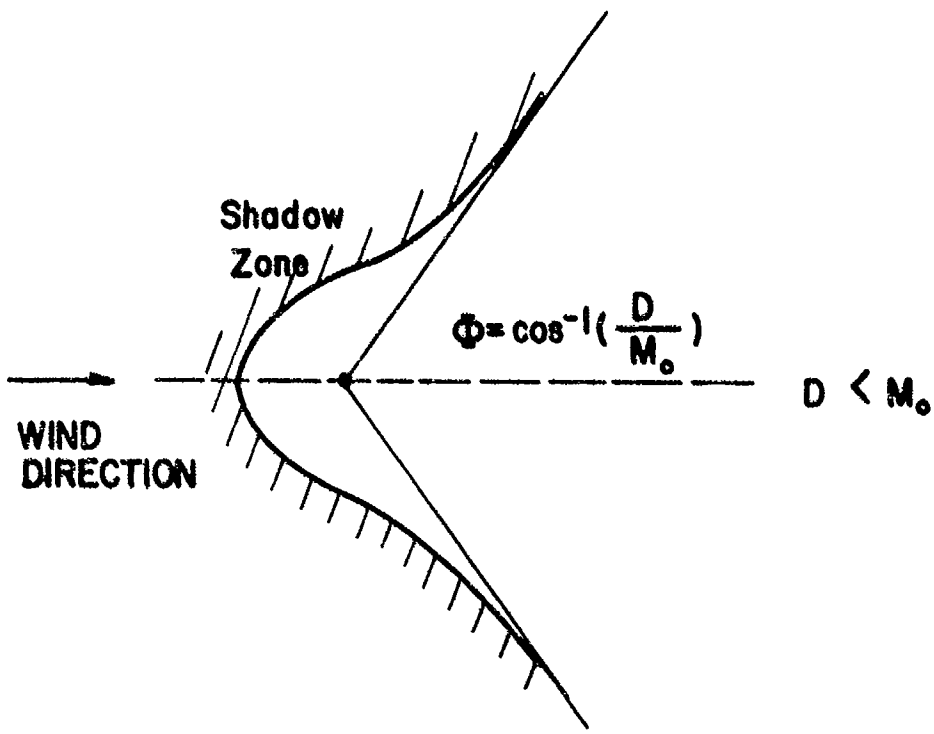

b) Effect of wind greater than temperature effect.

Fig. 17. Schematic diagram of position of shadow boundary in the presence of temperature and wind gradients; see Eq. (91).

For general use of the graph shown in Fig. 16 let $\delta \sim \beta \sim 1$ (as is often approximately true) and let T_1 be 293°A (20°C); then using k = 0.4 and the value of c_o given in Appendix I at 20°C (i.e., c_o = 34,400 cm/sec) the quantity B may be written

$$B = (1.71 \times 10^{-3}) \left[a - 0.042 \left(\frac{u_*}{u_{200}}\right) u_{200} \cos\phi \right] \qquad (93)$$

where $\underline{a}$ is in °C and u_{200}, the wind velocity at a height of 200 cm, is in cm/sec. The constant $\underline{a}$ may be obtained from on-site measurements of the temperatures T, T_o at two different heights z, z_o and using the expression

$$a = \frac{(T-T_o)}{\ln(z/z_o)} \quad , \qquad (94)$$

obtained from integrating Eq. (72) and letting $\delta = 1, \Gamma = 0$; typical values of $\underline{a}$ are given in Table 7. Values of (u_*/u_{200}) for various types of surface are given in Table 8.

To determine r_s, the horizontal distance to the shadow zone boundary for given z, z_o, ϕ and for given meteorological and surface conditions one may proceed as follows:

1. Obtain from Fig. 16 the value of $\sqrt{\frac{B}{2}} \frac{r_s}{z_o}$ for the given (z/z_o)

2. Obtain B from Eq. (93) for the given u_{200}, ϕ, for the value of $\underline{a}$ obtained from field measurements, using Eq. (94) (see Table 8 and Fig. 13 for orders of magnitude), and the value of (u_*/u_{200}) from Table 9 for the given surface.

3. Multiply the value obtained in Step 1 by $z_o(2/B)^{\frac{1}{2}}$.

1.5.6 Wave Theory of Shadow Zone: Constant Velocity Gradient

Although the ray theory of the shadow zone predicts that no sound rays enter into the shadow region, it is well known that sound does exist in this region. This may be explained on the basis of wave theory, since a shadow region is penetrated by sound waves diffracted across the shadow boundary. The theory of shadow zone penetration has been developed by Pekeris[32] for the case of a constant sound velocity gradient in the ocean. He found that in the shadow zone formed by the surface of the ocean, in which the sound velocity was assumed to decrease linearly with depth, the intensity of sound decreased in an exponential manner along a horizontal path. His results have been recently extended, by Ingard and Pridmore-Brown[33],

to the cases where the ground is acoustically represented by a normal impedance boundary condition, and either the sound velocity or the air temperature (sound velocity proportional to the square-root of the temperature) varies linearly with height.

In this subsection the case of the constant velocity gradient will be examined; this case is found to be solvable exactly. (Since the work in the succeeding two subsections depends upon this case the method of solution will be given in some detail.) In subsection 1.5.7, a method of approximately determining the high-frequency attenuation in the shadow zone for an arbitrary sound velocity dependence upon height will be given, and applied to the case where the sound velocity is proportional to the square root of the height (constant air temperature gradient). Since the sound velocity determined by the micrometeorological data given in subsections 1.5.2 and 1.5.3 varies approximately as the logarithm of the height (see subsection 1.5.4), the high-frequency approximation for the sound attenuation will be applied also to the sound velocity of Eq. (81).

For analytic simplicity, the case of the constant velocity gradient is best solved in an "inverted" system of coordinates, where z is positive into the ground; the ground is at $z = \gamma$; the source is at $r = 0$, $z = \sigma$ and the receiver is at P(r,z), see Fig. 18a .

The sound velocity dependence upon height is:

$$c(z) = gz \tag{95}$$

where g is the sound velocity gradient. Although the velocity goes to zero at $z = 0$, i.e., at a distance γ above the ground, this is taken care of analytically by requiring outgoing waves as z approaches zero. It is to be noted that the velocity gradient is, in practice, given by the difference in sound velocities at source and ground, divided by the source-to-ground distance, $z_o = \gamma - \sigma$:

$$g = \frac{1}{z_o}\left[c(\text{ground}) - c(\text{source})\right] \tag{96}$$

(so that the gradient used here is a positive number). The distance from the ground to the zero-velocity point, $z = 0$, is therefore

$$\gamma = \frac{c(\text{ground})}{g} \tag{97}$$

This very large distance, of the order of 1.1×10^5 feet for a typical atmospheric gradient of $g = 0.01$ sec^{-1}, is well outside the region of physical interest.

The wave equation for the pressure in the case of linear velocity

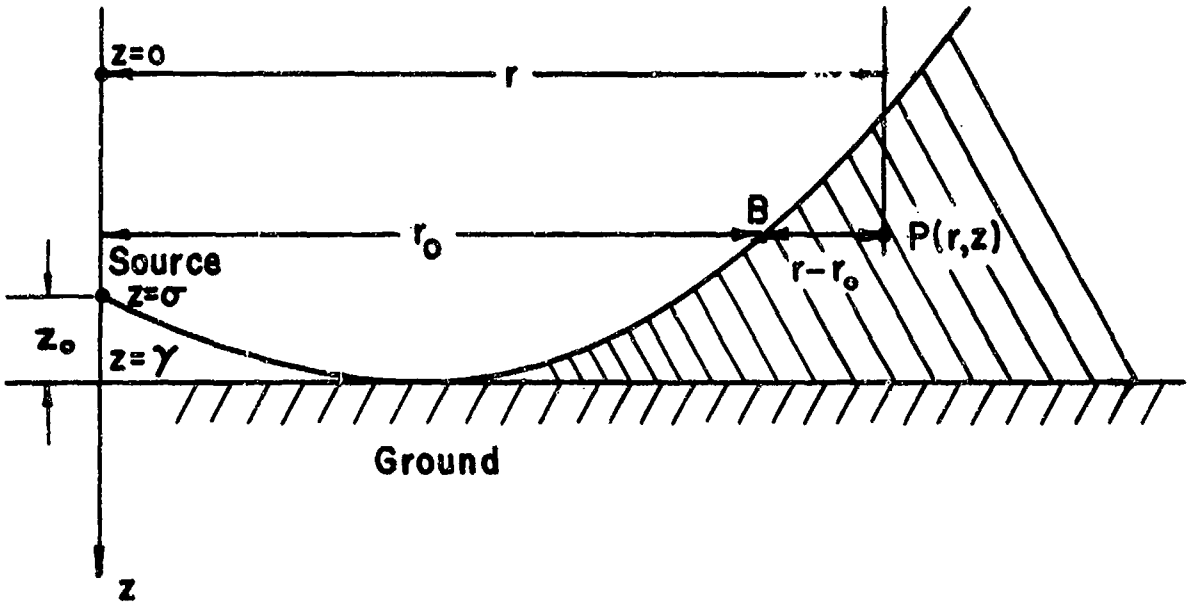

(a)

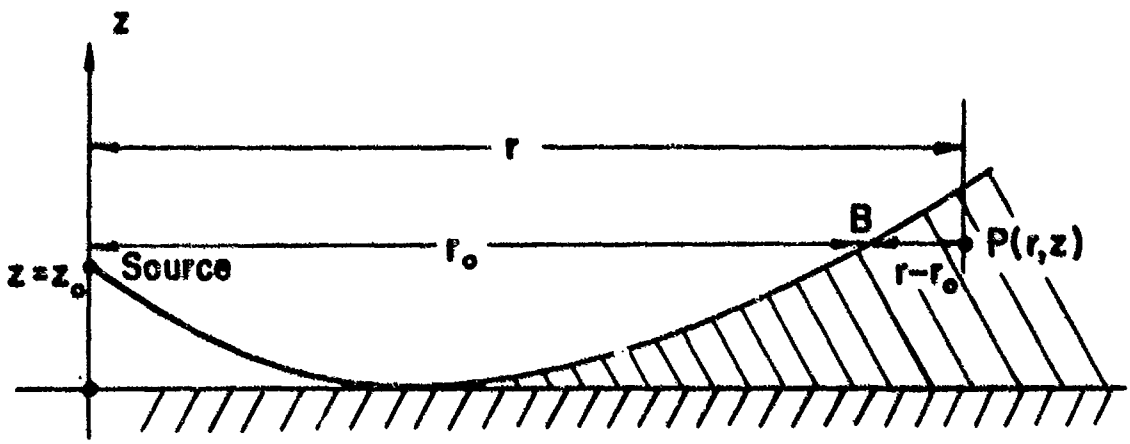

(b)

Fig. 18. Geometrical relations for the shadow zone wave theory; (a) "inverted" coordinate system for constant velocity gradient case; (b) "normal" coordinate system for constant temperature gradient case.

is

$$\nabla^2 p(r,z) + \frac{\omega^2}{g^2 z^2} p(r,z) = 0 \tag{98}$$

where the harmonic time dependence of p is $\exp(i\omega t)$. It is assumed that the ground is acoustically representable by a normal impedance condition:

$$p(r,o) = \frac{Z}{i\omega\rho}\left[\frac{\partial p(r,z)}{\partial z}\right]_{z=0} \tag{99}$$

where ρ is the density of air. By expressing the pressure as a Fourier-Bessel integral, solving the resulting z-dependent equation, and performing a contour integration, the solution may be obtained in terms of a Fourier-Bessel series[32]:

$$p(r,z) = 2\pi D \frac{(\sigma Z)^{\frac{1}{2}}}{\gamma^2} \sum_{m=1}^{\infty} \frac{H_o^{(2)}(k_m r)\, J_{in}(ik_m\sigma)\, J_{in}(ik_m z)}{\left(1+\frac{n^2}{x_m^2}\right) J_{in}^2(x_m) + J_{in}'^2(x_m)} \tag{100}$$

where D is a constant measuring the strength of the source, r is the radial distance from the source to receiver; $(\gamma-\sigma)$ is the height of the source above the ground (γ- z) is the height of the receiver above the ground; and γ is the distance from the ground to the z = 0 plane (see Eq. (97) and Fig. 18a); $H_o^{(2)}$ is the zero-order Hankel function of the second kind; J_{in} is the Bessel function of order $\underline{in}$; J'_{in} is its derivative with respect to its argument; and

$$n = \left[\frac{\omega^2}{g^2} - \frac{1}{4}\right]^{\frac{1}{2}} \tag{101}$$

The parameter x_m is the $m^{\underline{th}}$ solution (m = 1, 2, ...) of the equation:

$$J_{in}(x_m) + \left[\frac{2}{1 + \frac{2i\rho c_o \omega}{Zg}}\right] J'_{in}(x_m) = 0; \qquad x_m = ik_m\gamma \tag{102}$$

where ρ and c_o are the density and sound velocity (at the ground) of air, Z is the ground impedance, Eq. (99), and g is the velocity gradient.

In general, the series solution, Eq. (100), cannot be summed; however, for large ranges, the dependence of pressure on range can be found from the asymptotic expression for the Hankel function:

$$H_o^{(2)}(k_m r) \sim \sqrt{\frac{2i}{\pi k_m r}}\, e^{-ik_m r} \qquad k_m r >> 1 \tag{103}$$

Since the propagation constant k_m, found from Eq. (102), has a negative imaginary part which increases with increasing m, the terms of the series depend upon distance into the shadow zone as damped cylindrical waves. The attenuation coefficient of each term is given by:

$$\alpha_m = \frac{\sqrt{2}}{2} A_m \frac{\omega^{1/3} g^{2/3}}{c_o} \tag{104}$$

where the factor A_m depends upon the ground impedance and (slightly) on the frequency, and c_o is the sound velocity at the ground. Choosing a sound velocity of 1100 ft/sec, the attenuation is

$$\alpha_m = 12.5\, A_m\, g^{2/3} f^{1/3} \quad \text{db/1000 ft} \tag{105}$$

The dimensionless factors A_m are given for two different ground impedances in Table 9.

TABLE 9

Values of A_m in Eqs. (104), (105)

m	ρc-boundary	Hard boundary ($z = \infty$)
1	1.85	0.53
2	3.24	2.57
$m \geq 3$	$2.23(m - \frac{1}{4})^{2/3}$	$2.23(m - 3/4)^{2/3}$

Formulas for obtaining A_m in other cases are given in Reference 33.

Since the modes higher than the first are more strongly damped than the first mode, the propagation well into the shadow zone will be characterized by a single damped cylindrical wave of the type in Eq. (103) with an attenuation given by α_1, i.e., Eq. (104), (105), and Table 9 for $m = 1$. For the region far enough into the shadow zone so that only the first mode contributes to the sound field, the intensity at a point P(r,z) may be written as:

$$I(P) = I(B) \left(\frac{r_o}{r}\right) e^{-2\alpha_1 (r - r_o)} \tag{106}$$

where I(B) is the intensity on the shadow boundary at the same height as the receiver, r_o is the distance from source to B, r is the source-to-receiver distance, and α_1 is given by Eq. (104).

As an example, it may be noted that, for a typical gradient of $g = 0.01\ \text{sec}^{-1}$ and a 500 cps source the first mode is damped with an attenuation factor of 8.3 db/1000 ft for $Z = \rho c$, and 2.4 db/1000 ft for $Z = \infty$.

The theory of Pekeris (who considered the linear velocity case for a pressure-release surface) has been tested experimentally in underwater cases. It has been found that the attenuations predicted by the theory are greater (by less than a factor of two) than the measured values. This can be understood, since the effect of sound scattering from the rough sea surface, and from thermal inhomogeneities in the ocean, have not been taken into account; these would have the effect of increasing the sound intensity in the shadow zone. The attenuations found theoretically are therefore upper limits to the actual attenuations to be found experimentally, but probably give better than order-of-magnitude results.

1.5.7 Wave Theory of Shadow Zone: Constant Temperature Gradient

From the results of Pekeris, Ingard and Pridmore-Brown[32,33] have derived an approximate result for the shadow-zone attenuation of sound propagating over a normal impedance ground when the sound velocity is an arbitrary function of height; the approximation is valid for high frequencies.

A regular coordinate system is used (in contrast to the "inverted" one of Pekeris): the z-axis is positive upwards; the ground is at $z = 0$, the source is at $z = z_0$; and the receiver is at $P(r,z)$ (see Fig. 18b). Let the sound velocity be $c(z)$, and the velocity at the ground be $c(o)$; form the functions:

$$Q(z,\tau) = \left[\frac{\omega^2}{c^2(z)} - \frac{\omega^2}{c^2(\tau)}\right]^{\frac{1}{2}} \equiv \left[\frac{\omega^2}{c^2(z)} - k^2\right]^{\frac{1}{2}} \tag{107}$$

$$\mu(z,\tau) = \int_{\tau}^{z} Q(z,\tau)\, dz \tag{108}$$

where τ is a (complex) number to be determined. The equation:

$$\left[\frac{\mu(o,\tau)}{Q(o,\tau)}\right]^{\frac{1}{2}} H_{1/3}^{(2)}\left[\mu(o,\tau)\right] = \frac{Z}{i\omega\rho}\left[\frac{d}{dz}\left\{\left[\frac{\mu(z,\tau)}{Q(z,\tau)}\right]^{\frac{1}{2}} H_{1/3}^{(2)}\left[\mu(z,\tau)\right]\right\}\right]_{z=0} \tag{109}$$

(where Z, ω, ρ are the normal ground impedance, the angular sound frequency, and the density of air, respectively; $H_{1/3}^{(2)}$ is the Hankel function of the second kind of order 1/3) will determine an infinite number of roots τ_m. These will be, in general, dependent upon the sound frequency and the ground impedance. The (complex) propagation constant for each mode (which modes are similar to those of Eq. (100)) are given by:

$$k_m = \frac{\omega}{c(\tau_m)} \tag{110}$$

The attenuation factor for each mode is therefore:

$$\alpha_m = - \operatorname{Im} k_m \equiv - \operatorname{Im} \left[\frac{\omega}{c(\tau_m)}\right] \tag{111}$$

Well into the shadow zone only the first mode will be of importance, and the intensity will be given by Eq. (106). The above results are valid under the condition

$$Q^2 >> \frac{3}{4}\left(\frac{Q'}{Q}\right)^2 - \frac{1}{2}\frac{Q''}{Q} - \frac{5}{36}\left(\frac{Q}{\mu}\right)^2 \tag{112}$$

In reference 33, this has been applied to the case of sound propagation in a medium having a constant temperature gradient, i.e., a sound velocity of:

$$c(z) = c_o \sqrt{1 - \frac{b}{T_o} z} \tag{113}$$

where c_o is the sound velocity at the ground; T_o is the absolute temperature there; and $b = dT/dz$ is the (constant) temperature gradient. Eq. (113) gives a sound velocity gradient at the ground of:

$$g_o \equiv - \left[\frac{d\, c(z)}{dz}\right]_{z = 0} = \frac{c_o b}{2T_o} \tag{114}$$

Applying Eqs. (107) and (108):

$$Q^2 = \frac{\omega^2}{c^2{}_o \left(1 - \frac{bz}{T_o}\right)} - k^2 \tag{115}$$

$$\mu = \frac{\omega^2 T_o}{c^2{}_o\, b\, k} \tan^{-1}\left(\frac{Q}{k}\right) - \left(\frac{T_o}{b} - z\right) Q \tag{116}$$

It is found that for sufficiently high frequencies, such that

$$\omega/g_o >> 1 \tag{117}$$

Q and μ satisfy the condition Eq. (112). Letting $Q_o = Q(o,\tau)$ and $\mu_o \equiv \mu(o,\tau)$, Eq. (109) becomes, using Eq. (117):

$$\frac{i\omega\rho}{Z} \underline{v} \; Q_o \frac{H^{(2)}_{-2/3}(\mu_o)}{H^{(2)}_{1/3}(\mu_o)} \tag{118}$$

The roots $\mu_o^{(m)}$ are frequency dependent in general; however, for the case of hard ground ($z = \infty$), they are:

$$\mu_o^{(1)} = -0.685; \quad \mu_o^{(2)} = -3.90 \quad (Z = \infty) \tag{119}$$

For high frequencies, this gives attenuations of (see Eq. (111)):

$$\alpha_m = \frac{\sqrt{2}}{4}\left[-3\,\mu_o^{(m)}\right]^{2/3} \frac{\omega^{1/3} g_0^{2/3}}{c_o} \tag{120}$$

Far enough into the shadow zone so that only the first mode is of importance, Eq. (120) for m = 1 may be used in Eq. (106) for the intensity in the shadow zone.

Laboratory experiments have been performed in order to check the theoretical predictions. A small tank was heated in a manner to obtain a constant temperature gradient (b = 250°C/meter was used); measurements taken over a frequency range from 2700 cps to 10,400 cps for a hard boundary and for a ρc boundary (using glass wool) showed good agreement with theory. There seems to be little doubt that, under the idealized conditions assumed in subsections (1.5.6) and (1.5.7), the theoretical predictions will be fairly accurate.

1.5.8 Wave Theory of Shadow Zone: Logarithmic Velocity Dependence

In subsection (1.5.4) an expression for the velocity of sound (Eq. (81)) in the presence of wind and temperature varying with height was derived on the basis of the micrometeorological data of subsections 1.5.2 and 1.5.3. The problem of sound propagation in the atmosphere in the presence of a wind is no longer an isotropic one, and therefore requires the solution of a wave equation differing from the usual form, Eq. (98). It may be expected, however, that for wind velocities small compared with the sound velocity, an approximate solution may be obtained by using Eq. (81) for the sound velocity in the ordinary wave equation; an attenuation coefficient for sound in the shadow zone can therefore be derived using the methods of the previous subsection.

In the sound velocity equation, Eq. (81), the effects of wind and temperature are mixed; since the equation for the wind velocity variation with height is valid only for distances above the ground greater than ℓ, an "effective" wind velocity v_o will be used in the sound velocity equation, which will be assumed valid for $z \geq \ell$:

$$B = \frac{v_o}{c_o} \equiv m_o, \qquad z \geq \ell \tag{121}$$

$$c(z) = c_o(1 - m_o \ln \frac{z}{\ell}) \; ; \qquad z \geq \ell \tag{122}$$

where c_o is the sound velocity at $z = \ell$.

From Eqs. (107) and (108)

$$\mu = \frac{\omega}{c_o} \int_\tau^z \left\{ \left[1 - m_o \ln(z/\ell)\right]^{-2} - \left[1 - m_o \ln(\tau/\ell)\right]^{-2} \right\}^{\frac{1}{2}} dz \tag{123}$$

For small m_o, the value of μ on the ground can be approximated by

$$\mu_o \equiv \mu(\ell, \tau) \approx -\frac{2}{3} \frac{\omega \ell}{c_o} \sqrt{2 m_o} \left(\frac{\tau}{\ell} - 1\right) \ln^{\frac{1}{2}}\left(\frac{\ell}{\tau}\right) \tag{124}$$

where the value of $\mu(z,\tau)$ to be used in the boundary condition, Eq. (109), is its value at the effective ground surface $z = \ell$. For sufficiently high frequencies, and m_o not too small, it can be seen that $\tau \approx \ell$; therefore

$$\mu_o \approx \frac{2}{3} \frac{\omega \ell}{c_o} \sqrt{2 m_o} \ln^{3/2}(\ell/\tau) \tag{125}$$

This satisfies the condition for the validity of the approximation method Eq. (112), for

$$\frac{\omega \ell m_o}{c_o} >> 1 \tag{126}$$

The boundary condition, Eq. (107), for determining the roots $\mu_o^{(m)}$ is:

$$\frac{i\omega\rho}{Z} = \left(\frac{3\mu_o m_o}{\ell}\right)^{1/3} \left(\frac{\omega}{c_o}\right)^{2/3} \frac{H_{-2/3}(\mu_o)}{H_{1/3}(\mu_o)} \tag{127}$$

The roots are frequency dependent in general; however, for $Z = \infty$ they are:

$$\mu_o^{(1)} = -0.685 \; ; \qquad \mu_o^{(2)} = -3.90 \quad (Z = \infty) \tag{128}$$

The attenuation, from Eq. (110), (111), and (124) is:

$$\alpha_m = \frac{\sqrt{3}}{4}\left[-3\mu_o^{(m)}\right]^{2/3} \frac{\omega^{1/3} g_o^{2/3}}{c_o} \quad , \quad g_o = \frac{c_o m_o}{\ell} \tag{129}$$

where g_o is the sound velocity gradient at the surface. This expression will be compared with data in subsection (2.3.3).

It is to be noted that all of these high-frequency approximations to the attenuation coefficient, Eq. (104), (120), (129), have the same dependence upon frequency and sound velocity gradient; however, in view of some of the results of Pekeris, this should not be considered as a general result for all frequencies of interest. It may be expected, for

example, that changes of the velocity-height profile from the simple models used above, may markedly change the frequency dependence of the attenuation, especially at the lower frequencies.

1.5.9 Intensity in the Normal Zone; Channelling

In the three previous sections, expressions for the sound pressure due to a point source in a stratified medium were developed by means of wave theory; the expressions, given in terms of infinite series, were shown to be useful only inside the shadow zone, where only the first term of the series is of importance. There has been no such simple solution found for the "normal zone", i.e., the region between the source and the shadow boundary.

The ray-theory approximation to the normal zone sound field, valid for infinitely-high frequency, can be developed for an infinite medium. By means of appropriate images, the effect of a hard (or soft) boundary should be obtainable; however, non-infinite (and non-zero) impedance boundaries present special difficulties, and the problem of boundary effects needs investigation.

The sound intensity at a point P(r,z) in an infinite stratified medium, associated with the ray making an angle with the horizontal of θ_o at the source, see Fig. 14b, (i.e., the power per unit area at P carried between rays emerging from the source between angles θ_o and $\theta_o + d\theta_o$ and reaching P between angles θ and $\theta + d\theta$) is given by Reference 34:

$$I(r,z,\theta_o) = - \frac{F \cos\theta}{r(dr/d\theta_o)\sin\theta} \tag{130}$$

where F is the source power per unit solid angle; θ and θ_o are connected by Snell's law, Eq. (82), and r is the horizontal distance from the source (see Eq. (83)):

$$r = - \frac{c_o}{\cos\theta_o} \int_{\theta_o}^{\theta} \frac{\cos\theta \, d\theta}{(dc/dz)} \tag{131}$$

For the case of the constant sound velocity gradient (c = az), using the "inverted" coordinates of Fig. (18a), we obtain:

$$I = \frac{F\cos^2\theta_o}{4\pi r^2} \quad ; \qquad r = \frac{\sigma}{\cos\theta_o} (\sin\theta_o - \sin\theta) \quad \text{for } c = az \tag{132}$$

where $\sigma (= c_o/a)$ is the distance from the source to the z = o plane (see subsection 1.5.6). (It is to be noted that, for the intensity at a point P(r,z), one determines that value of θ_o which satisfies the second of Eqs. (132) and Snell's law, and uses this value of θ_o in the first of Eqs. (132).)

Due to the complexity of the equation of a ray traveling in a medium where the sound velocity depends logarithmically upon height (see Eq. (84)), it is doubtful that useful results can be obtained for this case by the above methods of analysis.

In the case of a sound velocity which increases with height above the ground (e.g., a temperature inversion), the sound rays are bent downward after leaving the source, and will all reach the ground after traveling some distance from the source; the distance will depend upon the sound velocity gradient and the angle of emission of the ray. Upon reflection from the ground, the process will be repeated, causing the sound rays to be periodically reflected from the ground as they travel outward from the source. This phenomenon, known as "channelling", can bring about a greater sound intensity at large distances from the source, than would be predicted by a simple inverse-square law. An analysis of this effect for the case of constant sound velocity gradient based on Pekeris' work, has been done by Haskell[35], but the results have not yet been extended to other cases of interest.

1.6 EFFECT OF RANDOM TEMPERATURE AND WIND INHOMOGENEITIES

1.6.1 Introduction

The effects on the propagation of sound of the height dependence of air temperature and wind velocity were discussed in subsection 1.5. There it was implicitly assumed that this height dependence (almost logarithmic) was constant in time and space, that is, a given height dependence was assumed to be independent of time and of horizontal position. Experimentally, it is found that the average temperature and wind velocity (speed and direction) are describable by a simple height dependence, but that there are variations about these mean values; these variations, or sound velocity inhomogeneities, are dependent upon time and position (horizontal and vertical), and lead to sound scattering, and the associated phenomena of intensity variations and fluctuations. An important characteristic of the inhomogeneities is their randomness, or irregularity in space and time.

If a sound beam passes through a region which contains inhomogeneities, i.e., one in which the sound velocity varies randomly about its mean value, sound may be scattered out of the beam, causing a decrease in intensity. Moreover, sound scattered from a sound field by inhomogeneities may cause an increase in intensity, at some points, above what would be ex-

pected in the absence of scattering; it is believed that the scattering of sound across the shadow boundary is responsible for the observation that sound intensities in the shadow zone are considerably higher than predicted by theory.

Since the inhomogeneities are time-dependent, that is, the magnitude of the deviation from the mean sound velocity depends upon time, the combination of "directly-received" and scattered sound will be time-dependent; the total received intensity will therefore change with time. The variations of the intensity may be subdivided into two types: "slow variations" or changes in the average intensity taking place over a period of minutes or more; and "fluctuations", or changes in intensity about the (slowly varying) mean value, taking place in a period of seconds, or less. (Obviously these definitions overlap, since they are two aspects of the same general phenomenon.) This division is useful from a practical point of view, since the variations in mean sound intensity may be expected to depend upon large-scale changes in sound conditions, e.g., changes in "average" wind velocity, while the fluctuations will depend upon the small-scale changes, or inhomogeneities, e.g., short gusts of wind.

Existing theoretical analyses of the effects of inhomogeneities usually do not take account of the presence of boundaries (the ground) or of the dependence of the mean sound velocity with height. It is often assumed (because of mathematical difficulties) that after the mean sound pressure is determined by using the mean sound velocity (varying with height), the effect of inhomogeneities may be given by assuming an infinite medium with a constant mean sound velocity (independent of height). It is expected that this should give, in most cases, the order of magnitude of the effect, and its dependence upon important parameters, such as sound frequency. Since the inhomogeneities are random functions of space and time, the effects due to them will also be random. Theoretical treatments of these effects are therefore designed to give information about average values, and root-mean-square deviations from average values.

After a short description of the methods of averaging used, the types of temperature and wind inhomogeneities to be expected in the atmosphere near the earth will be discussed; the analysis of specific problems will then follow.

1.6.2 Averages and Correlation Functions[36]

Consider a random function of space and time, $f(x,y,z,t)$, that is, a function whose value, at a point in space and at a given time, depends upon the variables $(x,y,z) \equiv \underline{r}$ and t in such an irregular manner that the relationship between values at two points (in space and time)

can be given only statistically. The time average, or mean, value of f is given by:

$$\bar{f}(\underline{r};\, T,\, t_o) = \frac{1}{T}\int_{t_o-\frac{1}{2}T}^{t_o+\frac{1}{2}T} f(\underline{r},\, t)\, dt \qquad (133)$$

In general, the average value will depend upon the time at which the average is taken, t_o, and upon the sampling length, T, as well as the position r. This dependence on t_o and T will obviously be of importance; for example, if $f(\underline{r},t)$ is a component of the wind velocity at a point, the average value of the wind will depend upon whether t_o is taken during a time of "strong" or "weak" wind, and whether T is large enough to take account of gross changes in wind speed, or just short gusts.

The time of averaging and the sampling length are closely connected to the type of changes considered, i.e., "slow variations" or "fluctuations". It is assumed in the theoretical developments to follow, that the length of time T is sufficiently long to include many short-time changes (fluctuations) in $f(\underline{r},t)$, but short enough so that any long-time changes (slow variations) in $f(\underline{r},t)$ take place in a length of time much larger than T. In this case, the average value $\bar{f}(\underline{r};\, T,\, t_o)$ will not depend upon T, but only upon the time of averaging; the fluctuations are then considered as deviations from the slowly varying average value. Since, in general, the slow variations will be assumed to depend upon large scale changes, they will not be of particular interest here; in the study of fluctuations, the averaging process may therefore be taken as though the mean value does not change. This mean value is therefore:

$$\left\langle f(\underline{r},t)\right\rangle = \lim_{T\to\infty} \frac{1}{2T}\int_{-T}^{T} f(\underline{r},t)dt \qquad (134)$$

Since the function $f(\underline{r},t)$ is assumed to be a random function of space as well as time, the same considerations hold in the case of a space average as held for the time average; the average should be taken over a volume large enough to include many small changes in $f(\underline{r},t)$ at any instant of time, but not so large as to include large-scale changes (e.g., the average should be over a region of space containing many gusts of wind, but such that every gust is "traveling" in a wind having the same velocity as the others):

$$\left\langle f(\underline{r},t)\right\rangle_V = \lim_{V\to\infty} \frac{1}{V}\int_V f(x,y,z,t)\, dx\, dy\, dz \qquad (135)$$

Measurements in acoustics usually involve sound pressure at a

point in space as a function of time, so that use of the time-averaging process in theories gives results more closely related to experiment than use of space averages[37]. However, since the theoretical developments are usually based upon "stationary" random variables, that is, variables whose average does not depend upon the time about which the time average is taken or upon the position about which the space average is taken (statistical homogeneity), both will give the same value for the average, that is, $\langle f \rangle = \langle f \rangle_V$, and the average does not depend upon position or time. This may be visualized by considering a wind with many gusts; for the time average, a stationary recording instrument averages over all the gusts carried past by the mean wind; for the space average, many recording instruments are used, placed throughout space, and the average taken by using the readings of all the instruments at one instant of time.

As will be seen in the next section, however, the micrometeorological variables are not statistically homogeneous, since they depend upon height above the ground; the time average will probably be the more useful one in theories using this fact.

The deviation from the mean is defined as:

$$\Delta_f(\underline{r},t) = f(\underline{r},t) - \langle f \rangle \tag{136}$$

The deviation has a mean value of zero. (When there is no chance of confusion the subscript will be dropped: $\Delta(\underline{r},t) \equiv \Delta_f(\underline{r},t)$.)

A measure of the randomness may be found by averaging the product of the deviation at a point in space at one time and the deviation at another point in space at another time:

$$\langle \Delta(\underline{r},t)\, \Delta(\underline{r}+\underline{\rho},\, t+\tau) \rangle = \lim_{T\to\infty} \frac{1}{2T} \int_{-T}^{T} \Delta(\underline{r},t)\Delta(\underline{r}+\underline{\rho},\, t+\tau)dt \tag{137}$$

where $\underline{\rho}$ is the vector distance between the two points in space, and τ is the time interval; the mean-square value of the deviation occurs for $\underline{\rho} = 0$, $\tau = 0$. As noted above, it is usual in the theoretical work to make the assumption of statistical homogeneity; the average in Eq. (137) will then depend only upon $\underline{\rho}$ and τ, the interval in space and time between the points whose deviations are being averaged.

If the function $f(\underline{r},t)$ is random, it may be expected that large values of the average appearing on the left hand side of Eq. (137) occur for small values of $\underline{\rho}$ and τ, since, if $\Delta(\underline{r},t)$ has some value, $\Delta(\underline{r}+\underline{\rho},\, t+\tau)$ will have "almost" the same value for small $\underline{\rho}$, τ: if $\Delta(r,t)$ has one sign (positive or negative), $\Delta(\underline{r}+\underline{\rho},\, t+\tau)$ will "most probably" have the same sign and the average will be made up of a series of positive terms. For large $\underline{\rho}$ or τ, the values of $\Delta(\underline{r}+\underline{\rho},\, t+\tau)$

should bear little relation to the values of $\Delta(\underline{r},t)$: for a given sign of $\Delta(\underline{r},t)$, the sign of $\Delta(\underline{r}+\underline{\rho}, t+\tau)$ may be positive or negative with "almost equal probability". The average, for large $\underline{\rho}$ or τ will therefore be made up of a series of terms having positive or negative signs with "almost equal probability"; the average therefore tends to zero for large $\underline{\rho}$ or τ. (If there is a periodicity in Δ, the average will also tend to be periodic; this is, however, excluded from truly random functions.)

The "correlation function" is defined by normalizing the average to a maximum value of unity:

$$R(\underline{\rho},\tau) = \frac{\langle \Delta(\underline{r},t)\, \Delta(\underline{r}+\underline{\rho}, t+\tau)\rangle}{\langle \Delta(\underline{r},t)\, \Delta(\underline{r}, t)\rangle} \tag{138}$$

Since the correlation function is often used for the case $\tau = 0$, the notation $R(\underline{\rho})$ will be used for $R(\underline{\rho},0)$. Under the condition of statistical homogeneity, $R(\underline{\rho},\tau)$ is a function of the vector distance, $\underline{\rho} = (\xi, \eta, \zeta) = (x_2-x_1, y_2-y_1, z_2-z_1)$, between the positions at which the deviations are taken; for the case of "isotropic homogeneity", $R(\underline{\rho},\tau) \equiv R(\rho,\tau)$ is a function of the magnitude of the distance between the points ($\rho = |\underline{\rho}|$), and does not depend upon direction.

Since it is expected that the correlation function goes to zero as either $\underline{\rho}$ or τ go to infinity, they may be integrated from zero to infinity over either variable. Thus may be defined, for the correlation function in general, characteristic lengths and a characteristic time. For the case of isotropic inhomogeneities, the characteristic length is:

$$\rho_o = \int_0^\infty R(\rho,0)\,d\rho \tag{139}$$

with corresponding definitions for characteristic lengths in the x, y or z directions for the anisotropic correlation function. The characteristic time is:

$$\tau_o = \int_0^\infty R(0,\tau)\,d\tau \tag{140}$$

1.6.3 Temperature Variations and Fluctuations

Although the slow variations in temperature are to be considered as relatively unimportant in the problems of sound scattering (since these are related to the "slowly varying" mean value of the received sound pressure), it seems best to discuss variations and fluctuations of temperature together, since they are the large-scale and small-scale aspects of the same problem of temperature changes.

As noted in subsection 1.5.2 and Fig. (13) the temperature gradient changes in size and sign during a 24-hour period. Table 10

TABLE 10

Diurnal temperature variations at various heights above the ground (note that the heights used are different for the two locations); from Sutton: Micrometeorology.

	Porton, England		Leafield, England	
Month	Height (meters)	Diurnal Variation (°C)	Height (meters)	Diurnal Variation (°C)
December	0.025	3.7	1.20	3.2
	0.30	3.3	12.40	2.2
	1.20	3.1	30.50	1.6
	7.10	2.7	57.40	1.2
	17.10	2.4	87.70	0.9
June	0.025	11.8	1.20	10.8
	0.30	10.2	12.40	8.8
	1.20	9.4	30.50	8.1
	7.10	8.3	57.40	7.4
	17.10	7.7	87.70	7.0

shows the diurnal variation of the temperature (in °C), at various heights above the ground, on clear days in Porton (open meadows) and Leafield (hilly pasture lands), England. As might be expected, the variations are greatest near the ground; the rate of decrease with height of the diurnal variation is much greater in summer than in winter. By expressing the temperature deviation from the mean by the first two terms of a Fourier series in time, the coefficients (which will be functions of the height) may be found:

$$\Delta T(z,t) = c_1 \sin(15t + \phi_1) + c_2 \sin(30t + \phi_2) \qquad (141)$$

In this expression the time, t, is expressed in hours past midnight, and the argument of the sines are in degrees (1 hour = 15 degrees); the values of the coefficients, c_1 and c_2 and the phase angles ϕ_1 and ϕ_2 are given

as functions of the height for Porton, England, and Ismailia, Egypt (near desert conditions) in Table 11. The summer conditions at Porton indicates that the temperature variation there can be represented, to a good approximation, by a single sinusoidal term in time; this is not true of the other conditions, however,

TABLE 11

Coefficients and phase angles for first two terms of a Fourier series representing the diurnal temperature variations at various heights above the ground (note that the heights used are different for the two locations, as well as the type of day used); from Sutton: Micrometeorology.

Month	Height (meters)	c_1(°C)	ϕ_1	c_2(°C)	ϕ_2
		Porton, England			
December (all days).	0.025	1.37	244°	0.84	59°
	0.30	1.23	238°	0.72	55°
	1.20	1.16	233°	0.64	52°
	7.10	1.03	225°	0.54	45°
	17.10	0.93	218°	0.46	40°
June (all days)	0.025	5.78	246°	0.48	108°
	0.30	5.14	238°	0.29	107°
	1.20	4.72	235°	0.25	110°
	7.10	4.10	228°	0.28	107°
	17.10	3.76	223°	0.31	103°
		Ismailia, Egypt			
December (clear days)	1.10	6.40	228°	1.97	61°
	16.20	4.06	219°	1.32	42°
	46.40	2.49	209°	0.98	28°
	61.00	1.94	204°	0.92	27°
August (clear days)	1.10	6.56	225°	1.41	50°
	16.20	5.28	219°	1.30	42°
	46.40	4.82	218°	1.41	31°
	61.00	4.69	219°	1.41	28°

There has been little experimental work concerned with the fluctuations of temperature. Sutton[38] reports, from a single set of observations at Leafield, England, that the magnitude of the temperature deviation from the mean varies approximately as $z^{-0.4}$, where z is the height above ground; however, this should not be considered as a general result.

There is some experimental evidence, which has a strong theoretical basis, that heat may be transferred by "bubbles" of warm air rising from the ground due to their buoyancy; this would be expected to take place under conditions of warm clear weather with a low wind, so that the ground becomes quite hot. The mean temperature field at any height would be closely related to the time-averaged effect of these bubbles' passage past a point. Sutton[39] estimates, from the Leafield data, that about four bubbles per minute rise from the ground, having a velocity of about 25 cm/sec at a height of 2 meters; the heat capacity per bubble, if the latter are assumed as planes, is about 0.05 cal/cm^2.

It may be expected that the temperature fluctuations are strongly related to such factors as temperature gradient, solar radiation, and wind fluctuations; the amount of data, however, is small, and is not in a form which can be used in the theoretical work (i.e., correlation functions). A statistical analysis of recent data should give useful parameters for the acoustical problems.

1.6.4. Wind Fluctuations

There is somewhat more known about the fluctuations in wind velocity than about temperature fluctuations, but not much of what is known is readily applicable to the theories of acoustic scattering. In an analysis of turbulence over meadows (by Scrase, quoted by Sutton[40]), it has been found that of the total turbulent energy associated with wind fluctuations, at least two thirds of the energy is associated with fluctuations lasting, at a point, less than five seconds. Fluctuations lasting for the order of a few minutes are found, as well as variations of a much larger time scale.

In general, it is found that the fluctuations in wind speed (in the x, y, and z directions) are approximately proportional to the mean wind speed, for small temperature-gradient conditions, at heights above about 20 meters from the ground. Below this height, the average magnitude (without regard to sign) of the fluctuations in the direction of the wind and across the wind are about equal, but the vertical fluctuation is somewhat smaller than the others; at heights of about 2 meters, the root-mean-square cross-wind fluctuation is more than two times greater than the root-mean-square vertical fluctuation.

The "gustiness" may be defined as the average magnitude of the speed fluctuations, in the x, y, and z directions, divided by the mean wind speed:

$$g_x = \frac{\langle |u - \langle u \rangle| \rangle}{\langle u \rangle} ; \; g_y = \frac{\langle |v| \rangle}{\langle u \rangle} ; \; g_z = \frac{\langle |w| \rangle}{\langle u \rangle} \qquad (142)$$

where u, v, w are the components of the instantaneous wind velocity in the x, y, z directions, respectively, $\langle u \rangle$ is the mean wind speed (taking the x-axis along the mean wind direction, and $\langle v \rangle = \langle w \rangle = 0$.) The gustiness is, therefore, a measure of the speed fluctuations in the direction of the mean wind and the fluctuation in mean wind direction (from g_y and g_z).

Best[41] has evaluated g_x for winds over a level field with grass from 1 to 2 cm high; the averages were computed by taking readings of the instantaneous wind velocity every ten seconds for a total time of three minutes. The experiments were conducted under the following conditions; height above ground varied from 2.5 to 200 cm; mean wind speeds (at a height of 200 cm) varied from 50 to 800 cm/sec; temperature gradients (between 10 and 110 cm height) varied from -0.015 to 0.01°C/cm. It was found g_x varied from 0.1 to 0.2, and was approximately independent of the mean wind (so that the average magnitude of the deviation is about 10 to 20% of the mean wind). The frequency of occurrence of values of g_x had no well-defined variation with height in the above range; it was independent of the temperature gradient for measurements of g_x between 2.5 and 10 cm above ground, but above 25 cm, g_x decreased as the temperature gradient went from negative to positive.

There is less information about the lateral (cross-wind) and vertical gustiness g_y and g_z; at 200 cm above grassland the maximum values of g_y and g_z are nearly independent of mean wind speed for negative temperature gradients, but increase sharply with increasing wind speed for positive gradients; for constant mean wind, both g_y and g_z decrease as the temperature gradient goes from negative to positive values. Under all conditions, at this height the ratios of the maximum values of g_y to g_z is about 1.8. As a function of height, the ratio of the maximum values of g_y to g_z was found to vary from about 2.9 at 25 cm to 1.4 at 506 cm; as noted above, the ratio is about unity for heights above 20 meters.

Sutton has shown, from data taken at 200 cm above grassland (grass up to 30 cm high), that the autocorrelation function (correlation between velocity fluctuation affecting a particle at time t and $t + \xi$) may be given by:

$$R(\xi) = \left(\frac{N}{N + \langle \Delta^2 \rangle \xi}\right)^n ; \qquad (143)$$

$N = 100$ cm/sec, $n = 0.15$; $\langle \Delta^2 \rangle = 6.51 \times 10^3$ cm/sec

This autocorrelation function is approximately related to the previously defined correlation function, subsection 1.6.2 by $R(\xi) \cong R(\langle u \rangle \xi, \xi)$, since a particle travels a distance $\langle u \rangle \xi$ in time interval ξ.

1.6.5 Scattering of Sound by Temperature Inhomogeneities

The problem of the scattering of a plane sound wave by temperature inhomogeneities has been solved by Pekeris[42], and the corresponding attenuation of a sound beam due to scattering, by Jacomini.

Consider a medium whose sound velocity has a mean value of c_o, and which has small random variation in space about the mean:

$$c(x,y,z) = c_o + \Delta c(x,y,z); \qquad \langle c \rangle = c_o; \ \frac{\Delta c}{c_o} \ll 1 \tag{144}$$

The wave equation for the pressure amplitude is, approximately,

$$\nabla^2 p + k^2 p = 2k^2 \left(\frac{\Delta c}{c_o}\right) p \quad ; \qquad k = \frac{\omega}{c_o} \tag{145}$$

The solution for an initial plane wave of sound traveling in the z direction is (assuming a time dependence of exp $[-i\omega t]$):

$$p(x,y,z) = e^{ikz} - \frac{k^2}{2\pi} \int \frac{\Delta c(x',y',z')}{c_o} \, p(x'y'z') \, \frac{e^{ikr'}}{r'} \, dv' \tag{146}$$

where (x,y,z) is the observation point, $\exp(ikz)$ is the initial plane wave, and the integral gives the scattered pressure contribution from the inhomogeneities; (x', y', z') is the position of a scatterer, and $r'^2 = (x-x')^2 + (y-y')^2 + (z-z')^2$. Since the magnitude of the velocity changes are assumed small, the pressure amplitude in the integral may be approximated by the initial plane wave. The power scattered into an infinitesimal solid angle $d\Omega = \sin\theta \, d\theta \, d\phi$ (where (r, θ, ϕ) are the spherical coordinates of the observation point (x,y,z)) at a large distance from the scattering volume is

$$E d\Omega = \frac{1}{\pi} I_o k^4 \, d\Omega V \left\langle \left(\frac{\Delta c}{c_o}\right)^2 \right\rangle \int_o^\infty R(\rho) \frac{\sin(2K\rho)}{2K\rho} \rho^2 d\rho \ ; \tag{147}$$

$$K = k \sin \theta/2$$

where I_o is the intensity of the initial plane wave, V is the volume of the medium containing the scatterers, and the space-correlation function is (see Eq. (132) for $r = 0$)

$$R(\xi,\eta,\zeta) = \frac{1}{\left\langle \left(\frac{\Delta c}{c_o}\right)^2 \right\rangle} \left\langle \left[\frac{\Delta c(x,y,z)}{c_o}\right] \left[\frac{\Delta c(x+\xi,\ y+\eta,\ z+\zeta)}{c_o}\right] \right\rangle \quad (148)$$

and statistical isotropy has been assumed:

$$R(\rho) = R(\xi,\eta,\zeta) \ ; \qquad \rho = \left[\xi^2 + \eta^2 + \zeta^2\right]^{\frac{1}{2}} \quad (149)$$

The plane wave attenuation coefficient may be found in the following manner: by integrating Eq. (147) over all angles (assuming that the angular spread of the initial beam is zero) the total power scattered by the inhomogeneities in the volume V may be found; the intensity attenuation coefficient, 2α (using α as the amplitude attenuation coefficient) is the ratio of the power scattered out of V to the power entering V. For initial intensity I_o, this is

$$2\alpha = \frac{1}{I_o V} \int E \, d\Omega \quad (150)$$

Using Eq. (147), this becomes:

$$2\alpha = 2k^2 \left\langle \left(\frac{\Delta c}{c_o}\right)^2 \right\rangle \int_o^\infty R(\rho) \left[\cos(2k\rho) - 1\right] d\rho \quad (151)$$

For a correlation function:

$$R(\rho) = e^{-\rho^2/a^2} \quad (152)$$

the intensity attenuation coefficient is:

$$2\alpha = \sqrt{\pi} \left\langle \left(\frac{\Delta c}{c_o}\right)^2 \right\rangle k_o^2 \, a\left(1 - e^{-k_o^2 a^2}\right) \quad (153)$$

This attenuation, increasing approximately as the square of the frequency, has not been well checked as yet by experimental work. Under the assumption of the Gaussian correlation function, Eq. (152), the scattered radiation has a directionality pattern proportional to $\exp\left[-a^2k^2 \sin^2(\theta/2)\right]$, so that its half-power point occurs at angles from the incident beam axis of

$$\theta = \pm 2 \sin^{-1}\left(\frac{\ln 2}{ak}\right)^{\frac{1}{2}} \text{ radians} = \pm \frac{95}{ak} \text{ degrees} \quad (154)$$

where (ak) is assumed large (sound wavelength small compared with inhomogeneity size); for audible frequencies, θ will usually be no more than a few degrees. Since the scattering angles, Eq. (154) are so small, it is to be expected that higher-order scattering would send sound back into the acoustic beam and hence decrease the effective attenuation. Eq. (153) is therefore, probably, an upper limit to the attenuation.

A somewhat more general development of plane-wave scattering theory has been given by Ellison[43] who considers the correlation between the intensity received at two points in a plane perpendicular to the direction of the incoming wave. Since there does not seem to be much application of this theory to the air acoustics problem the results shall not be given; it should be noted, however, that contributions to the Fourier transform of the intensity correlation function at a particular wave number comes from the same wave number of the Fourier transform of the refractive index correlation function.

A ray theory of attenuation due to scattering, arising from the use of a directional receiver, has been developed by Givens[44], et. al; in view of the discrepancies[45],[46] between ray and wave theories for the general scattering problem, there is some doubt as to whether this method is applicable quantitatively in atmospheric acoustics problems.

1.6.6 Fluctuations due to Temperature Inhomogeneities

Since the temperature inhomogeneities (as well as the wind inhomogeneities) change with time, the received scattered pressure will also change with time. If a series of sound pulses are received, the pressure amplitude of each pulse varies rapidly with time, and the time-average amplitude varies from pulse to pulse in a random manner about a mean value. A theory has been developed by Mintzer[45] for the fluctuation of the mean pulse amplitude from a point source of sound (in an infinite medium), and has been compared with underwater measurements. It is assumed in the development that the sound velocity at a point varies slowly enough with time, so that there is little change in sound velocity during the passage of a pulse past the point; this is found to be true if the pulse length T is much less than the characteristic period τ_o of the inhomogeneity (see Eq. (140), and if the characteristic length $\underline{a}$ (Eq. (139)) and period τ_o are related by $a/\tau_o << c_o$, where c_o is the mean sound velocity.

The method of analysis is similar to that of the previous section, except that the pressure fluctuations considered are those of the average pressure amplitude of a pulse, $\bar{p}$, and an initial spherical wave is assumed. If the coefficient of variation, V, is defined as the ratio of the standard deviation from the mean to the mean pressure amplitude

$$V^2 = \frac{\langle | \bar{p} - \langle \bar{p} \rangle |^2 \rangle}{|\langle \bar{p} \rangle|^2} \tag{155}$$

It is found that (for distances from the source large compared with the characteristic length)

$$V^2 = 2k^2 \sigma^2 r \int_0^\infty R(\xi) d\xi \tag{156}$$

where r is the distance from source to receiver, and

$$\sigma^2 R(\xi) = \left\langle \left[\frac{\Delta c(x,y,z,t)}{c_o}\right] \left[\frac{\Delta c(x+\xi, y, z, t)}{c_o}\right] \right\rangle \tag{157}$$

Here x is the coordinate along the line from source to receiver and σ is the rms value of $\Delta c/c_o$. For a Gaussian correlation function

$$R(\xi) = e^{-\xi^2/a^2} \tag{158}$$

the coefficient of variation is, for $k_o a >> 1$ (wavelength small compared with inhomogeneity size)

$$V = \left[\sqrt{\pi}\, k_o^2 \sigma^2 a\right]^{\frac{1}{2}} r^{\frac{1}{2}} \tag{159}$$

This formula has been subject to test in the underwater case[45], where acoustic measurements were made in deep water using 24 kc sound;[47] measurements have also been made[48] of the rms value of $\Delta c/c_o$, and of $\underline{a}$, the correlation distance. The theory and experiments agree very well.

The above work has been extended[49] to determine the time dependence of the fluctuation in pulse amplitude. Let the correlation function of the deviation from the mean pulse amplitude at a point in space be

$$\Phi(\tau) = \frac{\langle \Delta p(\underline{r},t)\ \Delta p(\underline{r}, t+\tau) \rangle}{\langle [\Delta p(\underline{r},t)]^2 \rangle} \tag{160}$$

and the correlation function of the deviation from the mean sound velocity be

$$R(\tau) = \left\langle \left[\frac{\Delta c(x,y,z,t)}{c_o}\right] \left[\frac{\Delta c(x,y,z,t+\tau)}{c_o}\right] \right\rangle \tag{161}$$

It is found that

$$\Phi(\tau) = R(\tau) \tag{162}$$

so that (under the conditions noted in the first paragraph of this subsection) a measurement of the correlation of successively received signals should give the time correlation of the velocity changes.

1.6.7 Scattering of Sound by Wind Inhomogeneities. I

As was noted in subsection 1.5, the interaction of sound waves with a wind is an anisotropic problem, and is therefore of a considerably more difficult nature than the problem with a variable temperature; this is reflected in the fact that a single scalar potential for the particle velocity cannot be used in the case of a wind, but that a vector potential must be introduced as well. However, Obukhov[50] has, by introduction of a suitably defined scalar "quasipotential", developed a simple method of taking account of vortical flow for flows of small Mach number (flow velocity much less than sound velocity). Using this method, Blokhintzev[51] has developed a single scattering approximation for the attenuation of a plane sound wave due to scattering from a turbulent region. The power scattered from a plane wave directed along the z-axis by a volume V of the turbulent medium into an infinitesimal solid angle $d\Omega$ becomes:

$$Ed\Omega = \frac{1}{4\pi^2} I_o k_o^4 \, d\Omega \, V \frac{1}{c^2} \left\langle (v_z)^2 \right\rangle \int_V dV \, e^{i(\underline{K}\cdot\underline{\rho})} \left[M_{zz}(\rho) + \frac{1}{k_o^2}\nabla^2 M_{zz}(\rho) + \frac{1}{4k_o^4}\nabla^2\nabla^2 M_{zz}(\underline{\rho}) \right] \tag{163}$$

where the vector $\underline{K}$ is given in terms of the unit vectors in the direction of the incident wave $\underline{i}_z$ and the scattering direction $\underline{n}$ (at spherical coordinate angle θ from the z-axis):

$$\underline{K} = k(\underline{n} - \underline{i}_z) \; ; \quad |\underline{K}| = 2k \sin(\theta/2) \tag{164}$$

and the correlation function of the z-component of the turbulent velocity (that is, the turbulent velocity component in the direction of the incident wave) is defined as:

$$\left\langle (v_z)^2 \right\rangle M_{zz}(\underline{\rho}) = \left\langle v_z(\underline{r}) \, v_z(\underline{r} + \underline{\rho}) \right\rangle \tag{165}$$

In general, the correlation function depends on the direction, as well as the magnitude of $\underline{\rho}$.

From dimensional considerations, and noting that, to the approximation ($v/c << 1$), used in deriving the above expression, the flow is incompressible, Blockhintzev derives a correlation function

$$M_{zz}(\underline{\rho}) = \gamma \int_{q>q_o} e^{-i(\underline{q}\cdot\underline{\rho})}\, q^{-11/3} \left(1 - \frac{q_1^2}{q^2}\right) dq_1 dq_2 dq_3 \left\langle (v_z^2) \right\rangle^{-1} \quad (166)$$

where γ is a constant estimated at about 0.2 (by Obukhov), and the integration is over values of the turbulent field wave number q greater than a value q_o where

$$\left(\frac{2\pi}{q_o}\right)^3 \simeq V \quad (167)$$

(The "constant" γ presumably depends upon wind speed.)
This restriction on the minimum value of the turbulent wave number, is equivalent to a restriction on the maximum value of the wavelength associated with the turbulence; i.e., the turbulent wavelengths of interest should be less than a representative length of the scattering volume ($V^{1/3}$); any larger scale turbulence will have an essentially constant velocity over the scattering region and will not contribute.

Using Eq. (166) in Eq. (163), and determining the intensity attenuation coefficient as in subsection 1.6.5, Eq. (150)

$$2\alpha = \frac{3}{5}(2\pi)^{1/3}\, \mu^{5/3} \left(\frac{2\pi\gamma^{\frac{1}{2}}\lambda^{1/3}}{c_o}\right)^2 \frac{1}{\lambda} \quad (168)$$

where μ is a dimensionless parameter much greater than unity and λ is the sound wavelength. Using data of Sieg's (to be discussed in Section II) Blokhintzev evaluates μ to be equal to 10 (a reasonable value); the weak frequency dependence (as $f^{1/3}$) "does not contradict Sieg's experimental results"[51]. This result should be the subject of further experiments.

1.6.8 Scattering of Sound by Wind Inhomogeneities. II

A more exact formulation than Blockhintzev, of the scattering of sound by turbulence (i.e., wind inhomogeneities), has been given by Lighthill[52] and independently by Kraichnan[53], based on the general theory of the interaction of sound and turbulence by Lighthill.

Lighthill has shown (from the usual equations of a compressible fluid) that the motion of a compressible fluid may be written as a wave equation in the fluid density with a "forcing" term dependent upon the velocity of the fluid. Neglecting deviations from adiabatic flow in the turbulence and the effects of viscosity, the equation for the density of the fluid is

$$\frac{\partial^2 \rho}{\partial t^2} - c^2 \nabla^2 \rho = \sum_{i,j=1}^{3} \frac{\partial^2 (\rho u_i u_j)}{\partial x_i \partial x_j} \tag{169}$$

where ρ is the density, and u_i, u_j are the components of fluid velocity in the x_i, x_j direction ($x_1 = x$, $x_2 = y$, $x_3 = z$). By dividing the fluid velocity into turbulent and acoustic components, and considering the turbulent-acoustic interaction term (the acoustic-acoustic term is negligible from the usual small-amplitude acoustic assumption; the turbulent-turbulent term gives rise to turbulence-induced sound, which has a small effect for low Mach numbers), a first approximation to the scattering can be obtained as in Eq. (146). For high frequency sound (wavelength small compared to characteristic size of the turbulence, see Eq. (139)), the power scattered from the turbulent volume into the solid angle $d\Omega$ is approximately

$$E d\Omega \approx 2 I_o k^2 \, d\Omega V \left\langle (v_z/c_o)^2 \right\rangle \int_0^\infty M_{zz}(0,0,\zeta) d\zeta; \qquad k\zeta_o >> 1 \tag{170}$$

where I_o is the incident intensity, k the sound wave number, the correlation function is

$$\left\langle (v_z)^2 \right\rangle \; M_{zz}(\xi,\eta,\zeta) = \left\langle v_z(x,y,z) \; v_z(x+\xi, \, y+\eta, \, z+\zeta) \right\rangle \tag{171}$$

and ζ_o is the characteristic length of turbulence in the z-direction, given by the integral in Eq. (170) (see Eq. (139)).

For isotropic turbulence, the high-frequency approximation ($k\zeta_o >> 1$) is not needed; the scattered power is given for any ratio of turbulence "size" to wavelength by:

$$E d\Omega \simeq \frac{I_o k^2}{8} \, d\Omega \, V \cos^2\theta \; \mathrm{ctn}^2(\theta/2) \, \mathcal{E}(2k \sin\tfrac{1}{2}\theta) \tag{172}$$

when $\mathcal{E}(K)$ is the Fourier transform (i.e., the spectrum) of the turbulent energy per unit mass of the fluid:

$$\mathcal{E}(K) = \tfrac{1}{2} \int_{-\infty}^{\infty} \left\langle v_z(\underline{r}) v_z(\underline{r} + \underline{\rho}) \right\rangle \; e^{-iK\rho} \, d\rho \tag{173}$$

where the correlation function is a function only of $\rho = |\underline{\rho}|$, since isotropic turbulence is assumed. It is to be noted from Eq. (172) above, that the scattered energy goes to zero at $\theta = 90^\circ$ and $\theta = 180^\circ$; for $\theta = 0^\circ$,

the energy spectrum goes to zero as $(2k \sin\frac{1}{2}\theta)^4$, so that there is a zero in scattered energy at $\theta = 0^\circ$ as well.

For sound wavelengths smaller than the scale of turbulence, the intensity attenuation due to scattering becomes:

$$2\alpha \simeq 8\pi^2 \frac{\omega^2}{c^2} \left\langle \left(\frac{v_z}{c}\right)^2 \right\rangle \int_0^\infty M_{zz}(0,0,\zeta)\, d\zeta \qquad (174)$$

It is not known, as yet, how well the above theory corresponds to experiment; in view of the good agreement with experiment of Lighthill's theory of noise generation by turbulence, it seems probably that the above scattering theory should give results close to experimental results.

1.7 DIFFRACTION OVER A WALL

1.7.1 Previous cases treated in Section I represent idealized situations in that, in each case, the air is assumed either unbounded, or bounded below by an infinite homogeneous plane. In field problems one is compelled to consider more complex cases. Thus in practice it is important to know how sound propagates over a hilly terrain or around obstacles such as trees or buildings. We shall make no attempt to treat the general problems here, but confine ourselves to the special case of propagation over a long wall of given height. In a given field situation the "wall" might be an extended hill, a long building, a row of trees, or, of course, a man-made wall of boards or stone.

1.7.2 Appropriate methods for treating this problem are available from the classical Fresnel diffraction theory, long used in optics[54]. For definition of symbols see Fig. 19.

In Fig. 19 the source of sound is at Q, and P is a point at which the sound level is to be calculated. The point P_o is directly above or below P and on the "line of sight" from Q; i.e., the line QP_o just grazes the "wall". The distances from the wall to Q and P_o are a and b, respectively, while the vertical displacement of P below P_o is d_o; the latter quantity is positive for P below P_o, negative for P above P_o. In the Fresnel theory it is assumed that $a \gg \lambda$, $b \gg \lambda$, $d_o \ll (a + b)$ and $d_o \ll (b/a)(a+b)$. Define a quantity v such that

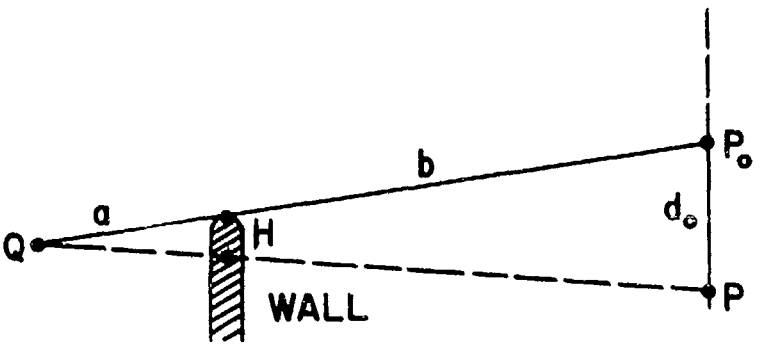

Fig. 19. Geometrical parameters for problem of diffraction over a wall.

$$v = d_o \cdot \left[\frac{2a}{b(a+b)\lambda}\right]^{\frac{1}{2}} \tag{175}$$

where λ is the acoustic wavelength. Then the sound pressure p at P is given by

$$p = A\left[X^2 + Y^2\right]^{\frac{1}{2}} \cos(\omega t + \theta) \tag{176a}$$

where ω is the angular frequency and

$$X = \int_v^\infty \cos \frac{\pi x^2}{2}\, dx\,, \tag{176b}$$

$$Y = \int_v^\infty \sin \frac{\pi x^2}{2}\, dx\,, \tag{176c}$$

$$\theta = \tan^{-1}(Y/X) \tag{176d}$$

and A depends on a, b and the source strength, but is independent of d_o.

Table 12 gives X and Y for positive and negative values of v

ranging from 0 to 6.95. From these the amplitude and phase of p/A may be calculated for any given a, b, d_o and λ. The same results are given in another form in Fig. 20. Here the Cornu Spiral is shown, obtained by plotting for each v-value a point whose vertical displacement with respect to a given point 0 is X, and whose vertical displacement with respect to the same point is Y. Hence, to determine the relative pressure amplitude and phase at a point P characterized by a given v-value one need only draw a vector from 0 to the point corresponding to the v-value in question: the horizontal component of this vector thus gives X, its vertical component Y. The length of the vector is $\left[X^2 + Y^2\right]^{\frac{1}{2}}$ and the angle measured counterclockwise to the vector from the horizontal gives $\tan^{-1}$ (Y/X) and hence the angle θ.

TABLE 12

The Fresnel Integral

v	X	Y	v	X	Y
6.95	-0.0207	0.0409	5.50	0.0216	-0.0537
6.90	0.0268	0.0376	5.45	-0.0269	-0.0519
6.85	0.0461	-0.0060	5.40	-0.0573	-0.0140
6.80	0.0169	-0.0436	5.35	-0.0490	0.0338
6.75	-0.0302	-0.0362	5.30	-0.0078	0.0595
6.70	-0.0467	0.0085	5.25	0.0390	0.0464
6.65	-0.0161	0.0451	5.20	0.0611	0.0031
6.60	0.0310	0.0369	5.15	0.0447	-0.0427
6.55	0.0480	-0.0078	5.10	0.0002	-0.0624
6.50	0.0184	-0.0454	5.05	-0.0450	-0.0442
6.45	-0.0292	-0.0398	5.00	-0.0637	0.0008
6.40	-0.0496	0.0035	4.90	-0.0002	0.0650
6.35	-0.0240	0.0440	4.80	0.0662	0.0032
6.30	0.0240	0.0445	4.70	0.0086	-0.0672
6.25	0.0507	0.0046	4.60	-0.0673	-0.0162
6.20	0.0324	-0.0398	4.50	-0.0261	0.0658
6.15	-0.0146	-0.0496	4.40	0.0617	0.0378
6.10	-0.0495	-0.0165	4.30	0.0506	-0.0540
6.05	-0.0424	0.0311	4.20	-0.0418	-0.0633
6.00	0.0005	0.0530	4.10	-0.0738	0.0242
5.95	0.0434	0.0312	4.00	0.0016	0.0796
5.90	0.0514	-0.0163	3.90	0.0777	0.0248
5.85	0.0181	-0.0513	3.80	0.0519	-0.0656
5.80	-0.0298	-0.0461	3.70	-0.0420	-0.0750
5.75	-0.0551	-0.0049	3.60	-0.0880	0.0077
5.70	-0.0385	0.0405	3.50	-0.0326	0.0848
5.65	0.0074	0.0559	3.40	0.0615	0.0704
5.60	0.0483	0.0300	3.30	0.0942	-0.0192
5.55	0.0544	-0.0181	3.20	0.0336	-0.0933

Table 12
(continued)
The Fresnel Integral

v	X	Y	v	X	Y
3.10	-0.0616	-0.0818	-1.30	1.1386	1.1863
3.00	-0.1058	0.0037	-1.40	1.0431	1.2135
2.90	-0.0626	0.0899	-1.50	0.9453	1.1975
2.80	0.0325	0.1085	-1.60	0.8655	1.1389
2.70	0.1075	0.0471	-1.70	0.8238	1.0492
2.60	0.1110	-0.0500	-1.80	0.8336	0.9508
2.50	0.0426	-0.1192	-1.90	0.8944	0.8734
2.40	-0.0550	-0.1197	-2.00	0.9882	0.8434
2.30	-0.1266	-0.0531	-2.10	1.0815	0.8743
2.20	-0.1363	0.0443	-2.20	1.1363	0.9557
2.10	-0.0815	0.1257	-2.30	1.1266	1.0531
2.00	-0.0118	0.1566	-2.40	1.0550	1.1197
1.90	0.1056	0.1266	-2.50	0.9574	1.1192
1.80	0.1664	0.0492	-2.60	0.8890	1.0500
1.70	0.1762	-0.0492	-2.70	0.8925	0.9529
1.60	0.1345	-0.1389	-2.80	0.9675	0.8915
1.50	0.0547	-0.1975	-2.90	1.0626	0.9101
1.40	-0.0431	-0.2135	-3.00	1.1058	0.9963
1.30	-0.1386	-0.1863	-3.10	1.0616	1.0818
1.20	-0.2154	-0.1234	-3.20	0.9664	1.0933
1.10	-0 2638	-0.0365	-3.30	0.9058	1.0192
1.00	-0.2799	0.0617	-3.40	0.9385	0.9296
0.90	-0.2648	0.1602	-3.50	1.0326	0.9152
0.80	-0.2230	0.2507	-3.60	1.0880	0.9923
0.70	-0.1597	0.3279	-3.70	1.0420	1.0750
0.60	-0.0811	0.3895	-3.80	0.9481	1.0656
0.50	0.0077	0.4353	-3.90	0.9223	0.9752
0.40	0.1025	0.4666	-4.00	0.9984	0.9204
0.30	0.3001	0.4958	-4.10	1.0738	0.9758
0.10	0.4000	0.4995	-4.20	1.0418	1.0633
0.00	0.5000	0.5000	-4.30	0.9494	0.9204
-0.10	0.6000	0.5005	-4.40	0.9383	0.9622
-0.20	0.6999	0.5042	-4.50	1.0261	0.9342
-0.30	0.7994	0.5141	-4.60	1.0673	1.0162
-0.40	0.8975	0.5334	-4.70	0.9914	1.0672
-0.50	0.9923	0.5647	-4.80	0.9338	0.9968
-0.60	1.0811	0.6150	-4.90	1.0002	0.9350
-0.70	1.1597	0.6721	-5.00	1.0637	0.9992
-0.80	1.2230	0.7493	-5.05	1.0450	1.0442
-0.90	1.2648	0.8398	-5.10	0.9998	1.0624
-1.00	1.2799	0.9383	-5.15	0.9553	1.0427
-1.10	1.2638	1.0365	-5.20	0.9389	0.9969
-1.20	1.2154	1.1234	-5.25	0.9610	0.9536

Table 12.
(continued)
The Fresnel Integral

v	X	Y	v	X	Y
-5.30	1.0078	0.9405	-6.15	1.0146	1.0496
-5.35	1.0490	0.9662	-6.20	0.9676	1.0398
-5.40	1.0573	1.0140	-6.25	0.9493	0.9954
-5.45	1.0490	0.9662	-6.30	0.9760	0.9555
-5.50	0.9784	1.0537	-6.35	1.0240	0.9560
-5.55	0.9456	1.0181	-6.40	1.0496	0.9965
-5.60	0.9517	0.9700	-6.45	1.0292	1.0398
-5.65	0.9926	0.9441	-6.50	0.9816	1.0454
-5.70	1.0385	0.9595	-6.55	0.9520	1.0078
-5.75	1.0551	1.0049	-6.60	0.9690	0.9631
-5.80	1.0298	1.0461	-6.65	1.0161	0.9549
-5.85	0.9819	1.0513	-6.70	1.0467	0.9915
-5.90	0.9486	1.0163	-6.75	1.0302	1.0362
-5.95	0.9566	0.9688	-6.80	0.9831	1.0436
-6.00	0.9995	0.9470	-6.85	0.9539	0.0060
-6.05	1.0424	0.9689	-6.90	0.9372	0.9624
-6.10	1.0495	1.0165	-6.95	1.0207	0.9591

We are particularly interested in the loss L in sound level caused by the wall. Expressed in db, this loss at any point P may be defined as

$$L = 20 \log_{10} (p/p') \quad , \tag{177}$$

where p is the pressure amplitude at P, and p' is the pressure amplitude which would exist there if the wall were absent. To a sufficiently good approximation we may take the reference pressure p' to be equal to the pressure that exists at a point vertically above P, at a point far enough above the wall so that the latter has negligible effects on the sound level. Hence in using Eq. (177) to evaluate L, p is determined for a v-value corresponding to P, while p' is evaluated for $v = -\infty$. (From Table 12 or from Fig. 20 we see that $X = Y = 1.00$ for $v = -\infty$ and hence that $p' = A\sqrt{2}$). Hence L is a function only of the v corresponding to P.

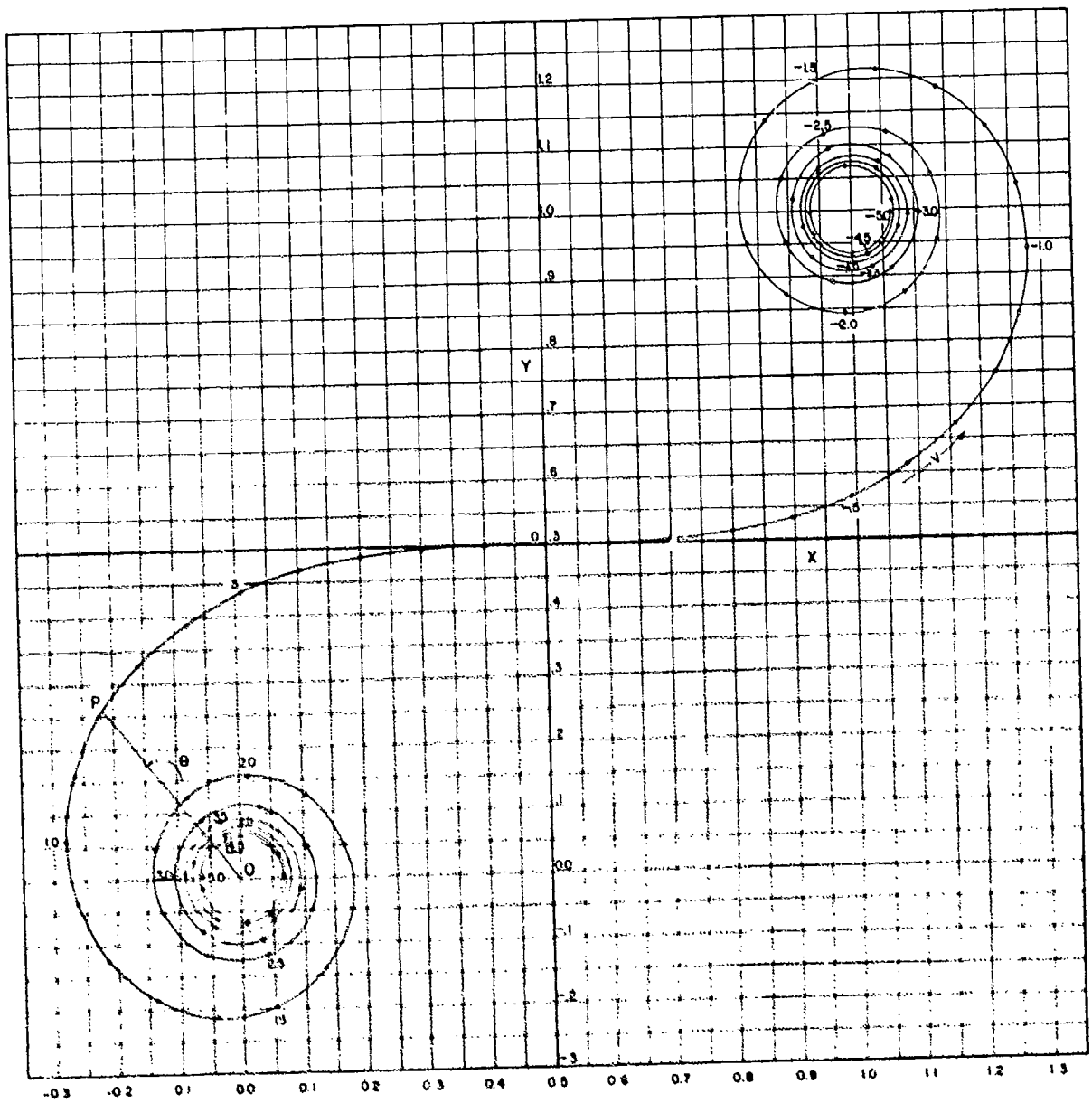

Fig. 20. The Cornu Spiral representation of the Fresnel Integrals X and Y, Eqs. (176).

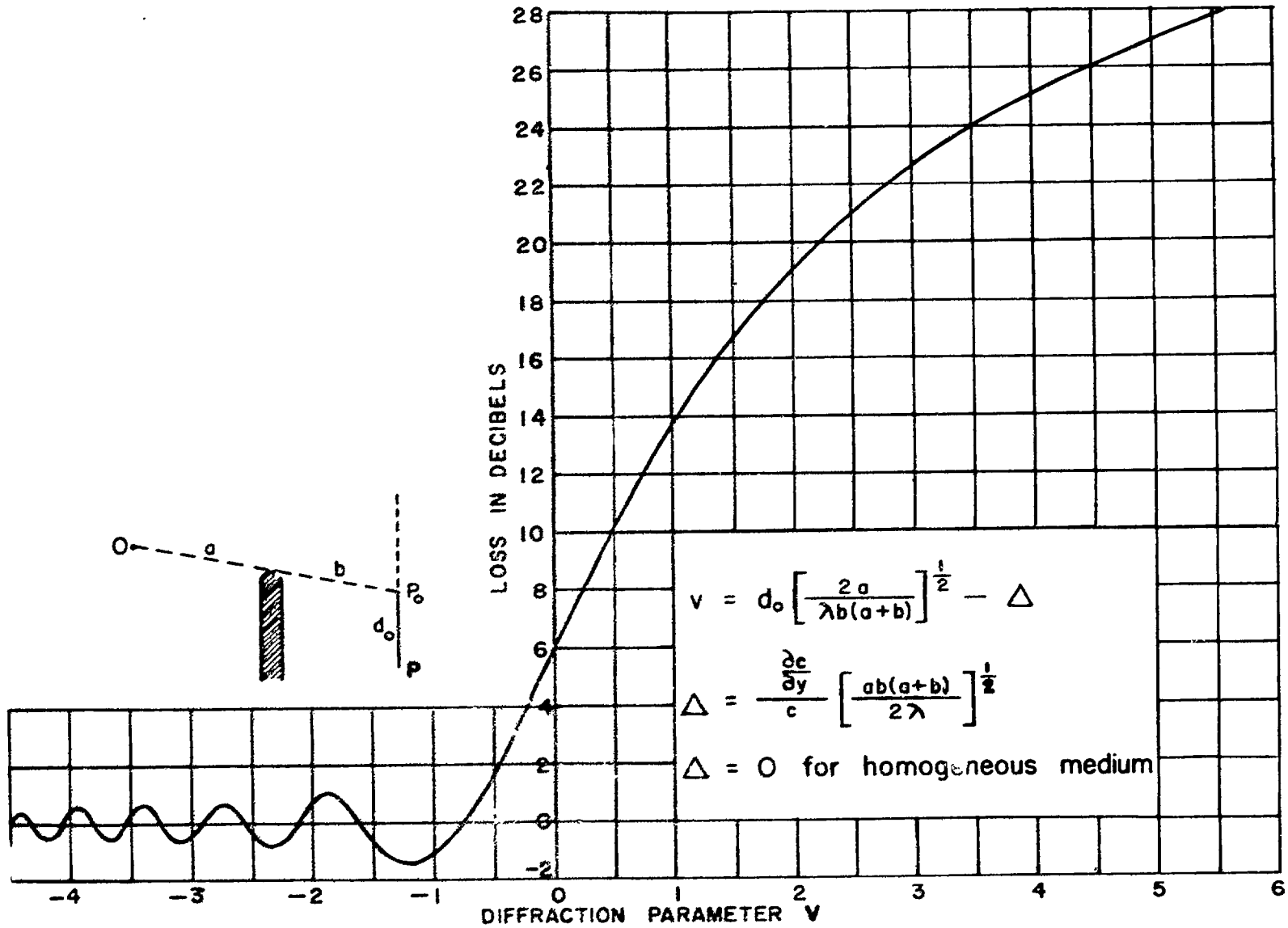

Fig. 21 Loss in sound level caused by a wall, as a function of the parameter v. The latter is defined in the insert, both for the case of a homogeneous medium and for the case of a medium in which there is a constant vertical gradient ($\partial c/\partial y$) of sound velocity c; λ is the acoustic wavelength.

Fig. 21 shows a plot of L versus v. To use this in a particular problem one determines the appropriate v from Eq. (175), then obtains L from the graph.

1.7.3 Fehr[55] has previously given a graph for calculating the loss caused by a wall. We shall not reproduce his graph here, since it is essentially the same as Fig. 21, but shall nevertheless discuss it briefly for later reference. Fehr's chart plots "wall loss" against a quantity N which, like v, depends on a, b, d_o and λ. The losses so plotted are, for assumed values of a, b, d_o and λ, 6 db less than those given in Fig. 21, being referred to the level at the shadow boundary rather than to a point far above the wall. In terms of the sketch in Fig. 19 Fehr's theory thus gives the loss at any point P relative to the sound level at P_o. The quantity N given by Fehr is

$$N = \left[\sqrt{a^2 + H^2} - a\right] - \left[\sqrt{b^2 + H^2} - b\right], \qquad (178)$$

where, referring to Fig. 19, H is the perpendicular distance from the source-receiver line QP (shown dotted in Fig. 19) to the upper edge of the wall, and is related to d_o by the equation

$$H/d_o = a/(a + b) . \qquad (179)$$

In the important case where both a and b are much greater than H, Eq. (178) reduces to

$$N = v^2/2 \qquad (180)$$

where v is given by Eq. (175). In the latter case one may get from Fig. 21 the same values for the wall loss as would be determined from Fehr's chart by the following steps:

(1) Calculate v for given a, b, λ and d_o from Eq. (175).
(2) Determine from Fig. 21 the loss for this v.
(3) Subtract 6 db from the loss given in Step (2).

If either a or b is not large with respect to H in which case the approximations made in arriving at the plot in Fig. 21 do not hold, one obtains Fehr's result by the same procedure except that Step (1) is replaced by Steps (1a) and (1b) given below:

(1a) Calculate N for given a, b, λ and d_o by Eq. (178).
(1b) Determine v from Eq. (180), using the value of N from Step (1a).

This latter procedure is apparently an empirical one, rather than one arrived at theoretically.

1.7.1 The results given in subsections 1.7.2 and 1.7.3 apply only if reflections of the ground may be neglected. Let us suppose instead that the source position Q is at a height z_o above a highly reflecting surface such as concrete. The reflected sound may then be regarded as coming from an image source, equal in magnitude and phase to the real source but at a distance $2z_o$ vertically below it, i.e., at a distance z_o below the surface. For this case the field at a point P due to both direct and reflected sound may be obtained by determining p from Eqs. (176) (either by use of Table 12 or Fig. 20) for both real and image source, then adding the two contributions, remembering to take phase into account as well as amplitude.

If the surface is not highly reflecting, the image concept no longer applies generally and the theory becomes much more difficult to apply. No useful solution is known for this case.

1.7.2 If a sound velocity gradient exists in the air due, e.g., to wind, rays traveling over the wall are bent upward or downward with consequent important changes in sound level. For the idealized case of a constant gradient one may still use the results given above in Eq. (176) and Fig. 21, if in the expression for v the distance d_o is replaced by a new quantity d. The latter, as indicated in Fig. 22 gives the vertical distance to the shadow boundary from the point of observation P. If rays are bent upward, we have $d > d_o$ and the loss in sound level caused by the wall at points P below P_o is greater than

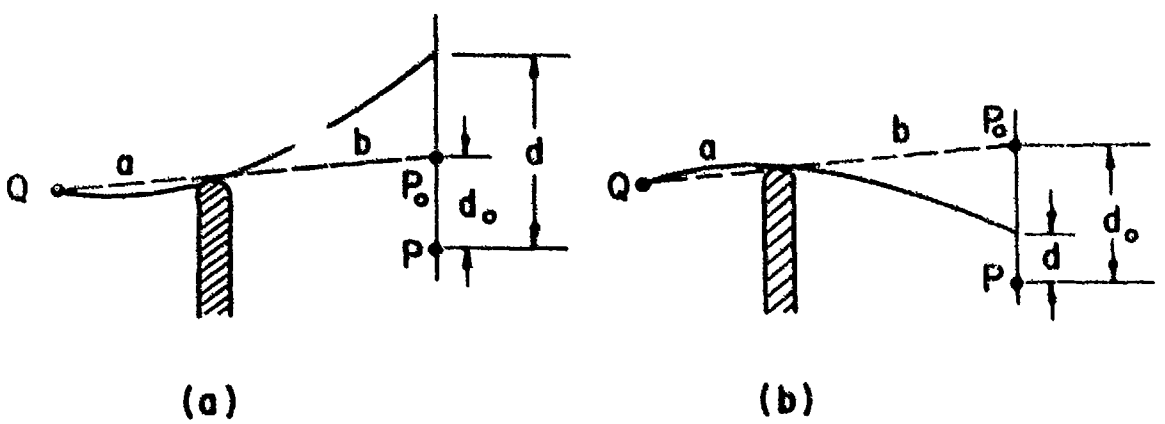

Fig. 22. Geometrical parameters for problem of diffraction over a wall in the presence of a vertical gradient of sound velocity.

if the rays were straight. If rays are bent downward we have $d < d_o$ and the loss at such points is less. Specifically, it can be shown that if a constant gradient ($\partial c/\partial y$) of the sound velocity c exists (y being assumed measured upwards) then, to an appropriate approximation,

$$d = d_o - \frac{b(a+b)}{2} \cdot \frac{\partial c/\partial y}{c} \qquad (181)$$

In summary, the loss at P due to a wall when a constant vertical gradient of sound velocity exists may be determined from Fig. 21 by properly evaluating v; in the expression for v the quantity d_o must be replaced by d, the latter being given by Eq. (181).

1.8 PROPAGATION OF HIGH AMPLITUDE SOUND*

1.8.1 Introduction

The theory in subsections 1.2 to 1.7 is all based on the usual linearizing approximations of acoustics. It is assumed there that the amplitudes of the alternating pressures, velocities, and displacements in a sound field are all small enough so that the inherently nonlinear basic hydrodynamic and thermodynamic laws may be simplified by dropping out certain terms.

It has been found experimentally that the results predicted by the linearized theory which results from this simplification fit many of the observed facts very well for the relatively weak sound waves typically encountered, e.g., in speech and music. In fact, most of the usual theory of acoustics and ultrasonics is based on this simplification, as may be verified by consulting standard text books. Nevertheless, there are actions which occur even at fairly ordinary sound levels which cannot be explained at all by linearized theory. Among these are the setting up of vortices in a Kundt's tube (which vortices, in turn, are responsible for the familiar formation of periodically spaced dust piles), and the steady torque exerted by sound waves on a Rayleigh disc. To explain these, it is necessary to take some account of nonlinear terms in the basic equations[56]. When sound levels of the order of those

---

*The authors wish to acknowledge the considerable help given by Professor R. B. Lindsay in the preparation of this subsection.

existing near powerful modern aircraft are considered, the linearized theory can no longer be expected (in general) to be quantitatively applicable. Indeed, phenomena which are hardly noticeable at ordinary sound levels play a very conspicuous role in intense sound fields, making the situation appear to be even qualitatively different from the weak field case.

Unfortunately for practical applications, the problems of high amplitude acoustics are very difficult; so far only the simplest of situations have been given detailed attention. There are, at present, only a few problems for which solutions exist which are suitable for application in the field. The need for extensive basic research in this general area is obvious.

The available literature on this general subject includes information on the following topics:

(1) Changes in wave shape, i.e., generation of harmonics and formation of shock fronts in a propagating wave,
(2) Propagation of shock fronts,
(3) Steady forces, i.e., radiation pressure, exerted by sound waves on obstacles or inhomogeneities.
(4) Steady circulatory motions, i.e., acoustic streaming set up by sound waves upon interacting with boundaries or with each other.

It is beyond the scope of this report to give a detailed review here of these various subjects. We shall confine ourselves to a very brief discussion of available information on topics (1) and (2).

1.8.2 Plane waves

Most of the available theory on "finite amplitude" wave propagation is for traveling plane waves. Assuming that absorption processes (such as were considered in subsections 1.2 and 1.3) are negligible, an exact equation describing the motion of a disturbance in air along the x axis is given by

$$\frac{\partial^2 z}{\partial t^2} = \frac{\gamma p_0}{\rho_0} \frac{\partial^2 z}{\partial x^2} \left(1 + \frac{\partial z}{\partial x}\right)^{-\gamma-1} \qquad (182)$$

x = rest position of an element of the medium

z = displacement of an element from its rest position

t = time

γ = ratio of specific heats

p_o = ambient pressure of the medium

ρ_o = ambient density of the medium

(It may be noted that x is a Lagrangian coordinate[57].)

Eq. (182) is nonlinear due to the term containing $(\partial z/\partial x)$ on its right hand side. If the strain is very small, so that $\partial z/\partial x \ll 1$, Eq. (182) reduces to the usual linear wave equation. A harmonic series solution to Eq. (182) was obtained by Fubini-Ghironi[58]; for points not too far from the (plane) sound source and for source amplitudes that are not too great the displacement is given by

$$z(x,t) = a_o + \sum_{n=1}^{\infty} a_n Z^n x^{n-1} \cos n\omega(t - x/c), \qquad (183)$$

where Z is the displacement amplitude of the source, and the a_n are constants independent of Z and x. According to this solution a sinusoidally vibrating plane source will generate a disturbance which starts out (at x = 0) as a simple sinusoidal traveling wave; however, as it travels away from the source its wave form changes as harmonics appear and grow in amplitude. That this distortion does occur has been verified experimentally; Thuras, Jenkins and O'Neill[59] found that Eq. (183) describes rather well the rate at which the second harmonic grows in amplitude when a plane wave, originally sinusoidal, propagates down a tube.

As stated before, the solution in Eq. (183) is valid only when x and Z are sufficiently small. Specifically it can be shown that a condition for the validity of Eq. (183) is that x should be small compared with a characteristic distance X given by,

$$\pi(\gamma + 1) X \approx \lambda c/U, \qquad (184)$$

where λ is the wavelength of the fundamental, c is the velocity of sound and $U \equiv \omega Z$ is the velocity amplitude of the source. Alternatively, we may write X in terms of the pressure amplitude p_s at the source as

$$X = A \lambda p_o/p_s , \qquad (185a)$$

where the dimensionless constant A is given by

$$A = \frac{\rho_o c^2}{(\gamma + 1)\pi p_o} \qquad (185b)$$

Evaluating the constants for air at atmospheric pressure (Appendix I), we obtain

$$X = 0.133\,\lambda c/U = 0.184\ \ p_o/p_s \tag{186}$$

The "exact" series solution of Fubini-Ghiron (not given here) is, of course, valid for larger amplitudes and greater distances than is the approximation to it given in Eq. (183). Nevertheless, even the "exact" solution breaks down at distances comparable to, or greater than X; at about this distance the solution becomes multiple-valued and loses physical significance. The difficulty evidently lies with the starting differential equation, Eq. (182); it is apparently not possible to describe the propagation at distances comparable to or greater than X without taking into account sound absorption processes, such as viscosity.

Fay[60] used a differential equation, modified from Eq. (182), in which shear viscosity is taken into account. He has given a series solution to this equation which, for x comparable to or greater than X, yields for the peak excess pressure p_e in a plane wave at distance x from a harmonic source of angular frequency ω the absolute value:

$$|p_e| = A\,\alpha_v \sum_{n=1}^{\infty} \frac{\sin nk\,x}{\sinh n\,\alpha_v(x_o+x)} \tag{187}$$

in which

$$A = \frac{16\,c\,\gamma\,p_o}{(\gamma+1)\omega}$$

$$\alpha_v = \frac{2}{3}\,\frac{u\,\omega^2}{\rho_o c^3}$$

ρ_o, p_o, γ as in Eq. (182)

$$k = \frac{\omega}{c}$$

c = small amplitude wave velocity = $(p_o\,\gamma/\rho_o)^{\frac{1}{2}}$

x_o = arbitrary constant to be determined by initial conditions.

Specifically, the constant x_o may be given in terms of the pressure amplitude p_s at the source (x = 0) as

$$x_o = \frac{4\,\rho_o\,c^3}{\gamma\,\pi\,f\,p_{eo}} \tag{188a}$$

where p_{eo} is the value of $|p_e|$ at $x = 0$; letting $\rho_o c^2 = \gamma p_o$ and $\lambda = c/f$ in the above expression we obtain

$$x_o = 1.27\,\lambda p_o/p_{eo} \qquad (188b)$$

It will be seen that x_o is of the same order of magnitude as the previously defined X, Eq. (186). Examination discloses that (187) leads to a limiting stable wave shape for sufficiently large values of x, and, indeed, to one that possesses a saw-tooth character. The pressure amplitude p_n of the n^{th} harmonic is just p_1/n where p_1 is the amplitude of the fundamental. The envelope of the maxima of the resultant excess pressure falls off inversely as $1/(x_o+x)$. As a matter of fact, whether the sum in (187) is approximated algebraically or by an equivalent integral, the excess pressure amplitude takes the form

$$|p_e|_{max} = \frac{4\,\rho_o c^3}{\gamma \pi f} \cdot \frac{1}{x_o+x} = \frac{1.27\,p_o\lambda}{(x_o+x)} \qquad (189)$$

where f is the actual frequency. It has here been assumed that

$$\frac{k\pi x}{a_v(x_o+x)} >> 1 \qquad (190)$$

which turns out to be satisfied in air at frequencies not exceeding one megacycle, provided $x/(x_o+x) > 10^{-4}$. This means x_o must not be too large or the excess pressure amplitude at the source too small. For very small source intensities the formula (189) breaks down.

If we fit Eq. (189) by an equivalent exponential curve of the form

$$|p_e|_{max} = Ce^{-\alpha x} \qquad (191)$$

it turns out that the equivalent attenuation coefficient α is given, in nepers/cm, by

$$\alpha = \frac{1}{x_o+x}, \qquad (192)$$

and is therefore a function of x, which indeed may be very slowly varying if x_o is rather large.* For points sufficiently near $x = 0$ we may

*It has recently been shown by Rudnick[61] that theory for the propagation of repeated shock fronts, where the Rankine-Hugoniot relations are applied, yields an attenuation coefficient identical in form with that given by Fay's theory, Eq. (192).

neglect x in the denominator of Eq. (192); using the expression for x_o given by Eq. (188b), evaluating constants for air at 20°C (Appendix I) and converting α to units of db/1000 ft, we obtain

$$\alpha = 6.10\ f p_s/p_o\ , \qquad (193)$$

where the frequency f is in cycles/sec. If, for example, the frequency is 100 cps and p_{eo} is 0.1 atm, the coefficient α has the value 61 db/1000 ft, valid for $x \ll x_o$.

1.8.3 Quasi-spherical waves

The results discussed above for plane waves are most useful as a guide in estimating the order-of-magnitude of effects. However, it is not to be expected that these results would be quantitatively valid for fields generated by real sources of finite size and with typical directivity patterns. So far as is known to the authors, there is not yet available any theory which is directly applicable to such fields as exist near aircraft.

As a guide, however, it is worthwhile to consider briefly certain experimental results obtained in the laboratory, using a piston-like source. C. H. Allen[62] made detailed measurements of the sound pressure in high amplitude fields generated by a piston 12.2 cm in diameter moving sinusoidally at a frequency of 14.6 kc. Pressure measurements were made out to distances of 200 cm from the source. Though the generated sound wave was sinusoidal near the source, harmonics were generated as it traveled, so that with increasing distance from the source it approached a sawtooth shape, as in the case of plane waves.

Allen was able to fit his data for quasi-spherical waves to empirical formulae which show striking analogies to the theoretical results for plane waves. The laws according to which harmonics are generated in a traveling wave were found to be very similar for the two cases. The main difference found was that the harmonics grow more slowly in a "spherical" wave of given amplitude than in a plane one (this result is perhaps not unreasonable since the amplitude of a spherical wave is continually decreasing, due to geometric spreading). The distance from a source of given amplitude to a point where a stable sawtooth wave may be said to be eventually fully developed is thus much greater for the quasi-spherical wave than for a plane one.

Allen found that after the drop in intensity due to spherical spreading was taken into account there remained for each harmonic an attenuation which was practically uniform throughout the range of 200 cm from the source, though increasing with the intensity level at the source. The latter result is qualitatively predicted by Eq. (189)

deduced from Fay's plane wave theory, though the former is not strictly in agreement with (189). However, it is of interest to compare the actually observed attenuation for the fundamental with average attenuations over the range 0 - 200 cm, as predicted by (189). The results are shown in Table 13. The order of magnitude agreement is rather suggestive in spite of the obvious inadequacy of the theory.

TABLE 13

Comparison of theory (Eq. (189)) with Allen's experimental results[62].

Source level (x = 3.8 cm)	Experimental attenuation	Average attenuation from Eq. (189)	Attenuation near source from Eq. (189)
146 db re threshold	0.0062 db/cm	0.0060 db/cm	0.0064 db/cm
151	0.013	0.010	0.011
156	0.027	0.017	0.021
161	0.035	0.027	0.036

SECTION II

OUTDOOR MEASUREMENTS

2.1 INTRODUCTION

In this section we review results obtained from acoustic measurements made in the field, i.e., in actual out-of-door situations. Here the sound field is often very complex, varying greatly in both time and space, and cannot be represented by any one of the idealized situations described in Section I. It is difficult to completely separate the effects of different factors in outdoor experiments since, e.g., weather parameters are not at the control of the experimenter, and surface parameters are only partly so. Nevertheless, careful planning of outdoor measurements does permit considerable information to be gained on the relative importance of different factors. Theory can then sometimes be applied to the problems with fair success. In the following discussion of various outdoor experiments we present the more pertinent of the experimental findings in each case, and also describe, whenever possible, how well these findings agree with the theory described in Section I.

(This review includes only those studies which appear to give suitable quantitative information on sound propagation losses in the lower atmosphere. The application assumed is that of sound propagation from sources to points no greater than a few miles distant. Experimental studies using explosive sources, where distances up to 100 miles or more are involved, are not included; the emphasis in these experiments is on arrival times of the blast waves. Also, the instrumentation does not permit accurate determination of overall losses and, especially, does not allow frequency analysis of these losses. For articles giving recent results, as well as bibliography, see Richardson and Kennedy[63], and Johnson and Hale[64]. Likewise excluded from this review are experimental studies carried out without the aid of modern instrumentation. Discussions and bibliography of early work are given by King[65], Sieg[67] and Ingard[66].)

In much of the work to be discussed below the results consist of field data on sound levels at various distances R from a sound source, the sound propagation path being either from air to ground, or else along a relatively flat ground surface. In reducing these data for presentation the investigators often assume that Eq. (2) applies; the experimental results are therefore plotted in such a way as to yield the attenuation coefficient α which applies under the given conditions.

In the procedure commonly followed for obtaining α the sound

level data are first used to compute losses at various distances R relative to the level at a given reference distance R_o. Use is then made of Eqs. (9) which show that when Eq. (2) holds the loss at any point relative to a reference point consists of two parts, a 1/R loss and exponential loss. The former can be computed for given R and R_o, being given by 20 $\log_{10}$ (R/R_o); the exponential loss at each point is then determined by simply subtracting the 1/R loss from the total loss. Finally, the exponential loss so obtained is plotted versus the distance $(R-R_o)$ and a straight line is fitted to the data; applying Eq. (10) the slope of this line (e.g., in units of db/1000 ft) yields α, the loss coefficient for the conditions under investigation.

It is, of course, clear from theoretical considerations (see Section I) that the sound field cannot always be described by the simple law given in Eq. (2). This is particularly true when refraction or ground effects (see subsections 1.4 to 1.6) are involved. One therefore cannot expect to specify the acoustic field in every case by simply stating a loss coefficient α. The loss coefficients given below must, therefore, in many cases, be regarded as approximate and as applicable only under the special conditions of the experiment.

Studies of sound fields in the out-of-doors, which are useful for our purposes, date from about 1940. Since that time several reports and publications have appeared in which attenuation measurements are given for sound of well defined frequency, being generated by loudspeakers, whistles or shock-excited resonant tubes. Several studies have also been made using sound generated by actual aircraft, either in flight or on the ground. In this case, the sound consists of a band of noise; the laws of attenuation characteristic of different parts of the spectrum are obtained by use of electric filters at the output of the receiver transducer. In subsection 2.2 we review investigations of sound propagation in the atmosphere, over an approximately plane earth surface in which the monochromatic type of sound source is used; in subsection 2.3 similar studies are discussed in which the sound consists of actual aircraft noise. The special subjects of diffraction over a long building or wall, propagation through wooded areas, and transmission through the earth are taken up in subsections 2.4, 2.5 and 2.6.

2.2 PROPAGATION OF SINGLE-FREQUENCY SOUND

2.2.1 Sieg (1940)[67]

The earliest paper containing any appreciable amount of quantitative data on sound attenuation is due to Sieg. The latter made studies of sound propagation from a loudspeaker mounted 35 feet above the ground; his frequency range was 200-4000 cps. Sound levels at various distances out to 1650 ft from the source were measured on a number of different days with Barkhausen, as well as with Siemens, noise meters by an observer at ground level, i.e., probably at points about 5 or 6 feet above the ground. (The aim was to study propagation of speech and music from public address systems.) The sound field on any given day was assumed described by Eq. (2) and the loss coefficient α determined in the manner described in subsection 2.1.

TABLE 14

Loss Coefficient in the Out-of-Doors, from Sieg.

Frequency (cps)	250	500	1000	2000	4000
α (db/1000 ft) "good conditions"	4.6	5.2	6.7	6.7	12.2
α (db/1000 ft) "bad conditions"	17.4	19.8	20.1	23.4	33.2
average α	10.4	10.4	11.0	12.8	18.9
(average α_{mol})	0.0	0.0	1.2	3.0	8.8

Table 14 summarizes his results. Typical values of α are given for "good propagation conditions" as well as for "bad propagation conditions". The former are for days described as "quiet", "quiet and cloudy" or "quiet, with inversion (temperature increasing with height)". In all cases "bad propagation conditions" are for windy days when the wind vector has a component opposing the direction of sound propagation. Also given in Table 14 are theoretical values of α_{mol} (subsection 1.2.3) computed by Sieg. (It appears that in Sieg's calculations of α_{mol}, the latter was assumed to depend only on frequency and relative humidity, independent of temperature. As is evident from the discussion in subsection 1.2.3, this assumption is in error, not only because α_{max} is temperature-dependent but, more important, because f_m depends mainly on the absolute humidity h. The latter can be quite different, of course, for situations where the relative humidity is the same, but for which the temperature is

different.) The classical absorption coefficient α_{class} (subsection 1.2.2) was neglected, being small compared to α_{mol} in the frequency range considered. It is clear that the observed attenuation is always greatly in excess of α_{mol}, both for "good" and "bad" propagation conditions.

In the case of the "bad propagation conditions" much of the observed loss may have been due to shadow effects. To show the likelihood of this we refer to the universal shadow boundary curve in Fig. 16. Assuming the ratio (z/z_o) of receiver height to source height is about 0.15 we obtain from Fig. 16:

$$(r_s/z_o)\ (B/2)^{\frac{1}{2}} \sim 0.5 \qquad (194)$$

To estimate B we refer to Eq. (93). Here one may let (u_*/u_{200}) be approximately 0.07, a value given in Table 8 for low meadow grass; 1000 cm/sec may be chosen as a typical value for $(u_{200} \cos\phi)$, since Sieg quotes wind velocity components of 600 to 1200 cm/sec directed against the sound for his "bad propagation conditions"; according to Table 7 the constant a, characterizing the temperature gradient, perhaps does not exceed 0.1 or 0.2 in magnitude and hence may be neglected in this case. One therefore obtains $B \sim 4.9 \times 10^{-3}$ from Eq. (93). Using this result in Eq. (194) we obtain

$$(r_s/z_o) \sim 10; \qquad (195)$$

since the source height z_o is about [illegible] distance r_s to the shadow zone at the receiver height of 5 ft is 350 ft, or a little over 100 meters. Since Sieg's measurements are over a range up to 500 meters, or 1650 ft, it would appear from this estimate that under his "bad propagation conditions" the receiver was usually in the shadow zone. Hence the high losses observed under these conditions are very likely due (at least, in part) to wind-produced sound shadows.

In the case of "good propagation conditions" temperature and wind gradients were (judging from the author's remarks) probably too small to cause shadows, and other mechanisms must be sought to account for the residual excess attenuation.

It is natural to wonder whether terrain effects, such as were described by theory in subsection 1.4, might be involved here. Referring to Fig. 10 let us consider the situation where the source-receiver distance R_1 is 1000 ft. Since the source height z_o is 35 ft the angle ψ is about 0.035 radians.

The sound pressure at any point in the field is given by Eq. (50); to evaluate the factor $F(\rho)$ appearing there we must first determine the quantity ρ. In so doing we choose the expression for $\rho^{(2)}$ in Eq. (53).

Turning to Eq. (46), we assume ζ is the order of unity, as is presumably reasonable for land covered with vegetation. (Sieg states that his measurements were made at different times during a year, and that the vegetative covering therefore varied from one set of measurements to another.) The quantities $\sin\psi$ and $\zeta \sin\psi$ can thus be neglected in Eq. (53) so that the latter reduces to

$$\rho^{(2)} = \frac{k_1 R_2}{2i\zeta^2} = \frac{\pi R_2}{i \lambda \zeta^2} , \tag{196}$$

where λ is the wavelength of the sound in air. At the lowest frequency, 250 cps, used by Sieg λ is 4.5 ft so that $(\pi R_2/\lambda)$ is about 700. Hence, if as assumed earlier, ζ is of the order of unity the magnitude of the quantity $\rho^{(2)}$ will be very much greater than unity at all frequencies employed by Sieg. Referring to Eq. (55) we see that we may therefore write $F(\rho) \simeq 1/2\rho$ to a very good approximation. Using this result in Eq. (50) and carrying through approximations consistently one obtains

$$p \simeq G\, e^{ikR_1}/R_1 , \tag{197}$$

where

$$G = 1/R_1 \cdot \left[2\zeta(z + z_0) + i\lambda\zeta^2/\pi - 4\pi i z z_0/\lambda\right] \tag{198}$$

This result is subject to the conditions that ζ be of the order of unity, $\sin\psi << 1$ and $k_1 R_1 >> 1$. Under these conditions G is always less than 1, and gives the factor by which the pressure amplitude is reduced due to the ground. When $z = 0$ the result given by Eqs. (197) and (198) reduces to that given by Eq. (64) for points on the earth's surface. For $\zeta = 1$ and z, z_0, λ and r equal to 5 ft, 35 ft, 4.5 ft and 1000 ft, respectively, we find that G is given approximately by its last term $(-4\pi i\, zz_0/\lambda R_1)$ and is equal to about 0.5. The db loss caused by the ground is $(-20 \log_{10} G)$ or, in this case, 6 db. For r greater than 1000 ft the loss due to the ground will increase by 6 db for each doubling of the distance.

For frequencies greater than 250 cps (i.e., for wavelengths less than 4.5 ft) or for distances less than 1000 ft the loss caused by the ground would not be as great and the approximation used in obtaining Eq. (198) would be less valid.

We return now to the question of how to interpret the excess

losses observed by Sieg under "good propagation conditions" (Table 14). In comparing the α-values given there with the result of the very rough calculations given above it should be remembered, first of all, that the ground loss does not vary linearly with distance and hence one cannot actually calculate a loss per unit distance coefficient in this case. Also, the calculated loss is subject to uncertainty because of insufficient information about the ground impedance; i.e., in Sieg's case ζ may differ greatly from unity.

Nevertheless, it is of interest to note that the ground loss, namely, 6 db, calculated at a distance r of 1000 ft from the source is about the right magnitude to explain the observed α at 250 cps, assuming the latter to be an averaged quantity. At higher frequencies, however, the calculated ground loss at 1000 ft is probably much smaller than the values of α given in Table 14. It would therefore appear that a complete accounting for Sieg's α-values for "good propagation conditions" will require consideration of other mechanisms in addition to ground effects.

It was suggested by Blokhintzev[51] that the excess attenuation observed by Sieg might be due to scattering by turbulence; indeed calculations made of single scattering from a sound beam, using rather arbitrary, though not unreasonable, assumptions regarding the turbulence give order-of-magnitude agreement with Sieg's observation. Unfortunately, rather fundamental questions remained to be answered regarding application of scattering theory to propagation from a real source in a real atmosphere. The mechanism involved in such a situation as Sieg's will perhaps not be known until experiments are done in which micrometeorological conditions (subsections 1.5 and 1.6) are determined in more detail and methods devised to isolate the parts played by different factors.

2.2.2 Schilling, Givens, Nyborg, Pielemeier and Thorpe (1946)[68]

Propagation of high frequency sound in the out-of-doors was the subject of fairly detailed investigation by Schilling and co-workers. Though their frequency range (10-25 kc) is above the range to be emphasized in this report, the work is of interest here since the problems involved are similar. Their sources were small whistles (operated by air from small pressure tanks); condenser microphones were used as receiving transducers.

Special tests showed that terrain effects described in subsection 1.4, were unimportant for their experimental conditions. Acoustical shadow effects were often encountered and could be identified. It was found possible to predict where shadow regions would exist by ray calculations based on detailed micrometeorological data. For measuring attenuation coefficients shadow effects were avoided by mounting

both source and receiver about 5 ft above the ground, source-receiver separations being seldom greater than 300 ft.

Typical loss coefficients are given in Fig. 23; the corresponding temperatures ranged from 75° to 88°F, and the relative humidities from 78 to 100%. In determining these coefficients use was made of theory which takes into account the effect of scattering on the response of a directional receiver (i.e., a considerably more elaborate scheme than that described in subsection 2.1 was used in determining α). The coefficients given in Fig. 23 are those which would presumably have been obtained, if a nondirectional receiver had been used in taking the measurements. (Had the original data on sound level vs. distance been simply fitted to Eq. (2), without the above correction, the apparent attenuation coefficients would be greater than those given, by amounts up to about 50 db/1000 ft.) Shown for comparison are absorption coefficients ($\alpha_{class} + \alpha_{mol}$) calculated from the theory for classical and molecular absorption given in subsection 1.2.2 and 1.2.3. The shaded area indicates the range within which the calculated values lie for the given conditions. The mean observed (corrected) value of α exceeds the mean theoretical absorption coefficient by amounts varying from 22 db/1000 ft at 10 kc to 100 db/1000 ft at 30 kc.

2.2.3 Eyring (1946)[69]

The work here referred to deals with various aspects of audible sound (75 - 10,000 cps) propagation through jungle areas in Panama. We cite here only certain results which pertain to the present topic. For comparison with findings on transmission through wooded areas Eyring made a few sets of measurements in the open, over different kinds of ground cover. In these measurements the sound was generated by loudspeakers; for frequencies up to 4800 cps these were actuated by electrical noise, while the frequencies 7000 and 10,000 cps were generated by use of single-frequency signals, in the more usual manner. Sound levels were measured by means of a high speed recorder actuated by the filtered output of suitable microphones.

In his determination of sound levels, Eyring was able to isolate the effects of certain factors, as did Schilling, et al. Shadow zones were found whose boundaries were sharp enough to recognize at frequencies above 2000 cps, but were blurred at lower frequencies. Losses associated with shadow zones were found especially (a) near noon on calm sunny days (i.e., when B, Eq. (93) was large due to a strong temperature effect) or (b) when a wind opposed the sound (i.e., when B was large due to wind gradients). By raising source and receiver sufficiently, or by choosing times when atmospheric conditions were suitable, Eyring was able to make transmission measurements in which shadow zones had no influence.

In one set of measurements the sound was propagated over a paved tarvia surface near noon on a sunny day. The relative humidity was 55 percent and the temperature 80°F. The source was kept at 5 feet above the ground, but at each receiver position the microphone was elevated sufficiently to move it out of the shadow and into the beam.

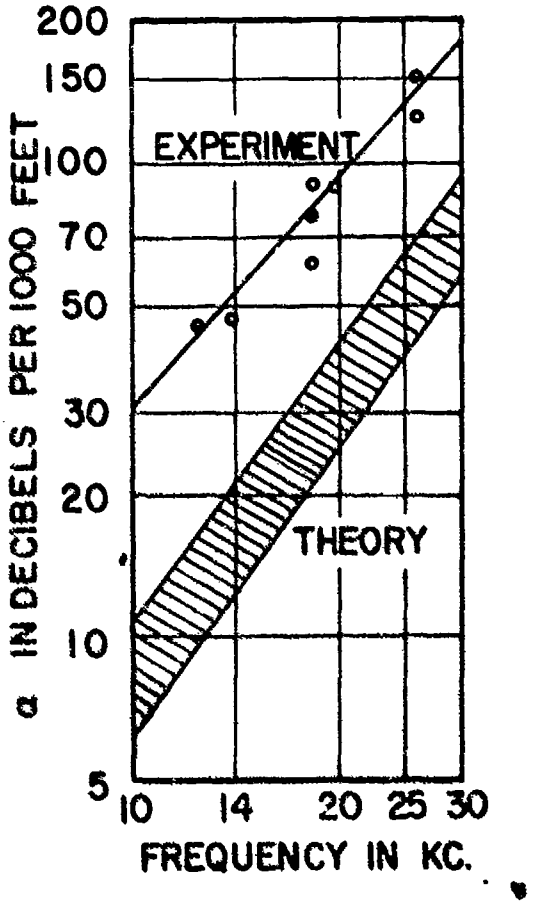

Fig. 23. Loss coefficient α vs frequency from outdoor measurements of Schilling and co-workers[68]. Theory gives ($\alpha_{class} + \alpha_{mol}$) from Eqs. (11), etc. Upper limit of shaded area is for assumed conditions of 75°F, 78% relative humidity; lower limit is for 88°F, 100% relative humidity.

The data on received sound levels vs source-receiver separation were fitted to Eq. (2) by the method described in subsection 2.1; loss coefficients obtained in this way for the different frequencies or frequency bands are given in the first row of coefficients in Table 15. Also shown in Table 15 (in the second row) are values of $(\alpha_{mol} + \alpha_{class})$ calculated from Eqs. (11), etc. for the given conditions of humidity and temperature.

TABLE 15

Loss Coefficients over Various Kinds of Terrain (from Eyring[69])
(All loss coefficients are in db/1000 ft)

Frequency (cps)	75 150	150 300	300 600	600 1200	1200 2400	2400 4800	7000	10,000
Hard surface: RH=55%, T=80°F								
Observed α	0.	0.	10.	0.	15.	11.	20.	45.
$(\alpha_{mol} + \alpha_{class})$	0.1	0.1	0.1	0.1	0.4	1.7	6.8	13.7
Hard surface: RH=95%, T=76°F								
Observed α	-	-	-	-	-	-	15.	27.
$(\alpha_{mol} + \alpha_{class})$	-	-	-	-	-	-	4.0	7.9
6-12 in. grass								
Observed α	2.5	6	9	-	-	-	-	-
18 in. grass								
Observed α	2.5	9	30	30	-	30	30	60

Measurements were also made at 7000 and 10,000 cps on a day when no appreciable wind or temperature gradients existed; there was therefore no need to elevate the microphone in this case. The resulting attenuation coefficients are shown in the third row of coefficients in Table 15; in the fourth row calculated values of $(\alpha_{mol} + \alpha_{class})$ are shown for the given atmospheric conditions, namely, 95% relative humidity and 76°F.

Measurements were also made over grass-covered ground, pains being

taken to avoid refraction or shadow effects. Loss coefficients computed from these data are shown in the fifth and sixth rows of Table 15. Evidently the ground covering plays a very important role in determining sound propagation losses. The temperature and relative humidity are not given for these latter cases, but are perhaps not greatly different than those for the experiments over tarvia. It is evident, particularly at the lower frequencies, that losses in sound level due to molecular absorption are considerably smaller than those due to the ground covering.

It is of interest to calculate the loss in 1000 ft expected due to ground loss, assuming conditions are such that Eqs. (197) and (198) are valid. As will be explained further in Section III the losses over 6 - 12 in. grass are given fairly well by letting $z = z_0 = 5$ ft, $R_1 = 1000$ ft and by assuming $\zeta \simeq 5\tau$. On this basis one obtains for $-20 \log_{10} G$ at 112 cps, 225 cps and 450 cps, respectively, the values 1.7, 6.8 and 9.8 db, to be compared with the values 2.5, 6 and 9 db given in Table 15 for the three lowest frequency bands. On the other hand, it is not clear how to account for the large losses obtained over 18 in. grass.

2.2.4 Delsasso and Leonard (1953)[70]

Work has recently been reported on propagation of low frequency sound (125-1000 cps) over a path length of about 8500 ft at an altitude of 10,000 ft. The site was in a mountainous region near Bishop, California. Source and receiver were mounted on towers set up on adjacent mountain peaks; the source-receiver line thus passed high over a valley which lay between the two peaks.

The source of sound was a small oxygen-acetylene cannon fired at intervals of a few seconds by a timing device. This arrangement provides a short pulse of sound having frequency components in the desired range. Appropriate filters in the receiving system selected the particular frequency to be used on any one test. Received pulses were displayed on an oscilloscope and recorded photographically.

The total loss over a distance of 8400 ft was measured by comparing the sound level at the main receiver microphone, which is at a distance of about 8500 ft from the source, with the level at a reference microphone, located about 100 ft from the source. By assuming the validity of Eq. (2) the loss coefficient α for any given pulse was determined from the measured ratio of pressure amplitudes caused at the two microphones by that pulse.

The report cited gives the results in tabular form. For each set of measurements, consisting of a series of pulses at a given frequency, the tables give the relative humidity, temperature, atmospheric pressure, wind direction and wind speed, as well as the maximum, minimum and average values of α observed in the set. Tables 16 - 19 below and Figs. (24 - 27) give a summary of their results. In Tables 16 - 19 the various columns give, in order, (1) the set number, (2) wind direction, (3) wind speed, (4) relative humidity (RH), (5) temperature (T), (6) the average observed loss coefficient (α_{Exp}) and (7) the theoretical absorption coefficient (α_{Theo}), given by the sum ($\alpha_{class} + \alpha_{mol}$) as in Eqs. (11), etc. No entry is made for (α_{Theo}) when the computed value is less than 0.1 db/1000 ft. In all cases the direction of sound propagation was from west to east.

TABLE 16

Loss Coefficients at High Altitudes: Delsasso and Leonard[70]

1000 cycles

No.	Wind		RH	T	α_{Exp}	α_{Theo}
	Dir.	Speed(ft/sec)	(%)	°F	db/1000 ft	
A 2	SE	12	21	64	2.29	1.64
4	SW	7	21	61	2.06	1.79
9	E	10	23	68	2.23	1.03
16	SW	5	52	55	1.76	0.44
18	S	10	34	52	2.12	1.24
20		0	55	56	1.71	0.37
24	SW	5	52	55	2.23	0.42
25	W	7	27	64	2.29	0.94
30		0	31	51	2.53	1.44
33	ENE	4	37	40	1.94	1.94
38	W	12	24	58	2.18	1.44
41	SW	7	25	58	2.06	1.44
42	NW	3	40	47	2.06	1.24
43	NW	2	41	46	2.29	1.14
55	N	3	25	59	1.88	1.34
65		0	73	51	1.88	0.28
67	S	8	24	61	0.83	1.29

TABLE 16
(continued)

No.	Wind Dir.	Wind Speed(ft/sec)	RH (%)	T °F	α Exp db/1000 ft	α Theo db/1000 ft
B 6d	W	7	34	46	2.35	1.64
7	ENE	4	40	40	2.18	1.79
9d	NE	6	18	39	2.56	5.84
10	ENE	6	33	41	1.71	2.44
11	E	8	33	45	2.29	1.94
12	SE	6	34	52	2.52	0.97

TABLE 17
Loss Coefficients at High Altitudes: Delsasso and Leonard[70]

500 cycles

No.	Wind Dir.	Wind Speed(ft/sec)	RH (%)	T °F	α Exp db/1000 ft	α Theo db/1000 ft
A 1	E	15	21	64	2.12	0.34
5	E	5	21	65	2.64	0.39
10	E	8	26	66	1.76	0.23
14	S	10	40	50	1.06	0.26
15	SW	7	16	52	1.30	1.31
17	SW	7	16	52	1.53	1.41
21	SE	9	24	68	1.36	0.24
22	W	10	27	64	1.53	0.25
29	E	10	58	59	1.36	
31	NE	7	27	65	2.24	0.23
39	W	5	20		2.35	0.51
44	W	6	48	57	1.88	0.11
47	W	7	48	55	2.06	0.14
49	NE	3	26	60	0.715	0.30
50	E	11	15	67	1.48	0.62
53	S	10	17	64	1.88	0.58

TABLE 17
(continued)

No.	Wind Dir.	Wind Speed(ft/sec)	RH (%)	T °F	α_{Exp} db/1000 ft	α_{Theo} db/1000 ft
56	W	7	32	55	2.41	0.29
57	E	3	24	61	2.29	0.35
61	NE	5	25	59	1.82	0.37
64	W	8	17	61	2.23	0.69
70	SW	10	60	42	2.23	0.185
71	E	10	17	64	1.88	0.61
72	W	8	17	61	1.94	0.55
B 6c	W	7	34	46	0.012	
8	NE	7	65	27	2.00	0.40
9c	NE	6	18	39	1.94	2.11
13	ENE	7	33	41	1.82	0.62
18	E	3	33	36	2.06	0.93
20	S	8	32	48	1.59	0.42
21	N	8	29	50	1.65	0.47
22	SE	5	35	51	1.36	0.31
24	E	8	41	48	1.88	0.30
26	NE	4	23	47	1.53	1.00

TABLE 18
Loss Coefficients at High Altitudes: Delsasso and Leonard[70]

250 cycles

No.	Wind Dir.	Wind Speed(ft/sec)	RH (%)	T °F	α_{Exp} db/1000 ft	α_{Theo} db/1000 ft
A 3	E	8	27	63	0.947	
6	E	5	22	61	1.18	0.11
11	E	7	24	69	0.538	
19	S	9	34	52		
23	S	8	30	54		
28	E	4	30	45	0.83	0.14
34	W	9	29	49	0.48	0.13
37	NW	8	12	54	0.538	0.46

TABLE 18
(continued)

No.	Wind Dir.	Wind Speed(ft/sec)	RH (%)	T °F	α_{Exp} db/1000 ft	α_{Theo}
45	SW	8	18	53	0.831	0.28
51	SW	5	23	42	0.715	0.29
52	SW	10	63	41	1.30	
54	W	1	56	54		
58	E	10	18	66	1.24	0.11
59	SE	2	94	45	0.48	
60	W	15	25	56	1.01	0.105
62	NE	5	20	68	0.538	
63	E	9	45	50	0.596	
68	E	8	38	59	0.772	
69	W	15	38	54	1.24	
B 2	SW	5	45	52	0.537	
4			30	45	1.01	0.14
6b	W	7	34	46	1.47	0.10
9b	NE	6	18	39	1.36	0.59
14	W	9	29	49	0.362	0.12
16	SW	5	45	52	1.30	
19	NE	4	35	39	0.362	0.16
23	E	3	37	36	0.947	0.15
25	E	5	21	62	0.713	

TABLE 19
Loss Coefficients at High Altitudes: Delsasso and Leonard[70]
125 cycles

No.	Wind Dir.	Wind Speed(ft/sec)	RH (%)	T °F	α_{Exp} db/1000 ft	α_{Theo}
A 7	E	5	21	61	0.187	
8	W	3	34	61		
12	E	10	27	66		
13	E	8	29	61	0.128	
32	E	4	24	39	0.187	
35	NE	6	26	57		
36	NE	5	30	57	0.012	
46	SE	9	47	60	0.363	
48	S	8	44	51		
66	E	8	37	57		

TABLE 19
(continued)

No.	Wind Dir.	Wind Speed(ft/sec)	RH (%)	T °F	α_{Exp} db/1000 ft	α_{Theo}
B 1	E	2	34	37	0.129	
3	SW	6	59	30	1.30	
5	E	4	29	39	0.421	
6a	W	7	34	46	0.012	
9a	NE	6	18	39	0.129	0.13
15						
17	SSE	12	34	50	0.772	

In Figs. (24 - 27) are plotted (as crosses) all values of (α_{Exp}) obtained from the above tables; the horizontal coordinate of each plotted point is the absolute humidity. For comparison the theoretical absorption coefficients (α_{Theo}) are also given (as circles). The latter are calculated for the humidities and temperatures applicable to the different sets of measurements and, like α_{Exp}, are plotted against absolute humidity.

Also shown in each plot is a smooth theoretical curve giving ($\alpha_{mol} + \alpha_{class}$) vs absolute humidity for a fixed temperature of 60°F. This curve may be compared with the individual theoretical points, which show scatter in the vertical direction because of temperature variations from one set to another. It is seen that, in spite of this scatter, the individual points cluster fairly closely about the fixed-temperature theoretical curve. (Indeed an advantage of plotting α against absolute humidity, as is done in Figs. (24 - 27), is that the theoretical absorption coefficient is then much less sensitive to variations in temperature than when relative humidity is the independent variable.

According to Figs. (24 - 27) the values of α obtained experimentally in the out-of-doors show considerable vertical scatter; much of this scatter probably is due to time-varying temperature and wind structure in the medium, whose effect is to cause large fluctuations in the amplitude of transmitted signals (see subsection 1.6). (However, the authors do not give appropriate data from which the fluctuation amplitudes can actually be determined.) If we let $\bar{\alpha}$ (h) be the mean value of the experimental α-values in the immediate vicinity of any given humidity h we find that $\bar{\alpha}$ does not vary greatly with h over the range studied in these experiments. Measured values of $\bar{\alpha}$ tend to be roughly in agreement with theory at the lower humidities, but to exceed theoretical values by greater and greater amounts as one goes to higher humidities.

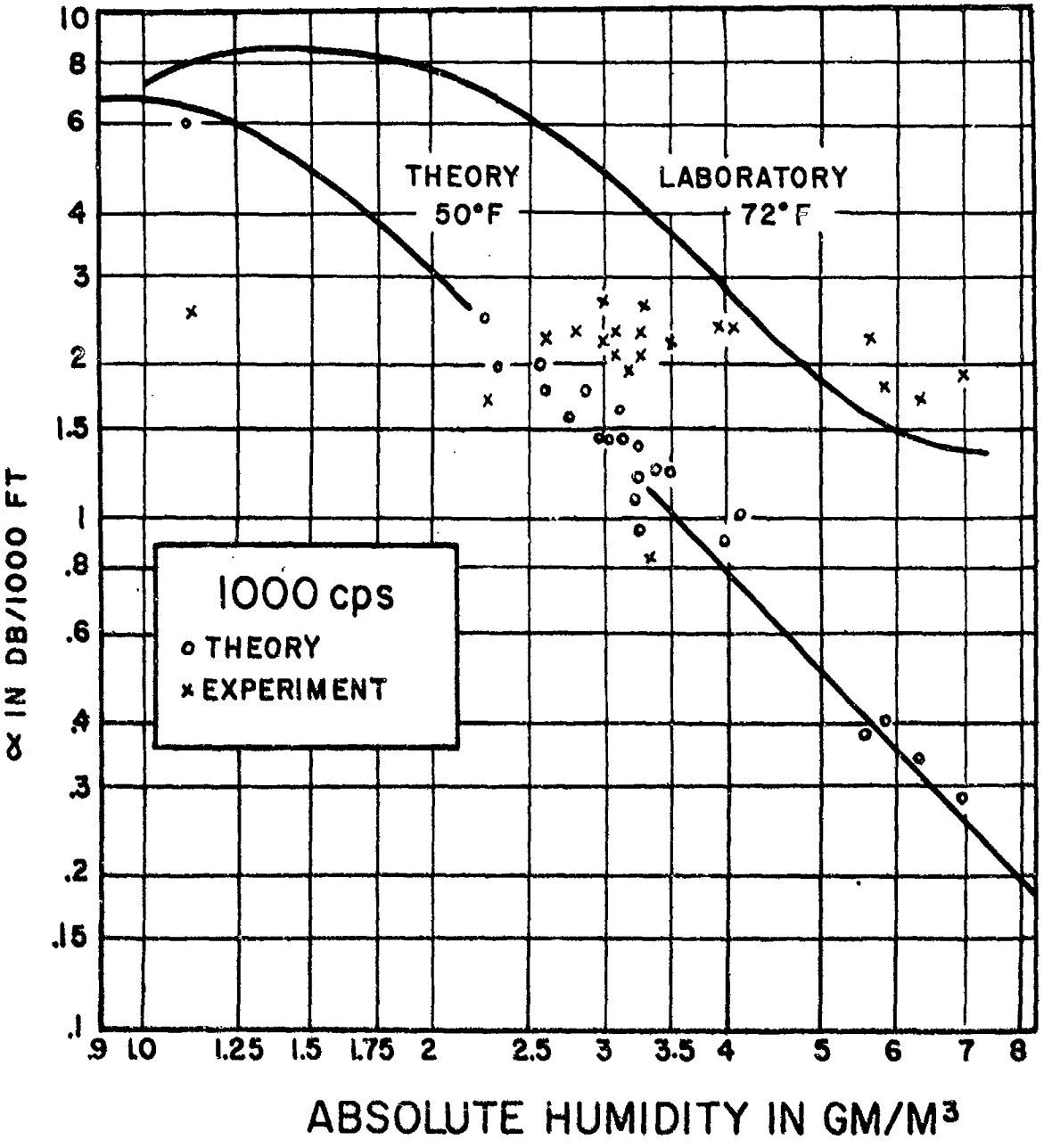

Fig. 24 Loss coefficients in open air, from Delsasso and Leonard[70]: 1000 cps.

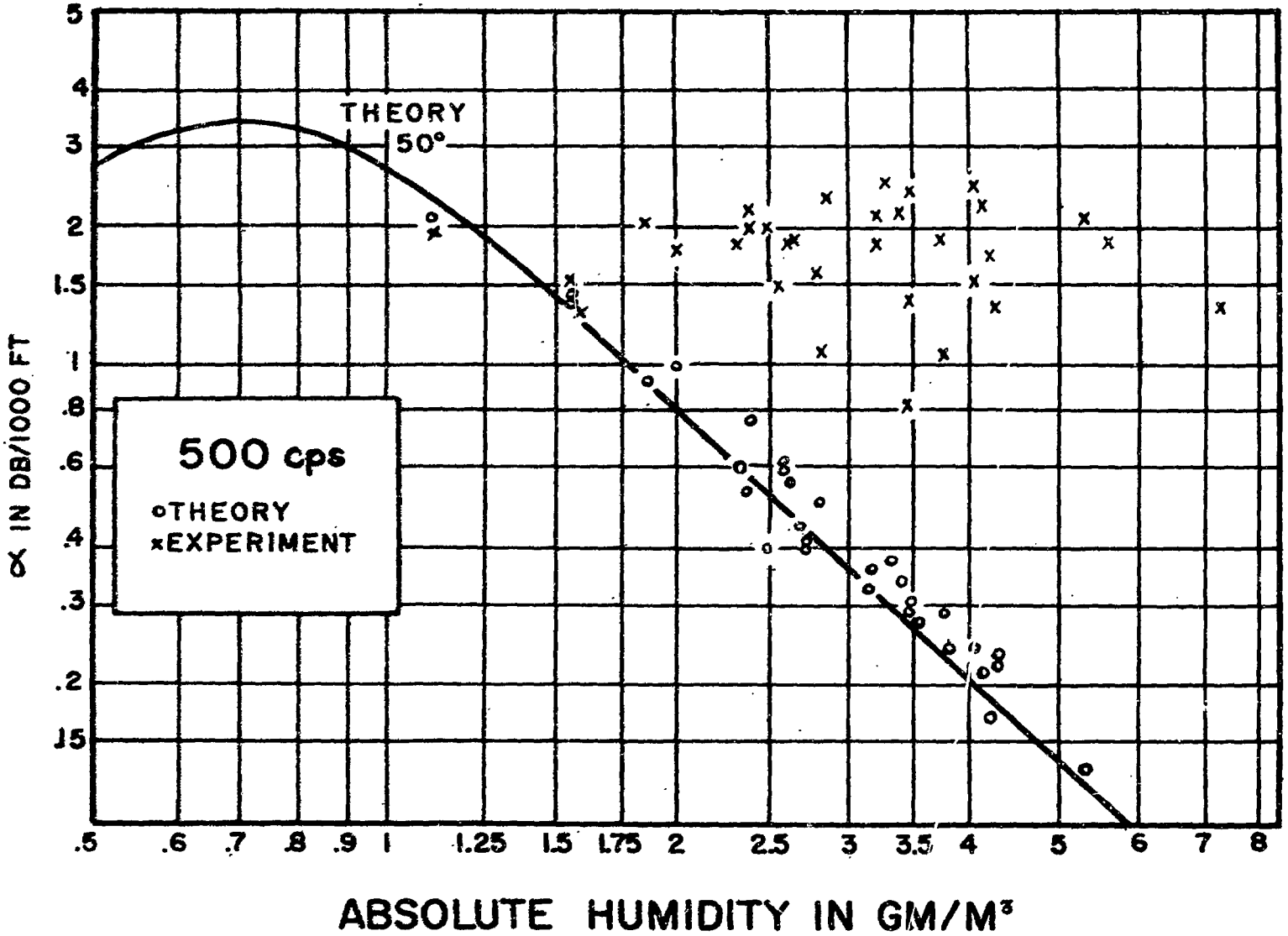

Fig. 25 Loss coefficients in open air, from Delsasso and Leonard[70]: 500 cps

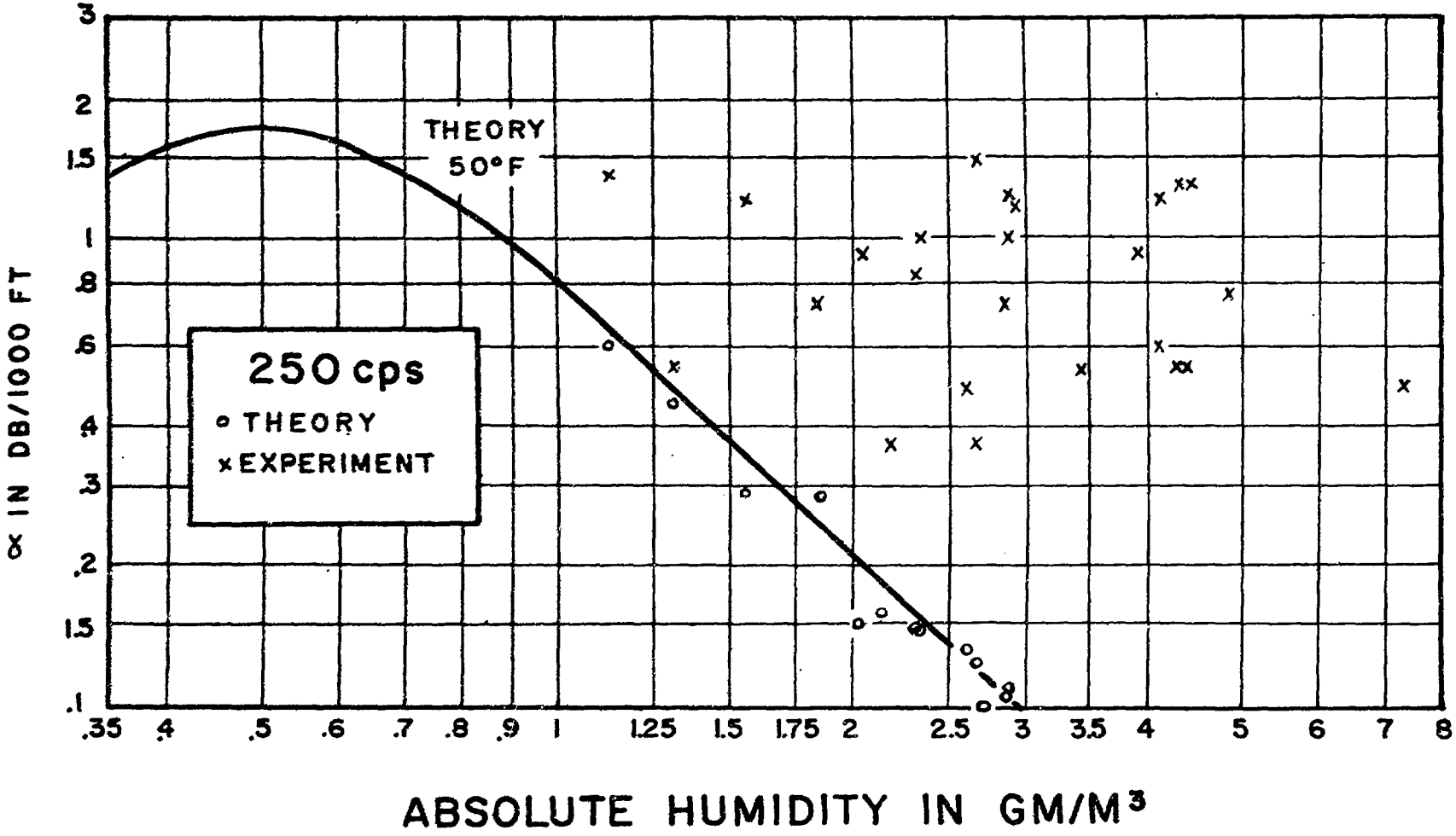

Fig. 26 Loss coefficients in open air, from Delsasso and Leonard[70]: 250 cps

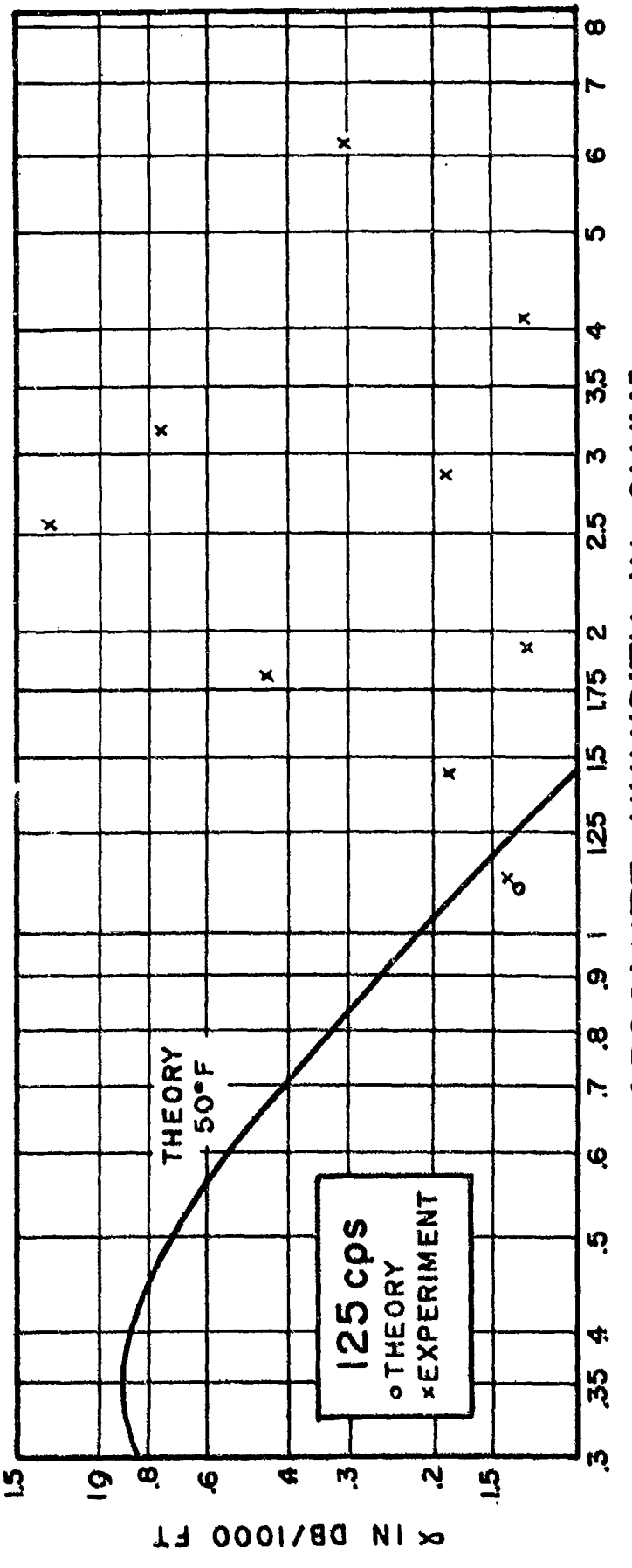

Fig. 27 Loss coefficients in open air, from Delsasso and Leonard[70]: 125 cps

The cause of the discrepancy at higher humidities is unknown. It should, of course, be remembered (subsection 1.2.4) that data taken in the laboratory also show excess losses at high humidities. In Fig. (24) is shown a curve of α vs h plotted by Delsasso and Leonard, based on laboratory measurements at 1000 cps. We see that the loss coefficients given by this curve are even higher than most of the field values. (The fact that the laboratory curve is for 72°F, while the mean temperature for the field data is near 50°F is probably not of great importance in explaining the great discrepancies between theory, field data and laboratory data; according to theory an increase of temperature from 50° to 70°F should increase absorption coefficients by about 25%.)

Horiuchi[71] has recently suggested that a considerable part of the attenuation observed by Delsasso and Leonard may be due to scattering by turbulence (see subsection 1.6). There are certain difficulties in connection with this explanation, however. One is that the experimental α does not appear to increase significantly with increasing wind speed, though such an increase would be expected from the hypothesis (since the turbulence increases with wind speed; see subsection 1.6). Another difficulty is that the sound source of Delsasso and Leonard is probably essentially non-directional at 1000 cps and less; hence it is not clear how one should proceed in calculating losses due to scattering (see subsection 1.6).

2.3 PROPAGATION OF AIRCRAFT NOISE

2.3.1 Regier (1947)[72]

Measurements were made by the above author to determine the sound level on the ground directly below an airplane in normal flight, as a function of its altitude. The airplane used was a light trainer having a 2000 rpm, 400 horsepower nine-cylinder engine directly connected to a two-blade (9 ft diameter) propeller. Horizontal flights were made at approximately 165 mi/hr at altitudes from 300 to 5000 ft. All measurements were made on the same day. The sky was clear; there was a slight breeze; the relative humidity was 40% and the temperature 72°F on the ground.

Regier determined acoustical levels with a General Radio sound level meter, without filters; the maximum indication of the meter, positioned at the ground, was noted for each flight, as the plane passed overhead. The data given are, therefore, of the nature of "total" sound levels, rather than levels for different discrete frequencies. Regier states, however, that for the airplane in question most of the sound

energy is in the 70 - 300 cps frequency range.

The observed sound levels at the ground are plotted (on semi-log paper) against airplane altitude R in Fig. 28 . For comparison a straight line is plotted in the same figure, representing the sound level variation which would be expected if the (1/R) law were valid, i.e., if the pressure amplitude at the ground were given by Eq. (2) with $\alpha = 0$. (Since the observed level would then be given by 20 $\log_{10}$ (A/R) it can be readily shown that in this case the sound level should decrease by about 6 db for each distance-doubled. (See subsection 3.2.1.))

Since Regier's data fit the given line rather well α is apparently negligible for the conditions of his experiments. This may not be surprising, since at such a low frequency as 300 cps and for the weather conditions noted, computed values of α_{class} and α_{mol} are only 0.004 and 0.02 db/1000 ft, respectively. One could nevertheless not be sure α is negligible without experimental confirmation; it will be remembered that Sieg's measurements made along the ground at frequencies in the same range, viz., 250 cps, yielded α-values from 4.6 to 17.4 db/1000 ft. Also, we shall see that Hayhurst's data, for propagation along the earth, give large values for α.

It appears that Regier's case, that of low frequency sound propagated vertically, is one of the few situations of interest where the 1/R law holds with satisfactory accuracy out-of-doors. However, even here, the author points out a small effect which might suggest an attenuation constant α that is not quite negligible. He states that the sound output of the plane may be expected to increase with altitude at the rate of about 0.4 db/1000 ft. Hence the data plotted in Fig. 28 ought, on this basis, to have been corrected for this, if they are to represent the facts for a constant source. The fact that a good fit to a straight line (i.e., to the 1/R law) exists in spite of this suggests that an exponential loss (see subsection 1.1.3) exists such that the loss coefficient α is about equal to 0.4 db/1000 ft; as the airplane goes to higher altitudes, the increase in source output would then be just cancelled by increased exponential losses due to a longer propagation path.

2.3.2 Parkin and Scholes (1954)[73]

Considerably more information on how sound propagates vertically from aircraft to ground has become available very recently. Parkin and Scholes measured sound levels at the ground on six different days, in frequency bands up to 8 kc, due to a light transport monoplane flying overhead at various altitudes up to 2000 ft.

The plane was a D.H. 104 Dove made by the DeHavilland Aircraft Company. It is twin-engined, powered by piston engines rated at about

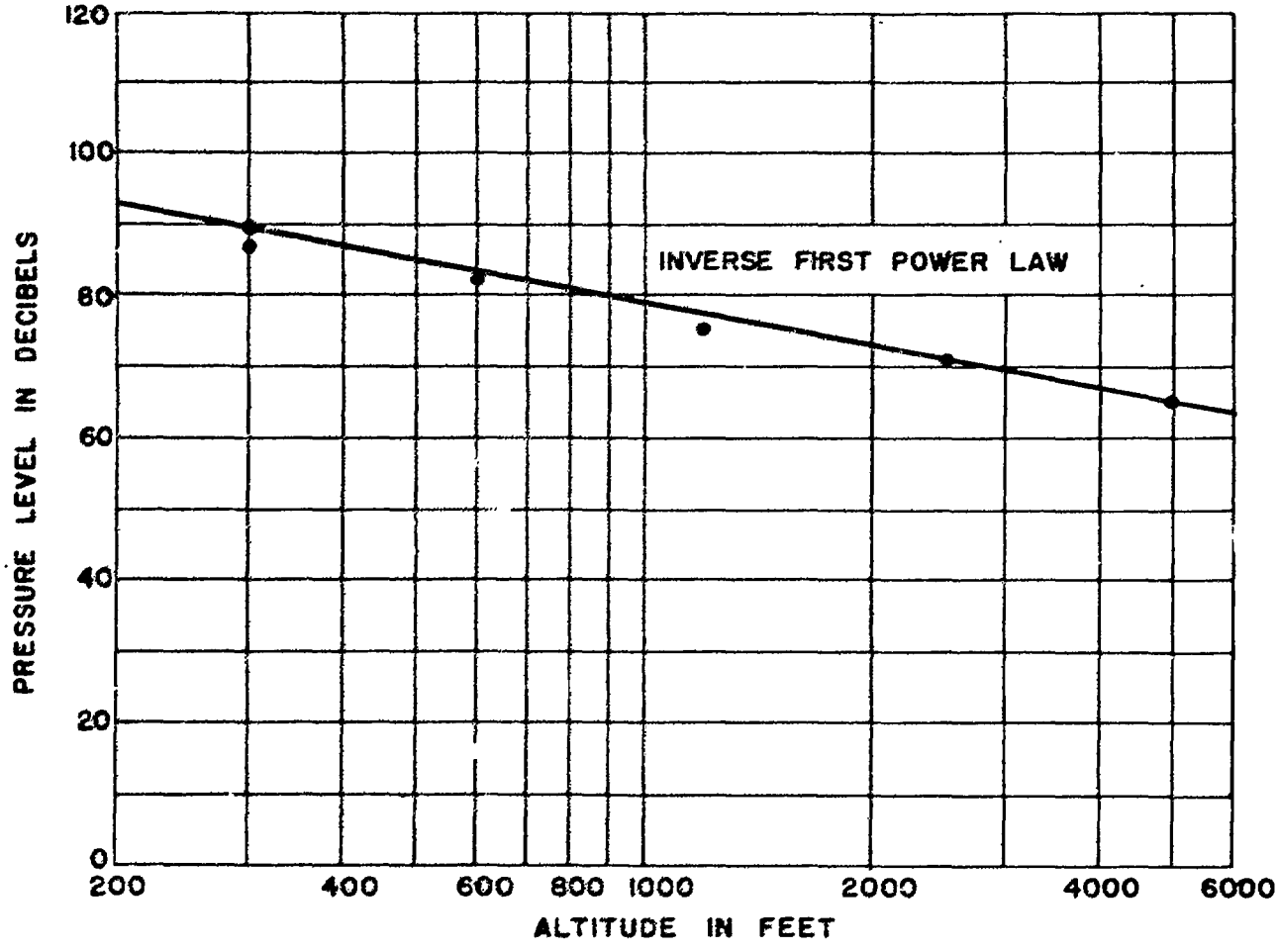

Fig. 28 Pressure level at ground due to overhead aircraft, vs height of aircraft, from Regier[72]. Noise spectrum centered at about 300 cps.

350 hp at 4000 ft, and has three-blade propellers 7.5 ft in diameter.

The signal from a condenser microphone mounted 5 ft high in the center of an airfield was recorded on magnetic tape and subsequently analyzed through one-third octave filters onto a high speed level recorder. The authors note that the recorder indicates something near the peak level of an input waveform rather than the mean rectified level. Also, they state that the trace on each record showed rapid fluctuations, and that mean lines were drawn by eye through these traces. The maximum values reached by these mean lines were noted; these maxima gave the levels which, at low frequencies, occurred when the aircraft had just passed overhead, and which at high frequencies (due to changing directionality of the source) occurred a short time later. Plots of sound level in various frequency bands versus distance from the aircraft sound source were thus made by associating each maximum level, determined in the manner just discussed, with the assumed distance to the source when the maximum occurred. The data for any given frequency band, on a given day, were fitted to Eq. (2), following the procedure described in subsection 2.1, and the corresponding loss coefficient α determined. Results for the six trials are given in Fig. 29 . Also shown are calculated values of the absorption coefficient ($\alpha_{mol} + \alpha_{class}$) based on Eqs. (11), etc. It is remarkable that loss coefficients observed by Parkin and Scholes in the out-of-doors are sometimes actually less than those predicted by Eqs. (11) - an unusual occurrence. In general, the Parkin and Scholes data are in moderately good agreement with Eqs. (11). This suggests that the latter equations may be rather useful in the problem of predicting noise levels due to aircraft nearly overhead.

2.3.3 Hayhurst (1953)[74]

Data has also recently become available on propagation of aircraft noise over a horizontal path along the ground. Due to the close bearing of this work on practical field problem, the results will be described here in some detail. Hayhurst made nineteen sets of measurements, extending over a period of three months. He used a filtered receiver, covering the audible range of frequencies; sound levels were measured at a series of points out to 2500 ft from the source.

The source of sound was a Bristol Hercules 630 14-cylinder aero-engine driving, through a reduction gear of 0.444:1, a four-bladed wooden propeller 13.25 ft in diameter. The engine, mounted in the airframe of a Vickers Viking aeroplane, was operated at the constant setting of 30 inches of mercury manifold pressure and 1900 rpm, and at this power setting developed about 750 hp. Sound pressure levels were measured on a Standard Telephones and Cables noise meter with electric filters inserted to analyze the levels in eight octaves between 37.5 and 9600 cps. The microphone was on a tripod 4 ft above the ground.

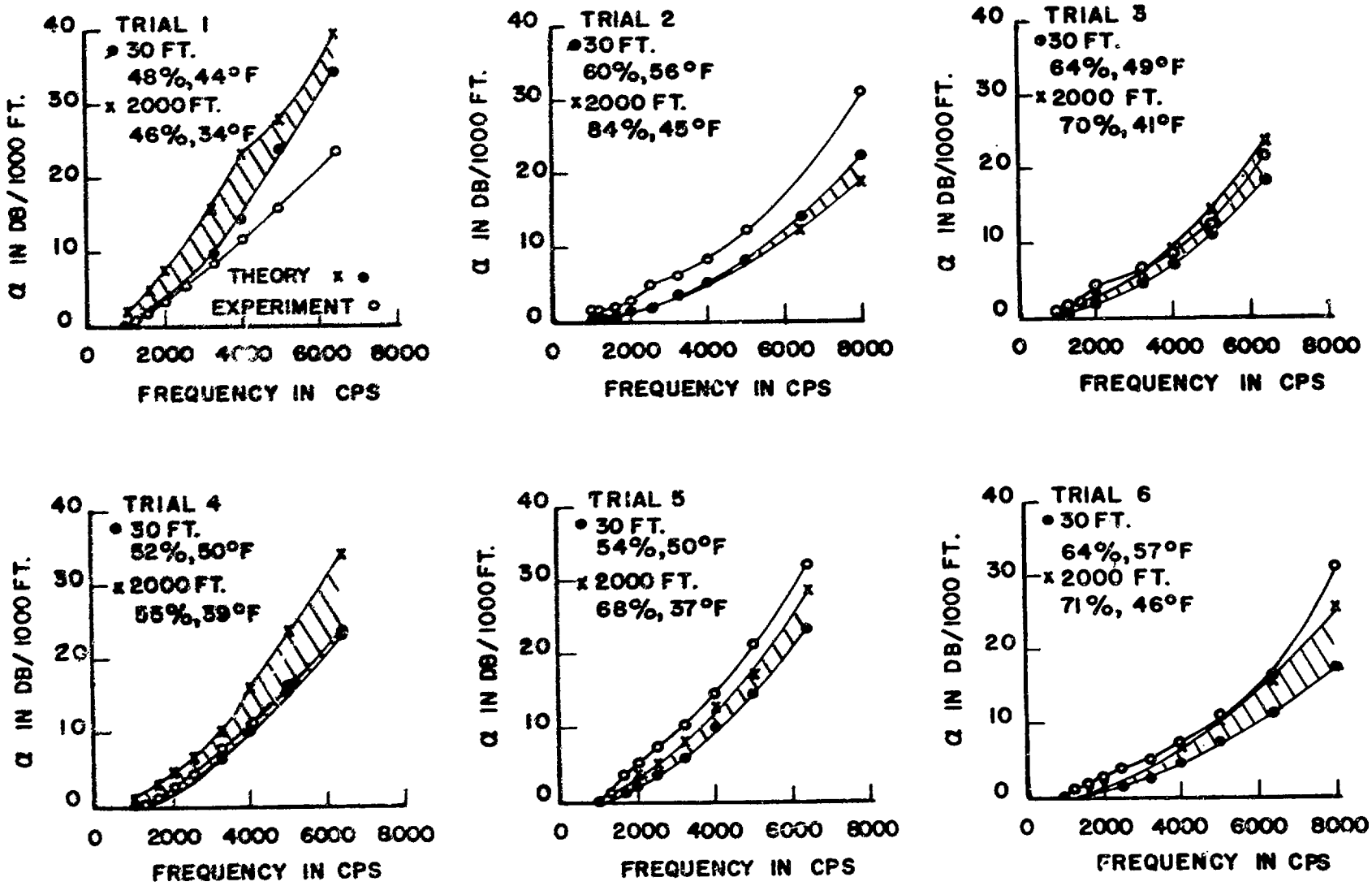

Fig. 29 Loss coefficients vs frequency for sound propagation from aircraft to ground, from Parkin and Scholes. Open circles, experimental; filled circles, calculated absorption coefficients ($\alpha_{class} + \alpha_{mol}$) for conditions at 30 ft; crosses, calculated values at 2000 ft.

In each trial the sound level in each octave band was determined at various distances from the source, and the results fitted to Eq. (2) by the process described in subsection 2.1. The loss coefficients α so obtained are given in Table 20 (from Hayhurst with slight modifications). For each set of measurements made on a given day, the temperature, relative humidity, scalar wind, and vector wind are given, as well as other coefficients in the different bands. By scalar wind is meant the wind speed, i.e., the magnitude of the wind velocity. By vector wind is meant the component of wind velocity directed towards the source from the receiver.

Examining the loss coefficients in any given frequency band, one finds considerable variation from one set of measurements to another. In exploring causes of these variations, Hayhurst found that, of the several measured meteorological factors, the vector velocity gave (by far) the best correlation with the attenuation coefficients. This is exemplified in Fig. 30 (from Hayhurst) which shows loss coefficients for the 300 - 600 cps band plotted against the corresponding vector wind.* It is evident that the component of wind blowing against the direction of sound propagation has a very great effect on the attenuation in this frequency band. Similar plots were made for the other octaves and significant correlations were again found, for all except the lower two and upper octaves. (Of these exceptional cases the attenuation due to wind was apparently so small as to be masked by experimental errors in the lower two bands, while measurements were too few in the upper one.)

From these plots, Hayhurst determined the rate of change of attenuation with vector wind in the various frequency bands considered: the results are plotted vs frequency in Fig. 31 (from Hayhurst). It should be remembered that the rate-values given are statistically significant only for the five octaves covering the frequency range 150 - 4800 cps.

No significant correlation was found to exist between loss coefficients and scalar wind. This suggests that the effects noted are not due to scatter of sound by turbulence, since this should occur regardless of wind direction (see subsection 1.6). Instead the losses caused by the wind are probably due to acoustical shadows (see subsection 1.5).

---

*The loss coefficients given in Table 20 are, of course, for different relative humidities. With the hope of reducing scatter due to this variable, Hayhurst adjusted all coefficients to 50% relative humidity, presumably by means of Kneser's theory, and it is these adjusted coefficients which are plotted in Figs. 30-31, 33 . He states, however, that the corrections were comparatively small.

TABLE 20
Loss Coefficients Over a Concrete Runway,
from Hayhurst[74].

Set	T (°C)	RH (%)	Scalar Wind mi/hr	Scalar Wind ft/sec	Vector Wind mi/hr	Vector Wind ft/sec	Loss Coefficients in db/1000 ft 37.5 – 75	75 – 150	150 – 300	300 – 600	600 – 1200	1200 – 2400	2400 – 4800	4800 – 9600
1	11	51	16.1	23.6	2.8	4.1	- 7.1	- 4.3	- 1.8	- 2.2	- 4.5	+ 3.1	+ 4.1	+32.9
2	12	49	12.6	18.6	8.1	11.8	+ 2.5	+ 5.7	+ 9.9	+20.7	+19.3	+20.6	+39.0	+52.3
3	7	59	16.1	23.6	15.8	23.2	- 5.5	- 3.2	+25.6	+23.6	+29.4	+42.8	+46.0	
4	10	43	12.7	18.6	- 9.8	-14.4	+ 2.0	+ 0.9	+ 0.8	+ 0.4	+ 0.1	+ 2.7	+14.0	+21.2
5	11	70	25.3	37.2	0.	0.	- 0.6	+ 4.1	+ 7.3	+ 9.6	+ 9.0	+ 8.5	+16.6	+33.4
6	8	51	10.4	15.2	-10.2	-15.0	+ 3.5	+ 1.1	- 1.7	- 1.9	- 3.8	+ 3.5	+11.3	+38.9
7	12	37	5.8	8.4	- 5.3	- 7.8	- 0.8	+ 0.8	+ 1.2	+ 4.2	+ 3.8	+ 6.1	+15.2	+37.0
8	13	51	15.0	22.0	- 5.1	- 7.4	- 7.4	- 3.6	- 4.6	- 5.4	- 4.4	- 7.1	+10.6	+19.4
9	13	51	15.0	22.0	+ 5.1	7.4	+13.4	+ 1.2	+10.1	+15.1	+25.2	+38.2	+43.4	+33.0
10	8	73	13.8	20.2	0.	0.	0.	+ 4.1	+ 1.6	+ 4.4	+ 6.3	+ 3.8	+14.9	+26.0
11	15	45	11.5	16.9	- 2.0	- 2.9	- 2.0	- 9.0	- 7.0	+ 4.0	+12.0	+23.0	+20.0	+17.0
12	18	36	5.8	8.4	3.7	5.4	+ 7.8	+ 6.5	+10.3	+13.0	+15.6	+ 7.9	+13.4	+23.4
13	18	36	5.8	8.4	- 3.7	- 5.4	+15.6	+ 6.2	+ 5.5	+11.7	+17.1	+20.7	+24.7	+40.4
14	19	29	9.2	13.5	1.6	2.4	0.	- 4.0	+ 7.0	+ 3.0	+ 4.0	+ 4.0	+18.0	+22.0
15	13	73	9.2	13.5	8.1	11.8	+ 1.9	+ 7.9	+10.7	+13.0	+15.2	+19.1	+45.4	+38.0
16	11	67	9.2	13.5	5.9	8.6	+ 0.2	+ 1.4	+ 5.7	+ 5.8	+ 7.0	+18.4	+26.4	+48.4
17	6	55	12.7	18.6	8.1	11.8	+ 2.5	+ 5.5	+12.3	+23.4	+24.9	+19.9	+34.2	+41.0
18	7	70	17.3	25.4	-16.2	-23.8	- 3.1	- 2.6	- 2.1	- 1.8	- 1.2	+ 0.1	+ 3.6	+22.4
19	7	89	11.5	16.9	- 5.8	- 8.4	+ 1.9	+ 5.0	+ 4.2	+ 0.5	- 0.1	- 1.3	+ 4.2	-38.2

Other data of Hayhurst's support the conclusion that his results are strongly influenced by the sound shadows due to wind. Two sets of measurements were made to determine the effect of receiver height. Sound level determinations were made, as before, at various distances from the source. At each distance, readings were taken with the receiver microphone at four different heights, namely, at 0, 10, 20 and 30 feet above the ground.

In one set of measurements there was a wind of 5 knots in the direction of the sound. Here it was not possible to pick out any variation of attenuation with height.

In the other set there was a wind of 7 knots opposed to the sound propagation direction; here there was a progressive increase of sound level with height. The results, in terms of effective loss coefficients at the several heights, are shown in Fig. 32. Since this height-effect occurs only for an upwind, it is evidently not due either to scattering or to terrain influences. It must, therefore, be due to acoustical shadows caused by wind gradients.

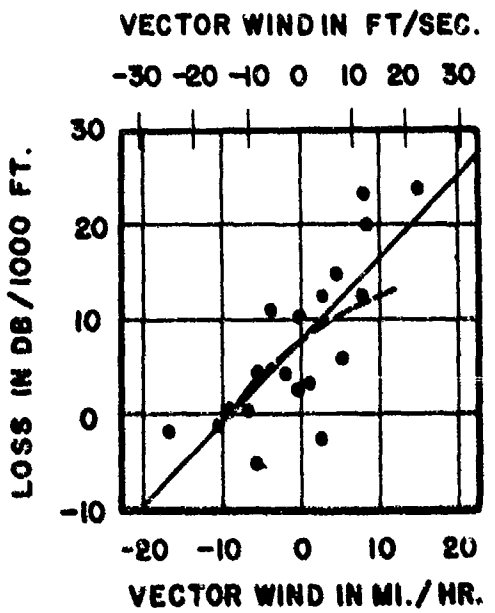

Fig. 30 Loss coefficients vs vector wind, i.e., component of wind velocity opposed to sound propagation direction, from Hayhurst[74]. Dashed curve is from theory for losses due to sound shadows, Eq. (129).

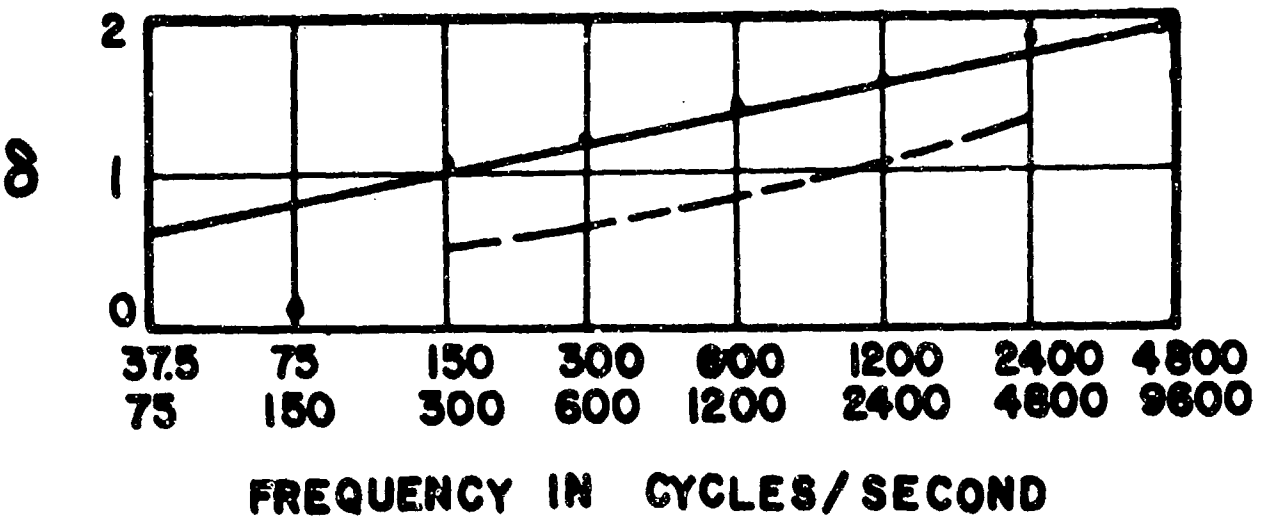

Fig. 31 Plot vs frequency of δ, the rate of change of loss coefficient with vector wind, in (db/1000 ft) per (mi/hr), from Hayhurst (with modified units); for 300 - 600 cps frequency band.

Referring back to plots such as Fig. 30, Hayhurst extracted from these the loss coefficient at zero vector wind for each frequency band. The results are shown in Fig. 33, the attenuation coefficients being corrected for 50% relative humidity as described above. One cannot here specifically compare each experimentally-determined value of α with the corresponding value of $(\alpha_{mol} + \alpha_{class})$, since the data given in Fig. 33 are for a range of humidities and temperatures. Upper and lower limits can be assigned to the theoretical values, however. Since all results given here have been adjusted for an assumed relative humidity of 50%, the uncertainty in $(\alpha_{mol} + \alpha_{class})$ may be assumed due mainly to variations in temperature. Under the conditions of temperature, humidity and frequency which apply here it is found rather readily that $(\alpha_{mol} + \alpha_{class})$ is a decreasing function of temperature, when the relative humidity is assumed fixed. Hence an upper limit to the theoretical absorption coefficient would be obtained by assuming the lowest possible value for the temperature, and a lower limit by assuming the highest temperature.

In Fig. 33 the indicated points on curve A give upper limits to $(\alpha_{mol} + \alpha_{class})$ for mid-frequencies of the various octave bands, and for an assumed relative humidity of 50% and temperature of 43°F; those on curve B give lower limits for the same frequencies, based on an assumed relative humidity of 50% and temperature of 66°F. The shaded band

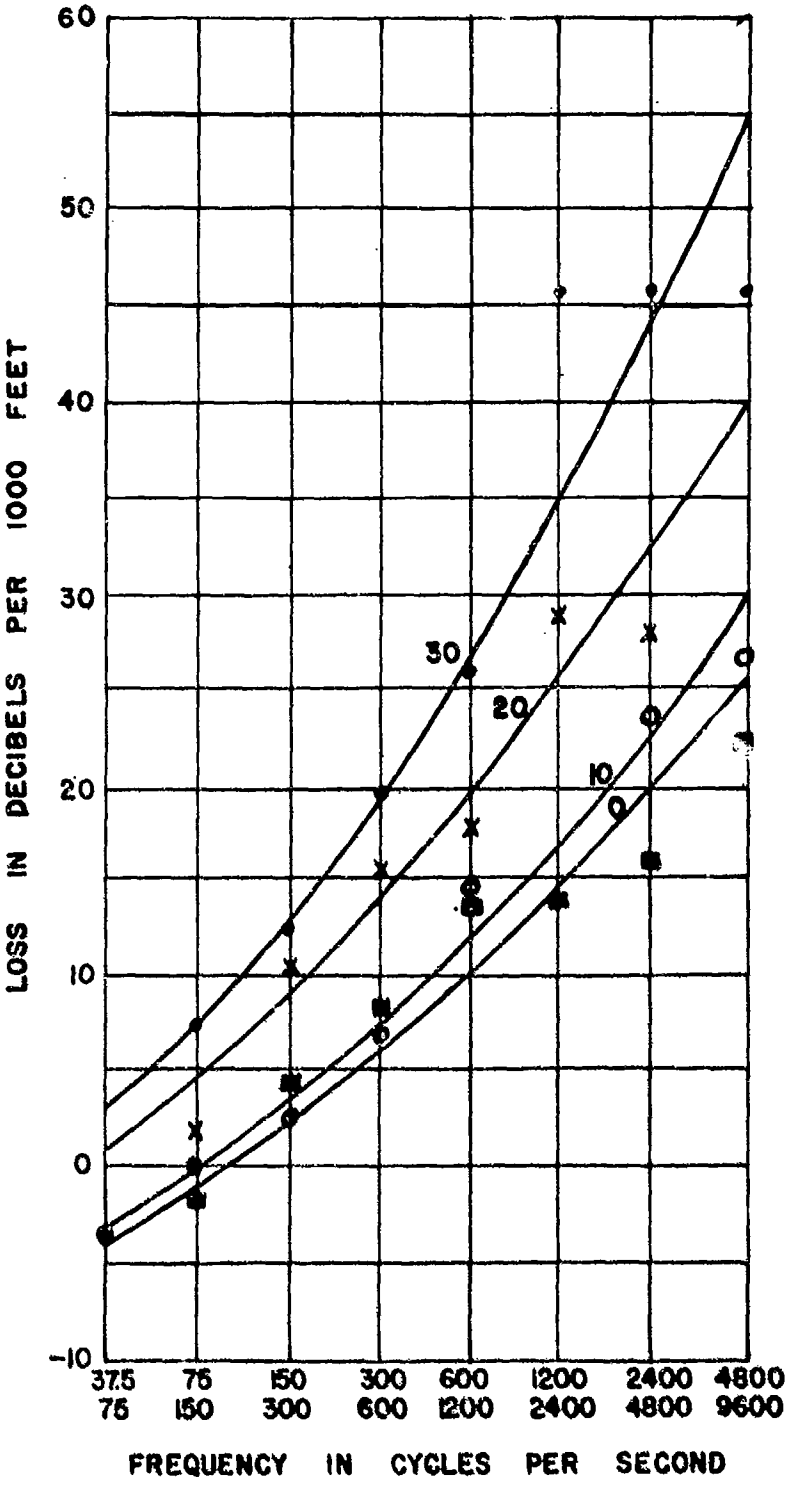

Fig. 32 Loss coefficients vs frequency for various receiver heights, from Hayhurst[74]. The numbers attached to the curves give corresponding receiver heights in feet.

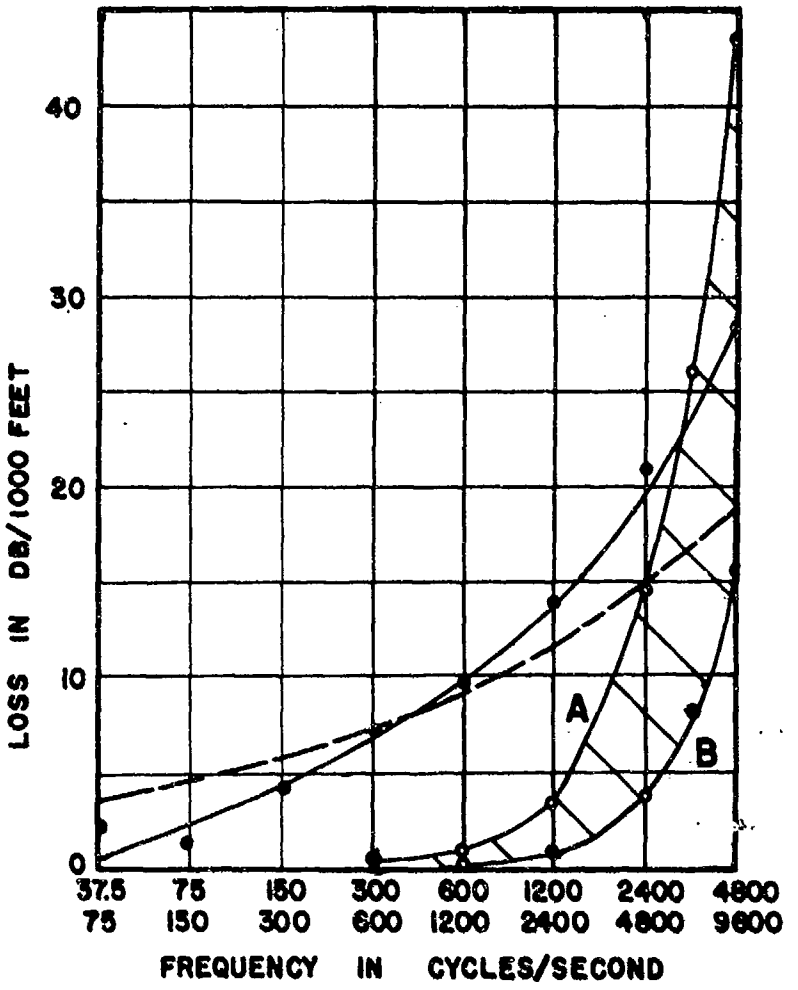

Fig. 33 Loss coefficients vs frequency at zero vector wind, from Hayhurst[74]. Filled circles are experimental values. Shaded area gives theoretical absorption coefficients from Eqs. (11). Dashed curve is from theory for losses due to sound shadows, Eq. (129).

bounded by curves A and B thus represents the possible range of theoretical absorption coefficients as a function of frequency. It is seen in Fig. 33 that at all except the higher frequencies, the observed α is considerably in excess of ($\alpha_{mol} + \alpha_{class}$). For example, the observed α for the 600 - 1200 cps band is about 10 db/1000 ft, whereas the mean theoretical value (for 900 cps) is about 0.5 db/1000 ft.

These results are in contrast to those of Regier (subsection 2.3.1) and also those of Parkin and Scholes (subsection 2.3.2). The latter usually found losses which were considerably less than reported by Hayhurst, and which, when not negligible, were comparatively well ac-

counted for by the sum ($\alpha_{mol} + \alpha_{class}$). The principal difference between the two field situations is that in Hayhurst's case the propagation is along a path parallel to the earth, while in the other cases the propagation is nearly along a vertical path. It seems likely that the vertical-path propagation should be comparatively unaffected by ground absorption; since also, the path is parallel to the direction in which the major changes occur in wind and temperature (i.e., the z-direction), there should be no refraction effects, such as shadows.

It is of some interest to apply the theoretical results of subsections (1.5.5) and (1.5.8) to Hayhurst's data; it will be seen that although these results do not give correct absolute values for the losses due to wind, etc. the predicted variation of the loss with frequency and wind speed are in rather good agreement with Hayhurst's observations. The sound velocity is expected to be from Eq. (81)

$$c = c_o \left(1 - B \ln \frac{z}{z_o}\right) \tag{199}$$

where c_o is the sound velocity at the source, i.e., at height z_o; B is given by Eq. (93)

$$B = (1.71 \times 10^{-3}) \left[a - 0.042 \left(\frac{u_*}{u_{200}}\right) u_{200} \cos\phi\right] \tag{200}$$

The factor a comes from the temperature gradient, Eq. (72) or (94); (u_*/u_{200}) may be found from Table 8; u_{200} is the wind speed in cm/sec, at 200 cm above ground; and ϕ is the angle between the wind direction and the line from source to receiver. It is difficult to estimate u_{200} from Hayhurst's data, since the wind was measured at the London Airport Meteorological Office, about one mile from the site of the acoustical measurements; moreover, the presence of buildings around the site of the wind measurements will probably cause a different variation of wind speed with height than that found at the acoustical site. It shall be assumed, however, that the wind measurements give an approximate measure of the wind speed at the area of the acoustical measurements.

If it is assumed that the wind measurements were made at a height of 10 meters (30 ft) above the ground (i.e., in a tower), the wind speed at 200 cm would be, using the logarithmic wind speed dependence of Eq. (74)

$$u_{200} = u_{10} \frac{\ln(200/\ell)}{\ln(10{,}000/\ell)} \tag{201}$$

where u_{10} is the measured wind speed (at the assumed 10 meters height),

and ℓ is the roughness length. Since the measurements were taken in an area where there were mainly concrete runways, presumably with some grass areas, it will be assumed that ℓ = 0.1 cm, (u_*/u_{200}) = 0.052; Eq. (200) becomes

$$B = (1.71) \times 10^{-3} \left[a + 0.08\, u_m \right], \tag{202}$$

where $u_m = - u_{10} \cos\phi'$ is the measured vector wind speed in miles per hour from receiver to source, and ϕ' is the angle between the wind direction and the line from receiver to source (i.e., $\phi' = \pi - \phi$). In order to estimate the size of a, the effect of the temperature gradient, it is to be noted that the loss coefficient in the 300 to 600 cps band, Fig. 30, falls to zero at about -9 mi/hr; it is assumed (for purposes of rough estimates) that this is that speed at which the wind gradient just cancels the temperature gradient. For positive wind (i.e., directed from receiver to source) or negative winds less than -9 mi/hr a shadow always exists. At negative wind speeds of magnitude greater than 9 mi/hr, the sound is assumed refracted in such a manner as to increase the sound intensity near the receiver above the simple inverse-square law (however, there is no quantitative theory of this effect of "sound channelling"). On the basis of this assumption B = 0 for a vector wind of -9 mi/hr; this gives a value of a of 0.72°C.

This value of a is somewhat larger than the representative values found above grass areas given in Table 7; if any effects of attenuation due to the ground or inhomogeneity scattering (giving a non-zero loss for the case of the wind cancelling the temperature effect) were assumed to exist one would obtain a smaller value for a.

The position of the shadow boundary may be found from Fig. 16; for zero vector wind (u_m = 0 in Eq. (202)) the value of B is

$$B = (1.71a) \times 10^{-3} = 1.23 \times 10^{-3}. \tag{203}$$

Since the sound source is mounted in an airframe, it will be assumed that the source of sound is about 8 ft above the ground; the receiver height is given by Hayhurst to be 4 ft. From Fig. 16 it is found that, for $z/z_o = \frac{1}{2}$:

$$r_s = (0.75)\, z_o \sqrt{\frac{2}{B}} = 242 \text{ ft}. \tag{204}$$

Since the attenuation was computed by Hayhurst from measurements taken between 100 and 2500 ft, most of the measurements were taken in the shadow zone; the attenuation is therefore expected to be due to shadow zone attenuation.

According to the high-frequency approximation to the shadow zone

attenuation for the sound velocity depending on the logarithm of the height, subsection (1.5.8), the first mode attenuation for an infinite impedance (hard) boundary is, from Eq. (129)

$$\alpha_1 = \frac{\sqrt{3}}{4} (3\mu_o)^{2/3} \frac{\omega}{c_o}^{1/3} \left(\frac{v_o}{\ell}\right)^{2/3} , \qquad (205)$$

where μ_o is in this case equal to 0.685, and where v_o ($= c_o m_o$) is the "effective" vector wind speed, i.e., a fictitious wind speed which includes the temperature effect. Since the temperature effect in Hayhurst's results is equivalent to a wind speed of about 9 mi/hr, the effective wind speed will be taken as

$$v_o = u_m + 9 \qquad \text{(mi/hr)} \qquad (206)$$

where u_m is Hayhurst's reported vector wind speed. It is to be noted that the minimum frequency for the validity of this high-frequency approximation, obtained from Eq. (126), is much greater than the frequencies used in the experiments ($f >> 5 \times 10^5$ cps); it is only in cases of larger wind velocity gradients and roughness lengths that it applies. It is interesting to note, however, that, although the theory gives here magnitudes of attenuation about 100 times too great, the dependence on wind speed and frequency are fairly close to the experimental results. If the attenuation at 450 cps is arbitrarily fitted to Hayhurst's experimental attenuation for the 300 - 600 cps band for zero vector wind (using the effective wind speed of Eq. (206)), the attenuation becomes

$$\alpha_1 = 0.225\ f^{1/3}\ (u_m + 9)^{2/3} \text{ db/1000 ft}; \quad u_m \text{ in mi/hr.} \qquad (207)$$

The dashed line of Fig. 30 shows the attenuation as a function of wind speed for f = 450 cps; addition of the classical and molecular absorption (between lines A and B of Fig. 33) would give results quite close to the experimental results. The dashed line of Fig. 33 shows the attenuation as a function of frequency (using the mid-frequency of each band) for zero vector wind; the dashed line of Fig. 31 shows the values of the rate of change of α, with wind speed, for zero wind speed.

The effect of a non-infinite ground impedance is shown in Hayhurst's measurements over grass-covered areas, where the attenuation is increased comparatively slightly above the attenuation found at his original site (mainly concrete). It is to be expected that μ_o will be changed from the value used for the infinite-impedance case, and most probably will be dependent upon frequency (see Eq. (108) etc.), although no quantitative estimate can be made. Since a basic assumption in the analysis given in subsection 1.5.8 was that the ground is representable by a uniform acoustic impedance, it is doubtful that the theoretical results will apply to Hayhurst's measurements, which were over non-uniform

grass and concrete areas.

There does not seem to be any method of quantitatively comparing with theory the results on the change in attenuation with receiver height. Using Fig. 16, the computed approximate distances to the shadow boundary are shown in Table 21 for the various receiver heights (assuming a source height of 8 ft). It is to be noted that for all heights, the receiver was in the shadow region for much of the range of measurements. As the height of the receiver increases the shadow boundary occurs farther and farther from the source. The experimentally measured attenuation is expected to decrease with receiver height since the sound then has a shorter distance to pass through the shadow zone to reach the receiver when the latter is, say, near the end of the range; this is in qualitative agreement with Hayhurst's measurements, Fig. 32.

TABLE 21
Computed distance to shadow boundary (r_s) for various receiver heights (z) assuming a source height of 8 ft.

z (ft)	r_s (ft)
0	130
10	370
20	550
30	710

2.3.4 Ingard (1953)[75]

In a recent review article, data are given obtained from transmission measurements made over a concrete runway and over sand overgrown with thin grass not quite two feet high. These data and the interpretations given them are of much interest here.

Ingard's results are for aircraft noise, generated by a propeller driven airplane; the source is estimated to be 10 feet above the ground. The receiving microphone, mounted on a truck, was also 10 feet above the ground. In determining sound levels, recordings were made on magnetic tape, then later analyzed with General Radio Octave Band Filters.

Measurements were made on a windy day, at different angles with respect to the wind direction; they were also made on a quiet evening, when no appreciable steady wind or temperature gradients existed. Considerable information was derived from the measurements

by proceeding in the steps given below.

1. The data on sound level vs source-receiver separation over a concrete runway, 200 ft wide, on a quiet evening, were fitted to Eq. (2) and the attenuation coefficient obtained by the method described in subsection 2.1. This latter was assumed to give the loss per unit distance due to air alone. The results are given by the dashed curve in Fig. 34.

2. The measurements over the concrete runway and over grass-covered sand were compared, both having been made on the same quiet evening. Differences were assumed due to surface losses over grass. The loss thus computed at the different frequencies is shown by the solid curve in Fig. 34. Ingard shows that the frequency dependence and magnitude of the loss are reasonable on the basis of the theory presented in subsection 1.4.

3. The measurements over sand on a windy day included determination of sound levels at a series of source-receiver separations and for the angles 0°, 45°, 90°, 135° and 180° between the direction of sound propagation and the mean wind direction. These sound levels were compared with those measured over sand on a quiet evening. The actual amount in decibels by which the sound level at any point on the windy day was exceeded by that at the same point on the quiet evening was assumed to be the loss due to wind at that point. (An assumption thus made is that the losses due to absorption described in subsection 1.2., are not significantly different for the two situations. According to Fig. 34 errors due to this assumption are likely to be negligible except at the higher frequencies, since the absorption itself is appreciable only for frequencies above 1000 cps.)

A figure showing typical results may be seen in Ingard's paper. No wind losses were observed for small source-receiver distances; this is to be expected, since then the receiver has, presumably, not yet reached the shadow zone boundary. Losses begin to appear rather abruptly at R = 200 ft for $\phi = 180°$ (sound propagation against the wind), and at about R = 400 ft for $\phi = 135°$ and $\phi = 90°$. The losses occurring in the cross-wind case, i.e., $\phi = 90°$, and are due to shadows caused by temperature gradients; those occurring at 135° and 180° are due to shadows caused by both wind and temperature gradients. No significant losses occur in the cases of propagation at 45° and 0° (with the wind); in these cases the sound is refracted downwards, and does not form a shadow.

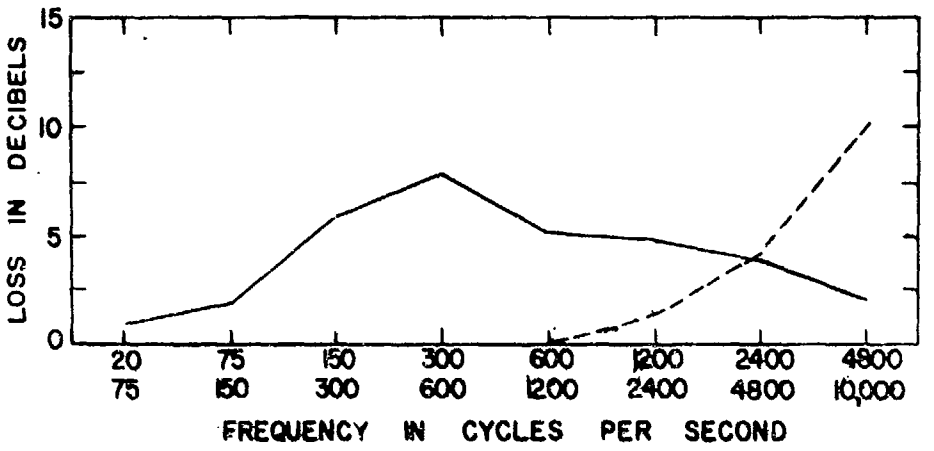

Fig. 34 Observed losses (in excess to 1/R loss) in open air experiments over two kinds of terrain, from Ingard[75]. Dashed curve gives losses due to air alone, as observed over concrete runway. Solid curve gives losses over grass covered sand, less those due to air above. The source-receiver separation is 1000 ft in each case.

An indication of the magnitude of the losses due to wind is given in Fig. 35. Here are shown the observed shadow zone losses (computed as indicated above) at a source-receiver separation R of 1000 ft, for the audible range of frequencies and for different angles ϕ. Ingard emphasizes that these data should only be regarded as typical and not of general validity; the results are very much a function of the distance R.

One feature of these curves, remarked on by the author, is of considerable interest. This is that the losses at a given point do not increase monotonically with frequency (as might have been expected from the theory in subsection 1.5), but instead pass through a maximum, then level off or decrease with increased frequency. Ingard suggests that this is due to scattering of sound into the shadow zone by temperature or wind inhomogeneities, as was discussed in subsection 1.6. As yet, there is no complete theory for dealing with this very important problem.

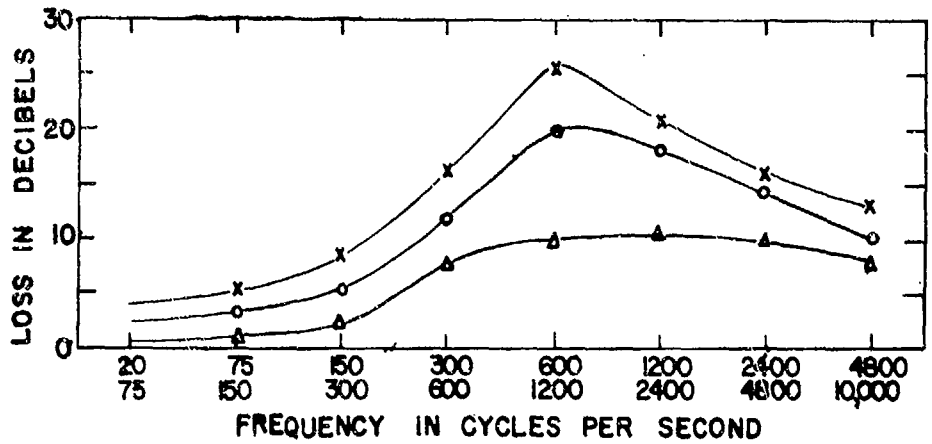

Fig. 35 Losses due to wind for fixed source-receiver separation of 1000 ft, from Ingard[75]. Crosses, circles and triangles represent angles ϕ (see Fig. 1) of 180°, 135° and 90°, respectively, between wind direction and sound propagation direction.

2.4 ACOUSTIC SHIELDING BY STRUCTURES

2.4.1 Stevens and Bolt[76]

Measurements have recently been reported on the propagation of sound around a long building. A 6F6 Navy aircraft was the noise generator; the source was effectively about 7 feet above the ground. Sound levels were determined by making magnetic tape recordings at various points, then later analyzing these with one-third octave band filters. A scaled schematic drawing of the arrangement is shown in Fig. 36. The building around which measurements were made was a hangar 33 ft high, 200 ft wide and 800 ft long. Surrounding the hangar was a wide flat area of sand covered with thin grass. In the experiments described the aircraft noise source was placed at different points relative to the hangar and for each source position the sound field was mapped out by recordings made at various points, especially behind the hangar.

We shall discuss here only a part of their results. In Fig. 36

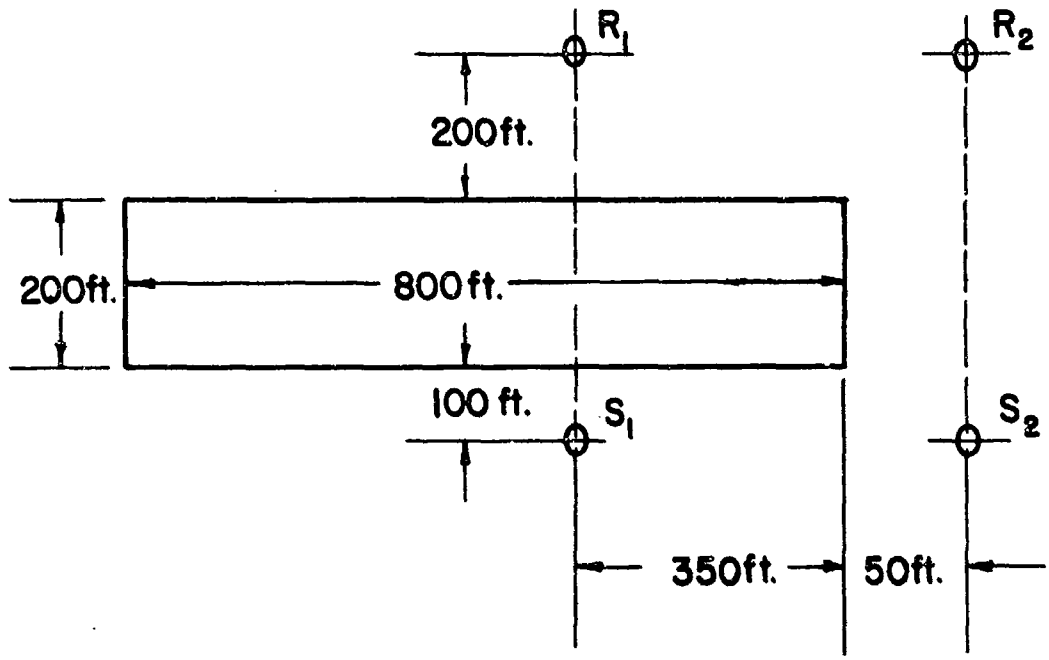

Fig. 36 Scaled drawing of arrangement for measuring acoustic shielding by hangar, from Stevens and Bolt[76].

the points S_1 and S_2 show two source positions used; R_1 and R_2 show two corresponding receiver positions. Both of the source-receiver lines $S_1 R_1$ and $S_2 R_2$ are about 500 feet long; however, the acoustical paths are significantly different in the two cases. Thus, the hangar is interposed as a barrier between source and receiver when the former is at S_1, the latter at R_1. On the other hand, the path $S_2 R_2$ is fairly well clear of any obstacle. The actual amount in decibels by which the sound level at R_2 (when the source is at S_2) exceeds that at R_1 (when the source is S_1) is called the noise reduction caused by the hangar.

In Fig. 37 are shown typical results obtained at low wind velocities. Here the observed noise reduction is given by the solid curve for frequencies ranging from 50 to 10,000 cps. For comparison, the dashed curve shows the reduction predicted by Fehr's theory (see subsection 1.7.3). Though the order of magnitude of the reduction is given correctly by this theory, there are obvious discrepancies. From plots like this for a variety of source and receiver positions, the authors

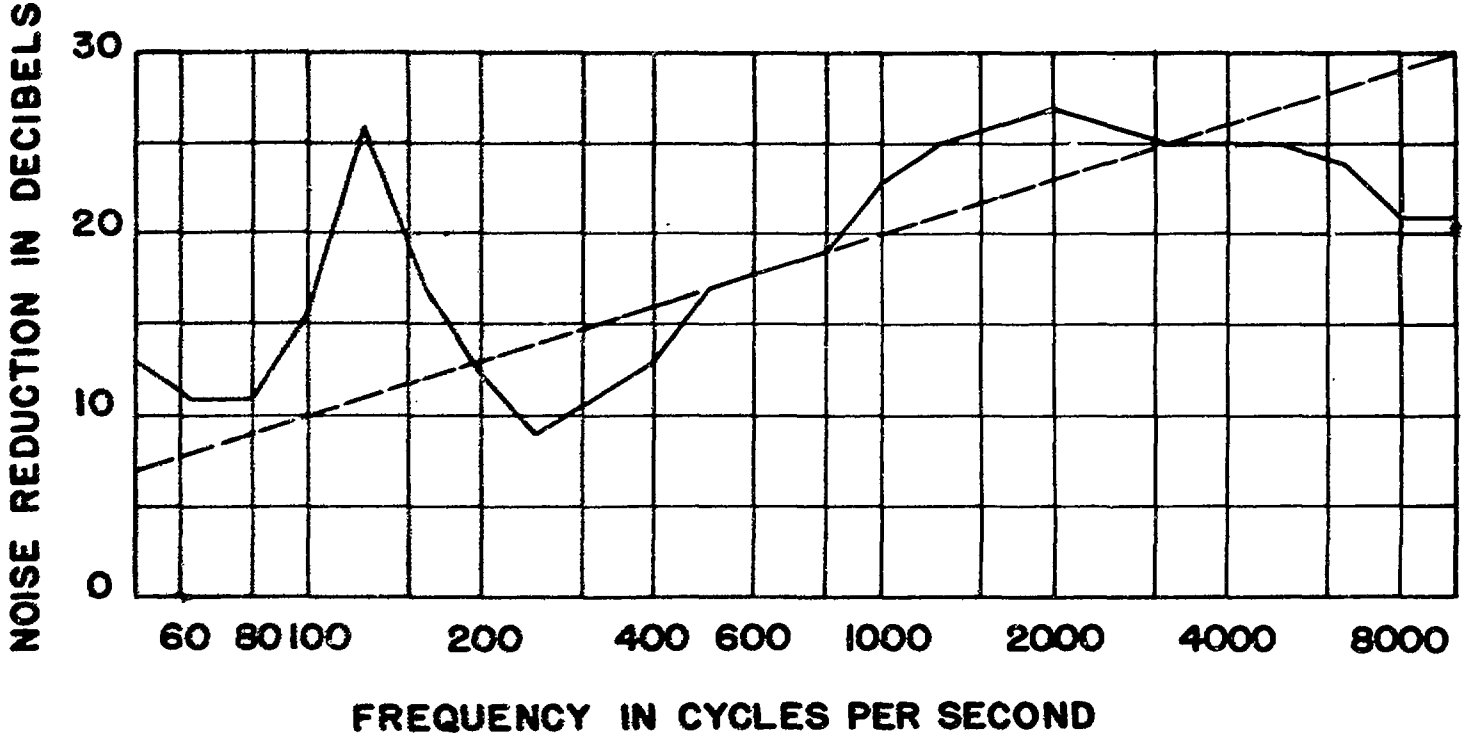

Fig. 37 Noise reduction caused by hangar, from Stevens and Bolt[76]. Solid curve gives experimental values; dashed curve gives Fehr theory.

were able to identify several features which proved to be characteristic, and also to develop explanations for them. These are reviewed briefly below.

1. A large peak in the noise reduction occurred at around 120 cps. The authors explain this as due to interference between sound coming directly from the source and that reflected from the ground surface (see subsection 1.7.4). in this case a concrete apron. If the source were on the ground, or if the ground were a poor reflector, this effect should be absent.

2. A dip in the curve occurs, characteristically between 200 and 1000 cps. This is explained by the authors as due to the fact that the terrain, especially on the receiving side of the hangar, does not interact with the sound field in the same way when sound propagates along path S_1R_1 as when it travels S_2R_2. In the latter case, a terrain loss (see subsection 1.4) may be expected; the probable magnitude of this loss may be seen in Fig. 34 which is for about the same conditions. From this figure, we see that the greatest terrain loss is at around 500 cps.

   As indicated in subsection 1.7.4 there is at present no theory, nor are there direct experimental results, for giving quantitative estimates of losses incurred along such a path as S_1R_1, due to the terrain between the hangar and receiver. It is reasonable, however, as explained by the authors, that the loss here should not be as great as that along S_2R_2, since, intuitively speaking, in the latter case the sound grazes the ground while in the former case the sound travels over the hangar and hence is less affected by the ground. It is to this decrease in terrain loss that the dip in the 200-1000 cps range is attributed. If the ground were such that no terrain loss occurred along S_2R_2, this effect would presumably be absent.

3. For frequencies above 3000 cps the noise reduction due to an acoustical shadow cast by the hangar tends to be rather less than that predicted by Fehr's theory. This is believed by the authors to be due to scattering of sound into the shadow by turbulence in the atmosphere. Theory (see subsection 1.6) predicts that the amount of scattering due to turbulence increases with the frequency. Hence the decrease in noise reduction because of this

effect should be, as was found experimentally, especially marked at high frequencies. The amount of scattering also depends, of course, on the degree of turbulence; the latter, in turn, depends on the wind velocity. Evidence on the latter point comes from other results obtained by the authors. By making measurements on different days, the authors found that the hangar caused less noise reduction, by as much as 12 decibels, for frequencies above 200 cps when a cross wind of 20 mph was present than when there was no wind.

The results shown in Fig. 37 do not apply if the source is very near to the hangar. In this case, Fehr's graph is found to predict noise reductions much greater than those observed. This is believed due to approximations in the diffraction theory (see subsection 1.7) on which his graph is based. An empirical correction is suggested by the authors for this case, namely, that the expression for N in Eq. (178) should be multiplied by $\left[1 + (H^2/A^2) \right]^{-1}$.

An additional conclusion reached by the authors, on the basis of a large number of observations, is that the observed losses are in general greater - on the average, by about 3 db - than would be predicted by the Fehr chart. (Alternatively, the losses are about 3 db less than those given directly by Fig. 21.)

2.4.2 Hayhurst (1953)[77]

Further data on sound reduction by structures is given by Hayhurst. The latter describes results obtained in tests of acoustic shielding by experimental walls of corrugated cement asbestos sheeting (1/4 in. thick) up to 40 ft high and 50 ft long. It was found that noise from a Viking aircraft (see subsection 2.3.3), placed 20 ft behind the wall, was reduced by approximately 20 - 25 db over the 37.5 - 10,000 cps frequency range at all points forward of the wall, up to distances of about one mile. We shall not attempt here to discuss the results in detail. Because of the nature of the data it is rather difficult to make comparisons with the theory described in subsection 1.7; however, Stevens and Bolt[76] state that the Hayhurst results appear to be in fair agreement with the predictions of the Fehr chart.

2.5 SOUND TRANSMISSION THROUGH FORESTED AREAS

An idea of how much loss is suffered by sound in propagating through a variety of forests or wooded areas is given by Eyring[69] in the same paper referred to previously. Such information may be useful in cases where part of the transmission path from source to receiver is through a region populated with leafy trees, with or without underbrush.

Eyring and his group made their measurements in the jungles of Panama; loudspeakers were used as sound sources. Measurements in any given jungle area were made by operating the source at some point in the interior of the area, then determining sound levels at various distances with microphones and recording equipment. In all cases source and receiver were 5 ft above the ground. Data on sound levels *vs* source-receiver separations were fitted to Eq. (2) and determinations thus made of the loss coefficient α for different frequencies in the various jungles.

Fig. 38 gives the Eyring results in the form of zones or bands, each representing the range of loss coefficients to be expected in a given type of jungle, as a function of frequency. The jungles are typed in terms of (1) the greatest distance at which a moving white object can be seen, and (2) the estimated density of the foliage. The author warns that these results are particularly valid for jungles in tropical regions and may be in error elsewhere. However, Schilling, *et al*[78] in their work at higher frequencies, found that Panama jungles are not striking different acoustically than forests in Pennsylvania. Hence we might expect Fig. 38 to be useful for making transmission loss estimates even for forested areas in the United States.

2.6 PROPAGATION OF SOUND THROUGH THE GROUND

As has become clear in previous discussion (e.g., subsection 1.4) the sound received at a given point P (see Fig. 1) depends not only on the nature of the atmosphere, in which both the source point Q and the receiver point P are immersed, but also on the acoustical properties of the earth. If the earth is highly absorbing only a shallow surface layer will have an appreciable effect on the sound field at Q. This appears to be the case for porous soils, for which both theory and experiment indicate very high attenuation coefficients, of the order of 0.5 db/cm and higher for frequencies above 500 cps[22, 79, 80]. Hence, under these conditions the sound may be said to travel from Q to P by paths which

are essentially through air alone and only to a negligible extent through the ground.

The question arises whether there might be special conditions, say, at low audible frequencies and/or for compacted or water-soaked soils, where a significant portion of the sound from Q would arrive at P by way of the earth. In particular, ground-conducted sound might be expected to be important when the air path from P to Q is poor, e.g.,

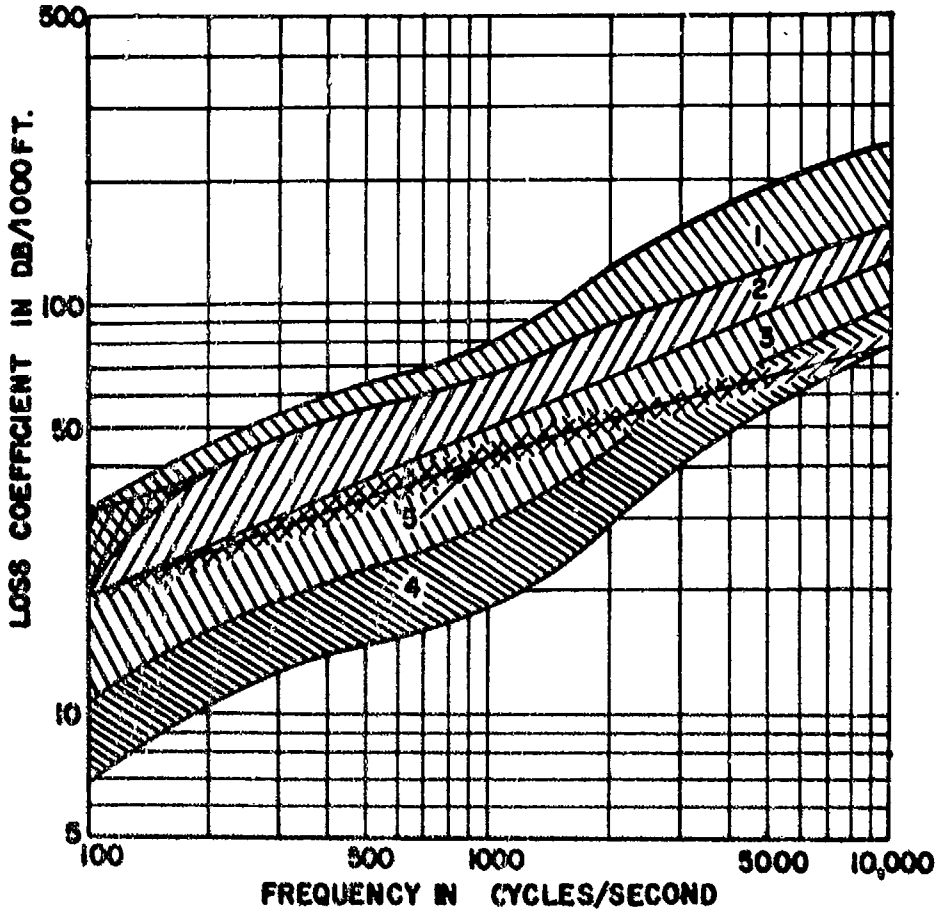

Fig. 38 Loss coefficients in jungles or forests, from Eyring. Numbers in zones represent different jungles as follows:

(1) Very leafy; one sees a distance d of approximately 20 ft.
(2) Very leafy; d = 50 ft.
(3) Leafy; d = 100 ft.
(4) Leafy; d = 200 ft.
(5) Little leafy undergrowth, large bracketed trunks; d = 300 ft.

if Q were in an acoustic shadow, caused either by a wall (subsection 1.7) or by refraction (subsection 1.5). Unfortunately, there does not exist suitable field data by means of which the contribution due to ground-propagated sound can be estimated with satisfactory accuracy. There are indications, however, that this contribution is not usually highly important.

For example, seismologists find that earth vibrations caused by artificial surface disturbances can be detected only at relatively short ranges; the disturbance due to a 200 lb lead weight dropped from a height of 20 ft has been found to be detectable at distances no more than 300 ft, using a seismograph (natural frequency about 15 cps) capable of detecting surface movements of the order of several Angstroms[31] ($1\ \text{Å} = 10^{-8}$ cm). It is true that by using explosives seismologists are able to obtain detectable surface vibrations up to distances of several miles, but it is important to realize that this is accomplished only by use of <u>buried</u> charges[82]. The general method is to place an explosive cartridge at the bottom of a drilled hole, typically 25 ft deep, then pack the hole firmly with dirt and water before detonation. The earth vibrations transmitted from an equivalent charge exploded on the earth surface is very much less, by factors of as much as 50 or 100; the ineffectiveness of such a surface charge is partly due to the surface ground layer being a poor medium for sound transmissions. By contrast to the relatively short ranges of ground waves resulting from surface blasts, it is commonly found that the simultaneously generated <u>air-transmitted</u> sound is detectable at distances of 100 miles or more from the source[63,64].

Other information on wave propagation in the ground, in this case over very short ranges, comes from dynamic tests on soils[83,84]. The latter are made by applying an alternating force to a given small area of the ground, then measuring the vertical ground amplitude at various distances r from the source. Typical data[83] at r = 50 ft for the 20-30 cps range indicate ground amplitudes of 20-50 Å at that distance per kilogram of impressed force at the source. It has been found[84] that the amplitude of vibration varies approximately inversely with distance r from the source. Hence the data quoted above may be expressed in equation form approximately as

$$\epsilon_g \leq 0.078\ F/r, \tag{208}$$

where the vibration amplitude ϵ_g is in Angstroms, the amplitude F of the exciting force is in dynes and r is in centimeters. (Eq. (208) states that ϵ_g will be equal to or less than 50 Å at a distance r of 50 ft (1525 cm) when F is one kilogram (9.8×10^5 dynes).)

In the case to which Eq. (208) applies the ground vibrations

were set up by a heavy plate pressed against the earth, upon which was impressed an alternating vertical force by mechanical or other means. For purposes of the present report we are interested in situations where forces are applied to the ground by such sources as noisy aircraft which generate sound in air as well as in the ground. In the absence of experimental data directly applicable to this problem it is worthwhile to calculate for a somewhat idealized case the particle amplitude in air expected at a distance r from the source due to air-transmitted sound, and compare this with the vibratory amplitude at the earth's surface due to the ground wave, as given by Eq. (208).

In making this comparison we assume a volume-type source, i.e., one whose action consists of a periodic injection and withdrawal of air from a given localized region in the atmosphere. Specifically, we suppose that air is uniformly admitted and withdrawn from a region consisting of a thin sheet of area A immediately above the ground. (For example, we might suppose the region to be in the shape of a cylinder whose lower base, of area A, is in the plane of the ground surface and whose height is very small.) Let the total instantaneous volume rate of influx of air into this region be $q_o \sin \omega t$; the instantaneous vertical velocity of the air in the source region will then be $(q_o/A) \sin \omega t$. If the horizontal dimensions of the source are of the order of $(\lambda/2)$ or less (where λ is the sound wavelength in air) the particle amplitude ξ_a in the air-transmitted wave will be given approximately by

$$\xi_a = q_o/2\pi cr, \tag{209}$$

where r is the distance from the source and c the velocity of sound in air. Eq. (209) may be derived easily from standard theory for sound propagation from a volume source[85], in which theory one neglects the effects of absorption and refraction processes in the air, such as were considered in Section I. If one substitutes for c a typical value for ordinary temperatures (Appendix I) and expresses ξ_a in Å one obtains

$$\xi_a \simeq 450\, q_o/r \tag{210}$$

where q_o and r are in cgs units.

From similar theory[86] one may estimate the amplitude F of the alternating force exerted on the ground over the total source area. If, as previously assumed, the horizontal dimensions of the source are of the order of $(\lambda/2)$ or smaller, the amplitude F will be of the order of $(\rho_o c q_o)$ or smaller, i.e.,

$$F \leq \rho_o c q_o \tag{211}$$

Combining Eqs. (208) and (211), and evaluating ρ_o and c for air at a typical temperature (Appendix I) we obtain

$$\xi_g < 3.5\ q_o/r, \tag{212}$$

where q_o and r are in cgs units while ξ_g is in Angstroms. Comparing this expression for ξ_g with Eq. (210) for ξ_a we see that the ground transmitted vibratory amplitude at a given distance r is less than the air-transmitted particle amplitude at the same distance by at least a factor of 125, or about 42 db.

In considering the result of this very rough calculation two points should be kept in mind. First, the experimental data upon which Eqs. (208) and (212) are based cover only a very short range, up to r = 50 ft; it is not known how accurately Eq. (208) would represent typical facts for much larger values of r. Second, in obtaining Eqs. (209) and (210) for ξ_a the losses due to absorption and refraction in the air transmissions path were assumed negligible. When the latter assumption is not valid, as would be particularly the case in a region of "acoustic shadow", the ratio (ξ_a/ξ_g) would be considerably diminished.

SECTION III

APPLICATIONS TO PRACTICAL PROBLEMS

3.1 INTRODUCTION

In this section are presented special graphical aids and suggested procedures for applying the results of Sections I and II to actual field situations. In general terms, the overall problem is assumed to be this: given a source of specified properties, located at a specified site, to predict the sound level distribution in the surrounding region, at points up to several miles from the source.

In many commonly-encountered situations an accurate solution to this problem is far beyond the grasp of present day acoustics. If the land surrounding the source is rolling, of uneven constitution, or overlaid irregularly with trees or physical structures the difficulties are obvious; to attempt exact analysis in such a case would clearly be impractical.

Even if the terrain near the site is flat and uniform, the vagaries of the atmosphere often provide an inhomogeneous medium of such complexity as to present very great analytical difficulties. In many actual cases the various aspects of the propagation problem, taken up separately in the subsections of Section I, cannot be isolated and treated separately, but must be confronted simultaneously. The task then presents itself of predicting the sound field in a medium where

(1) viscosity, heat conduction, molecular relaxation and other basic mechanisms play a part,
(2) fog or smoke is present,
(3) the underlying surface is a reflector, scatterer and/or absorber,
(4) random temperature and wind inhomogeneities exist,
(5) time-independent gradients of temperature or wind-speed exists, and
(6) phys l structures obstruct the sound propagation pat .

As indicated, there is no solution for this very general problem. However, there is useful information described in Section I and II which is applicable to certain important special situations. For example, it appears to be fairly well known how to calculate sound levels on the ground due to a source nearly overhead. This is a very important case since the results may be applied to calculations of the maximum levels to which people under a take-off course are exposed. This problem is taken up later in this section, as are a number of others.

In what follows, we present in subsection 3.2 a number of graphs and nomograms for convenience in computing or estimating acoustic losses due to various causes. In subsection 3.3 typical problems are discussed which arise in the field; suggested procedures for handling these are given wherever possible.

3.2 COMPUTATIONAL AIDS

3.2.1 The 1/R Law

In some special cases the pressure amplitude p at any point P (whose distance from the source is R) is given by Eq. (2) with α equal to zero; the dependence of p on R in this simple case is then called the (1/R) law or inverse first power law. As indicated in subsection 1.1, the loss in decibels of the sound level at P relative to that at a reference point P_o (at a distance R_o from the source), is given for this case by

$$\text{"(1/R) Loss"} = 20 \log_{10} (R/R_o) \qquad (213)$$

Fig. 39 shows a plot of the 1/R loss, also at times referred to as the divergence loss, geometrical loss, etc. (see subsection 1.1.3) versus the distance ratio (R/R_o). Since semi-log coordinates are used, the resulting graph is a straight line. The 1/R loss increases by equal numbers of decibels when the ratio (R/R_o) increases by equal factors; e.g., the loss increases by 6 db for each doubling of the distance R (R_o being assumed constant), and by 20 db for each ten-fold increase of R. The greatest loss per unit distance occurs, of course, near the source; the same geometric loss is encountered in traveling the 100 ft interval from 100 to 200 ft, as in the 1000 ft interval from 1000 to 2000 ft, etc.

The graph in Fig. 39 shows the (1/R) loss for ratios (R/R_o) from 1 to 2000. It is easy to take account also of ratios out of this range; to do this one uses the result that any additional factor of 10^n in (R/R_o) increases the loss by 20n db. For example, the loss for $(R/R_o) = 65{,}000$ may be obtained by the following steps.

(1) Write the ratio in the form: 650×10^2 (since "650" lies between 1 and 2000).
(2) Find from Fig. 39 that the (1/R) loss is 56 db for $(R/R_o) = 650$.
(3) Note that n = 2; hence 20n = 40 db.

LOSS IN DECIBELS
0
10
20
30
40
50
60
70
DISTANCE - RATIO (R / R₀)
1
2
4
6
8
10
20
40
60
80
100
200
400
600
1000
2000

(4) Add results of Steps 2 and 3. The loss for $(R/R_o) = 65{,}000$ is: 56 + 40 = 96 db.

An alternative presentation for use in computing the loss due to spherical divergence is given in Table 22. Here the (1/R) loss is given for values of (R/R_o) varying from 1.0 to 9.9. The loss for ratios (R/R_o) outside the range of the table are obtained, as above, by remembering that an additional factor of 10^n in (R/R_o) increases the loss by 20n db.

3.2.2 The $R^{-1} e^{-\alpha R}$ Law

Returning to Eq. (2) we now consider the more general case when α is not zero; the given equation is then approximately applicable to a wide variety of situations, as was found in Sections I and II. As stated in subsection 1.1.3 the loss in sound level at any point P relative to that at a reference point P_o may then be considered as made up of two parts: the first is a (1/R) loss, as discussed in the previous subsection; the second is called an exponential loss and is given in decibels by

$$\text{Exponential loss} = \alpha (R-R_o), \qquad (214)$$

where α is in decibels per unit of distance, the latter unit being chosen, of course, to agree with those of the distance $(R-R_o)$. Knowing α one may obtain the loss at P relative to P_o by the following steps:

(1) Obtain the (1/R) loss from Fig. 39 or Table 22.
(2) Calculate the quantity $\alpha(R-R_o)$.
(3) Add the results of Steps (1) and (2).

For example, one proceeds as follows to obtain the loss in sound level at 2000 ft from a source relative to that at 100 ft for an assumed loss coefficient of 6.0 db/1000 ft:

(1) From Fig. 39 the 1/R loss for a distance ratio of 20 is 26.0 db.
(2) The quantity $\alpha(R-R_o)$ is (6.0)(1900/1000) = 11.4 db.

← Fig. 39 Chart giving (1/R) loss at a distance R from a source, relative to the level at a distance R_o.

TABLE 22

Inverse First Power Loss in Decibels for Given Values of the Ratio (R/R_o)

R/R_o	.0	.1	.2	.3	.4	.5	.6	.7	.8	.9
1	0.0	.8	1.6	2.3	2.9	3.5	4.1	4.6	5.1	5.6
2	6.0	6.4	6.8	7.2	7.6	8.0	8.3	8.6	8.9	9.2
3	9.5	9.8	10.1	10.4	10.6	10.9	11.1	11.4	11.6	11.8
4	12.0	12.3	12.5	12.7	12.9	13.1	13.3	13.4	13.6	13.8
5	13.9	14.2	14.3	14.5	14.6	14.8	15.0	15.1	15.3	15.4
6	15.6	15.7	15.8	16.0	16.1	16.3	16.4	16.5	16.7	16.8
7	16.9	17.0	17.1	17.3	17.4	17.5	17.6	17.7	17.8	18.0
8	18.1	18.2	18.3	18.4	18.5	18.6	18.7	18.8	18.9	19.0
9	19.1	19.2	19.3	19.4	19.5	19.6	19.6	19.7	19.8	19.9

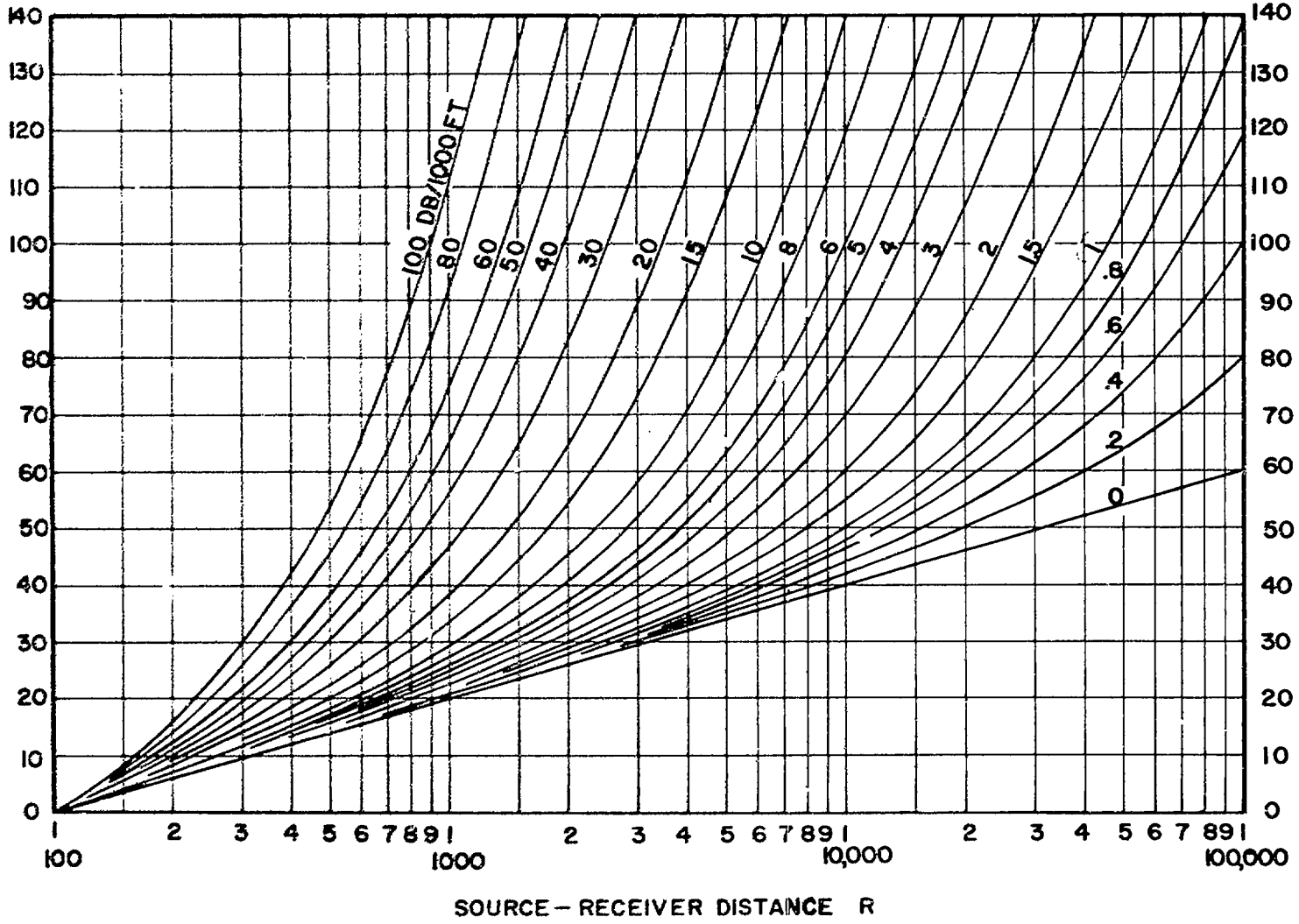
140
130
120
110
100
90
80
70
60
50
40
30
20
10
0
100 DB/1000 FT
80
60
50
40
30
20
15
10
8
6
5
4
3
2
1.5
1
.8
.6
.4
.2
0
1
2 3 4 5 6 7 8 9 1
100
1000
10,000
100,000
SOURCE – RECEIVER DISTANCE R

(3) The total attenuation is (26.0 + 11.4) = 37.4 db.

As a more convenient method for obtaining the same result Fig. 40 may be used. The latter gives plots of the total loss (1/R loss plus exponential loss) as a function of R for different values of α ; R_o is assumed, in all cases, to be 100 ft. As an example of the use of Fig. 40 one may easily verify the correctness of the result obtained by carrying out Steps (1), (2) and (3) above.

For any value of R_o greater than 100 ft the total loss incurred between R_o and R may be obtained from Fig. 40 by the following steps:

(1) Determine the loss from 100 ft to R from Fig. 40.
(2) Determine the loss from 100 ft to R_o from Fig. 40.
(3) Subtract the result of Step (2) from that of Step (1).

As an example, the loss between 800 ft and 2000 ft for α = 6 db/1000 ft is obtained as follows:

(1) Loss from 100 ft to 2000 ft = 37.5 db.
(2) Loss from 100 ft to 800 ft = 22.5 db.
(3) Loss from 800 ft to 2000 ft = 15.0 db.

For any value of R_o less than 100 ft the total loss incurred between R_o and R may be obtained as follows:

(1) Determine the loss from R_o to 100 ft. This will usually be mainly a (1/R) loss, obtained from Fig. 39. (For the frequency range of main interest losses due to attenuation by the medium would be usually fairly small for distances less than 100 ft.)
(2) Determine the loss from 100 ft to R, using Fig. 40.
(3) Add the results of Steps (1) and (2).

As an example, the loss between 70 and 2000 ft for α = 6 db/1000 ft is obtained as follows:

(1) Loss from 70 to 100 ft $\simeq$ 3 db (the error due to neglecting the exponential loss here is about 0.2 db).
(2) Loss from 100 to 2000 ft = 37.5 db.
(3) Loss from 70 to 2000 ft = 40.5 db.

← Fig. 40 Chart giving total loss ((1/R) loss + exponential loss) at a distance R from a source relative to the level at a distance of 100 ft, for various values of the loss coefficient α .

3.2.3 Loss Coefficients for Homogeneous Air

3.2.3.1 In order to predict losses when Eq. (2) holds, one must, of course, know what value to assume for the loss coefficient α. In making estimates, it is often very helpful to know the results of theory (subsections 1.2.2 and 1.2.3) and laboratory experiments (subsection 1.2.4) on loss coefficients in homogeneous air. For applying these results to practical problems, we suggest specific computational procedures below, and also give a number of graphs or nomograms which present the theoretical and laboratory results in different ways. For some purposes, a given one of these presentations will be the most suitable; for other purposes another will be best.

3.2.3.2 According to theory the attenuation in homogeneous air is given by the sum of α_{class}, given by Eq. (11b) etc., and α_{mol}, given by Eq. (18). The former may be obtained for any frequency at any given temperature from Fig. 2. The latter may be calculated by using Figs. 3, 4 and 6, following the steps given in subsection 1.2.3. One finds that in many cases α_{class} is negligible with respect to α_{mol} for the given conditions; the theoretical value of α for homogeneous air is then essentially just α_{mol}.

The experimental values of α, obtained in the laboratory are also given in Figs. 3, 4 and 6. To find the laboratory value for given conditions, one may follow the same four steps given in subsection 1.2.3, with the exception that in Steps (2) and (3) the experimental results rather than the theoretical curves should be used for h_m and (α / α_{max}), respectively. (Step (1) is unaffected since experimental results for α_{max} agree very well with the theory.)

From Fig. 6 we see that the observed values of (α/α_{max}) do not fall off to zero at high humidities, as the theory would predict, but instead level off at about 0.2; stated differently, the values of α for any given frequency level off to about 0.2 times the α_{max} for that frequency. A rough "rule of thumb" for recalling the Delsasso and Leonard laboratory α at the higher humidities would thus be as follows:

(1) Determine α_{max} for the given temperature and frequency from Fig. 3;
(2) Multiply the result of Step (1) by 0.2.

To determine α_{max} for conditions outside the range of Fig. 3 one may refer to Fig. 41. Here are given plots of α_{max} versus frequency for frequencies ranging from 10 cps to 10 kc and for temperatures from 0° to 100°F. To determine α_{max} for frequencies outside the range of

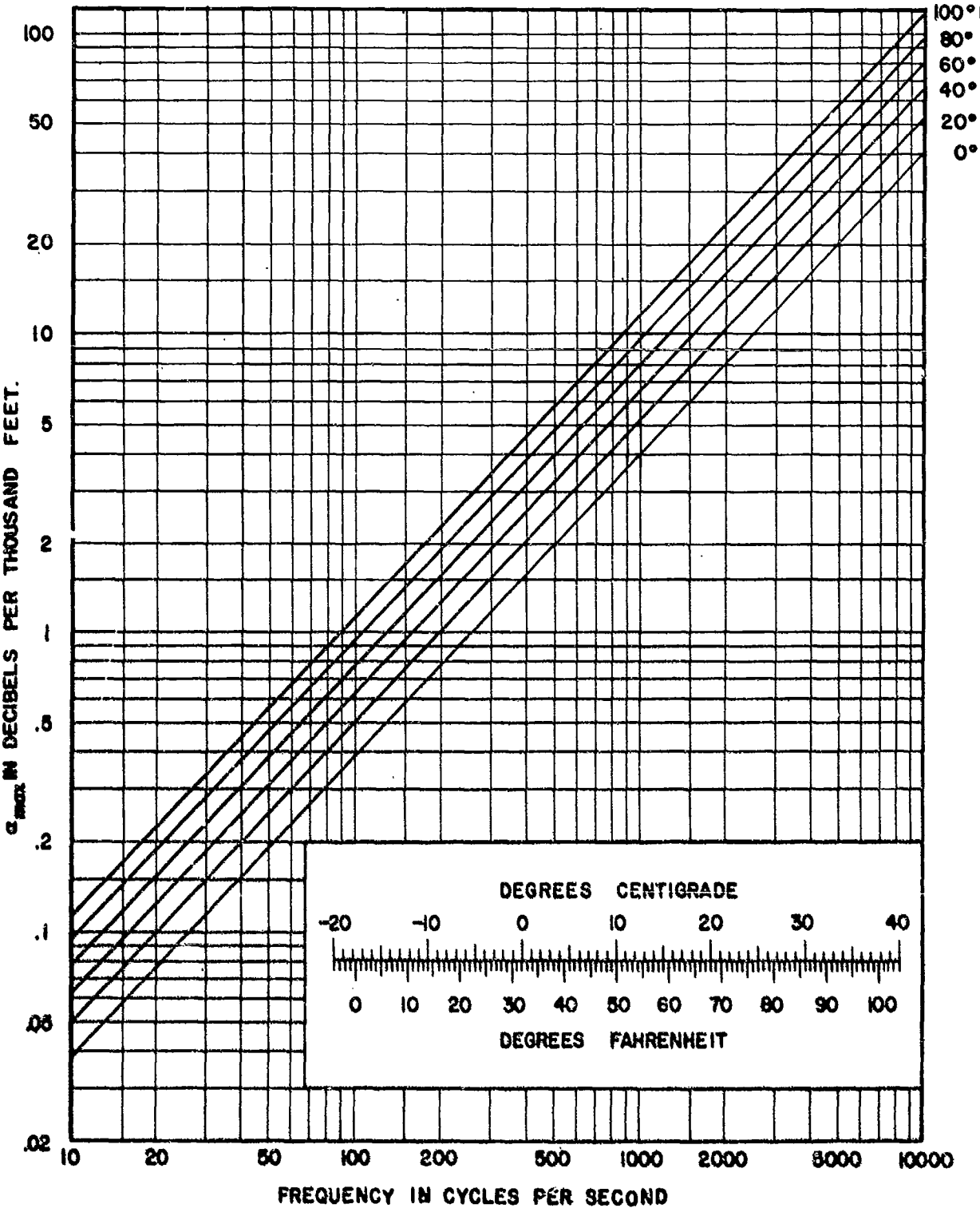

Fig. 41 Extended plot of maximum molecular absorption coefficient α_{max} versus frequency at various temperatures.

the graph one may simply use the fact that α_{max} is proportional to frequency. Thus to determine α_{max} at 250 kc and 40°F, one notes from Fig. 41 that α_{max} is 16 db/1000 ft at 2.5 kc and 40°F, then multiplies this value by 100 obtaining 1.6 db/ft for the given frequency.

3.2.3.3 For the specific frequencies of 500, 1000, 2000 and 4000 cps the theoretical results are presented in more convenient form in Figs. 42 - 45.

For definiteness, consider Fig. 42 which is for 500 cps. This figure really consists of two graphs. The lower graph contains a family of straight lines; these are plots on log-log paper of relative humidity against absolute humidity h for different temperatures. The upper graph contains a family of curves which are plots on log-log paper of α vs the absolute humidity h at various temperatures.

To determine α, one effectively obtains the absolute humidity from the given relative humidity and temperature by using the lower graph, then finds α for this h-value and the given temperature from the upper graph. A typical path to be followed in making a computation is shown by the broken line A B C D; for this example, the relative humidity is assumed to be 66% and the temperature 42°F. The detailed procedure is as follows:

(1) Select the relative humidity on the vertical axis of the lower graph; this determines A.
(2) Extend a horizontal line to the left from A until it intersects that member of the family of straight lines, representing relative humidity vs h, which corresponds to the given temperature. (As in this example, the particular family member for the given temperature will usually not actually appear; its position must be inferred by interpolation.) This intersection determines the point B.
(3) Extend a vertical line upward from B until it intersects that (interpolated) member of the family of α vs h curves which correspond to the given temperature. This intersection determines the point C.
(4) Extend a horizontal line to the right (or left) from C; its intersection D on the vertical axis gives the desired value of α_{mol}.

For any other temperature and humidity one proceeds similarly, of course; also, the same procedure is to be used in determining α_{mol} from Figs. 43,44 and 45 for 1000, 2000 and 4000 cps, respectively.

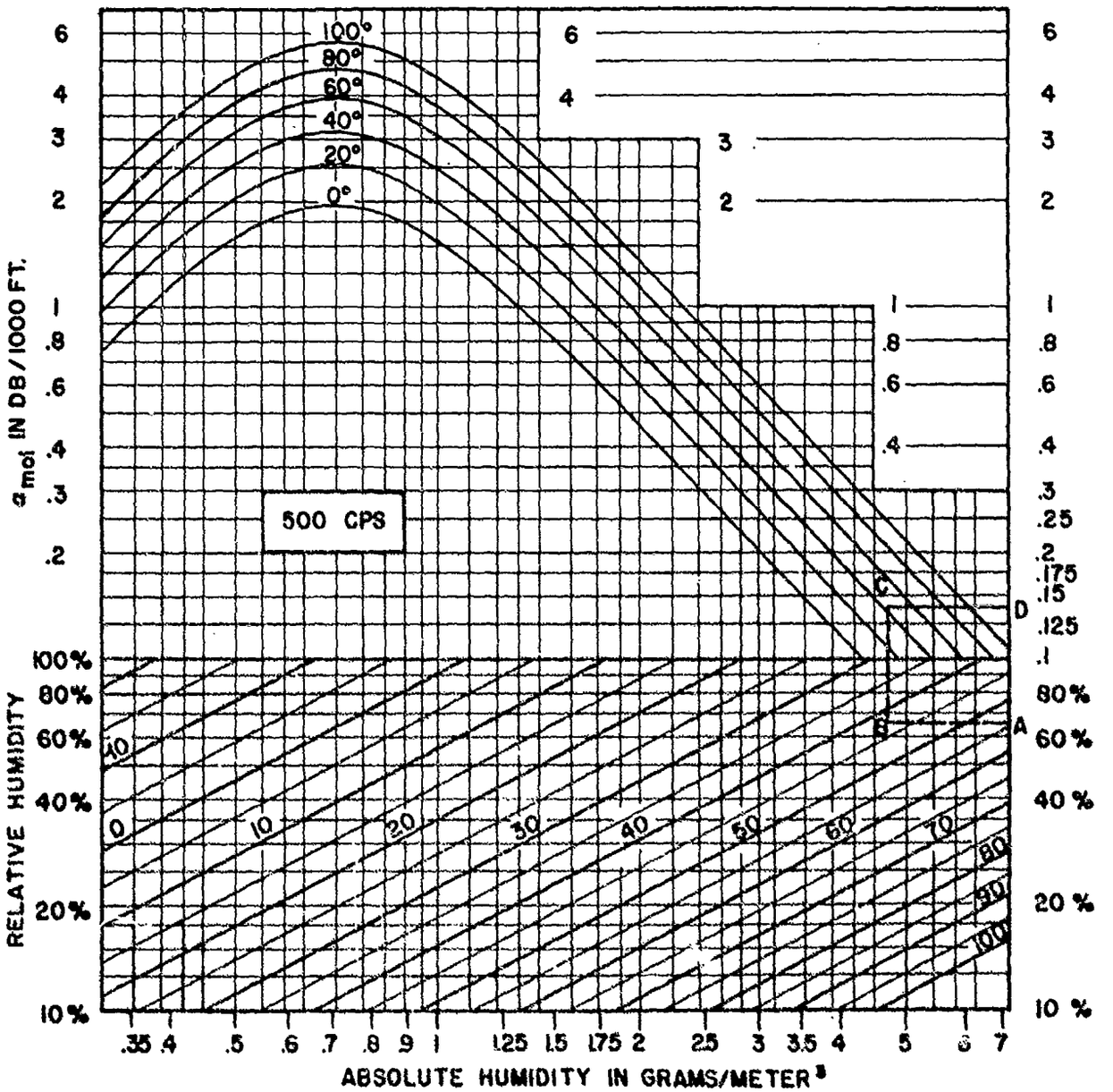

Fig. 42 Nomogram for calculating α_{mol} for given temperature and humidity conditions at a frequency of 500 cps. See text for instructions in use.

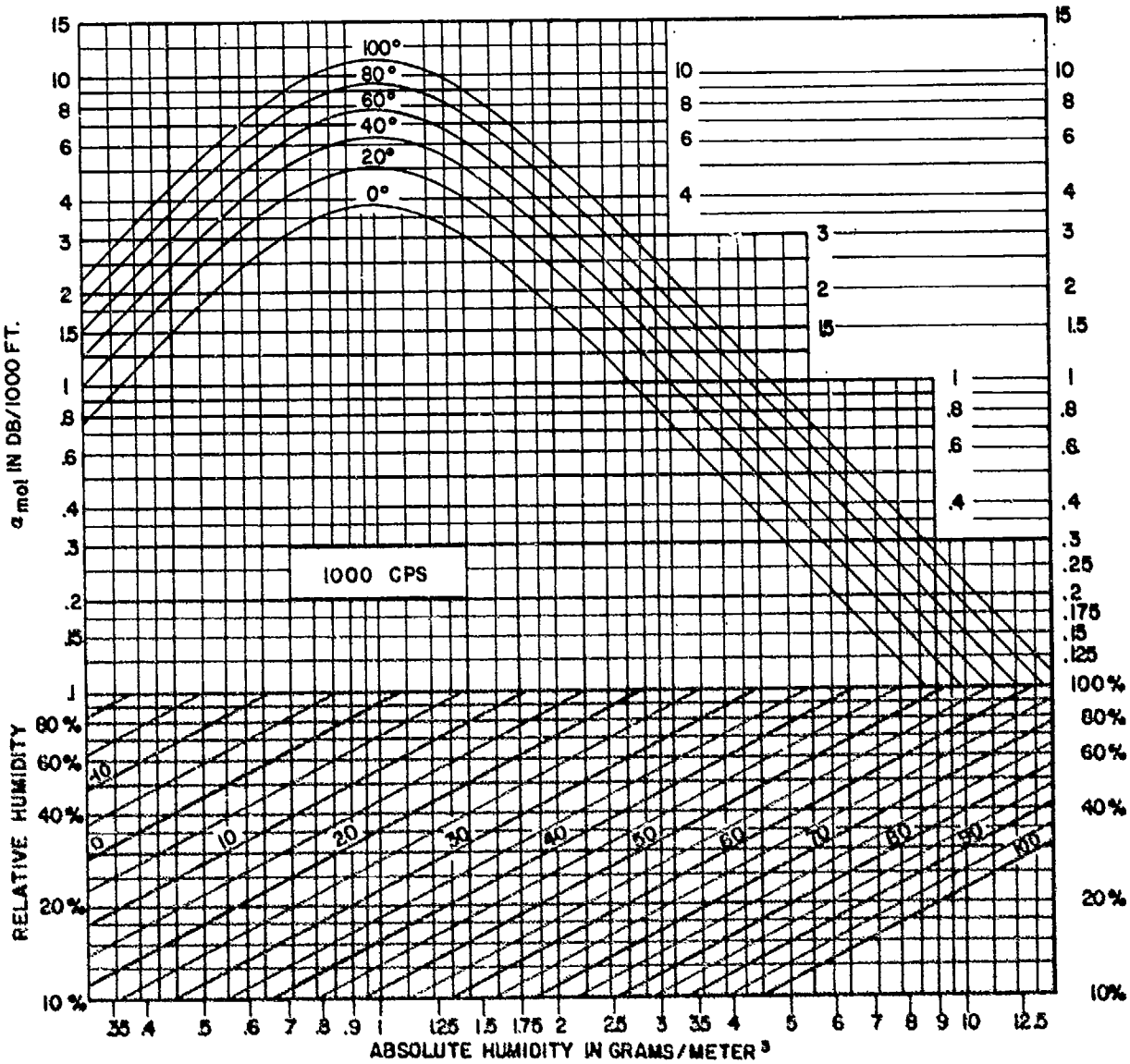

Fig. 43 Nomogram for calculating α_{mol}; 1000 cps

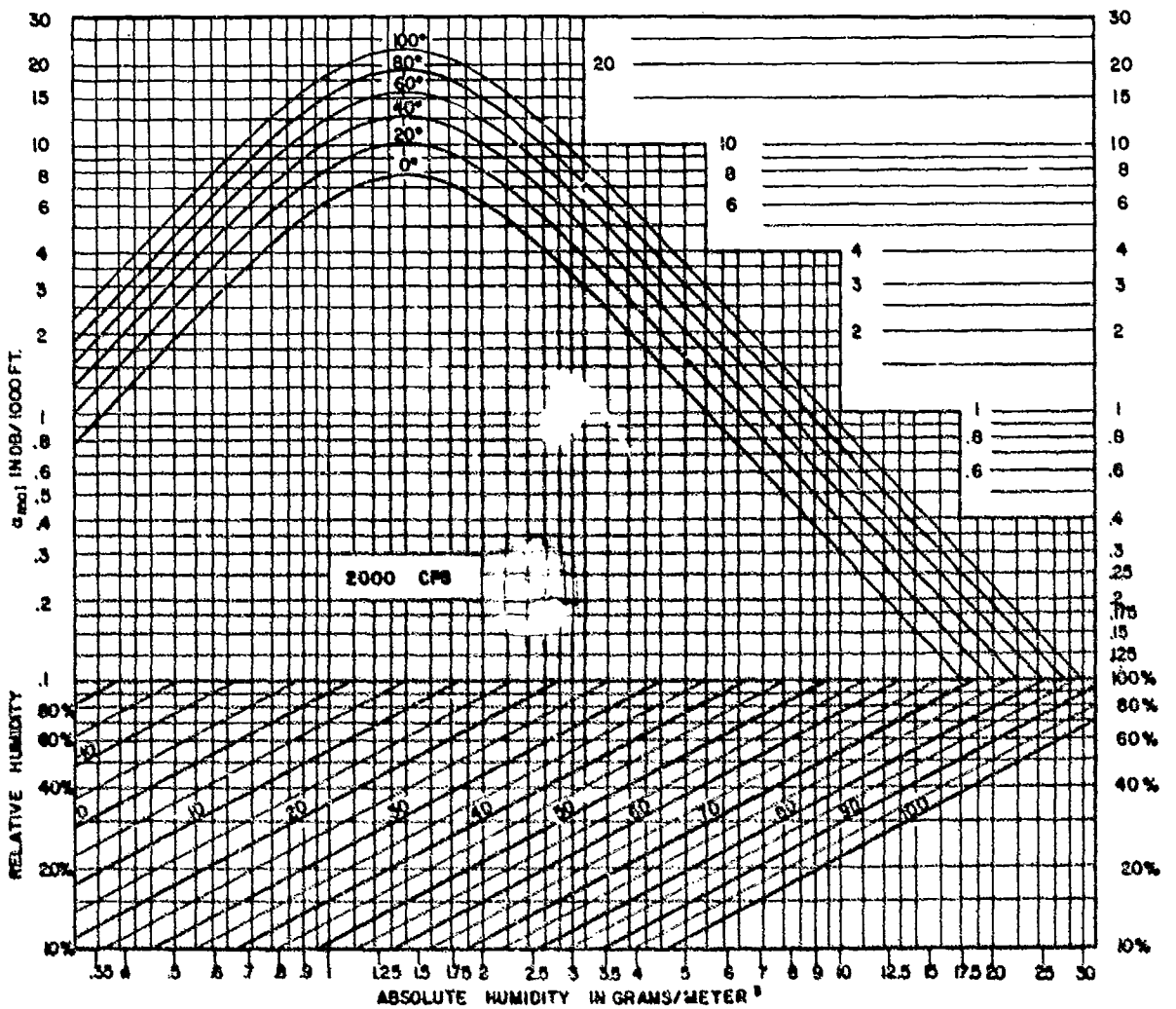

Fig. 44 Nomogram for calculating α_{mol}; 2000 cps

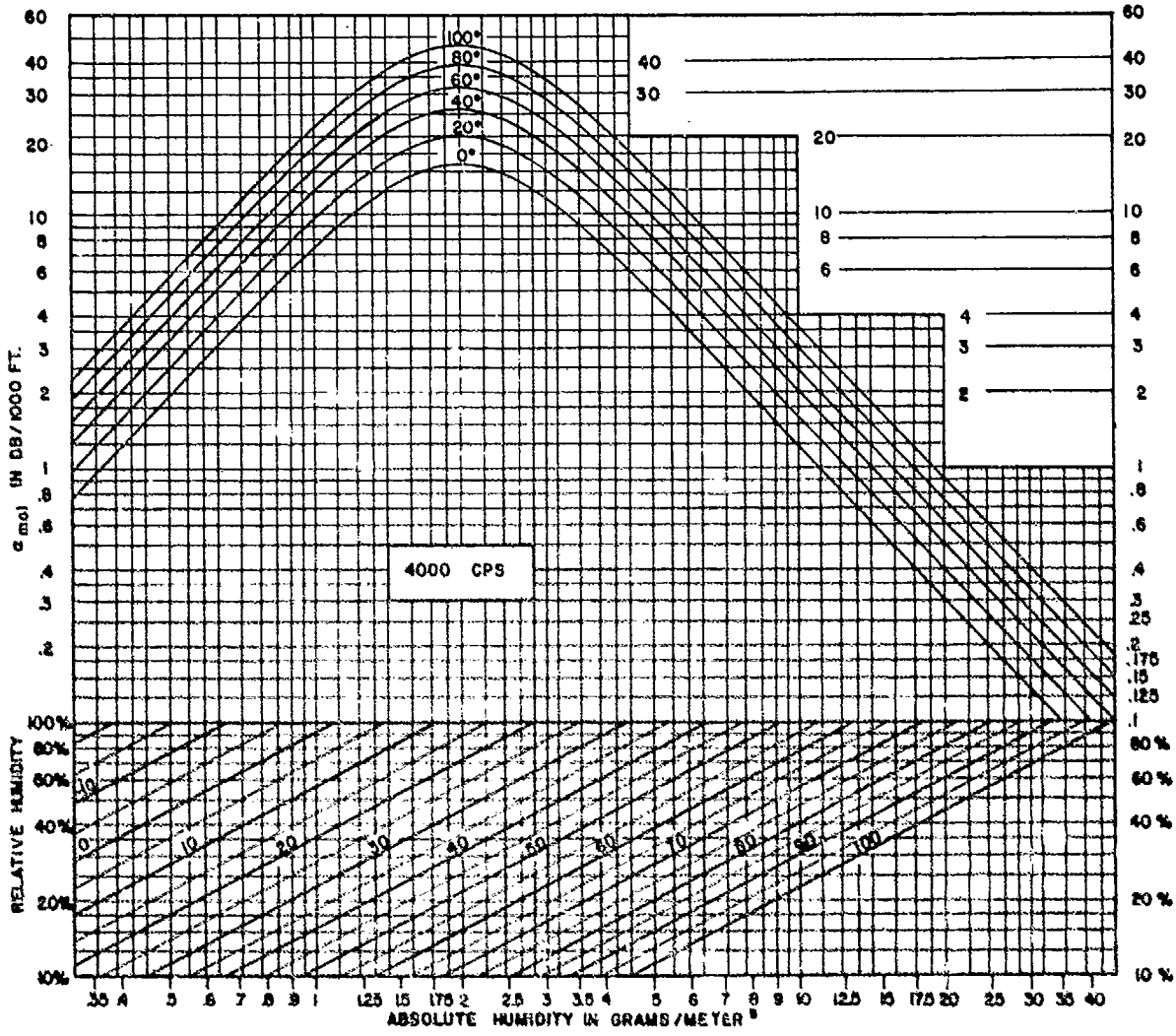

Fig. 45 Nomogram for calculating α_{mol}; 4000 cps

3.2.3.4 For frequencies other than those to which Figs. 42 - 45 apply one may use Fig. 46. The latter is similar to the former figures in that plots of relative humidity vs h at different temperatures are given in a lower graph, and plots of α vs h in an upper one. However, Fig. 46 differs from the previous ones in that here the α vs h curves are all for the same temperature (60°F) but are for different frequencies. A final correction for temperature requires an additional step. The general procedure for using Fig. 46 to calculate α at any given temperature, humidity and frequency is as follows:

(1) For given temperature and relative humidity determine h from the lower graph.
(2) For this h and the given frequency determine from the upper family of curves the value of α as it would be for the given absolute humidity if the temperature were 60°F; designate this value as α_{60}.
(3) Make a final correction for temperature. This may be done by any of several procedures to be suggested later.

The line ABCD shows a typical path to be followed in carrying out the first two of the above steps for calculating α_{60}; it is assumed that the temperature, relative humidity and frequency are 83°F, 53% and 3250 cps, respectively. The points A and B are determined from the given relative humidity, and temperature as in Fig. 42. A vertical line is then extended upward from B until it intersects that (interpolated) member of the upper family which corresponds to the given frequency. This intersection determines the point C. A horizontal line is then extended to the right from C; its intersection D' with the vertical axis gives α_{60}, in this case equal to 0.73 db/1000 ft.

For carrying out the final step indicated above, namely, to make a final temperature correction, one may use any one of the alternative methods (a), (b) or (c) given below:

(a) From the table shown as an insert in the lower right hand portion of Fig. 46, find the correction factor G for the given temperature. Multiply G by α_{60} to obtain α for the given temperature, relative humidity and frequency. For the given example G is 1.25 and hence α is 0.91 db/1000 ft.

Fig. 46 Nomogram for calculating α_{mol} at arbitrary frequency, temperature and humidity. See text for instructions in use. →

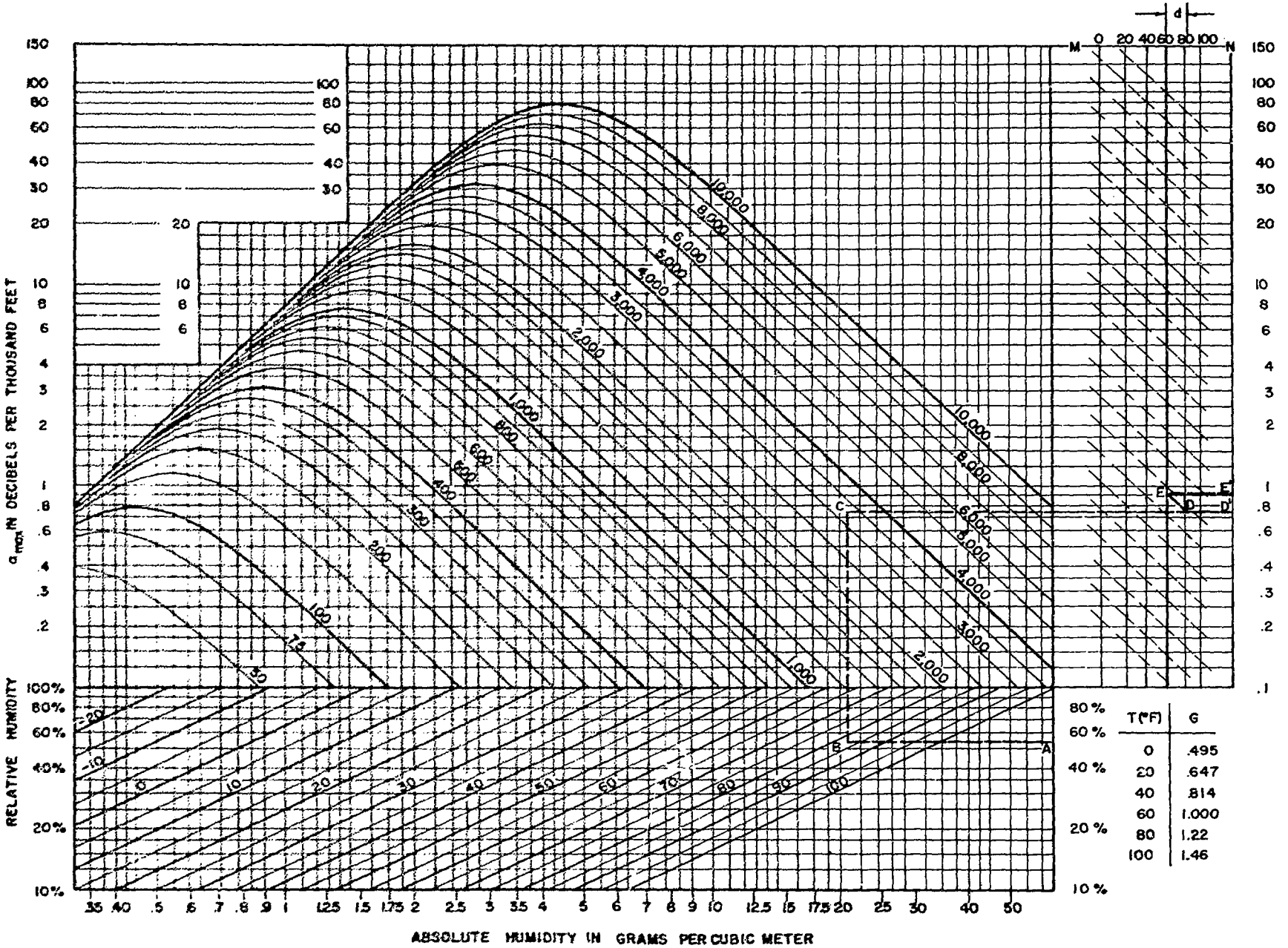
α_{max} IN DECIBELS PER THOUSAND FEET
RELATIVE HUMIDITY
ABSOLUTE HUMIDITY IN GRAMS PER CUBIC METER
d
M
N
0 20 40 60 80 100
A
B
C
D
D'
E
E'
T(°F) G
0 .495
20 .647
40 .814
60 1.000
80 1.22
100 1.46
80 %
60 %
40 %
20 %
10 %

(b) Using scale MN in the upper right hand portion of the figure mark off (by use of dividers or other suitable means) the distance from the point corresponding to 60°F to that corresponding to the given temperature; call this distance d. (As an example, the distance d to be measured for the case of 83°F is indicated above the scale.) The scale is such that d is proportional to the logarithm of the temperature correction factor G. Returning to the point D' measure the distance d either upward or downward from D' depending, respectively, on whether the temperature is greater or less than 60°F. The point E' so arrived at (i.e., the point a distance d above or below D') gives α for the given temperature, relative humidity and frequency. It may be verified that for the given example one obtains by the method α = 0.91 db/1000 ft, as before.

(c) Note the intersection D of the horizontal line CD' with that (interpolated) vertical line, extended downward from scale MN, which corresponds to the given temperature. Draw a 45° line (parallel to the dashed guide lines) from D; the intersection E of this line with the heavy vertical line which extends downward from the 60° mark on MN gives the desired value of α, it being understood that the scale according to which α is obtained from E is the scale on the extreme right of the figure. One may, in fact, draw a horizontal line to the right from E and read α from its intersection E' on that scale. It will be readily seen that this procedure is equivalent to that described in alternative (b).

3.2.3.5 Still another graphical method of calculating α_{mol} from Eq. (18) is afforded by a nomogram originated by Kneser[87] and extended by Pielemeier[88]. This nomogram (Fig. 47) gives α_{mol} for a wider range of parameters than Fig. 46, though with less accuracy. A broken dashed line indicates a typical path followed in making a computation; the temperature, relative humidity and frequency are assumed to be 15°C, 50% and 3000 cps, respectively. To determine α_{mol} from the nomogram for the given conditions, one may proceed as follows:

Fig. 47 Nomogram for calculating α_{mol} at arbitrary frequency, temperature and humidity, from Pielemeier[88]. →

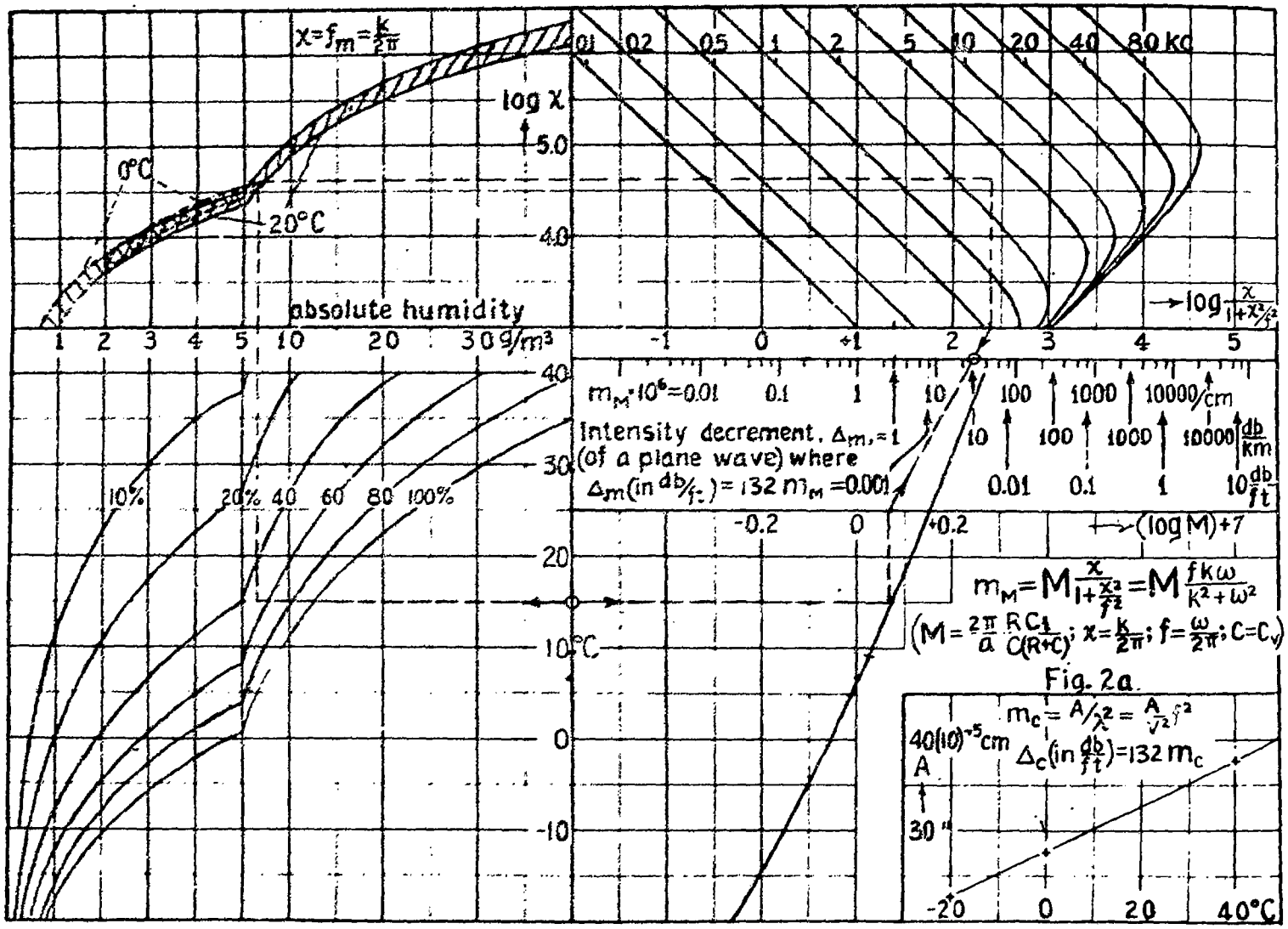
$\chi = f_m = \frac{k}{2\pi}$
log χ
5.0
4.0
0°C
20°C
absolute humidity
1 2 3 4 5 10 20 30 g/m³
40
30
20
10°C
0
-10
10% 20% 40 60 80 100%
.01 .02 .05 1 2 5 10 20 40 80 kc
$\rightarrow \log \frac{\chi}{1+\chi^2/f^2}$
-1 0 +1 2 3 4 5
$m_M \cdot 10^6 = 0.01$ 0.1 1 10 100 1000 10000/cm
Intensity decrement, $\Delta_{m_1} = 1$
(of a plane wave) where
$\Delta_m (\text{in } \frac{db}{ft}) = 132\, m_M = 0.001$
10 100 1000 10000 $\frac{db}{km}$
0.01 0.1 1 10 $\frac{db}{ft}$
-0.2 0 +0.2 $\rightarrow$ (log M)+7
$m_M = M \frac{\chi}{1+\frac{\chi^2}{f^2}} = M \frac{fk\omega}{k^2+\omega^2}$
$\left(M = \frac{2\pi}{a} \frac{RC_1}{C(R+C)};\ \chi = \frac{k}{2\pi};\ f = \frac{\omega}{2\pi};\ C = C_v\right)$
$m_c = A/\lambda^2 = \frac{A}{\sqrt{2}} f^2$
40(10)⁻⁵cm
A
$\Delta_c (\text{in } \frac{db}{ft}) = 132\, m_c$
30
-20 0 20 40°C

Fig. 2a.

(1) Starting at 15°C on the temperature axis in the lower quadrant, trace left to the 50% curve (by interpolation).
(2) Trace upward to the middle of the shaded area in the upper left quadrant.
(3) Trace to the right to the 3 kc curve in the upper right quadrant.
(4) Trace downward to the scale marked "log $\chi/(1+\chi^2/f^2)$".
(5) Start again at 15°C on the temperature axis in the lower quadrant; trace to the right to the curve in the lower right quadrant.
(6) From the latter trace upward to the scale marked "(log M) + 7".
(7) Connect by a straight line, the points arrived at in Steps (4) and (6). The intersection of this line with the scale marked "$m_M \cdot 10^6$" gives the intensity absorption coefficient in units of cm^{-1}.
(8) Multiply the number obtained in Step (7) by 1.32×10^5 to obtain α_{mol} in db/1000 ft for the given conditions.

Some of the symbols appearing on the nomogram are different than those used in the body of this report. Thus χ corresponds to the f_m in Eq. (18) and M corresponds to $(2\alpha_{max}/f)$ where α_{max} is given by Eq. (21b).

For ranges of parameters where both Fig. 46 and Fig. 47 apply the former is capable of higher accuracy, mainly because of the highly compressed log scale from which m_M is read in Fig. 47.

3.2.3.6 As shown earlier in this report, there is considerable evidence from both laboratory and outdoor experiments that the theoretical absorption coefficient ($\alpha_{mol} + \alpha_{class}$), as given by Eqs. (11) etc., does not give the correct result under all conditions. Particularly at the higher absolute humidities and lower frequencies (see Fig. 7), observed values of α are considerably in excess of the theoretical predictions. Especially for these conditions it would therefore seem preferable to base one's estimates of α for given field conditions on experimental rather than theoretical values.

The most recent laboratory results on α for homogeneous air are those given by Delsasso and Leonard. Their results (already discussed in some detail in subsection 1.2.4) are presented in Figs. 48 and 49; the plots of α versus absolute humidity given here are from the smooth curves fitted by Delsasso and Leonard to their data. From a set of results like these, for six different frequencies and three temperatures one might hope to be able to estimate α for any given

conditions by interpolation or extrapolation. Plots for converting from relative to absolute humidity are in the lower part of each figure, to aid in interpolation, etc. The recommended procedure to follow in estimating α for given conditions, say 60% relative humidity (RH) and 80°F, is as follows:

(1) Determine the absolute humidity h corresponding to 60% RH and 80°F; obtain h = 15 gm/m^3.
(2) Determine α at 71.2°F and 94.5°F for the given absolute humidity, i.e., for h = 15 gm/m^3; interpolate between these α-values.

(This procedure should usually be much more accurate than an alternative procedure where one determines α for the given relative humidity, i.e., 60% at both 71°F and 94.5°F, then interpolates.) Unfortunately such interpolation cannot be done with accuracy or confidence except over rather limited ranges of conditions. Data are not given at temperatures which are spaced closely enough to justify linear interpolation. This is especially obvious in the temperature range between 35° and 71°F, since results for these two temperatures are very different from each other.

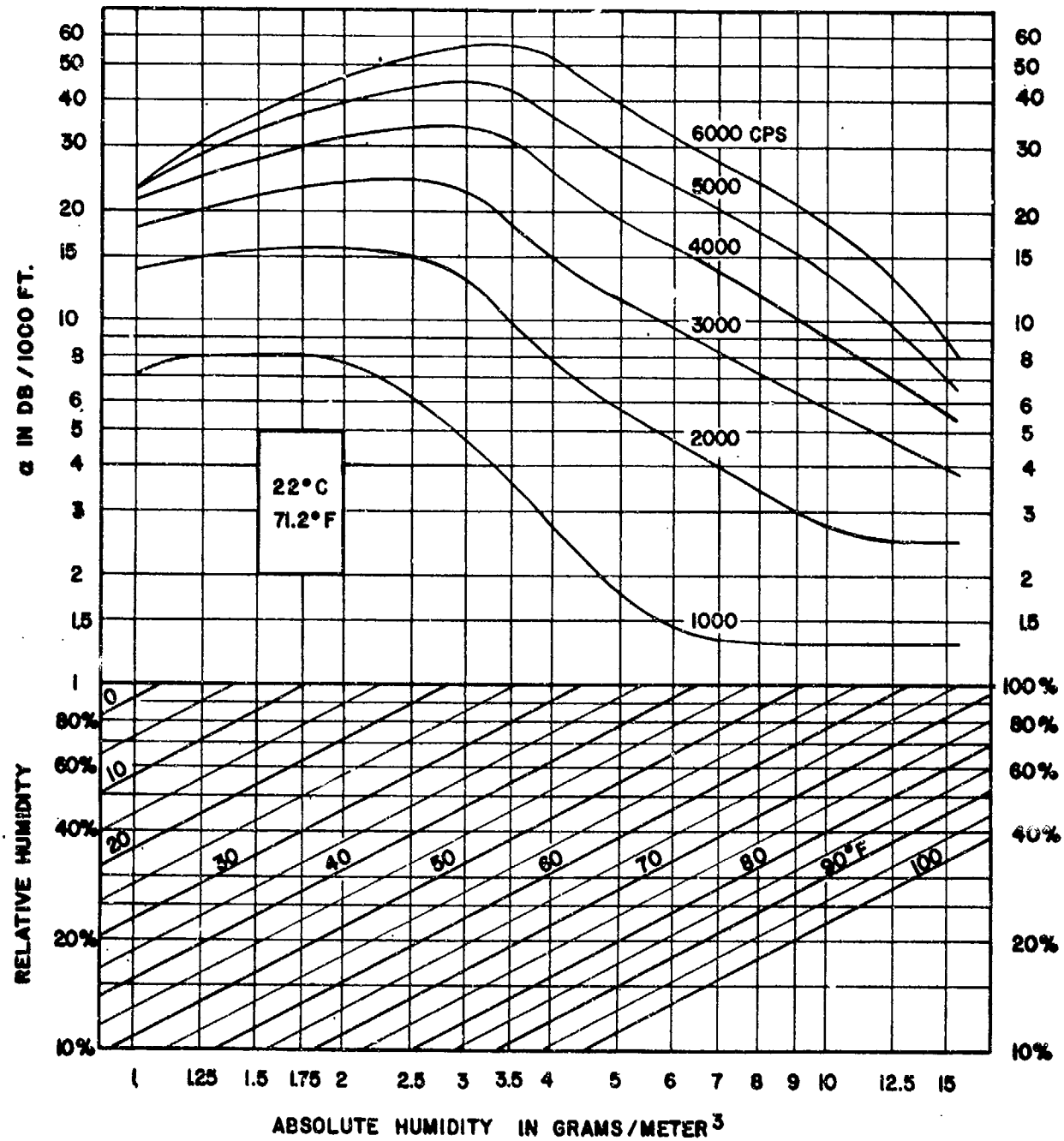

Fig. 48 Nomogram for determining laboratory α for air at 22°C; data from Delsasso and Leonard.

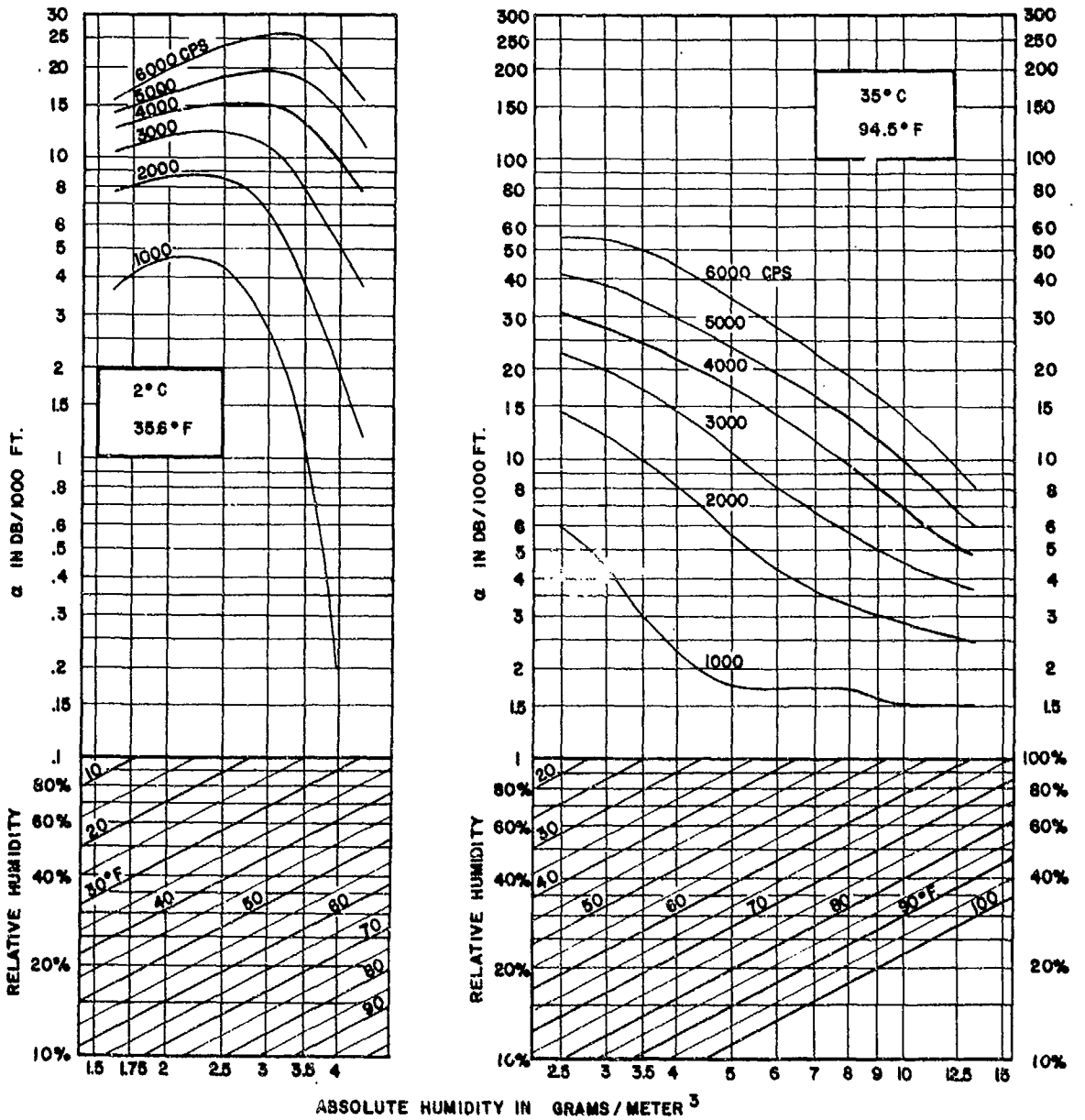

Fig. 49 Nomogram for determining laboratory α for air at 20C and 35°C; data from Delsasso and Leonard.

3.3 TYPICAL PROPAGATION PROBLEMS

3.3.1 Propagation Vertically from Aircraft to Ground

For persons living in residential areas at distances of, say 1 to 20 miles from an airport, the greatest disturbances probably occur at points rather directly under a take-off course. A problem of great importance, therefore, is that of predicting the sound level near the ground due to an aircraft nearly overhead, e.g., such that the line from aircraft to observer makes an angle of less than 45° with the vertical.

Fortunately, this situation appears to be one for which fairly reliable predictions can be made. The data of Parkin and Scholes (subsection 2.3.2) indicate that the pressure amplitude at the ground varies approximately inversely with the distance R from an aircraft noise source to observer for cases when the source is nearly overhead at frequencies below 1000 cps. The results of Regier (subsection 2.3.1) for frequencies around 300 cps are in agreement with this. For frequencies above 1000 cps, Parkin and Scholes find that Eq. (2) holds, where α is no longer negligible but is given moderately well by the theoretical absorption coefficient ($\alpha_{mol} + \alpha_{class}$).

Presumably a distinguishing characteristic of the conditions of Parkin and Scholes, and of Regier, is that in their cases the propagation path, being nearly vertical, is little affected by the ground (subsection 1.4) or by sound shadows (subsection 1.5). Also in their cases the air may be relatively homogeneous so that scattering by turbulence, etc., (subsection 1.6) is of reduced importance. From such considerations one would expect the results of Regier, and of Parkin and Scholes, to agree with those of Delsasso and Leonard (subsection 2.2.4) taken at high altitudes between mountain peaks. For under the latter conditions it might also be expected that terrain losses and refraction effects would be negligible. Examining the results we find the agreement apparently not as good as would thus be indicated; in the Delsasso-Leonard experiments the losses are appreciably greater than for a (1/R) law. Their average loss coefficients α are about 2.2, 1.6, 0.8, and 0.5 db/1000 ft respectively, for the frequencies 1000, 500, 250 and 125 cps.

The cause for this apparent discrepancy is unknown. However, it should be realized that the results of Parkin and Scholes are based on measurements at altitudes only up to 2000 ft and those of Regier are for altitudes only up to 5000 ft. Hence errors of 2 to 4 db in the sound level data (not unreasonable for level measurements on highly fluctuating signals) could account for the difference between their quoted results and those of Delsasso and Leonard. It will be realized, too, of course, that if in the practical problem to be solved one is concerned only with

aircraft at altitudes less than 2000 ft, the discrepancies noted are not of great significance.

On the basis of what has been said, a recommended procedure is given below for predicting sound levels on the ground due to an aircraft nearly overhead. It will be assumed that the pressure amplitude at any point on a reference sphere surrounding the source is known as a function of frequency. It will also be supposed that a given flight path is under consideration. The procedure outlined below is suggested for predicting the sound level at a ground observer point P due to noise generated by the aircraft when at a point Q along its flight path. (It will be realized that this sound level at P due to the source at Q will not occur when the moving source is at Q, but some time later, determined by the time for sound to travel from Q to P.)

For convenience in speaking of source specifications, suppose a special set of rectangular coordinate axes, say (x', y', z'), is fixed in the aircraft noise source with origin at the source. Let the reference sphere be of radius R_o, centered at the origin; let P_o be any point on this sphere, its directions cosines with respect to (x', y', z') being (ℓ, m, n), respectively. It will be assumed below that the source specification for a given frequency band consists of data giving the pressure amplitude p_o for that band at every point P_o (ℓ, m, n) on the reference sphere.

Recommended Procedure:

(1) Determine the distance R from the aircraft to the observer for the assumed points P and Q.
(2) Determine the direction (ℓ, m, n) of the line $\overline{QP}$ from the aircraft to observer with respect to the source axes (x', y', z').
(3) Refer to the source specifications for the reference pressure p_o at the given frequency f and at the reference point P_o (ℓ, m, n).
(4) Obtain the pressure amplitude p at the observer point P directly from the equation

$$p/p_o = (R_o/R) \exp -\left[\alpha(R - R_o)\right] , \qquad (215)$$

where p_o is the pressure at P_o (ℓ, m, n). Alternatively, obtain the loss in decibels of the sound level at P relative to that at P_o. As given in Eqs. (9), the latter consists partly of a $(1/R)$ loss and partly of an exponential loss. The former may be determined by reference to Fig. 39 or Table 22 in subsection 3.2.1. The latter may be computed simply from Eq. (204) if α is known. Alternatively, if α is known, the total loss may be obtained by use of Fig. 40 as described in subsection 3.2.2.

By any of the methods for carrying out Step 4 it is, of course, necessary to know the constant α. According to the results of Parkin and Scholes one can obtain a fair estimate of α by determining the theoretical absorption coefficient

$$\alpha_{theo} = \alpha_{class} + \alpha_{mol} \tag{216}$$

for the given meteorological conditions, using methods described in subsection 3.2.3. However, the Parkin and Scholes results are for rather specialized conditions, since their absolute humidities are always less than about 6 gms/m^3. It is recommended that α_{theo} be regarded generally as a lower limit to α, and that experimental results be consulted, when available for the conditions of interest, for estimates which may be more nearly correct.

Thus for frequencies of 1000 cps and below, one may estimate α on the basis of the outdoor results of Delsasso and Leonard (Figs. 24 - 27 and Tables 16 - 19) if the meteorological conditions for which these results are applicable seem to correspond reasonably closely to those for the problem at hand. It will be remembered that the observed α of Delsasso and Leonard tends to be in excess of α_{theo} by a ratio which increases with increasing absolute humidity.

At frequencies of 1000 cps and above one may refer to the laboratory data of Delsasso and Leonard (Figs. 48 and 49; subsection 3.2.3); these are in fair agreement with results previously reported by Knudsen. It will be remembered that here also the observed α exceeds α_{theo} by a ratio which increases with absolute humidity.

3.3.2 Propagation along the Ground

3.3.2.1 Introduction

Another important problem is that of propagation along the earth from a source near the ground to a receiver near the ground. Unfortunately, the situation here can be very complicated due to refraction phenomena combined with effects due to interaction with terrain. Since satisfactory information about the general problem does not exist it is helpful to consider special cases, in each of which given factors play predominant roles. In subsections 3.3.2.2 to 3.3.2.4 special situations are taken up, which correspond to certain specified actual conditions; in each case are described recommended methods for handling the problem, based on such information as is available.

3.3.2.2 Hard ground surface; quiet cloudy day

If the ground is paved, or is water-soaked earth, one may assume

that the acoustic impedance is infinite (see subsection 1.4); terrain losses are then negligible, although image effects may enter. If, in addition, the atmosphere is relatively free of wind and temperature gradients and if the source and receiver heights z_o and z are small compared with their horizontal separation r, then the governing equation for the pressure amplitude is simply, from Eq. (2),

$$p = (1/r)\, e^{-\alpha r} \tag{217}$$

The quantity α in this equation is presumably given by the loss coefficient in homogeneous air (subsection 1.2). The recommended method for calculating losses under the conditions noted is thus as follows:

(1) Determine the loss coefficient for homogeneous air under the given conditions of temperature and humidity by methods described in subsection 3.2.3;
(2) Calculate the total loss (1/R loss plus exponential loss) by methods described in subsection 3.2.2.

If r is not large compared to z and z_o, the pattern is complicated by maxima and minima due to interference between direct and reflected sound. If α is assumed negligible, the general result for the complex pressure amplitude for any z_o, z and r is given by Eq. (58).

Unfortunately, there are few or no available experimental data bearing on the special case treated here.

3.3.2.3 Earth covered with vertical-stemmed vegetation; quiet cloudy day

We suppose here that the medium which forms the lower boundary to the air is itself porous and such that air moves through it easily in the vertical direction, but with difficulty in the horizontal direction. Then one may assume the normal impedance condition holds (subsection 1.4, Case 2). For source-receiver distances large enough so that $\sin\psi \ll \xi \ll (1/\sin\psi)$ and $k_1 R \gg 1$ (see subsection 1.4), the decibel loss at any point relative to that at a reference point R_o will be given by the 1/R loss plus the quantity

$$\text{Terrain loss} = -20 \log_{10} G = 20 \log_{10} (r/r_1) \tag{218a}$$

where

$$G = r_1/r\ , \tag{218b}$$

and

$$r_1^2 = 4\zeta^2 (z + z_o)^2 + \left(\frac{4\pi z z_o}{\lambda} - \frac{\lambda\zeta^2}{\pi}\right)^2 \quad . \qquad (218c)$$

(The above result comes from Eqs. (197) and (198).) Hence to calculate the terrain loss for conditions under which Eqs. (218) are valid one may determine r_1 from Eq. (218c), then calculate the loss for any given r from Eq. (218a). (One may use Fig. 39 or Table 22 for decibel ratios.) The <u>total loss</u> at a distant point relative to the level at a nearer point would include the terrain loss, the (1/R) loss, and other kinds of losses which may be important.

Example:

Calculate the loss in level at a point 1000 ft from a source, relative to that at a 10 ft distance, taking into account the (1/R) loss as well as terrain loss. Let $\zeta = 1$, $z = z_o = 10$ ft and $\lambda = 2.5$ ft.

(1) The (1/R) loss is $20 \log_{10} (1000/10) = 40$ db (see Fig. 39 or Table 22).
(2) The terrain loss at 1000 ft relative to the level at 10 ft (assuming negligible terrain loss at this latter close distance) is $20 \log_{10} (1000/r_1)$ where r_1, as given by Eq. (218c), is 502 ft. From Fig. 39 or Table 22 the terrain loss is therefore 6.0 db.
(3) The total loss at 1000 ft is the sum of the separate losses computed above, or Total loss = 40 db + 6.0 db = 46.0 db.

As stated previously, Eqs. (218) give the terrain loss accurately only at sufficiently large distances r from the source. For points near a given source the terrain loss is negligible and the sound level will follow the law.

$$\text{Sound level in db} = 20 \log_{10} (A/r) \quad , \qquad (219a)$$

where A is a constant proportional to the source strength; it is assumed in Eq. (219a) that atmospheric absorption is negligible. When Eq. (219a) holds the loss increases by just 6 db per distance-doubling (see subsection 3.2.1). For the same source to which Eq. (219a) applies the sound level at large distances will be given by

$$\text{Sound level in db} = 20 \log_{10} (Ar_1/r^2) \qquad (219b)$$

The total loss in this case amounts to 12 db per distance-doubling; one might say that one-half of this, i.e., 6 db/doubling, is due to 1/R loss while the other half is terrain loss.

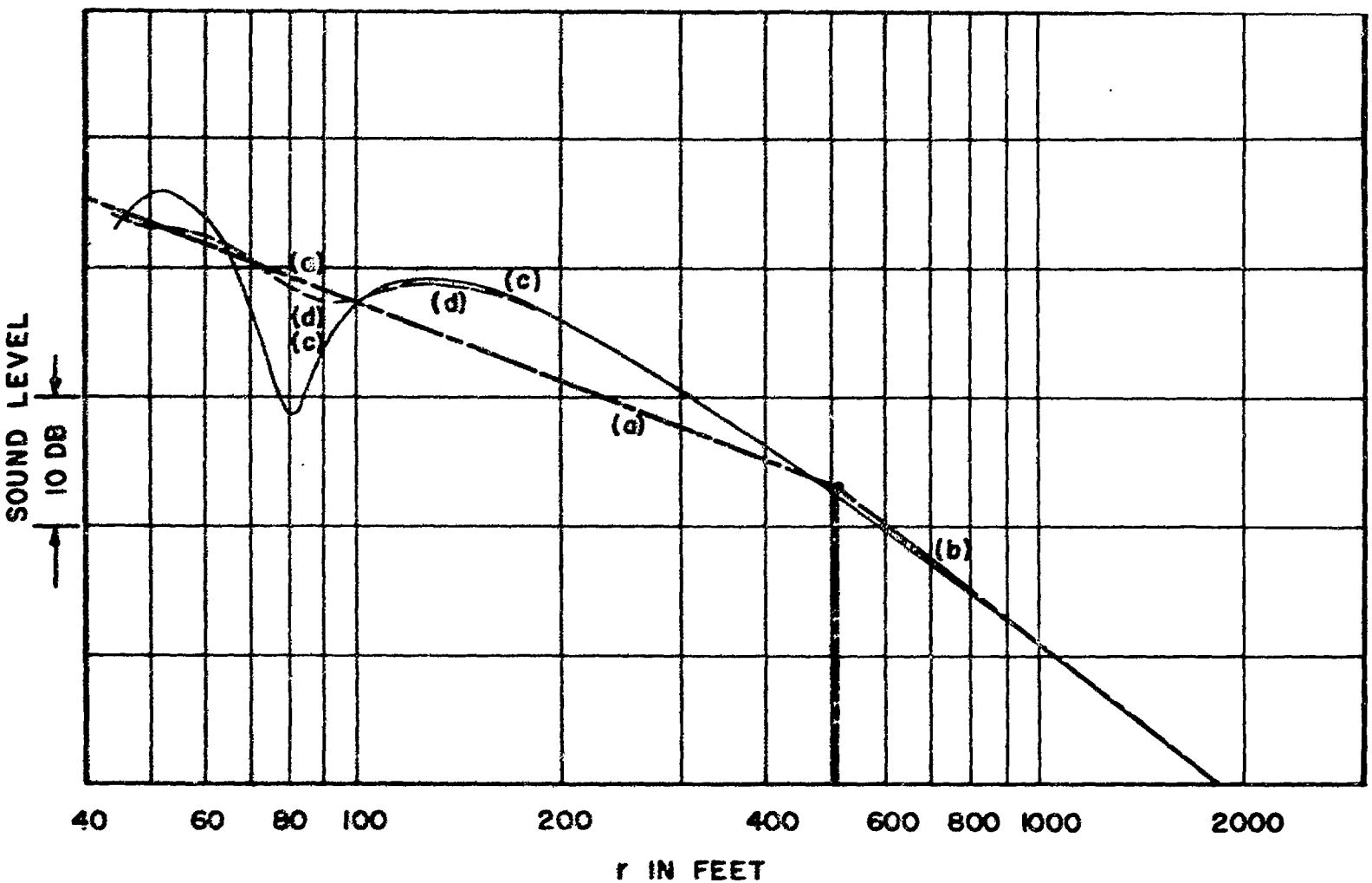

Fig. 50 Sound level over impedance boundary vs horizontal separation r between source and receiver; $z = z_0 = 10$ ft, $\zeta = 1$. Curve (a) is a plot of Eq. (219a); curve (b) is for Eq. (219b), for a pure tone of 450 cps. Curves (c) and (d) are from Franken[89]; (c) for a pure tone of 450 cps; (d) for a (300-600 cps) band of noise.

At $r = r_1$ one obtains the same sound level from both Eqs. (219). (This might be regarded as an accidental happening; neither of the approximate formulae given by Eqs. (219) is accurately valid at $r = r_1$.) A graph of these equations may easily be obtained by plotting sound level vs r on semi-log paper, as in Fig. 50. Here Eqs. (219) are plotted for the case $\zeta = 1$, $z = z_o = 10$ ft, $\lambda = 2.5$ ft (frequency = 450 cps) considered in the above example. The straight line (a) has a slope of 6 db/distance-doubling and thus represents Eq. (219a). The straight line (b) represents Eq. (219b); it therefore has a slope of 12 db/doubling, and joins line (a) at $r = r_1$, i.e., at $r = 502$ ft.

For comparison with the approximations represented by lines (a) and (b), Fig. 50 also shows the results of more accurate application of the theory for terrain losses (subsection 1.4); the curves (c) and (d) are from a report by Franken[89]. The solid curve (c) gives the results for a pure tone of 450 cps; maxima occur at about 50 and 150 ft, and a sharp minimum at 70 ft; these maxima and the minimum are due to interference between direct and reflected sound. The dashed curve (d) is for the same condition except that the source now generates an octave band of noise (300 - 600 cps) rather than a pure tone. For $r \geq 100$ ft there is little difference between curves (c) and (d); however, for $r \leq 100$ ft the difference is marked in that the maximum at 50 ft, and the minimum at 80 ft are much reduced for the case of the noise band.

It is to be seen that line (a), representing Eq. (219a), fits the accurate theory for a band of noise fairly well for $r \leq 100$ ft, and that line (b), representing Eq. (219b), represents the facts with good accuracy for $r \geq 502$ ft. In the vicinity of 150 - 300 ft the accurate theory predicts sound levels up to 6 db greater than is given by Eq. (219a), i.e., by line (a). The reason for this deviation is that Eq. (219a) takes no account of reflected sound and hence, of course, does not predict the maximum at 150 ft, which is due to constructive interference between reflected and direct sound. This maximum is, in general, to be expected at $r = r_m \simeq 4\pi z_o/\lambda$.

Comparisons of Eqs. (219) with more exact theory for other values of ζ and at other frequencies yield about the same results as are seen in Fig. 50. Hence a simplified scheme suggests itself, which is sufficiently accurate for many purposes. A recommended procedure for calculating the terrain loss in a given octave band due to a noise source when source and receiver are fairly near the ground is as follows:

(1) For $r \geq r_1$ use Eq. (219b);
(2a) For $r \leq r_1$ use Eq. (219a) if rough estimates are sufficient, specifically, if errors up to

6 db in the vicinity of $r = (4z z_o/\lambda)$ may be ignored;

(2b) For more accuracy in the region $r \ll r_1$ use the general theory for pure tones in subsection 1.4, bearing in mind that minima and maxima will be smoothed out in the actual case of a band of noise;

(2c) For highest accuracy follow the method of Franken[89] in obtaining results for the case of a noise-band source.

Unfortunately, available experimental data are not sufficiently extensive to indicate just how closely the above procedure describes the losses which occur out-of-doors over a real earth. However, the theory should, at least, prove very useful in order-of- magnitude estimates.

When Eqs. (218) or (219b) are valid, the terrain loss at any given distance r is determined entirely by the parameter r_1. From Eq. (218c) we see that r_1 is minimum with respect to λ, and hence also with respect to frequency, when λ is equal to λ_m, where

$$\lambda_m = 2\pi\sqrt{z\, z_o}/\zeta \quad , \tag{220}$$

and that the minimum value of r_1 is

$$r_{1m} = 2\zeta(z + z_o) \tag{221}$$

The greatest terrain loss for any r, z, z_o and ζ is thus for $\lambda = \lambda_m$ and is given by $20 \log_{10} (r/r_{1m})$; the loss decreases monotonically (1) as λ increases for $\lambda > \lambda_m$, and (2) as λ decreases for $\lambda < \lambda_m$. The maximum in loss vs frequency is a rather broad one as may be seen by considering the expression for r_1 obtained by letting $z = z_o$ and $\lambda = n\lambda_m$ in Eq. (218c):

$$r_1 = r_{1m}\left[1 + (1/4)(n - n^{-1})^2\right]^{\frac{1}{2}} \quad , \tag{222}$$

where $r_{1m} = 4z\zeta$. When $n = 1$, Eq. (222) yields $r_1 = r_{1m}$; for frequencies an octave above or below the frequency f_m corresponding to λ_m (i.e., $n = 2$ or $n = \frac{1}{2}$) one obtains $r_1 = 1.25\, r_{1m}$; for two octaves above or below f_m ($n = 3$ or $1/3$) the result is $1.67\, r_{1m}$, and at three octaves it is $2.13\, r_{1m}$. Hence for any given z, z_o, r and ζ for which Eq. (222) applies the terrain loss at frequencies one, two and three octaves, respectively, from f_m will be less by only 1.9, 4.4 and 6.5 db from that at f_m.

Unfortunately for application of these equations, it is not

known what values of ζ are appropriate for typical kinds of ground. One might hope that some information might be obtained by fitting Eqs. (218) to given field data; thus if λ_m were known for given z and z_o one could determine ζ from Eq. (220). For example, Eyring's data (subsection 2.2.3, Table 15) were fitted reasonably well by assuming $\lambda_m = 2$ ft, corresponding to a frequency of about 560 cps. On this basis, letting $z = z_o = 5$ ft, ζ turned out to be $5\pi = 15.7$. As another example, the data on terrain loss vs frequency given by Ingard[75] in Fig. 34 appear to be fitted best by assuming $\zeta = 4\pi = 12.6$. On this basis, from Eq. (220), $\lambda_m = 5$ ft so that the maximum terrain loss at r = 1000 ft is about 6 db.

3.3.2.4 Sandy terrain; quiet cloudy day

We now consider the case where the lower medium is porous and such that air motions in the pores take place with equal ease or difficulty in all directions. By proceeding from the theory in subsection 1.4 it is possible to show that when $k_1 R_1 >> 1$ and $\sin\psi << (Z_2/Z_1 a) << (1/\sin\psi)$, where

$$a = \left[1 - (k_1/k_2)^2 \cos^2\psi\right]^{\frac{1}{2}} \simeq \left[1 - (k_1/k_2)^2\right]^{\frac{1}{2}} , \qquad (223)$$

one obtains approximate formulas identical with Eqs. (218) except that ζ is replaced by $(Z_2/Z_1 a)$. Hence the recommended procedure is the same as in the previous subsection (3.3.2.3) with the exception that ζ is to be replaced everywhere by $(Z_2/Z_1 a)$.

If the soil is similar to sand and the frequency not too great one may estimate the ratio $(Z_2/Z_1 a)$ by a theory such as that recently advanced by R. W. Morse[22]. The latter theory adapts basic equations presented previously for acoustical porous materials, to the case of granular media. By a reasonable choice of certain parameters a surprisingly good fit to data on actual porous soil is obtained. Using results of this theory and making the assumption that the imaginary part of the propagation constant in soil is much less than the real part, one obtains

$$\frac{Z_2}{Z_1} \simeq P^{-1}(c_1/c_2) , \qquad (224)$$

where P is the porosity of the soil (volume of air in the soil per unit volume of soil), c_2 is the velocity of sound in soil and c_1 the velocity of sound in air. Typical values for P and $(c_1/c_2) = (k_2/k_1)$ are 0.6 and 1.4 respectively. Using these values one obtains $(Z_2/Z_1 a) \simeq 3.3$.

3.3.3 Propagation through Fog

On a quiet foggy day (so that wind and temperature gradients are very small) and under conditions (i.e., sound either traveling nearly vertically to ground from an overhead source, or traveling horizontally along an "acoustically hard" boundary) such that terrain losses are negligible, one may expect the pressure amplitude due to a given source to decrease with distance according to Eq. (2), where

$$\alpha = \alpha_{hom} + \alpha_{e-c} + \alpha_{o-w} \tag{225}$$

In the above equation α_{hom} is the loss coefficient α which would be obtained for homogeneous air, i.e., in the absence of fog (see subsection 1.2); α_{e-c} and α_{o-w} are, respectively, the coefficients due to fog given by Epstein and Carhart (subsection 1.3.2) and by Oswatitsch and Wei (subsection 1.3.3). Graphs for computing α_{hom} have already been discussed in detail in subsection 3.2.3; graphs and tables are given in subsection 1.3 for calculating α_{e-c} and α_{o-w} for a uniform fog of specified density and droplet size. Here we merely give estimates, by application of the respective theories, of losses to be expected for typical fogs.

According to results given by Houghton[90] the water content of fogs under his conditions of observation is sometimes as great as 0.3 gm/m^3 but is more usually around 0.1 gm/m^3. (A glance at the conversion chart, Fig. 51, Appendix II, makes it clear that the water content in droplet form is thus much less than the mass of water in molecular or vapor form for typical temperatures and humidities.) Observed droplet diameters vary from over 10^{-2} cm down to the order of microns; "averages" for different fogs vary from 9 to 75 microns.

Table 23 below gives values of α_{e-c} and α_{o-w} computed at frequencies f of 0.1, 1.0 and 10 kc, respectively, for uniform fogs of assumed droplet radii ξ of 5, 10 and 25 microns, respectively; in each case the water content is assumed to be 0.1 gm/m^3.

For the frequencies considered in Table 23, it is seen that for a given water content, e.g., in gm/m^3, both α_{e-c} and α_{o-w} increase as the droplet size decreases. We also note that for the given conditions α_{e-c} increases with frequency while α_{o-w} decreases with increasing frequency. The latter is evidently important only at the lower frequencies.

It may be mentioned that α_{e-c} is an additive quantity. For example, the coefficient α_{e-c} due to a fog consisting of two droplet-groups A and B is just the sum of the coefficients for groups A and B,

TABLE 23

Computed Loss Coefficients for Fogs

ξ (microns)	f cps	α_{e-c} (db/1000 ft)	α_{o-w} (db/1000 ft)
5	100	0.2	0.2
	1,000	1.2	2.7×10^{-2}
	10,000	1.7	3.0×10^{-4}
10	100	0.17	2.5×10^{-2}
	1,000	0.35	4.7×10^{-4}
	10,000	0.49	4.7×10^{-6}
25	100	0.06	1.9×10^{-4}
	1,000	0.07	1.9×10^{-6}
	10,000	0.11	1.9×10^{-8}

separately. Use can be made of this principle in determining α_{e-c} for a realistic fog in which there is a distribution of particle sizes. In this case the distribution may be divided into groups such that in Group 1 there are n_1 particles per unit volume of approximately uniform radius ξ, in Group 2 there are n_2 of radius ξ, etc. The value of α_{e-c} can be determined for each group separately, then added to give α_{e-c} for the combination.

On the other hand, α_{o-w} is <u>not</u> an additive quantity. This is exemplified by the fact that for a uniform fog α_{o-w} is not, in general, directly proportional to the number n_o of droplets per unit volume. In fact, under some circumstances α_{o-w} decreases when n_o increases. For the case of a fog in which there is a distribution of droplet sizes the Oswatitsch-Wei theory is not applicable in its present form; development is needed to adapt the theory to this general problem.

SECTION IV

RECOMMENDATIONS FOR FUTURE RESEARCH

4.1 INTRODUCTION

It is evident from Sections I and II that considerable gaps exist in our knowledge of how sound propagates in the lower atmosphere. Although, as was shown in Section III, some practical situations can be treated fairly adequately, there are others where analytical description of the sound field is subject to much uncertainty, and still others where such description can hardly be given at all. Obviously much research remains to be done before satisfactory solutions can be given of the overall problem to which this report is devoted. Specifically, this problem is:

Given the characteristics of a sound source, radiating into the atmosphere, to predict the pressure amplitude at any point in the surrounding region.

Development of a practical system of procedures for making such predictions with accuracy requires a broad program of research. In planning a program for this purpose, an important consideration is that useful results are needed as soon as possible; at the same time it must be realized that some of the questions to be answered are rather basic ones which require long range approach. To meet needs of the present as well as those of the future, and to do this in a sound and economical manner, it is necessary that research be carried on at several different levels. Thus a balanced research program would include the following:

(1) Theoretical investigations both on basic mechanisms and on applications of these to practical situations.
(2) Laboratory experiments to check existing theories and to guide new theoretical approaches.
(3) Experimental work under actual field conditions, or under conditions which simulate those which obtain in practice.

In the following subsections various possibilities for research are suggested and described; particular attention is given to certain special topics which the available literature, reviewed in Sections I and II, shows to be inadequately understood.

4.2 THEORY AND LABORATORY EXPERIMENTS

4.2.1 Losses in moist air

As pointed out in subsection 1.2 there is need for improved theory to account for attenuation of sound in air, especially at high humidities and at low frequencies. Development of such theory would, no doubt, call for laboratory experiments specially designed to check various features of the theory. In addition, it has been seen in subsection 1.2.4 and 3.2.3 that laboratory measurements are also needed to accomplish the following specific objectives:

(1) Extend the range of measurements to higher absolute humidities.
(2) Determine, if possible, the cause of uncertainties in present data, in particular, unresolved questions as to the correct values of h_m for different frequencies and as to the shape of α vs h curves (see Figs. 4, 5 and 6).
(3) Obtain data at other temperatures than those (35.6°, 71.6° and 95°F) used by Delsasso and Leonard, especially at temperatures between 36° and 72°F. Such additional data would, of course, improve greatly the accuracy with which values of α to be applied at given temperature and humidity conditions can be obtained by interpolation from laboratory data.

4.2.2 Losses in Fog

Closely related to the problem of moist air, where the water content is considered to be in the form of a gas of H_2O molecules, is that of a fog or cloud, where some of the water exists as droplets (i.e., large aggregations of molecules which are held in suspension). Though theories now available (subsection 1.3) may be inherently capable of treating sound propagation in a real fog, the application to actual out-of-door situations is not possible at present for various reasons:

(1) Adequate information is not available on densities and drop-size distributions for fogs occurring in different parts of the United States. Furthermore, it is perhaps not possible to carry out a program of fog measurements, satisfactory for acoustical purposes, with methods now in use. Both the Epstein-Carhart and Oswatitsch-Wei theories suggest the possible acoustical importance of droplets with

radii of the order of microns or smaller. Development of experimental techniques is necessary before such small droplets can be accurately counted.

(2) The Oswatitsch-Wei theory needs to be generalized in order to make it applicable to real fogs, where droplets are not uniform in size.

(3) There are questions, only briefly discussed in subsection 1.3, regarding the values of the effective heat conductivity coefficient and diffusion coefficient to be used when the Oswatitsch-Wei theory is applied to small droplets with radii of the order of microns and smaller. These matters, discussed in Reference 13, should be given further consideration.

4.2.3 Ground Attenuation

By laboratory experiments the theoretical results of subsection 1.4 have been shown to be adequate for the description of sound propagation over a uniform ground; the theories should now be extended to the following cases:

(1) Propagation over non-uniform ground, i.e., where the surface is made up of patches of material (soil, grass, etc.) having different acoustical properties.

(2) Propagation over a non-planar ground, i.e., where the surface is uneven.

In view of recent papers concerning electromagnetic propagation over the above types of ground, these theoretical advances can probably be made without great difficulty. The results of these investigations, and the validity of any approximations which may be necessary, can best be tested by laboratory experiments using frequencies in the kilocycle range and, mainly, commercially available acoustical materials.

There is also much need for a systematic study to determine the acoustic quantities ζ, Z_2 and c_2 applicable to various typical kinds of ground and ground-covering.

4.2.4 Shadow Zone Problems

Since micrometeorological data indicate that the sound velocity depends on the logarithm of the height above the ground for both the temperature and wind velocity gradients, an analysis of sound attenuation in the shadow zone formed by this type of gradient should be undertaken. Since the wind-gradient problem is of a different character from the temperature-gradient problem, these will probably need to be carried out

separately, although it seems likely that the results of the simpler temperature-gradient problem will give a considerable amount of information useful for the more complicated wind-gradient problem. These analyses will probably involve a fairly long range program, since information is necessary concerning low-frequency attenuation where the usual approximation method (high-frequency approximation) is probably no longer valid. However, in view of the generality of the (almost) logarithmic temperature and wind-dependence upon height, the results would seem to be of considerable importance in out-of-doors sound propagation problems.

Theoretical investigations should be made of the sound field in the normal zone, i.e., between the source and the shadow boundary, as well as the sound field under conditions of "channelling" (field due to a positive temperature gradient or field in the downwind direction from a source in a wind).

It does not seem likely that the results obtainable from the above theories can be tested in the laboratory; but small-scale out-of-doors experiments where good micrometeorological information could be obtained would probably provide an adequate check on this theory. (See subsection 4.3.3.)

4.2.5 Scattering by Inhomogeneities

In view of the comparatively elementary state of present-day theories, as well as the lack of experimental data, it would seem advisable to plan a long range program of basic theoretical and experimental research into the problem of the scattering of sound by temperature and wind inhomogeneities. Some problems to be investigated are: the validity of the theories of Lighthill and Kraichnan, and their extension to more realistic types of inhomogeneities, e.g., where the parameters describing the inhomogeneities depend upon height above the ground; the (often unstated) approximations involved in Blokhintzev's theory of sound scattering in the atmosphere; the applicability to the air acoustics case of Mintzer's results on underwater sound fluctuations due to temperature inhomogeneities; the increase in sound level in the shadow zone due to scattering of sound from the normal zone.

Many of the above theoretical developments can be tested, as well as partially directed, by the results of laboratory experiments. Since a large amount of experimental, as well as theoretical, results have been obtained on turbulence in wind tunnels, it would seem admirable to attempt acoustic measurements on turbulence produced in a wind tunnel. There the turbulence parameters are, to a large extent, at the control of the investigator; specific factors and approximations in the theories of scattering by turbulence could then be tested.

It would also seem feasible to do experimental work on turbulence scattering by means of small-scale outdoor experiments; (see subsection 4.3.3).

4.2.6 Propagation of high amplitude sound

The overall propagation problem may involve "finite amplitude" phenomena when powerful sources are used. In this case the approximations of linear acoustics (upon which nearly all of the analysis in Section I of this report depends) are not valid near the source, but only at distances from it greater than some limiting distance, say, R*. Of course, the choice of R* is somewhat arbitrary and would, in general, vary with direction. For a very powerful source the distance R* may be so great that the sound field at this distance is affected by refraction in the medium, and by terrain effects. The pressure amplitude at a distance R* is then a fluctuating quantity, and its mean value depends on micrometeorological conditions as well as on the nature of the ground.

Measurements made to specify an aircraft source must be reproducible; i.e., the results must depend only on design and operation parameters of the aircraft and not on the micrometeorological state of the atmosphere, or on the terrain. Hence, source-specification measurements should preferably be made near to the source, say, at distances from it less than some limiting distance R** which depends on the micrometeorological and terrain conditions. When a very powerful source is used, or when refraction or terrain effects are especially great, the distance R** may be less than R*. Hence the problem of predicting the field surrounding a source, on the basis of given reproducible source measurements, requires consideration of the region between R** and R*.

A very difficult problem is posed in treating this region; here one must deal with high amplitude sound propagation through a refracting medium, subject to terrain influences. At the present time, results on high amplitude propagation are available only for rather elementary situations. The general problem can probably be approached only through a long range program of fundamental research. Phenomena characteristic of high amplitude sound fields which should receive attention include (1) wave distortion, generation of harmonics and shock wave formation, (2) reflection and refraction at oscillating boundaries, and (3) radiation pressure and acoustic streaming.

4.3 EXPERIMENTS OUT-OF-DOORS

4.3.1 Introduction

As was shown in the review of literature in Section II, the results of theory or laboratory experiments for idealized cases cannot be assumed to apply out-of-doors except where checked by actual experiment. According to the findings in Section II the only cases where results obtained out-of-doors are quantitatively in agreement with theory are those (subsections 2.3.1 and 2.3.2) dealing with sound propagation nearly vertically from aircraft to ground. To arrive at valid prediction methods it is therefore necessary to carry out extensive experimentation under actual outdoor conditions.

In spite of the inadequacy of theoretical results in their present form, these nevertheless serve a very useful purpose as guides in setting up experiments and interpreting the findings. Let us assume our goal is to obtain prediction methods whereby the pressure amplitude due to a specified aircraft source is given at any point in terms of a number of measureable parameters. (When, as is usually true, the pressure amplitude is a fluctuating quantity we should want our prediction scheme to give some index of the fluctuation magnitude as well as a suitable average of the pressure amplitude.) The findings for idealized cases, discussed in Section I, suggest that the following sets of parameters are of particular importance.

(1) Geometrical parameters: principally those giving the source and receiver positions and the source orientation.
(2) Parameters giving the average state of the air; principally the mean temperature and absolute humidity.
(3) Parameters determining acoustic properties of the ground; for example, the acoustic impedance or normal acoustic impedance of the ground. To some extent the acoustic quantities can be expressed in terms of other physical parameters such as porosity and flow resistance, in the case of porous soils, or such as density and elastic constants for "fluid" or solid soils.
(4) Parameters which describe the variation of sound velocity with height due to wind and temperature gradients. According to present-day micrometeorological formulae (subsections 1.5.2 and 1.5.3) the temperature-height profile can be expressed in terms of two parameters, which may be determined empirically from a few temperature measurements at different heights. These two parameters depend, among other things, on the solar radiation and on the heat capacity, conductivity and reflectivity of the ground. According to other micrometeorological formulae wind-height profiles also depend

mainly on two parameters, the roughness length ℓ for the given terrain, and the wind speed at some reference height. The acoustical effect of wind depends also, of course, on the angle between the wind direction and the source-receiver direction.

(5) Parameters describing "random" inhomogeneities in the atmosphere; correlation coefficients of various kinds are useful for this purpose (see subsection 1.6).

(6) Parameters describing fogs or smokes, if they exist; principally the particle-size distributions.

(7) Parameters describing irregularity of the terrain if such exists; such irregularity may be due to a hilly countryside, to a non-uniform vegetative covering, or to obstacles such as trees or buildings.

If one is to obtain a prediction formula from outdoor experiments alone, it would appear to be necessary to perform a large number of experiments under a great variety of conditions. In each experiment all of the parameters listed above should be determined, as well as the acoustical results. The experiments should be done for a wide variety of conditions, such that each parameter varies over its entire range of interest.

Suppose it were desired to have at least one acoustical measurement for each set of significantly different parameter values likely to be encountered in practice. It is not hard to show that the undertaking would be a prohibitively long and expensive one. Suppose, for example, that only four parameters A, B, C, D were felt to be important and that each were assumed to have only five significantly different ranges of values. (If, for example, parameter A were to stand for average temperature, the assumption might be that the temperature for any given experiments is specified well enough by stating into which of the following five ranges it falls: 0° - 20°; 20° - 40°; 40° - 60°; 60° - 80°; 80° - 100°F.) The total number N of combinations is then $(5)^4$ or 625. If the number of parameters is doubled N becomes $(5)^8$ or about 400,000; if also the number of different ranges of values for each parameter is doubled N becomes 10^8!

A comprehensive approach on a purely empirical basis would seem to be impractical. Several schemes present themselves as alternative approaches to the problem; these will be discussed in succeeding subsections.

4.3.2 Large-scale Out-of-door Experiments

One important method of obtaining results for use in prediction is to make measurements under actual field conditions over a long period

of time. Here one would use an airplane sound source and make continuous recordings of the instantaneous pressure amplitude at various points in the region surrounding the source. Observations would be made with the aircraft on the ground, as well as in the air following typical flight patterns; data would be taken at all times of day, under a representative sampling of weather conditions, at all seasons of the year, and over a period of years. A basic assumption on which the usefulness of this method depends is that the frequency of occurrence of various sets of conditions is the same for the selected site and period of measurements as it is, averaged over a long time period, for other sites of interest. If this is true, the time-averaged acoustical results of the experiment may be applied to the new situation which is felt to be comparable to the one studied.

It is evident that if the time-averages obtained from such an experiment are to be applicable to the wide variety of circumstances encountered in practice, the program of measurements must be much more extensive than any carried out heretofore. For example, Hayhurst's data are only for approximately horizontal propagation over a particular kind of terrain, are only for one source height and are (mainly) for one receiver height. The results of Parkin and Scholes are also for very restricted conditions, being only for nearly vertical propagation from aircraft to ground and for fairly low absolute humidities.

An experiment which is to yield results suitable for general use must include a comprehensive set of measurements where the sound travels obliquely to ground from an aircraft in flight, the source-receiver line QP thus making arbitrary angles with the vertical. Also a wider range of temperatures and humidity conditions should be investigated than are covered by the Parkin and Scholes data. In addition, different source and receiver heights should be used, various terrains should be investigated, etc. (See the list, given earlier in the subsection, of parameters which theory indicates to be important in propagation problems.)

Large scale experiments of the kind just described are very likely the best means of obtaining order-of-magnitude results for immediate and direct application to practical field problems. However, if the measurements are to be extensive enough to give reliable averages under a sufficient variety of conditions it is to be expected that the undertaking will be a large and costly one.

Though the emphasis in such an experiment is on long-time averages, the usefulness of the results would be increased if as many as possible of the important meteorological, micrometeorological and terrain parameters are measured at frequent intervals, and attempts made to correlate these with acoustical results. It is not to be

expected, however, that the effects of various factors could be completely separated from each other since, as indicated above, a very extensive set of measurements would be needed for this purpose. This is particularly true since, in a large scale experiment, the micrometeorological and terrain factors will often not be uniform throughout the region of interest. Also, some of the micrometeorological factors may vary rapidly with time; attempts to detect and measure in detail these short-time variations in large scale experiments would require prohibitively elaborate instrumentation.

4.3.3 Small-scale Out-of-Door Experiments

More detailed information for use in the prediction problem may be gained from out-of-door experiments designed especially to isolate and measure the effects of the various separate factors. Such experiments would probably best be done on a comparatively small scale, where source-receiver distances range up to, say, the order of 1000 ft. It is not difficult to find areas where the terrain is fairly uniform over distances of this magnitude. Also, when the region of interest is thus limited, it is feasible to set up appropriate instrumentation for giving detailed description of the micrometeorological factors.

Results obtained from small-scale investigations cannot usually be directly used in predicting levels at the greater source-receiver distances typically of interest in field problems. Nevertheless these investigations can serve a very useful purpose in determining the relative importance of various factors, in checking the adequacy of theories and in providing suggestive facts on which theories may be based. Specific questions which might usefully be answered by such experiments are:

(1) What is the minimum loss to be expected over ground? Is it ever true that the field in the region a few feet above the ground is given by Eq. (2), where a is given by the theoretical absorption coefficient (Eqs. (11)) (as found by Parkin and Scholes for the case of propagation from aircraft vertically to ground)? Alternatively, is it more nearly true that the minimum loss coefficient is given by the laboratory value for homogeneous air (subsection 1.2 or Figs. 48 and 49, subsection 3.2.3)? Experiments to answer these questions should be done under conditions where shadow effects (subsection 1.5) and terrain effects (subsection 1.4 are absent. They might be carried out over hard or water-soaked ground on a quiet cloudy day or night, or at great source-receiver heights.

(2) Are losses caused by fog or smoke important? Experiments to test this factor should be done under quiet conditions in the absence of terrain and shadow effects. If possible, comparison should be made between losses with the fog or smoke present and losses when the air is free of suspended matter, the temperature and absolute humidity (i.e., water vapor content) being the same in the two cases. So that theoretical predictions can be made to compare with experimental results, the density and particle-size distributions of suspensions should be measured by the best available methods.

(3) To what extent is the idealized theory for the field of a point source above a plane boundary applicable to actual situations out-of-doors? To test this theory accurately experiments should be carried out over uniform terrain under quiet conditions, in the absence of shadow or other refraction effects. Independent measurements should be made to determine the acoustical impedance or normal acoustical impedance of the terrain.

(4a) How accurately can the contour of an acoustic shadow boundary be predicted from micrometeorological data? To answer this question ray plots might be made on the basis of measured wind velocities and temperatures at various heights; calculations would best be compared with measurements made on relatively high frequency sound, say, 10 kc or higher, where shadow boundaries would be relatively sharply defined.

(4b) How accurately can the contour of an acoustic shadow boundary be predicted from micrometeorological empirical formulae? Here predictions based on Fig. (16) might be compared with experimental results obtained by using high frequency sound; the quantity B would have to be determined on the basis of a few temperature and wind measurements, as described in subsection 1.5.

(5a) How important are losses due to scattering by turbulence? Experiments to shed light on this question should be carried out in the absence of terrain or shadow effects; perhaps some of the experimental work should be done with both source and receiver rather high above the ground. (Possibly existing towers could be used for this purpose.) Tests should be made with both directional and non-directional sources. In the case of a highly directional source, comparison may be made with theory (see subsection

1.6). Losses due to scattering by turbulence should increase with wind speed. Detailed micrometeorological measurements, including determination of turbulence parameters, should accompany acoustic measurements.

(5b) How important are gains in sound level caused by scattering? If acoustic energy is conserved in the scattering process energy scattered from strong parts of a sound field should appear in the weak parts; in the case of a directional source, when losses appear along directions corresponding to maxima in a lobe pattern gains should appear along directions corresponding to minima. The extent to which this is true (and, more specifically, the extent to which acoustic energy is conserved) could be checked experimentally.

(6) To what extent can the sound field in a shadow zone be accounted for on the basis of diffraction theory (subsection 1.5) plus theory for scattering by turbulence (subsection 1.6)? Detailed acoustical and micrometeorological measurements would need to be made here.

4.3.4 Model Experiments

Still another way in which it may be possible to gain information about complex out-of-door situations is by means of models. By the latter is meant an arrangement whereby measurements are made on a very small scale, and the results applied directly to large scale situations by use of a simple scaling factor. For example, in aerodynamics and hydrodynamics much design information is obtained about airplanes and ships by tests in which small models are used.

There are also certain situations in acoustics where models may be used, with simple scaling factors. Thus suppose that in a given situation the sound pressure p varies sinusoidally in time with angular frequency ω, and that p is everywhere a solution of the usual acoustic wave equation. The time-independent form of the latter may be written as

$$\frac{\partial^2 p}{\partial x^2} + \frac{\partial^2 p}{\partial y^2} + \frac{\partial^2 p}{\partial z^2} + k^2 p = 0 \qquad (226)$$

where

$$k = \omega / c = 2\pi / \lambda \quad , \qquad (227)$$

the constants c and λ being, as usual, the sound phase velocity and wavelength. If we define new variables x_1, y_1, z_1 such that

$$x_1 = kx$$
$$y_1 = ky \qquad (228)$$
$$z_1 = kz$$

we find that Eq. 226) reduces to

$$\frac{\partial^2 p}{\partial x_1^2} + \frac{\partial^2 p}{\partial y_1^2} + \frac{\partial^2 p}{\partial z_1^2} + p = 0 \quad ; \qquad (229)$$

in these new variables the wave equation is independent of frequency. The pressure p for the given situation is a solution of Eq. (229), and also satisfies certain boundary conditions. The latter may consist of a statement that the normal derivative of p is zero on certain rigid surfaces (such as the earth surface, walls of buildings, artificial walls, etc.) and that p goes to zero at infinity. For any given frequency, say, that for which $k = k_a$ the equation of the rigid surfaces may be expressed in terms of $x_1 = (k_a x)$, etc., in the form

$$\phi\left[(k_a x), (k_a y), (k_a z)\right] = C \quad . \qquad (230)$$

For any other frequency, say, that for which $k = k_b$, the solution $p(x_1, y_1, z_1)$ of Eq. (229) which for $k = k_a$ satisfied boundary conditions on the surfaces described by Eq. (230) will now satisfy boundary conditions on the new surface

$$\phi\left[(k_b x), (k_b y), (k_b z)\right] = C \quad . \qquad (231)$$

The new surfaces, described by Eq. (231) are identical in shape with those described by Eq. (232) but are expanded according to the scaling factor $(k_a/k_b) = (\lambda_b/\lambda_a)$.

The application of this result is that the sound field to be expected on a large scale at low frequencies can (under appropriate circumstances) be determined by experiments on a small model at high frequencies. Specifically, suppose it is desired to know the sound field to be expected around a set of buildings and enclosures due to a source or set of sources at 200 cps. If the walls and ground surface may be assumed rigid, and if refraction effects can be assumed negligible, the desired information can be obtained by investigation of a model. This model might, for example, be scaled 1:100 so that all dimensions are reduced by this factor. The frequency of the source or sources (assumed very small), placed on the model in appropriate positions should then be 20,000 cps; i.e., the wavelength must be reduced by the same factor as other dimensions. The pressure amplitude (and phase, if desired) might then be determined by means of a small

probe microphone.

If the walls or ground are not rigid the boundary condition will, in general, be dependent on frequency in a manner that may be unknown and the above procedure will not be valid. Neither will the method usually be valid if losses in the medium are important, for then Eq. (226) no longer holds in its original form; the constant c must then be regarded as complex and dependent on frequency in a manner that is known only to a limited extent. It is true, however, that in special cases it may be possible to take account of attenuation of the medium by, e.g., adjusting the humidity, so that the absorption per wavelength at the high frequency used in the scaled model will be the same as for the actual low frequency being represented.

In the case of a refracting medium, as always exists out-of-doors, the situation can be represented to some extent by Eq. (226) if the sound velocity c is regarded as a function of space and time. At any given frequency c may, of course, be expressed in terms of the non-dimensional quantities (x_1, y_1, z_1).

The application of this result is that the field in a large scale situation in an inhomogeneous atmosphere at low frequencies can be determined by study of a small model at high frequencies, provided that the space scale of inhomogeneities in the medium is reduced by the same ratio as other geometrical quantities. If, as in the previous example it is desired to represent an out-of-doors situation at 200 cps by a 1:100 model, using 20,000 cps, one must somehow reduce the scale of the atmospherical structure by the same ratio. For example, if shadow zones are to be studied the wind or temperature gradients must be increased by a factor of 100; if scattering by turbulence is to be studied the mean size of "eddies" must be reduced by a factor of 100, etc. Such adjustment of the scale of inhomogeneities can be accomplished to some extent. It is well known, for example, that the scale of turbulence in the air can be varied artificially by passing the air through wire screens. Nevertheless, it is evident that the production of a micro-atmosphere which is a true model of a real out-of-door atmosphere would be a considerable research problem in itself.

BIBLIOGRAPHY

1. J. J. Markham, R. T. Beyer and R. B. Lindsay, Absorption of Sound in Fluids, Revs. Modern Phys. 23, 353 (1951)

2. H. O. Kneser, Interpretation of the Anomalous Sound Absorption in Air and Oxygen in Terms of Molecular Collisions, J. Acoust. Soc. Am. 5, 122 (1933)

3. V. O. Knudsen, The Absorption of Sound in Air, in Oxygen, and in Nitrogen - Effects of Humidity and Temperature, J. Acoust. Soc. Am. 5, 112 (1933)

4. V. O. Knudsen, The Absorption of Sound in Gases, J. Acoust. Soc. Am. 6, 199 (1935)

5. H. Knotzel, Absorption of Audible Sound in Air and Its Dependence on Humidity and Temperature, Akust. Z. 5, 246 (1940)

6. Report entitled, The Attenuation of Sound in the Atmosphere, prepared at the Department of Physics, University of California at Los Angeles, under Air Force Contract W-28-099-AC-228, Feb. 25, 1953. Also see reference 70.

7. H. C. Rothenberg and W. H. Pielemeier, Ultrasonic Absorption in Air, J. Acoust. Soc. Am. 22, 81A (1950). See also report entitled, Atmospheric Physics and Sound Propagation, prepared at the Department of Physics, The Pennsylvania State University, under Signal Corps Contract W36-039-SC-32001, Sept. 1, 1950.

8. J. Sivian, High Frequency Absorption in Air and Other Gases, J. Acoust. Soc. Am. 19, 914 (1947)

9. G. S. Verma, Effects of Humidity on Ultrasonic Absorption in Air at 1.46 Megacycles, J. Acoust. Soc. Am. 22, 861 (1950)

10. W. H. Pielemeier, Observed Classical Sound Absorption in Air, J. Acoust. Soc. Am. 17, 24 (1945)

11. P. S. Epstein and R. R. Carhart, The Absorption of Sound in Suspensions and Emulsions I, Water Fog in Air, J. Acoust. Soc. Am. 25, 553 (1953)

12. K. L. Oswatitsch, The Dispersion and Absorption of Sound in Fog, Phys. Zeit 42, 365 (1941)

13. Y. T. Wei, Absorption of Sound in Foggy Air at Low Audible Frequencies, Ph.D. Thesis, University of California at Los Angeles, June, 1950

14. I. Langmuir, Super-cooled Water Droplets in Rising Current of Cooled Saturated Air, General Electric Company, Schenectady, 1944

15. W. E. Howell, The Growth of Cloud Drops in Uniformly Cooled Air, Ph.D. Thesis, Mass. Institute of Technology, 1948

16. V. O. Knudsen, J. V. Wilson and S. Anderson, The Attenuation of Audible Sound in Fog and Smoke, J. Acoust. Soc. Am. 20, 849

17. I. Rudnick, The Propagation of an Acoustic Wave along a Boundary J. Acoust. Soc. Am. 19, 348 (1947)

18. U. Ingard, On the Reflection of a Spherical Sound Wave from an Infinite Plane, J. Acoust. Soc. Am. 23, 329 (1951)

19. R. B. Lawhead and I. Rudnick, Acoustic Wave Propagation along a Constant Normal Impedance Boundary, J. Acoust. Soc. Am. 23, 546 (1951)

20. G. A. Hufford, An Integral Equation Approach to the Problem of Wave Propagation over an Irregular Surface, Quart. of App. Math, 9, 391 (1951)

21. H. Bremmer, The Extension of Sommerfeld's Formula for the Propagation of Radio Waves over a Flat Earth to Different Conductivities of the Soil, Physica XX, 441, (1954)

22. R. W. Morse, Acoustic Propagation in Granular Media, J. Acoust. Soc. Am. 24, 696 (1952)

23. Cf.: Jahnke and Emde, Tables of Functions (Dover Publications, New York, 1943) p. 23

24. R. B. Lawhead and I. Rudnick, Measurements on an Acoustic Wave Propagated along a Boundary, J. Acoust. Soc. Am., 23, 541 (1951)

25. Physics of Sound in the Sea, N.D.R.C. Summary Technical Reports Division 6, Vol. 8, (Committee on Undersea Warfare, National Research Council)

26. O. G. Sutton, Micrometeorology (McGraw Hill Book Co., Inc. New York, 1953)

27. R. Geiger, The Climate Near the Ground, trans. by M. M. Stewart, et al (Harvard University Press, Cambridge, Mass. 1950)

28. O. G. Sutton, loc. cit., p. 207

29. E. L. Deacon, Vertical Profiles of Mean Wind in the Surface Layers of the Atmosphere, Geophysical Memoirs 91

30. O. G. Sutton, loc. cit., p. 232 ff.

31. E. L. Deacon loc. cit., p. 13 ff.

32. C. L. Pekeris, Theory of Propagation of Sound in a Half Space of Variable Sound Velocity Under Conditions of Formation of a Shadow Zone, J. Acoust. Soc. Am. 18, 295 (1946)

33. D. C. Pridmore-Brown and U. Ingard, Sound Propagation into the Shadow Zone in a Temperature-Stratified Medium above a Plane Boundary, J. Acoust. Soc. Am. 27, 36 (1955)

34. Physics of Sound in the Sea, loc, cit., p. 54

35. N. A. Haskell, Asymptotic Approximation for the Normal Modes in Sound Channel Wave Propagation, J. Appl. Phys. 22, 157 (1951)

36. Cf.: G. K. Batchelor, The Theory of Homogeneous Turbulence (Cambridge University Press, Cambridge, England, 1953) and Sutton, Ref. 10 p. 61 ff.

37. See H. Staras, J. Appl. Phys. 23, 1152 (1952) also D. Mintzer, Wave Propagation in a Randomly Inhomogeneous Medium III, J. Acoust. Soc. Am. 26, 186 (1953)

38. Sutton, Ref. 10, p. 210

39. Sutton, Ref. 10, p. 223

40. Sutton, Ref. 10, p. 251

41. A. C. Best, Transfer of Heat and Momentum in the Lower Layers of the Atmosphere, Geophysical Memoirs No. 65, 40-66 (1935)

42. C. L. Pekeris, Note on the Scattering of Radiation in an Inhomogeneous Medium, Phys. Rev. 71, 268 (1947)

43. T. H. Ellison, The Propagation of Sound Waves through a Medium with Very Small Random Variations in Refractive Index, J. Atm and Terr. Phys. 2, 14, (1951)

44. M. P. Givens, W. L. Nyborg, H. K. Schilling, Theory of the Propagation of Sound in Scattering and Absorbing Media, J. Acoust. Soc. Am. 18, 284, (1946)

45. D. Mintzer, Wave Propagation in a Randomly Inhomogeneous Medium I, J. Acoust. Soc. Am., Sept., 1953

46. D. Mintzer, Wave Propagation in a Randomly Inhomogeneous Medium II, J. Acoust. Soc. Am., Nov., 1953

47. M. J. Sheehy, Transmission of 24 kc Underwater Sound from a Deep Source, J. Acoust. Soc. Am. 22, 24 (1950)

48. L. Liebermann, The Effect of Temperature Inhomogeneities in the Ocean on the Propagation of Sound, J. Acoust. Soc. Am. 23, 563 (1951)

49. D. Mintzer, Wave Propagation in a Randomly Inhomogeneous Medium III, J. Acoust. Soc.,Am. 26, 186 (1953)

50. See Ref. 32, p. 21

51. D. Blokhintzev, The Acoustics of an Inhomogeneous Moving Medium, Trans. by R. T. Beyer and D. Mintzer, Research Analysis Group Report (Aug., 1952) Brown University. Cf. also D. Blokhintzev, J. Acoust. Soc. Am. 18, 322 (1945)

52. M. J. Lighthill, On the Energy Scattered from the Interaction of Turbulence with Sound or Shock Waves, Dept. of Mathematics, University of Manchester, A.R.C. 15, 432-F.M. 1825 (Dec., 1952)

53. R. H. Kraichman, The Scattering of Sound in a Turbulent Medium, J. Acoust. Soc. Am. 25, 1096 (1953)

54. R. W. Wood, Physical Optics,(The Macmillan Company, New York, 1934)

55. R. C. Fehr, The Reduction of Industrial Machine Noise, Proceedings of the Second Annual National Noise Abatement Symposium, Chicago, October 5, 1951, p. 93

56. Rayleigh, Theory of Sound (Dover Publications, New York, 1945), Par. 253 and Par. 352

57. H. Lamb, Dynamical Theory of Sound (Dover Publications, New York, 1945), Chap. 1

58. E. Fubini-Ghiron, Anomalous Propagation of High Amplitude Acoustic Waves, Alta. Freq. 4, 530 (1935)

59. A. L. Thuras, R. T. Jenkins and H. T. O'Neil, Extraneous Frequencies Generated in Air Carrying Intense Sound Waves, J. Acoust. Soc. Am. 6, 173 (1935)

60. R. D. Fay, Plane Waves of Finite Amplitude, J. Acoust. Soc. Am. 3, 222 (1931)

61. I. Rudnick, On the Attenuation of a Repeated Sawtooth Shock Wave, J. Acoust. Soc. Am. 25, 1012 (1953)

62. C. H. Allen, Sound Waves of "Stable" Form, J. Acoust. Soc. Am. 23, 630A (1951). See also report entitled, Atmospheric Physics and Sound Propagation, prepared at the Department of Physics, The Pennsylvania State University, under Signal Corps Contract W36-039-SC-32001, Sept. 1, 1950.

63. John M. Richardson and William B. Kennedy, Atmospheric Winds and Temperatures to 50-Kilometers Altitude as Determined by Acoustical Propagation Studies, J. Acoust. Soc. Am. 24, 731 (1952)

64. C. T. Johnson and F. E. Hale, Abnormal Sound Propagation Over the Southwestern United States, J. Acoust. Soc. Am. 25, 642 (1953)

65. Louis V. King, On the Propagation of Sound in the Free Atmosphere and the Acoustic Efficiency of Fog-Signal Machinery: An Account of Experiments Carried Out at Father Point, Quebec, September, 1913, Philosophical Transactions of the Royal Society A, 218, 211-293 (1919)

66. Uno Ingard, Review of the Influence of Meteorological Conditions on Sound Propagation, J. Acoust. Soc. Am. 25, 405 (1953)

67. H. Sieg, On the Propagation of Sound in Open Air and its Dependence on Weather Conditions, Elektrische Nachrichten Technik, Heft 9, Band 17, p. 193 (Sept., 1940)

68. Schilling, Givens, Nyborg, Pielemeier and Thorpe, Ultrasonic Propagation in Open Air, J. Acoust. Soc. Am. 19, 222 (1947)

69. C. F. Eyring, Jungle Acoustics, J. Acoust. Soc. Am. 18, 257 (1946)

70. L. P. Delsasso and R. W. Leonard, Field Measurements of the Attenuation of Sound in the Low Audio Range, J. Acoust. Soc. Am. 25, 835A (1953). See also Ref. 6.

71. J. Horiuchi, Scattering of Sound by Isotropic Turbulence, J. Acoust. Soc. Am. 26, 946A (1954)

72. A. A. Regier, Effect of Distance on Airplane Noise, N.A.C.A. Technical Note No. 1353, June, 1947

73. P. H. Parkin and W. E. Scholes, Air-to-Ground Sound Propagation, J. Acoust. Soc. Am. 26, 1021 (1954)

74. J. D. Hayhurst, The Attenuation of Sound Propagated Over the Ground, Acustica 3, 227 (1953)

75. U. Ingard, The Physics of Outdoor Sound, Proceedings of the Fourth Annual National Noise Abatement Symposium, Chicago, October 23, 1953.

76. K. N. Stevens and R. H. Bolt, On the Shielding of Noise Outdoors, J. Acoust. Soc. Am. 26, 938A (1954)

77. J. D. Hayhurst, Acoustic Screening by an Experimental Running-up Pen, J. Roy. Aero Soc. 57, 3 (1953)

78. Ultrasonic Signaling, O.S.R.D. Technical Report No. 5012, March 31, 1945

79. W. L. Nyborg, I. Rudnick and H. K. Schilling, Experiments on Acoustic Absorption in Sand and Soil, J. Acoust. Soc. Am. 22, 422 (1950)

80. Ferrero and Sacerdote, Acustica 1, 135 (1951)

81. C. A. Heiland, Geophysical Exploration (Prentice-Hall, Inc., New York, 1940), p. 484

82. C. A. Heiland, loc. cit., p. 489 ff.

83. C. A. Heiland, loc. cit.. Chap. 12

84. R. F. Brown, R. K. Cook and L. B. Tuckerman, National Bureau of Standard Report No. 3694, Propagation of Sound Waves Through the Ground, Ordnance Project No. TB 2-001 (Oct. 1, 1954)

85. Rayleigh, Theory of Sound (Dover Publications, Inc., New York, 1945), Par. 278, 280

86. Rayleigh, loc. cit., Par. 302. See also L. E. Kinsler and A. R. Frey, Fundamentals of Acoustics (John Wiley and Sons, Inc., New York, 1950), Chap. 7

87. H. O. Kneser, A Nomogram for Determining the Sound Absorption Coefficient in Air, Akust. Zeits 5, 256 (1940)

88. W. H. Pielemeier, Kneser's Sound Absorption Nomogram and Other Charts, J. Acoust. Soc. Am. 16, 273 (1945)

89. Peter A. Franken, The Field of a Random Noise Source above an Infinite Plane, Technical Report, N.A.C.A. Contract NAw-6405, Acoustics Laboratory, Mass. Institute of Technology

90. H. G. Houghton, On the Physics of Clouds and Precipitation, from Compendium of Meteorology, American Meteorological Society, Boston, Mass., 1951, p. 165.

91. P. Baron, Propagation of Sound through the Atmosphere and the Audibility of Warning Signals in the Ambient Noise, Annales des Telecommunications, 9, 258 (Oct., 1954)

92. U. Ingard, Field Studies of Sound Propagation Over Ground, Technical Report, N.A.C.A. Contract NAw-6341, Acoustics Laboratory, Mass. Institute of Technology, Oct. 29, 1954

APPENDIX I

VALUES OF PHYSICAL CONSTANTS

Table 24

Temperature Dependence of Various Constants

T_c	$\eta \times 10^6$	$K \times 10^5$	D_{o-n}	$\rho \times 10^3$	$c \times 10^{-4}$	c_p	γ
-150	83.0	2.58	0.045	2.88	2.20	.246	1.42
-100	114.2	3.59	0.082	2.043	2.62	.241	1.41
- 50	143.0	4.49	0.127	1.588	2.98	.241	1.41
0	170.9	5.53	0.181	1.289	3.31	.240	1.40
20	180.8	5.64	0.206	1.205	3.42	.240	1.40
40	190.4	5.94	0.231	1.130	3.55	.240	1.40
60	199.7	6.25	0.256	1.061	3.65	.240	1.40
100	217.5	6.81	0.314	0.948	3.87	.240	1.40

T_c: temperature in degrees Centigrade

η: viscosity coefficient: poise

K: coefficient of heat conductivity: cal cm^{-1} $sec^{-1}(^oC)^{-1}$

D_{o-n}: oxygen-nitrogen diffusion coefficient: cm^2 sec^{-1}

ρ: density of air at standard pressure: gm cm^{-3}

c: velocity of sound in air: cm sec^{-1}

c_p: specific heat of air at constant pressure: cal $gm^{-1}(^oC)^{-1}$

γ: ratio of specific heats for air

Values of the parameters in Table 24 are either from the International Critical Tables or from the following empirical formulae:

$$\eta = \frac{0.0759}{(T+120)} \cdot \left(\frac{T}{296}\right)^{3/2}$$

$$K = \frac{0.0212}{(T+125)} \cdot \left(\frac{T}{273}\right)^{3/2}$$

$$D_{o-n} = \frac{0.181}{p} \left(\frac{T}{273}\right)^{7/4}$$

$$c = (33{,}060) \cdot \sqrt{1 + 0.00371\, t}$$

$$\rho = \frac{0.001293}{1+0.00367\, t}\, p$$

In the above equations T is the absolute temperature (^{o}K), p is the pressure in atmosphere and t is the Centigrade temperature.

APPENDIX II

Formula and Graph for Converting Units of Humidity

Several methods are in common use for specifying the moisture content of air. Perhaps the most common is to give the relative humidity, i.e., the percentage ratio of the actual moisture content in air at given conditions to that which would exist at the same temperature if the air were saturated.

A second index of water content is the absolute humidity, giving the mass of water contained in unit volume of moist air. This index will be here designated as h_1 and will be assumed to be in units of grams per cubic meter.

Still another index used in the literature is the water-air molecular ratio, or the ratio of the number of water molecules to the number of air molecules contained in any given volume. The latter ratio, designated as h_2, is related to h_1 by the following approximate relation:

$$h_2 = (h_1/\rho_o)(M_a/M_w) , \qquad (232)$$

where ρ_o is the density of dry air, M_a is the mean molecular weight of air, and M_w is the molecular weight of water vapor. In using Eq. (232) M_a may be assumed to be 29.0, M_w to be 18.0 and ρ_o to be given for the temperature in question by Table 24.

Fig. 51 is a chart for converting units of humidity. The upper part of this graph shows plots of relative humidity versus absolute humidity h_1 at various temperatures. The lower part gives a nomogram for determining h_2 for a given h_1 and a stated temperature. Using the two plots jointly allows one to determine h_2 for any given relative humidity and temperature, as illustrated by the line ABCD for the specific conditions of 25% relative humidity and 37°F.

The procedure for determining h_2 for arbitrary relative humidity and temperature is as follows:

(1) Determine B from the given relative humidity and temperature.
(2) Drop a vertical downward from B; determine its intersection C with an (interpolated) horizontal line for the given temperature.
(3) Draw a line inclined at 45° with respect to the horizontal, i.e., parallel to the guide lines, from C to the heavy horizontal line (corresponding to 100°F) which gives the

scale of h_2. The intersection D gives the desired value of the molecular ratio. (The role of the line CD is to correct for the effect of the temperature dependence of ρ_o in Eq. (232); if the temperature is 100°F there is no correction.)

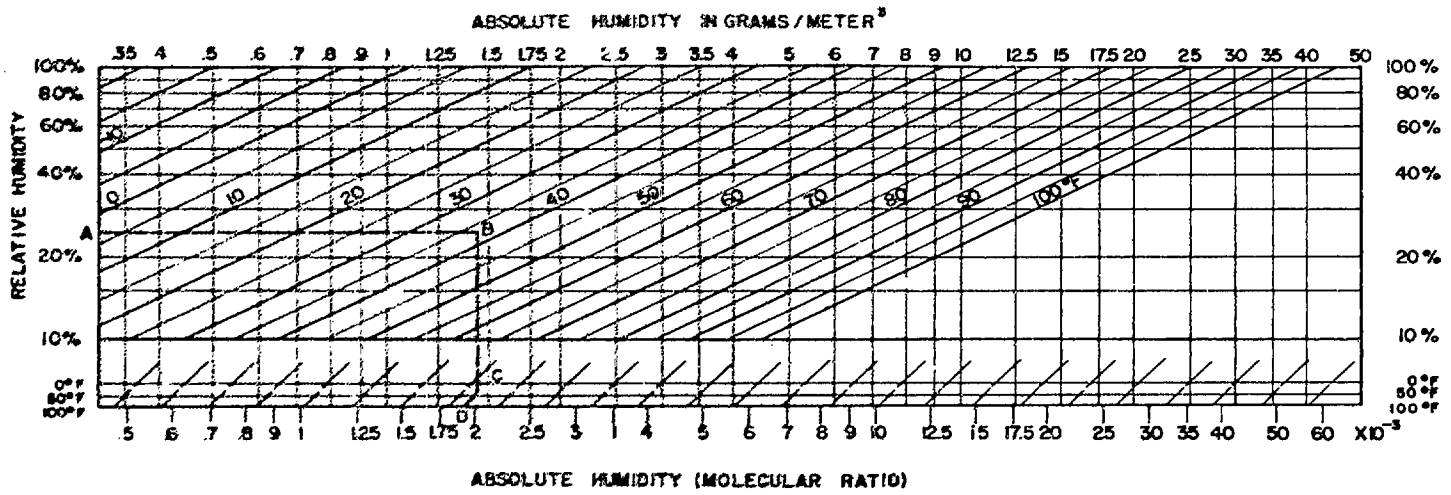

Fig. 51 Chart for converting units of humidity.

APPENDIX III

Computed Absorption Coefficients at Various Geographical Locations

According to the results of Parkin and Scholes (subsection 2.3.2) the loss coefficient for propagation from aircraft to ground (along a nearly vertical path) is given fairly well by the theoretical absorption coefficient

$$\alpha_{theo} = \alpha_{mol} + \alpha_{class} ,$$

given by Eqs. (11), etc. As explained in subsection 1.2 the quantity α_{theo} is dependent, under ordinary atmospheric conditions, mainly on the mean temperature and absolute humidity. This suggests that typical loss coefficients for different geographical regions, for the case of nearly vertical propagation, might be estimated on the basis of mean weather data for the respective regions. Such data are readily available; the temperature and humidity are among the quantities measured continuously at over 300 weather stations distributed throughout the United States. Detailed records and analyses may be obtained from the U. S. Weather Bureau.

Table 26 is representative of the results one obtains by using average meteorological data from various stations and calculating from these the corresponding average loss coefficients α_{theo}. For purposes of this table 81 stations were selected; these are listed in Table 25 along with code numbers for location on the U. S. map, Fig. 52, and for reference in Table 26.

In Table 25 the temperature (Temp) and humidity (RH) data are averages for the entire year and averages for the special months of January and July; these averages are based on records extending over a period of 40 years or more. On the basis of these average meteorological data loss coefficients α_{theo} were calculated (by use of the nomograms in Figs. 42 - 45) and are given in Table 26 for 0.5, 1.0, 2.0 and 4.0 kc. Values less than 0.1 db/1000 ft are not recorded.

The main general tendency to be noted in the results tabulated is due to the dependence of α_{mol} on absolute humidity; because of this dependence the attenuation tends to be high in cold weather (i.e., when the absolute humidity is low) and low in warm weather.

In using the representative data in Table 26 the results of Sections I and II should be carefully kept in mind. Thus the main conditions under which α_{theo} has been shown to give approximately correct results are those of the Parkin and Scholes experiments; in these the absolute humidities were fairly low. At the higher absolute

humidities one may expect the actual loss coefficients to be in excess of α_{theo} (see subsection 1.2).

In general, the values α_{theo} given in Table 26 should be regarded as lower limits to the loss coefficients to be expected in practice. Hence if the values of α_{theo} given there are used to estimate the sound level at the ground due to an overhead aircraft, these calculated sound levels will usually be upper limits to the actually realized sound levels.

Upper limits to the loss coefficients for the case of nearly vertical sound propagation would probably be given by

$$(\alpha_{theo})_{max} = \alpha_{class} + \alpha_{max} \simeq \alpha_{max}$$

where α_{max} is given by Eq. (21b) and by Figs. (3) and (41). At 68°F the values of α_{max} for 0.5, 1.0, 2.0 and 4.0 kc are, respectively, about 2.6, 5.2, 10.4 and 20.8 db/1000 ft.

In the case of sound propagation along a horizontal path all available evidence, as discussed in Section II and Appendix IV, indicates greater loss coefficients than are given by α_{theo}; this is especially true when source and receiver are near the ground, but also appears to be true at rather high altitudes (as in the case of the experiments of Delsasso and Leonard, subsection 2.2.4).

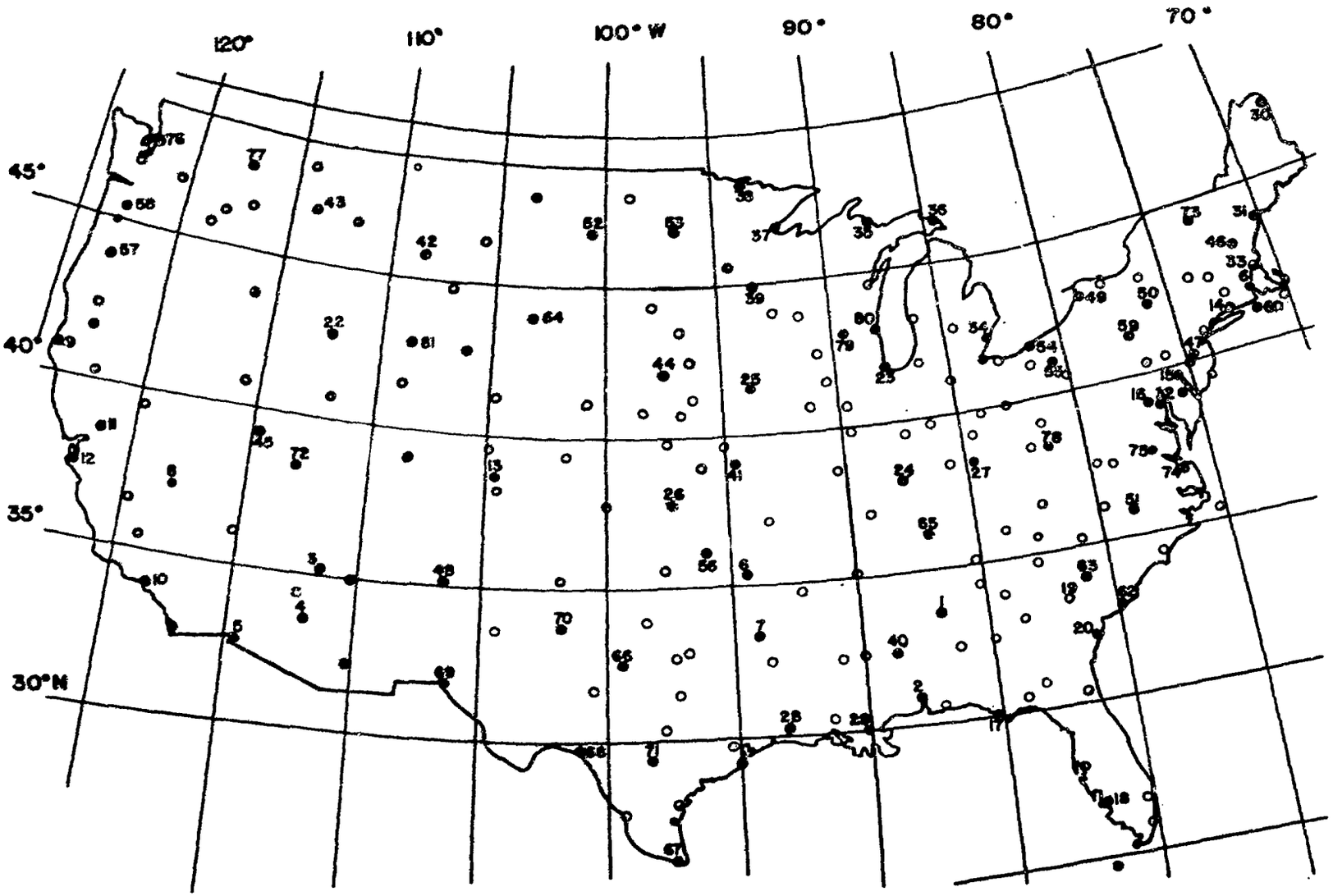

Fig. 52 Map of United States showing weather stations

Table 25

Code Numbers for Various Weather Stations

Code	State	City	Code	State	City
1	Alabama	Birmingham	28	Louisiana	Lake Charles
2		Mobile	29		New Orleans
3	Arizona	Flagstaff	30	Maine	Caribou
4		Phoenix	31		Portland
5		Yuma			
6	Arkansas	Fort Smith	32	Maryland	Baltimore
7		Texarkana			
8	California	Bishop	33	Massachusetts	Boston
9		Eureka			
10		Los Angeles			
11		Sacramento			
12		San Francisco			
13	Colorado	Colorado Springs	34	Michigan	Detroit
			35		Marquette
14	Connecticut	New Haven	36		Sault St. Marie
15	Delaware	Wilmington	37	Minnesota	Duluth
			38		International Falls
16	D. of C.	Washington	39		Minneapolis
17	Florida	Apalachiola	40	Mississippi	Meridian
18		Fort Myers			
19	Georgia	Augusta	41	Missouri	Kansas City
20		Savannah			
21	Idaho	Boise	42	Montana	Billings
22		Pocatello	43		Missoula
23	Illinois	Chicago	44	Nebraska	Norfolk
24	Indiana	Evansville	45	Nevada	Ely
25	Iowa	Des Moines	46	New Hampshire	Concord
26	Kansas	Wichita	47	New Jersey	Trenton
27	Kentucky	Lexington	48	New Mexico	Albequerque

Table 25
(continued)

Code	State	City	Code	State	City
49	New York	Buffalo	66	Texas	Abilene
50		Binghampton	67		Brownsville
			68		Del Rio
51	N. Carolina	Raleigh	69		El Paso
			70		Lubbock
52	N. Dakota	Bismark	71		San Antonio
53		Fargo			
54	Ohio	Cleveland	72	Utah	Milford
55		Youngstown			
56	Oklahoma	Tulsa	73	Vermont	Burlington
57	Oregon	Eugene	74	Virginia	Norfolk
58		Portland	75		Richmond
59	Pennsylvania	Williamsport	76	Washington	Seattle
			77		Spokane
60	Rhode Island	Block Island			
61		Providence			
62	S. Carolina	Charlestown	78	W. Virginia	Charlestown
63		Columbia			
64	S. Dakota	Rapid City	79	Wisconsin	Madison
			80		Milwaukee
65	Tennessee	Nashville	81	Wyoming	Lander

Table 26

Absorption Coefficients Computed from Weather Data at Various Stations

Code	Period	Temp (°F)	RH (%)	α in db/1000 ft 0.5 kc	1 kc	2 kc	4 kc
1	Jan.	49.3	70.0		0.4	1.6	6.2
	July	79.7	72.0		0.1	0.4	1.6
	Avg.	62.5	70.0		0.1	0.8	3.1
2	Jan.	54.5	79.2		0.2	1.0	3.8
	July	81.2	79.5		0.1	0.3	1.4
	Avg.	67.3	76.5		0.1	0.5	2.2
3	Jan.	35.1	60.0	0.3	1.1	4.6	17.1
	July	66.4	60.0		0.2	0.8	3.4
	Avg.	44.6	51.5	0.2	0.9	3.7	13.6
4	Jan.	54.5	56.7		0.4	1.7	6.9
	July	90.8	43.5		0.1	0.5	2.2
	Avg.	75.1	41.75		0.2	1.0	4.1
5	Jan.	61.5	36.7	0.2	0.7	2.6	11.1
	July	95.2	34.7		0.2	0.6	2.2
	Avg.	74.7	38.5		0.3	1.3	4.5
6	Jan.	42.9	73.7	0.1	0.5	2.2	8.5
	July	81.1	71.7		0.1	0.4	1.5
	Avg.	62.0	67.25		0.2	0.9	3.4
7	Jan.	49.3	73.2		0.4	1.4	5.6
	July	81.3	76.5		0.1	0.4	1.5
	Avg.	65.1	68.0		0.2	0.7	3.0
8	Jan.	43.5	37.5	0.4	2.6	8.6	22.6
	July	79.6	17.0	0.3	1.0	4.2	16.6
	Avg.	56.0	24.5	0.4	1.9	7.5	24.6
9	Jan.	51.0	82.0		0.3	1.0	4.1
	July	55.1	85.0		0.2	0.8	3.3
	Avg.	60.9	72.0		0.2	0.9	3.7
10	Jan.	58.8	66.0		0.2	1.0	4.1
	July	70.4	73.2		0.1	0.5	2.4
	Avg.	60.9	72.0		0.2	0.8	3.1

Table 26
(continued)

Code	Period	Temp (°F)	RH (%)	α in db/1000 ft 0.5 kc	1 kc	2 kc	4 kc
11	Jan.	51.8	86.5		0.2	1.0	3.7
	July	78.2	48.2		0.2	0.7	2.9
	Avg.	60.9	65.75		0.2	0.9	3.6
12	Jan.	53.1	84.7		0.2	0.9	3.4
	July	60.1	76.5		0.2	0.8	3.2
	Avg.	55.6	77.5		0.2	0.9	3.5
13	Jan.	37.6	40.5	0.4	1.5	6.7	20.6
	July	71.8	49.5		0.2	0.9	3.5
	Avg.	49.1	48.5	0.2	0.7	3.1	11.6
14	Jan.	34.2	76.0	0.2	0.8	3.1	12.6
	July	72.1	66.5		1.0	4.0	2.2
	Avg.	49.7	69.0		0.4	1.5	6.1
15	Jan.	37.6	77.7	0.1	0.6	2.5	9.6
	July	77.0	66.2		0.1	0.4	1.9
	Avg.	54.2	71.75		0.3	1.1	4.3
16	Jan.	40.7	71.7	0.1	0.6	2.5	9.9
	July	79.6	61.2		0.1	0.5	1.9
	Avg.	56.5	66.25		0.3	1.1	4.6
17	Jan.	55.9	81.0		0.2	0.9	3.4
	July	81.8	79.5		0.1	0.3	1.3
	Avg.	68.8	78.75		0.1	0.5	2.0
18	Jan.	63.6	78.7		0.2	0.6	2.5
	July	82.4	81.5			0.3	1.3
	Avg.	73.9	78.75		0.1	0.4	1.7
19	Jan.	50.0	75.2		0.3	1.3	5.4
	July	81.5	73.0			0.4	1.4
	Avg.	65.4	69.5		0.2	0.7	2.9
20	Jan.	53.4	73.5		0.3	1.1	4.4
	July	80.9	78.2			0.3	1.3
	Avg.	66.8	74.5		0.2	0.6	2.3
21	Jan.	41.0	74.2	0.1	0.5	2.2	8.6
	July	74.1	35.7		0.3	1.4	5.6
	Avg.	50.8	59.25	0.1	0.5	0.9	7.4

Table 26
(continued)

Code	Period	Temp (°F)	RH (%)	α in db/1000 ft 0.5 kc	1 kc	2 kc	4 kc
22	Jan.	36.2	75.5	0.2	0.6	2.8	10.6
	July	73.4	31.2	0.1	0.5	2.0	7.7
	Avg.	47.2	57.75	0.2	0.6	2.4	9.6
23	Jan.	29.2	78.7	0.2	1.1	4.0	15.6
	July	76.4	63.0			0.5	2.1
	Avg.	50.1	70.75		0.4	1.4	5.8
24	Jan.	37.9	80.5	0.1	0.5	2.2	8.6
	July	79.9	66.0			0.4	1.8
	Avg.	56.9	70.0		0.3	1.0	4.0
25	Jan.	24.1	86.2	0.3	1.2	5.2	17.6
	July	76.3	69.5			0.4	1.8
	Avg.	50.2	70.75		0.3	1.4	5.7
26	Jan.	37.4	72.2	0.2	0.7	2.8	11.2
	July	78.7	65.0			0.4	1.8
	Avg.	57.0	65.5		0.3	1.1	4.5
27	Jan.	39.7	79.2	0.1	0.5	2.1	8.6
	July	77.3	68.7			0.4	1.8
	Avg.	54.4	71.75		0.3	1.1	4.4
28	Jan.	55.9	75.7		0.2	1.0	3.9
	July	82.0	81.5			0.3	1.3
	Avg.	68.3	78.5		0.1	0.5	2.1
29	Jan.	58.3	74.5		0.2	0.9	3.3
	July	83.3	75.0			0.3	8.0
	Avg.	70.4	74.75		0.1	0.5	2.1
30	Jan.	15.8	74.5	0.7	2.5	9.0	18.1
	July	64.1	72.7		0.2	0.7	2.8
	Avg.	37.2	74.0	0.2	0.6	2.6	10.1
31	Jan.	28.5	79.5	0.3	1.1	4.3	14.6
	July	67.8	73.0		0.1	0.6	2.3
	Avg.	44.5	74.5	0.1	0.4	1.8	7.5
32	Jan.	41.7	73.7	0.1	0.5	2.2	8.6
	July	78.7	63.2			0.5	1.8
	Avg.	57.1	64.66		0.3	1.1	4.4

Table 26.
(continued)

Code	Period	Temp (°F)	RH (%)	α in db/1000 ft 0.5 kc	1 kc	2 kc	4 kc
33	Jan.	34.7	69.0	0.2	0.8	3.8	13.6
	July	73.2	66.0			0.5	2.2
	Avg.	50.7	65.75		0.4	1.5	6.1
34	Jan.	29.6	82.2	0.2	0.9	3.5	13.6
	July	74.0	62.7			0.6	2.2
	Avg.	49.3	70.25		0.4	1.6	6.1
35	Jan.	22.2	75.3	0.5	1.8	7.1	20.6
	July	67.0	64.3		0.2	0.7	3.0
	Avg.	42.2	73.0	0.1	0.5	2.1	8.1
36	Jan.	18.9	81.0	0.5	2.0	7.2	19.6
	July	63.8	79.7		0.1	0.6	2.4
	Avg.	39.3	77.25	0.1	0.6	2.3	9.4
37	Jan.	12.5	77.5	0.9	3.4	9.3	17.6
	July	64.2	75.2		0.2	0.7	2.7
	Avg.	39.2	75.75	0.1	0.5	2.4	9.4
38	Jan.	4.2	76.2	1.6	4.2	7.0	8.6
	July	64.5	71.7		0.2	0.7	2.8
	Avg.	36.3	73.25	0.2	0.7	2.8	9.6
39	Jan.	16.7	80.0	0.6	2.4	9.0	19.6
	July	72.5	68.0		0.1	0.5	2.2
	Avg.	45.6	68.5		0.5	1.9	8.3
40	Jan.	51.6	75.2		0.3	1.2	4.7
	July	80.8	76.7			0.4	1.4
	Avg.	64.5	73.5		0.2	0.7	2.8
41	Jan.	34.5	74.2	0.2	0.7	3.0	12.3
	July	81.2	57.5			0.5	1.9
	Avg.	56.1	65.75		0.3	1.1	4.4
42	Jan.	36.2	51.0	0.3	1.3	5.5	18.6
	July	74.3	39.5		0.3	1.2	4.7
	Avg.	47.2	58.0	0.1	0.6	2.5	9.6
43	Jan.	35.8	79.2	0.1	0.6	2.6	10.1
	July	67.8	39.0		0.4	1.6	6.5
	Avg.	44.1	66.25	0.1	0.6	2.3	9.0

Table 26
(continued)

Code	Period	Temp (°F)	RH (%)	α in db/1000 ft 0.5 kc	1 kc	2 kc	4 kc
44	Jan.	21.9	79.0	0.4	1.7	7.0	19.6
	July	76.3	60.6			0.5	2.1
	Avg.	48.3	67.0		0.4	1.8	6.9
45	Jan.	33.5	67.7	0.2	1.0	4.1	14.6
	July	69.1	37.7		0.4	1.8	6.8
	Avg.	45.2	46.0	0.3	1.1	4.4	16.6
46	Jan.	27.6	75.5	0.3	1.3	5.1	17.6
	July	69.8	68.2		0.2	0.6	2.4
	Avg.	44.8	71.0	0.1	0.5	1.9	7.4
47	Jan.	37.4	71.3	0.2	0.7	2.9	11.6
	July	76.2	66.6			0.5	1.9
	Avg.	53.5	56.33		0.3	1.4	5.4
48	Jan.	42.2	45.7	0.3	1.3	5.3	18.6
	July	80.0	43.0		0.2	0.8	3.2
	Avg.	56.6	45.0	0.1	0.5	2.4	8.9
49	Jan.	31.3	80.7	0.2	0.8	3.2	12.6
	July	71.6	67.0		0.1	0.6	2.2
	Avg.	47.5	73.0		0.4	1.6	5.9
50	Jan.	33.5	80.0	0.2	0.7	2.9	11.6
	July	71.4	67.7		0.1	0.6	2.3
	Avg.	48.4	75.25		0.3	1.4	5.5
51	Jan.	47.9	73.5		0.3	1.5	5.9
	July	80.2	67.5			0.4	1.7
	Avg.	61.1	71.5		0.2	0.8	3.2
52	Jan.	15.8	80.5	0.7	2.5	8.7	18.6
	July	69.9	65.7		0.2	0.7	2.6
	Avg.	41.7	67.75	0.1	0.6	2.7	10.0
53	Jan.	10.4	76.2	1.1	3.7	9.5	13.6
	July	69.9	68.5		0.2	0.6	2.4
	Avg.	40.9	71.75	0.1	0.6	5.3	9.9
54	Jan.	33.6	83.0	0.2	0.7	2.8	10.5
	July	74.4	63.5			0.5	2.2
	Avg.	50.6	71.25		0.3	1.5	5.7

Table 26
(continued)

Code	Period	Temp (°F)	RH (%)	α in db/1000 ft 0.5 kc	1 kc	2 kc	4 kc
55	Jan.	32.8	80.2	0.2	0.7	3.2	12.1
	July	70.9	68.0		0.2	0.6	2.3
	Avg.	49.8	74.0		0.3	1.3	5.5
56	Jan.	41.2	70.5	0.1	0.6	2.4	9.5
	July	80.4	70.5			0.4	1.6
	Avg.	60.6	67.5		0.2	1.0	4.0
57	Jan.	46.9	86.2		0.3	1.3	4.8
	July	65.2	63.7		0.2	0.8	3.4
	Avg.	52.4	77.5		0.3	1.0	4.1
58	Jan.	48.5	86.7		0.3	1.1	4.5
	July	68.0	66.7		0.2	0.6	2.7
	Avg.	54.6	75.25		0.2	1.0	4.1
59	Jan.	33.6	74.5	0.2	0.8	3.2	12.6
	July	73.9	66.0			0.5	2.1
	Avg.	50.7	72.50		0.3	1.4	5.5
60	Jan.	36.5	79.0	0.1	0.6	2.6	10.1
	July	69.5	77.0			0.5	2.0
	Avg.	49.9	80.75		0.3	1.2	4.7
61	Jan.	35.7	72.5	0.2	0.7	3.3	12.6
	July	71.2	71.0			0.5	2.1
	Avg.	49.4	70.5		0.4	1.6	6.0
62	Jan.	53.6	71.7		0.3	1.2	4.8
	July	81.1	81.0			0.3	1.3
	Avg.	66.6	77.0		0.1	0.6	2.2
63	Jan.	51.3	74.5		0.3	1.3	4.6
	July	82.3	69.7			0.4	1.5
	Avg.	64.4	65.0		0.2	0.8	3.2
64	Jan.	31.3	70.7	0.3	1.1	4.3	13.6
	July	72.5	61.5		0.2	0.6	2.4
	Avg.	46.1	60.5	0.1	0.6	2.3	8.8
65	Jan.	45.2	77.0		0.4	1.7	6.7
	July	79.7	73.0			0.4	1.6
	Avg.	60.1	69.5		0.2	0.9	3.7

Table 26
(continued)

Code	Period	Temp (°F)	RH (%)	α in db/1000 ft 0.5 kc	1 kc	2 kc	4 kc
66	Jan.	51.9	43.2	0.2	0.7	2.9	12.6
	July	84.0	57.0			0.4	1.8
	Avg.	64.1	58.75		0.3	1.0	3.9
67	Jan.	64.5	67.7		0.2	0.8	3.1
	July	85.8	72.2			0.3	1.3
	Avg.	73.6	77.25		0.1	0.4	1.7
68	Jan.	56.4	46.7	0.1	0.5	2.3	9.0
	July	89.7	46.7			0.5	2.1
	Avg.	69.8	61.0		0.2	0.7	2.8
69	Jan.	50.3	32.5	0.4	1.4	6.2	18.6
	July	83.5	43.0		0.2	0.7	2.8
	Avg.	66.0	39.5		0.4	1.9	7.1
70	Jan.	46.6	46.2	0.2	1.0	4.1	16.6
	July	80.6	55.0			0.5	2.1
	Avg.	59.5	56.25		0.3	1.4	5.6
71	Jan.	55.9	56.5		0.4	1.6	6.2
	July	86.1	61.2			0.4	1.6
	Avg.	66.2	67.75		0.2	0.7	2.8
72	Jan.	37.6	63.3	0.2	0.8	3.4	13.1
	July	76.6	43.0		0.2	0.8	3.1
	Avg.	49.0	52.0	0.2	0.6	2.6	3.4
73	Jan.	24.7	75.0	0.4	1.5	6.2	19.6
	July	71.2	63.5		0.2	0.6	2.4
	Avg.	44.5	73.75	0.1	0.4	1.9	7.4
74	Jan.	46.1	75.0		0.4	1.5	6.5
	July	79.7	72.7			2.4	1.5
	Avg.	59.2	72.5		0.2	0.8	3.3
75	Jan.	42.9	74.2	0.1	0.5	2.0	7.7
	July	79.9	66.0			0.4	1.7
	Avg.	57.7	71.25		0.2	0.9	3.5
76	Jan.	47.2	84.0		0.3	1.3	4.9
	July	65.4	72.7		0.2	0.7	2.6
	Avg.	53.2	75.25		0.3	1.1	4.2

Table 26
(continued)

Code	Period	Temp (°F)	RH (%)	α in db/1000 ft 0.5 kc	1 kc	2 kc	4 kc
77	Jan.	37.9	84.2	0.1	0.5	1.9	7.7
	July	69.3	40.2		0.4	1.5	5.9
	Avg.	47.1	63.75	0.1	0.5	2.0	7.8
78	Jan.	42.0	73.7	0.1	0.5	2.1	8.3
	July	76.5	72.7			0.4	1.7
	Avg.	55.8	70.25		0.3	1.0	4.0
79	Jan.	23.5	77.7	0.4	1.4	5.8	18.6
	July	72.4	67.2		0.1	0.6	2.2
	Avg.	46.9	72.0		0.4	1.6	6.2
80	Jan.	27.0	77.7	0.3	1.1	4.7	16.6
	July	72.6	67.5		0.1	0.5	2.1
	Avg.	47.7	72.25		0.4	1.6	6.1
81	Jan.	31.8	58.0	0.4	1.4	5.8	18.6
	July	73.5	35.7		0.4	1.6	5.8
	Avg.	43.2	56.25	0.2	0.8	3.2	12.6

APPENDIX IV

RECENT CONTRIBUTIONS

In this appendix we review very briefly work which has come to our attention too recently to be incorporated into the body of this report.

P. Baron (1938 - 1954)[91]

In this paper (1954) the author describes results of sound propagation studies carried out in 1938-9, but for which the findings were hitherto not available in published form. The purpose of these studies was to determine optimum installation conditions for a warning siren. An extensive set of measurements was made on sound levels at different distances up to 4500 meters (nearly 3 miles) from a siren mounted aloft, usually on a tower at a height of 35 m (115 ft); in nearly all cases the frequency was 390 cps; the receiver height was 1.5 m (about 5 ft). Data were taken under a variety of weather conditions at two different sites, and, for each site, at points distributed throughout an area surrounding the source; a total of about 6000 observations were made in all.

On the basis of these measurements a curve was plotted of average sound level vs distance R from the source. (Under conditions to which these results apply, the wind direction is perpendicular to the direction of sound propagation.) In addition to a (1/R) loss the results indicate an additional loss L. The latter, measured in decibels, varies linearly with R for distances ranging from 100 to 2000 m, the loss coefficient (see subsection 1.1) being about 7 db/1000 meters or 2.1 db/1000 ft in this region. At greater distances the effective loss coefficient is less; at 4000 m the loss L is only 22 db, so that the average loss coefficient over the path from 100 to 4000 m is about 5.5 db/1000 m or 1.7 db/1000 ft.

The author explains the decrease of the effective loss coefficient with distance in the 2000-4000 m range as due to the tendency for sound to propagate to short distances by paths near the ground, and to long distances along paths higher in the atmosphere; in the case of Baron's experiments this tendency is accentuated by the topography of the land which begins to slope upward at about a distance of 3000 m from the source. Further evidence that more loss is encountered in propagation along the ground than at higher altitudes is given by experiments in which height of the receiver is varied. When this is done the received sound level is always found to increase with receiver height, the greatest increase occurring at a distance R of about 250 m. For example, when the receiver is raised from a height

of 5 m to a height of 37 m the received level at 250 m increases by about 16 db; at greater distances the increase obtained by raising the receiver becomes gradually less, being only about 3 db at 4000 m.

No explanation is given by the author of just why the higher altitude sound propagation path should entail less loss. It is clear, however, that this general result is entirely consistent with results discussed in Section II of the present report. Thus the losses observed by Sieg (subsection 2.2.1), Eyring (subsection 2.2.3), Hayhurst (subsection 2.3.3) and Ingard (subsection 2.3.4) in measurements where the sound propagation path is near the earth are, as a whole, much greater than those found by Delsasso and Leonard (subsection 2.2.4), Regier (subsection 2.3.1) and Parkin and Scholes (subsection 2.3.2), where the path is mainly through air at relatively high altitudes. The same mechanisms for losses, namely, terrain effects and refraction phenomena, which were considered in connection with the findings in Section II are, no doubt, equally important in Baron's case. Referring back to the specific results presented in Section II, we observe that Baron's average loss coefficients (i.e., about 2 db/1000 ft) at 390 cps are:

(1) About the same order of magnitude as those found by Delsasso and Leonard at 250 cps and 500 cps (see Tables 17, 18 and Figs. 25, 26);
(2) Much smaller than those reported for about the same frequency by Sieg (about 5 db/1000 ft under "good conditions"; see Table 14) and by Hayhurst (about 5 db/1000 ft for zero vector wind; see Fig. 33);
(3) Greater than those indicated by Regier (subsection 2.3.1) and Parkin and Scholes (subsection 2.3.2); according to the latter investigators loss coefficients for frequencies as low as 390 cps are hardly measurable under the conditions of their experiments and hence must be less than 1.0 db/1000 ft.

The approximate agreement between the results of Delsasso and Leonard, obtained at high altitudes, and those of Baron, suggests strongly that in the case of propagation over distances up to several miles the propagation is mainly through the upper atmosphere. The question remains, however, as to why the losses obtained in both of these cases (i.e., Delsasso and Leonard in one case, Baron in the other) should be greater than those reported by Regier and by Parkin and Scholes.

In addition to information on mean sound levels or mean sound

losses Baron also gives a rather extensive discussion of variations or fluctuations in the levels. Plots are given showing the root-mean-square deviation from the mean sound level plotted vs the distance R. Also, typical recordings are shown for different frequencies and different heights of the siren; from these we see (1) that the fluctuation magnitude increases with distance R and with frequency and (2) that a change takes place in the character of the fluctuations, especially, that the latter become much slower when the siren is lifted from ground level to a height of 37 m.

Results are also given showing received sound levels plotted against $\cos\phi$, where ϕ is the angle between the direction of the wind and that of sound propagation. The scatter diagrams obtained are similar to those of Hayhurst (Fig. 30, subsection 2.3.3); as in the latter case, the observed correlation between sound level and wind direction is probably mainly due to sound shadows caused and/or modified by wind gradients.

In agreement with Hayhurst, the present author states that little, if any, correlation was found between observed sound levels and wind speed (direction not taken into account). This strongly implies that inhomogeneity scattering is very slight.

Ingard (1954)[92]

This reference contains additional details on measurements reported in Reference 75. Also, a new set of data is included on measurements of mean sound levels and fluctuations of pure tones of frequencies 200, 500, 1200, 1700, 2900 and 5000 cps simultaneously generated by a single loudspeaker; source and receiver heights were 6 ft; source and receiver were separated by distances up to 350 ft. Wind velocities were recorded simultaneously with sound levels on a tape recorder.

The results show the effects on sound levels of sound shadows due to wind and temperature gradients. Also of interest are some rather detailed plots of fluctuations vs source-receiver separation at various frequencies.